ABSTRACT

Title of Dissertation: OPTIMAL SCHEDULING OF EVACUATION OPERATIONS WITH CONTRAFLOW

Hayssam Hicham El-Sbayti, Ph.D. 2008

Dissertation Directed by: Professor Hani S. Mahmassani
Department of Civil and Environmental Engineering

Congestion due to evacuations can be catastrophic and life threatening. The sudden increase in demand will result in excessive loads on roads not typically designed to handle them, leading to network breakdown at the worst possible time. Moreover, since building new roads is infeasible, efficient utilization of the available network resources during disasters becomes one of the few options available to facilitate the movement of residents to safety.

One option is to address the demand side of the problem, through demand scheduling. By scheduling the evacuation demand over a longer period, the congestion is staved off and network degradation is delayed. Advising traffic on when to evacuate, where to evacuate, and which route to take has the potential to improve evacuation times, especially in no-notice emergency conditions. Another option is to address the supply side of the problem, through network re-design. By reversing the direction of wisely selected lanes in a process known as contraflow, a temporary increase in the operational capacity is achieved without any major infrastructure changes.

Both options, if planned correctly, have the potential to greatly ease network degradation and allow evacuees to reach safety sooner. Therefore, the ability to determine the joint optimal demand scheduling and network contraflow policies is of critical nature to the success of any evacuation plan. The objective of this study is to develop a simulation-based dynamic traffic assignment model that minimizes network clearance time at a minimum cost to the travelers by jointly considering demand scheduling and contraflow strategies.

OPTIMAL SCHEDULING OF EVACUATION OPERATIONS WITH CONTRAFLOW

By

Hayssam Hicham El-Sbayti

Dissertation submitted to the Faculty of the Graduate School of the
University of Maryland, College Park, in partial fulfillment
of the requirements for the degree of
Doctor of Philosophy
2008

Advisory Committee:

Professor Hani S. Mahmassani, Chair
Professor Eyad Abed
Professor Paul M. Schonfeld
Professor Bruce L. Golden
Assistant Professor Cinzia Cirillo

ACKNOWLEDGEMENTS

I wish to express my sincerest thanks to my advisor Dr. Hani S. Mahmassani, for his encouragement, patience, and guidance throughout the course of my Ph.D. study. My career has been strongly influenced by his dedication to excellent research work and his passion for the field of operations research and transportation science.

I am also grateful for the members of my doctoral examination committee, Dr. Paul Schonfeld, Dr. Bruce Golden, Dr. Eyad Abed, and Dr. Cinzia Cirillo for their comments and suggestions on my research work.

Special thanks are due to Dr. Xeusong Zhou and Dr. Chung-Cheng Jason Lu for their valuable contribution to the development of DYNASMART-P. I am also grateful for my colleagues Dr. Roger Chen, Dr. Xiao Qin, Dr. Xiang Fei, Dr. Ricardo Giesen, Mr. Samer Hamdar, Mr. Kuilin Zhang, Ms Sevgi Erdogan and Ms. Jing Dong for their support and friendship.

I am indebted to Dr. Khaled Abdelghany, Dr. Ahmed Abdelghany, Dr. Hossein Tavana, and in particular Dr. Yi-Chang Chiu and Dr. Nathan N. Huynh, who were very patient in providing the necessary guidance and advice in my early Ph.D. Study at Austin.

I would also like to thank Rebecca A. Weaver-Gill for providing immeasurable assistance throughout my graduate program.

Finally I would like to express my deep appreciation to my beloved wife, Nina Dannaoui for her unconditional support throughout my studies and my baby Leah Sbayti, for the bundle of joy that she is.

TABLE OF CONTENTS

LIST OF TABLES

LIST OF FIGURES

ABBREVIATIONS

ATT	Average Experienced Trip Time
AET	Average Evacuation Time
ALC	Average LNCT-DTA Cost
AON	All-Or-Nothing Assignment
ATIS	Advanced Traveler Information System
ATMS	Advanced Transportation Management System
BPR	Bureau of Public Roads
CF	Contraflow
CTM	Cell Transmission Model
DNLP	Dynamic Network Loading Problem
DSS	Decision Support Systems
DTA	Dynamic Traffic Assignment
FAT	Fixed Arrival Time
FEMA	Federal Emergency Management Agency
FIFO	First-In First-Out
GIS	Geographical Information Systems
ITS	Intelligent Transportation Systems

LNCT	Latest Network Clearance Time
LP	Linear Program
MNCT	Minimum Network Clearance Time
MSA	Method of Successive Averages
NMP	Nonlinear minimization problem
NRC	Nuclear Regulatory Commission
O-D	Origin-Destination
ODS	Optimal Demand Scheduling
ORS	Optimal Route Swap
STA	Static Traffic Assignment
SO	System Optimal
UE	User Equilibrium
VI	Variational Inequality
VMS	Variable Message Signs

NOTATIONS

Indices

a	Arc in the network
a^{-1}	Link running in opposite direction to a
n	Node in the network
k	Iteration number
r	Source (origin) node in the network
s	Sink (destination) node in the network
$\bar{s}$	Super sink destination
p	Path in the network
$\hat{p}$	Least marginal travel time path for (r,s,τ), $\hat{p} \in P_{r,s}^{\tau}$
$\hat{p}_{r,s}$	Least MNCT marginal time path for $r-s$
t	Index for time step, $t = 1,...,T$
τ	Index for departure (assignment) time period, $\tau = 1,...,T_{\tau}$

Sets

A	Set of directed arcs in network
$\overline{A}$	Set of reversible directed arcs in network, $a \in \overline{A}$
N	Set of nodes in network

R	Set of source (origin) nodes in the network
S	Set of sink (destination) nodes in the network
$\bar{S}$	Set of shelter/safety destinations in the network, $\bar{S} \subset S$
$\Gamma(n)$	Set of links that are downstream of node n
$\Gamma^{-1}(n)$	Set of links that are upstream of node n
$\bar{P}_{r,s}^{\tau}$	Set of active (non-zero flow) paths in $P_{r,s}^{\tau}$
$\bar{P}_{r,s}$	Set of active paths (non-zero flow) between $r-s$
$\hat{P}_{r,\bar{s}}^{\tau}$	Set of time-dependent least MNCT marginal time paths between $r-s$
J^{-}	Set of vehicles that will be switching to cheaper paths
$\Re_{r,s}$	Set of restricted path-departure times combination for $r-s$

Link-based Variables

$N_a(t)$	Physical capacity of link a at time step t
$y_a(t)$	Capacity (maximum physical storage or occupancy on link a at time step t
$u_a(t)$	Inflow on link a at time step t
$v_a(t)$	Outflow on link a at time step t
$x_a(t)$	Volume on link a at time step t
$c_a(t)$	Link travel time on link a at time step t
$\tilde{c}_a(t)$	Link travel time marginal on link a at time step t

$c_a^{\min}$ Minimum travel time on link a corresponding to free-flow conditions

$\omega_a(t)$ Number (algebraic) of lanes reversed on link a

α_a Shape parameter associated with link a

$\vartheta_a(t)$ Average speed on link a at time step t

$\vartheta_a^{\max}$ Maximum speed on link a

$\vartheta_a^{\min}$ Maximum speed on link a

$\kappa_a(t)$ Average density on link a at time step t

κ_a^{jam} Jam density on link a

κ_a^{cutoff} Cutoff density on link a

L_a Length of link a

L_a Length (miles) of link a

l_a Number of lanes in link a

$\xi_{r,s,p}^{\tau,a}(t)$ Time-dependent link-path index, equal to 1 if vehicles going from origin r to destination s during departure time τ are assigned to path τ are on link a during time step t; and 0 otherwise

Node-based Variables

$I_n(t)$ Total flow entering a node n in time step t

$O_n(t)$ Total flow exiting a node n in time step t

$d_{r,s}^{\tau}$ Traffic demand associated with the O-D pair $r-s$ at departure time τ

d_r Total demand at origin r to be evacuated

$\pi_{r,s}^{\tau}$ Minimum travel time for flow leaving origin r going to destination s during departure period τ

$\tilde{\pi}_{r,s}^{\tau}$ Minimum travel time marginal for flow leaving origin r going to destination s during departure period τ

$\hat{\pi}_{r,s}$ Minimum MNCT marginal time between $r-s$

$\bar{\pi}_{r,s}$ Minimum LNCT marginal time between $r-s$

$\Lambda_{r,s}^{\tau}$ Staging policy or the fraction of demand leaving origin r to destination s

Path-based Variables

$f_{r,s,p}^{\tau}$ Flow leaving origin r going to destination s assigned to path $p \in P_{r,s}^{\tau}$ during departure period τ

$P_{r,s}^{\tau}$ Set of all possible paths between r and s at departure time τ

$C_{r,s,p}^{\tau}$ Travel time for path $p \in P_{r,s}^{\tau}$

$\tilde{C}_{r,s,p}^{\tau}$ Marginal travel time for path $p \in P_{r,s}^{\tau}$

$\chi_{r,s,p}^{\tau}$ MNCT time incurred by the MNCT-DTA system for path $p \in P_{r,s}^{\tau}$

$\tilde{\chi}_{r,s,p}^{\tau}$ MNCT marginal time incurred by the MNCT-DTA system due to an additional vehicle on path $p \in P_{r,s}^{\tau}$

$\tilde{\chi}'^{\tau}_{r,\bar{s},p}$ Derivative of $\tilde{\chi}_{r,s,p}^{\tau}$ with respect to flow

$\gamma_{r,s,p}^{\tau}$ LNCT time incurred by the LNCT-DTA system for path $p \in P_{r,s}^{\tau}$

$\tilde{\gamma}^{\tau}_{r,s,p}$ LNCT marginal time incurred by the LNCT-DTA system due to an additional vehicle on path $p \in P^{\tau}_{r,s}$

$\tilde{\gamma}'^{\tau}_{r,\bar{s},p}$ Derivative of $\tilde{\gamma}^{\tau}_{r,\bar{s},p}$ with respect to flow

$\delta^{\tau}_{r,s,p}$ Unadjusted flow shift (algebraic) to path $p \in \overline{P}^{\tau}_{r,s}$

$\tilde{\delta}^{\tau}_{r,s,p}$ Amount of feasible flow shift (algebraic) to path $p \in \overline{P}^{\tau}_{r,s}$

δ_p Amount (algebraic) of flow shifted to path p

$\tilde{C}'$ Derivative of $\tilde{C}$ with respect to flow, i.e. $\tilde{C}' \equiv \partial\tilde{C} / \partial f$

Functions

$\Omega_a(t, \boldsymbol{f})$ Link flow-to-cost mapping function evaluated through simulation.

$\Phi^{\tau}_{r,s,p}(\boldsymbol{f})$ Path flow-to-cost mapping function evaluated through simulation.

$\boldsymbol{L}(\bullet)$ Lagrangian operator

$H(\bullet)$ Function that maps a given active path-departure-time couple (p,τ) to an index i

$\mathsf{P}(p)$ Probability that a vehicle on path p switches to optimal path $\hat{p}$ in a given (r,s,τ)

$G(N,A)$ Graph of network represented by the node set N and directed link set A

$F(t)$ Fraction of the total demand loaded by time t

Vectors and Matrices

$\boldsymbol{c}$ Vector of link travel times $c_a(t)$

$\tilde{\boldsymbol{c}}$	Vector of link travel time marginals $\tilde{c}_a(t)$
$\boldsymbol{y}$	Vector of link capacities $y_a(t)$
$\boldsymbol{u}$	Vector of inflow volumes $u_a(t)$
$\boldsymbol{v}$	Vector of outflow volumes $v_a(t)$
$\boldsymbol{x}$	Vector of link volumes $x_a(t)$
$\boldsymbol{d}$	Vector of time-dependent O-D demand $d_{r,s}^{\tau}$
$\boldsymbol{\pi}$	Vector of minimum travel-time marginals $\pi_{r,s}^{\tau}$.
$\tilde{\boldsymbol{\pi}}$	Vector of minimum path travel-time marginals $\tilde{\pi}_{r,s}^{\tau}$
$\hat{\boldsymbol{\pi}}$	Vector of minimum MNCT marginal travel times $\hat{\pi}_{r,s}$
$\breve{\boldsymbol{\pi}}$	Vector of minimum LNCT marginal travel times $\breve{\pi}_{r,s}$
$\boldsymbol{\xi}$	Vector of time-dependent link-path indices $\xi_{r,s,p}^{\tau,a}(t)$
$\boldsymbol{\delta}$	Vector of flow shifts (algebraic) in the network
$\boldsymbol{C}$	Vector of path travel times $C_{r,s,p}^{\tau}$
$\tilde{\boldsymbol{C}}$	Vector of path marginal travel times $\tilde{C}_{r,s,p}^{\tau}$
$\boldsymbol{f}$	Vector of dynamic flow assignments $f_{r,s,p}^{\tau}$
$\boldsymbol{f}^*$	Optimal flow pattern
$\boldsymbol{g}$	Set of auxiliary path assignments obtained by an AON assignment for the MSA algorithm

Other

$\lvert N \rvert$	Total number of nodes in network
$\lvert A \rvert$	Total number of directed arcs in network
Δ	Time step length (in seconds)
W	Network clearance time
T	Maximum number of time steps in planning horizon
$[0, W]$	Simulation interval (planning horizon)
$\overline{W}$	Target network clearance time
W^*	Minimum network clearance time
T_τ	Maximum number of departure (assignment) time periods planning horizon
$[0, W_\tau]$	Demand assignment interval
β	Demand loading curve response rate.
G_{SO}	Gap for the SO-DTA problem
$\tilde{G}_{\text{SO}}$	Relative gap for the SO-DTA problem
G_{UE}	Gap for the SO-DTA problem
$\tilde{G}_{\text{UE}}$	Relative gap for the SO-DTA problem
ε	Path convergence threshold
$V(\varepsilon)$	Number of cases, in which the absolute path flow difference for 2 successive iterations, $\left\lvert f_{r,s,p}^{\tau\,(\kappa)} - f_{r,s,p}^{\tau\,(\kappa+1)} \right\rvert \forall r, s, \tau, p$, is greater than ε

$\overline{V}(\varepsilon)$	Predetermined user-specified upper bound for $V(\varepsilon)$
θ	Denotes a descent direction
ρ	Denotes the step size along θ, $\rho \in [0,1]$
h^{-1}	Scaling term
$\hat{\rho}$	Swap rate
$\eta(t)$	Turnstile cost incurred by the system when a vehicle exits in time step t
G_{MNCT}	Gap for the MNCT-DTA problem
$\tilde{G}_{\text{MNCT}}$	Relative gap for the MNCT-DTA problem
G_{LNCT}	Gap for the LNCT-DTA problem
$\tilde{G}_{\text{LNCT}}$	Relative gap for the MNCT-DTA problem
M	A sufficiently large positive number
$\left\|\overline{P}_{r,s}^{\tau}\right\|$	Number of paths in $\overline{P}_{r,s}^{\tau}$

1 INTRODUCTION

Congestion in most major urban areas results in loss of productivity and environmental degradation but in the case of man-made or natural disasters, it can be catastrophic and life threatening. The sudden increase in demand will result in excessive loads on roads not typically designed to handle them, leading to network degradation and breakdown at the worst possible time. The prospect of evacuees being stranded in traffic and having to weather an extreme event on the streets is particularly terrifying. Moreover, since building new roads is infeasible, efficient utilization of the available transportation network resources during disasters becomes one of the few available options to facilitate the movement of residents to safety.

One option to efficiently use the available transportation network is to address the demand side of the problem, through demand scheduling. By scheduling and spreading the evacuation demand over a longer period, the congestion is staved off and network degradation is delayed. Advising traffic on when to evacuate, where to evacuate, and which route to take has the potential to improve evacuation times, especially in no-notice emergency conditions. While such a strategy is not new, it has been incorporated into traffic assignment models in the evacuation context only recently and as such, warrants further investigation.

Another option is to address the supply side of the problem, through network re-design. By reversing the direction of intelligently selected lanes in a process known as contraflow, a temporary increase in the operational capacity is achieved without any major infrastructure changes. Safety and confusion though, remain a major cause of concern. These very concerns have caused the state of Florida to decline the use of contraflow strategies during hurricane Floyd. On the other hand, South Carolina and Georgia have both successfully implemented their contraflow evacuation plans and their positive experience is generating a lot of interest in other states to include the contraflow option as part of their evacuation plans.

Both options, if planned correctly, have the potential to greatly ease network degradation and allow first responders and evacuees to reach safety sooner rather than later. Therefore, the ability to determine the joint optimal demand scheduling and network contraflow policies is of critical nature to the success of any evacuation plan. The subsequent sections of this chapter introduce the motivation for this work, the evacuation problems addressed in this study, the contributions of this work to the fields of transportation engineering, and outlines the remainder of this dissertation.

1.1 BACKGROUND AND MOTIVATION

Evacuation of urban centers is not a new field. Civilizations have always faced threats, whether natural (hurricanes, floods, earthquakes, etc…) or man-made (chemical spills, nuclear meltdowns, terrorist acts, etc…) that necessitated mass evacuations. Evacuation can be defined as the removal of residents from a dangerous area to safety in a timely and efficient manner. Two different evacuation scenarios can be considered, advance warning and no-notice. In the former, the estimation of the population at risk and the evacuation time compared to the hazard propagation time can be done a priori. Hence, time and potential risks are the key components of this type of evacuation. In the latter, evacuation occurs when insufficient warning has prevented the organizer from conducting a pre-emergency evacuation planning.

Evacuating a large population is an extremely difficult and complicated task that requires the coordination of several agencies. For recurrent events, such as hurricanes, emergency management agencies usually have a priori evacuation strategies. Citizens are usually given advanced warning about the trajectory of the threat and are advised on safety destinations. Still, most of these a priori strategies do not incorporate any form of staging or spreading of the demand and the examples are abundant. One just has to refer to the failure of evacuation plans during hurricanes Floyd, Andrew, and Katrina in preventing or even delaying network

gridlock despite ample warning periods.

For non-recurrent no-notice extreme events, evacuating a large population in the same manner as recurrent events, by mandating evacuation but without any form of staging, leads to premature congestion on the surface streets and excessive delays. Therefore, without intelligently advising the population on their optimal departure times, routes, and safety destinations, evacuees may get stuck on grid-locked roadways for excessive periods of time, which could be even more devastating, in the event the threat picks up speed or changes direction, than staying at home.

With traditional evacuation strategies proving no match for the excessive demand patterns generated from these extreme events, the best approach to address this problem is to integrate demand and supply management strategies, using Intelligent Transportation Systems (ITS) strategies, to enforce the desired strategies. The integration of these strategies can only be realistically analyzed using the Dynamic Traffic Assignment (DTA) capability. Traditional Static Traffic Assignment (STA) models have proved to be inappropriate for the generation of information strategies and route guidance instructions [Peeta (1994)] for they cannot adequately model the waiting phenomenon associated with travel. Furthermore, STA models cannot account for travelers' response to supplied real-time information and/or route guidance instructions. On the contrary, DTA models reflects the trip making decisions better, the resulting congestion, and the ability of trip-makers to adjust their trip choices in response to travel information.

A central question is how to route evacuees to safety. The most commonly used route choice principle in traffic assignment models is the User Equilibrium (UE) principle, which states that the travel costs on all actually used routes are equal and less than those (would be) experienced on unused routes [Wardrop (1952)]. The UE principle assumes that all travelers have perfect information about the different travel options, and that all travelers perceive

travel costs uniformly. Such an assignment principle has been also used in the context of evacuation models [Rathi and Solanki (1993), Hobeika and Kim (1998)].

While UE characteristics may be applicable for every-day traffic conditions, their applicability to emergencies is rather unclear. Evacuees will generally not have perfect information about all travel options in the network and as such, they may be inclined to follow route advisory information than their own especially if they had been stuck in gridlocked conditions in previous evacuations. Such an apparent willingness to adhere to route advisory information provides a great opportunity for planners to capitalize on it and provide a System Optimal (SO) type of information to minimize network clearance time. In an SO assignment, which is based on Wardrop's second principle [Wardrop (1952)], travelers will behave cooperatively when choosing their departure times and routes in order to minimize the total cost to the system. In other words, some travelers will have to be assigned to sub-optimal paths (from their perspective) for the benefit of the whole (system). Providing an SO type of information is the current trend in all evacuation studies [Sattayhatewa and Ran (2000), Chiu (2004), Tuydes and Ziliaskopoulos (2004, 2005a), Liu et al. (2005a, 2005b), Sbayti and Mahmassani (2006), Yuan et al. (2006), Chiu et al. (2007)] and this dissertation will be no exception.

Simulation-based DTA models are typically used for evacuation modeling since analytical DTA models suffer from several serious shortcomings. First, they lack a sound link-cost performance function. The use of Bureau of Public Roads (BPR) link performance and exit functions leaves much to be desired. Moreover, these functions cannot enforce First-In First-Out (FIFO) conditions and cannot take advantage of the recent developments in ITS, traffic modeling, and vehicle re-routing. In addition, the computing and memory requirements of analytical DTA models prohibit their applicability in reasonably sized urban networks.

On the other hand, the use of simulation-based DTA models raises the issue of solution

quality and optimality. While almost all simulation-based DTA models are capable of correctly propagating traffic and adhering to flow fundamentals, very few are capable of solving for, and for that matter guaranteeing, UE and SO conditions. Moreover, solving for an SO objective is even harder due to difficulties in estimating the link travel time marginals. Therefore, it is of utmost importance to have a theoretically sound simulation-based model that satisfies both UE and SO conditions, and at the same time adheres to traffic fundamentals, before attempting to solve evacuation problems.

Furthermore, currently available evacuation models lack several important features and functionalities. They are generally designed for a specific scenario such as a hurricane or a nuclear meltdown and as such cannot be applicable to a general evacuation scenario. Moreover, most models have been static in nature and therefore cannot account for the impact of information strategies on route selection, a key element to the success of any evacuation plan. Thirdly, these models mainly use the UE assignment principle, which may or may not be applicable, but in any case would produce worse evacuation times than using an SO objective. Furthermore, most models treat evacuation demand mobilization times as exogenous to the system and not as decision variables, which is not advantageous in no-notice extreme. Finally, most models do not optimize for contraflow operations, let alone account for it, and when they do, it is done rather simplistically.

1.2 PROBLEM STATEMENT AND OBJECTIVES

The overall problem addressed in this dissertation is to develop a methodology for emergency evacuation planning that simultaneously considers supply and demand management options in order to facilitate the mobility of evacuees to safety. The methodology is manifested in the development of a bi-objective simulation-based DTA model that aims at minimizing the network clearance time while keeping the total system trip time at a minimum given supply and demand constraints. The primary objective is to

minimize network clearance time; however, it must be achieved at a minimum cost to the system (average trip times for evacuees).

There are two primary problems to be solved within the overall problem. The first problem is to solve for the Optimal Demand Scheduling (ODS) policy that would minimize network clearance time at a minimum cost to the system. The second problem is to solve an SO discrete network re-design problem to determine the optimal lane-reversibility policy (capacity redistribution). The main output of this model is the set of lanes that need to be reversed that would minimize the total system trip time. The combination of these two problems results in solving the overall problem addressed in this dissertation, namely integrating supply and demand management options to minimize network clearance time while keeping cost to the system at a minimum.

1.2.1 Problem 1: The Optimal Demand Scheduling Problem

Consider a transportation network represented by a directed graph $G(N,A)$ with $|N|$ nodes and $|A|$ directed arcs. Let $r \in R \subset N$ and $s \in S \subset N$ denote an origin node and a destination node, respectively. Let the study period $[0,W]$ be discretized into T time steps of length Δ such that $W = T \cdot \Delta$, with a time index $t = 1,...,T$. Let the demand assignment period, $[0,W_\tau]$ be discretized into T_τ departure periods of length $\Delta_\tau \geq \Delta$ such that $T_\tau = W_\tau \cdot \Delta_\tau$, with a departure time index $\tau = 1,...,T_\tau$. Assume that W is long enough for all the traffic to clear the network, i.e. $W > W_\tau$. Let $f_{r,s,p}^{\tau}$ be the flow leaving origin r going to destination s assigned to path $p \in P_{r,s}^{\tau}$ during departure period τ. Assume that the total demand to be evacuated at each origin, d_r, is known a priori and that the network is empty at start of evacuation. The optimal demand scheduling (ODS-DTA) problem is therefore to find the vector of path-flow assignments $\boldsymbol{f}$, for all r,s,τ combinations that would minimize the network clearance time W while keeping the total system cost (total trip times) at a minimum.

Two sub-problems need to be solved sequentially to obtain the optimal demand scheduling pattern $\boldsymbol{f}^*$. The first sub-problem is the Minimum Network Clearance Time (MNCT) DTA problem whose main output is estimating the minimum network clearance time W^*. The second sub-problem is the Latest Network Clearance Time (LNCT) DTA problem whose main output is the time-dependent flow pattern that minimizes the total system trip time while reaching safety before a pre-specified target evacuation time, the minimum network clearance time W^* in this particular case. Both problems are addressed in detail in Chapter 4.

1.2.1.1 *Sub-problem 1: The Minimum Network Clearance Time Problem*

This main objective of this problem, as is with most evacuation models, is to determine the minimum network clearance time W^*. The problem may be stated as follows: given the total demand d_r to be evacuated and a set of safety destinations S; we wish to solve for time-dependent O-D path flows $f_{r,s,p}^{\tau}$ that minimizes the network clearance time W, subject to DTA constraints; where W is defined as $W \geq C_{r,s,p}^{\tau}, \ \forall r,s,\tau,p$ and $C_{r,s,p}^{\tau}$ represents path travel time for a vehicle traveling from r to s on path p at departure time τ. It entails the following:

- Formulating the MNCT-DTA problem as a minimization program and deriving its optimality conditions;
- Establishing solution existence by using underlying Variational Inequality (VI) problem;
- Reformulating the VI problem as an equivalent Nonlinear Minimization Program (NMP) via a gap function;
- Developing a simulation-based solution heuristic based on the derived optimality conditions to solve the MNCT-DTA problem; and
- Evaluating the solution heuristic on test and real urban networks.

1.2.1.2 *Sub-problem 2: The Latest Network Clearance Time Problem*

This main objective of this problem is to determine the demand scheduling policy to minimize the average trip time for evacuees subject to clearing the network within a fixed time $\overline{W}$. This problem may be generally stated as follows: given the total demand to be evacuated d_r and a set of safety destinations S; we wish to solve for time-dependent O-D path flows $f_{r,s,p}^{\tau}$ that minimizes the total system trip time subject to clearing the network within a target evacuation time $\overline{W}$ and DTA constraints. It entails the following:

- Formulating the LNCT-DTA problem as a minimization program and deriving its optimality conditions;
- Establishing solution existence by using underlying Variational Inequality (VI) problem;
- Reformulating the VI problem as an equivalent NMP via a gap function;
- Developing a simulation-based solution heuristic based on the derived optimality conditions to solve the LNCT-DTA problem; and
- Evaluating the solution heuristic on test and real urban networks.

1.2.1.3 *Combining the Sub-problems: Optimal Demand Scheduling Problem*

The objective of the MNCT-DTA problem is to minimize the network clearance time W, which may be substituted by minimizing the total turnstile costs (exit times) of individual evacuees [Hamacher and Tjandra (2002)]. In other words, the model is insensitive for variations in experienced trip times as long vehicles exit at the same time. For example, a vehicle departing at 8:00 AM and reaching the safety at 8:50 AM has the same contribution to the objective function of the MNCT-DTA as a vehicle departing at 8:15 AM and reaching safety at 8:50 AM despite incurring different trip times. Whereas for the LNCT-DTA problem with a target network clearance time of $\overline{W} = 8:50\ \text{AM}$, the second vehicle will have a lower contribution to the objective function (better) since its trip time is shorter.

It is desirable to minimize the network clearance time while keeping the total system trip time at a minimum, however, the somewhat conflicting objectives of the MNCT-DTA and the LNCT-DTA problems, results in a bi-objective problem whose solution is obtained in two sequential stages. In the first stage, an MNCT-DTA problem is solved to determine the minimum network clearance time W^*. In the second stage, an LNCT-DTA problem is solved with a target evacuation time W^*. We refer to the resulting problem as ODS-DTA and the resulting time-dependent O-D path flows $\boldsymbol{f}^*$ as the optimal demand scheduling flow pattern. These objectives are also addressed in detail in Chapter 4.

1.2.2 Problem 2: The Contraflow Network Design Problem

The supply management strategy considered in this dissertation is to find the optimal lane reversibility policy that would minimize the total system trip time. This problem entails finding the optimal capacity redistribution, expressed in terms of the number of lanes to be reversed for each link, ω_a. The resulting problem is essentially a network re-design problem whose objective is to minimize the total system trip time, subject to keeping the total network capacity fixed (i.e. cannot create capacity) and DTA constraints. This problem may be stated as follows: given a time-dependent demand (with fixed departure times) $d_{r,s}^{\tau}$, and a set of candidate links to be reversed, $\overline{A}$, we wish to find the number of lanes to be reversed ω_a for each reversible link $a \in \overline{A}$ to minimize total system trip time subject to supply, demand and DTA constraints. It entails the following:

- Formulating the CF-DTA problem as a minimization problem by modifying the base SO-DTA model and deriving its optimality conditions;
- Developing a simulation-based solution heuristic based on the derived optimality conditions to solve the CF-DTA problem; and
- Evaluating the solution heuristic on test and real urban networks.

These objectives are addressed in detail in Chapter 5.

1.2.3 The Overall Problem: Optimal Evacuation Demand Scheduling with Contraflow

The ORS-DTA problem and the CF-DTA problem are considered jointly in second half of Chapter 5. The resulting problem is referred to as ODS-CF-DTA and may be stated as follows: given a transportation network $G(N, A)$, total demand that needs to be evacuated at each origin d_r, the set of safety destinations S, and the set of reversible links $\bar{A}$, the problem is to determine the joint optimal 1) lane reversibility policy $\boldsymbol{\omega}^*$ and 2) the time-dependent O-D path flows $\boldsymbol{f}^*$ so as to minimize the network clearance time W, while keeping the total system trip time at a minimum.

The solution procedure for the ODS-CF-DTA problem is a two-stage procedure. In Stage I, the MNCT-DTA and CF-DTA problems are combined to solve for the optimal joint flow pattern and lane configuration that results in minimizing the network clearance time. The resulting problem is referred to as MNCT-CF-DTA and is solved in an iterative bi-level framework whereby an MNCT-DTA problem is solved in the lower level, given current optimal lane configuration to find the optimal flow pattern that minimizes network clearance time and a CF-DTA problem is solved in the upper level, given current optimal flow pattern, to find the optimal lane configuration that minimizes trip times in the network. The process iterates until convergence. In the second stage, an LNCT-DTA problem is solved, given the optimal lane configuration $\boldsymbol{\omega}^*$, minimum network clearance time $\boldsymbol{f}^*$, and using the MNCT-CF-DTA solution as the starting solution.

1.3 ORGANIZATION OF THE DISSERTATION

This dissertation is organized in six chapters. Following the problem definition, motivation, and objectives, chapter 2 presents a general overview of the literature related evacuation modeling. Chapter 3 reformulates the SO-DTA problem via a gap function, derives its optimality properties and solution algorithm. Chapter 4 formulates the MNCT-DTA and LNCT-DTA demand scheduling models and derive their optimality conditions and solution

algorithms. These models are also combined in Chapter 4 to obtain the ODS-DTA problem. Chapter 5 formulates the CF-DTA problem and derives its optimality conditions and corresponding solution algorithm. Chapter 5 also integrates the ODS-DTA and the CF-DTA problems and examines their combined impact on the same test cases in considered in chapter 4. Finally, chapter 6 presents the conclusions, and directions for future work.

2 LITERATURE REVIEW

This chapter provides a review of the relevant literature for this research and is organized into five sections. Section 2.1 lists existing computer evacuation models along with their features and drawbacks. Sections 2.2 and 2.3 discuss route choice and demand estimation in the context of evacuation. Section 2.4 provides a background review and relevant studies regarding the evacuation management strategies considered in this research, namely demand scheduling and contraflow. Finally, section 2.5 provides a brief overview of the DTA problem, the basis of all evacuation models formulated in this dissertation.

2.1 EVACUATION MODELING

Interest in evacuation modeling has started in the 1970s with an initial emphasis on hurricane evacuation [Urbanik (1978), COE and SWFRPC (1979)]. However, after the nuclear accident at the Three Mile Island in 1979, and the subsequent mandate issued by the nuclear regulatory commission (NRC) to develop evacuation plans for urban centers, emphasis has shifted to evacuation from nuclear sites [HMM Associates (1980), Urbanik and Desrosler (1981), Sheffi et al. (1982a, 1982b), KLD Associates (1984)]. Interest has returned to hurricane evacuation in 1990s, primarily because the most expensive (at the time) hurricane in United States in terms of damage, Hurricane Andrew, occurred in 1992 and the hurricane that generated the greatest evacuation in United States history, Hurricane Floyd, occurred in 1999. Since then, state departments of transportation have become more involved in emergency evacuation. Recently, and in the aftermath of September 11, 2001 terrorist attacks and Hurricane Katrina, greater attention is being allocated to the transportation aspects of evacuation.

To analyze an evacuation scenario, a number of different approaches have been used, ranging from empirical models to sophisticated simulation models. Most of the research has been concentrated on two distinct problems, evacuation of buildings and evacuation of urban

networks, like entire cities or coastal plains. Evacuation models for buildings have been discussed extensively in Chamlet (1982) and Choi et al. (1984, 1988) and will not be reviewed in this dissertation.

According to Lovas (1998) and Graat et al. (1999), the evacuation time – the time needed to complete an evacuation process – basically consists of three main time components: 1) the time required to detect a dangerous situation that warrants evacuation; 2) the time required to decide on a course of action (evacuate or do not evacuate), and 3) the time evacuees need to reach safety, which is also known in the literature as egress time. Since the behavioral and organizational factors are the main contributors, to the first two components, most evacuation models only emphasize the calculation of network clearance time (egress time) and treat the result as the lower bound of the real evacuation time, which will also be the approach taken in this dissertation.

2.1.1 Existing Evacuation Models

This section describes the existing emergency evacuation models and software. Evacuation models range from simple empirical models to sophisticated simulation models with the overall evacuation time as the major output. Furthermore, there are two approaches to model the behavior of evacuees in the network, namely macroscopic and microscopic. Macroscopic approaches consider the collective behavior of the evacuees and are mainly used to produce a good first estimate of the evacuation time. This estimate can be later used to analyze existing evacuation plans. On the other hand, microscopic approaches model behavior of individual evacuees and their interaction among others but are usually resource-intensive and can only be implemented using simulation techniques.

A nice review about evacuation modeling applied to large areas can be found in Southworth (1990), Sattayhatewa and Ran (2000), and Church and Sexton (2002). Most evacuation models, such as NETVAC [Sheffi et al. (1982a, 1982b)], DYNEV [KLD Associates (1984)],

and MASSVAC [Hobeika et al. (1985)] have been developed to solve a specific evacuation problem. For others, existing traffic simulation packages have been modified to incorporate evacuation modules and add-ons, requiring extensive modifications in most cases. Examples of traffic simulation packages used in evacuation applications include NETSIM [HMM Associates (1980), Urbanik and Desrosler (1981), Radwan et al. (1985)], MITSIM [Yang and Koutsopoulos (1996)], CORSIM [Sisiopiku et al. (2004)], PARAMICS [Cova and Johnson (2002, 2003), Church and Sexton (2002)], DYNASMART-P [Chiu (2004), Sbayti and Mahmassani (2006), Kwon and Pitt (2005)], and VISSIM [Han and Yuan (2005)].

The majority of evacuation models are computerized software packages in which the major emphasis is on traffic assignment. Earlier models such as DYNEV and MASSVAC adopted static traffic assignment principles, whereas almost all recent evacuation models consider the dynamic nature of traffic especially in the evacuation context [Chiu (2004), Chiu et al. (2005, 2007), Sbayti and Mahmassani (2006), Kwon and Pitt (2005), Tuydes (2005a, 2005b), Liu et al (2005a, 2005b, 2006)].

Despite the resurgence of evacuation modeling and related studies, it is not a new field. In fact, traffic management attempts have been recorded as early as in 1963, but are mostly limited to empirical solutions [Givens (1963)]. One of such models is the dissipation rate model [Houston (1975)], which uses a simple formula that correlates the size and population density with evacuation time. While simple and easy to use, the dissipation rate model does not account for network topography, evacuation activities, and intersection capacity and control.

Another empirical approach in evacuation is the use of capacity analysis techniques. The evacuation time is determined by allocating the estimated number of evacuees to their corresponding evacuation routes and dividing that number with the respective capacities. While an obvious improvement over the dissipation rate model, it still lacked the capability

to capture network topography and traffic dynamics.

Empirical models have a major limitation in that they do not capture the movement of traffic around the evacuation area. The first study to attempt to do so is the one conducted by H.M.M (1980), using NETSIM, a microscopic traffic simulator, to study the evacuation pattern surrounding four nuclear plants. However, the study has been conducted on a small network due to the huge (at the time) computing and memory requirements, which rendered their results inconclusive and unsatisfactory.

To improve on the H.M.M model, Sheffi et al. (1982a, 1982b) have developed NETwork eVACuation (NETVAC), a macroscopic traffic simulation model, to estimate the network clearance time surrounding nuclear power plant sites. NETVAC uses established aggregate traffic flow relations to move traffic along the network, accounting for queue formation and route selection in response to changes in link density, intersection control, and lane management strategies. Drivers are assumed to have some prior knowledge of the network topography in that they know the general direction to safety. The route selection process is myopic in the sense that, at each intersection, evacuees select the outbound link that can get them towards safety faster. Its use is, however, restricted to radial evacuation from a single point, rather than in a more general direction.

Another model that handles evacuations around nuclear plants is the Calculated Logical Evacuation And Response (CLEAR) microscopic simulation model developed by Moeller et al. (1982), which estimates the time required for a specific population density and distribution to clear a certain disaster area. The advantage of this model is that it accounts for the time required by individuals to prepare and gather for evacuation. Nonetheless, vehicles are only simulated on main arterial roads (to minimize computer resource requirements), and as such CLEAR cannot be used to model neighborhood evacuation applications.

A model that has been developed for the NRC commission and endorsed by the Federal

Emergency Management Agency (FEMA) is the macroscopic simulation model DYNamic EVacuation (DYNEV) by KLD Associates (1984). DYNEV, the most widely reported network evacuation model according to Southworth (1990), is derived through the enhancement of the sub-model simulation core in TRAFLO [Lieberman et al. (1980, 1983)]. The model adheres to the principles of flow continuity and performs static equilibrium traffic assignment – the main drawback of this model – to provide detailed link-level statistics. The key advantage of this model is its capability to identify bottlenecks along the evacuation routes.

As mentioned earlier in this chapter, most models do not account for human behavior during disasters. A model that does so is the EVAC PLAN PACK Model [PRC Voorhees (1982)], which is both a dynamic and probabilistic model. The human behavior is taken into account for determining the loading and response rate of evacuees. The model outputs evacuation time and personal-vehicular information, including congestion associated with the evacuation activity.

So far, all the models mentioned above are developed for evacuations around nuclear power plant failures. A model that is developed for a wider variety of evacuation situations is MASS eVACuation (MASSVAC) by Hobeika et al. (1985) and Hobeika and Jamei (1985). It is a real-time macroscopic simulation model that uses Dial's algorithm [Dial (1969)] to stochastically assign traffic onto major arteries. Traffic is propagated in the network based on BPR link performance functions.

MASSVAC estimates the network clearance times and identifies potential bottlenecks in the network. The major advantage of this model is its ability to produce detailed output at the microscopic level, which helps in assessing the impact of different intersection control and operational strategies on the evacuation process. The major disadvantage of this model is that it ignores the time required to reach major arterials, which usually leads to underestimating

the network clearance times. MASSVAC has been applied to several applications such as hurricane and nuclear power plant evacuations. Later on, Hobeika and Kim (1998) have updated MASSVAC by incorporating a static UE traffic assignment procedure to overcome the limitations of Dial's algorithm, which tends to assign traffic to overlapping paths. Not surprisingly, the UE assignment provides better results than that of Dial's.

The consultant Post, Buckley, Schuh and Jernigan (PBS&J) developed the Evacuation Travel Demand Forecasting System (ETDFS) in 2000 [PBS&J (2000a, 2000b, 2000c)]. This macroscopic model attempts to simulate and determine the impact of the inter-state evacuation traffic encountered in situations such as that produced by Hurricane Floyd.

2.1.2 Evacuation Decision Support Systems

With the advent of Geographical Information Systems (GIS) and its natural applications to transportation networks, it was only a matter of time before GIS capabilities were incorporated into evacuation models to develop evacuation Decision Support Systems (DSS). The aim of a DSS is to provide a planning package that integrates both the transportation and spatial aspects of evacuation applications. One of the first DSS for handling evacuations is TEVACS by Han (1990), which is effectively an adaptation of NETVAC for multi-modal networks. Han has used the model to evaluate different evacuation actions such as rearrangement of gathering points, traffic signal improvement and partial reversibility lanes on 6-lane highways. The study has concluded that integrated solutions have a bigger impact on reducing evacuation time compared to sum of benefits gained by partial improvements alone.

Another application of NETVAC is that of Abkowitz and Meyer (1996) who have introduced a GIS capability to NETVAC to use existing TIGER/line files and population data to determine the network degradation as well as evacuation times for fixed-point and traffic-corridor applications.

Tufekci and Kisko (1991) have developed the Regional Evacuation Modeling System (REMS), a decision support system capable of performing dynamic analysis including multiple scenarios such as hurricanes, chemical spills or nuclear accidents, with interactive data manipulation options that ultimately can be deployed in a real-time application. Lepofsky et al. (1993) also proposes GIS methods capable of performing transportation hazard analysis and incident management.

A more recent DSS for evacuation is the Oak Ridge Evacuation Modeling System (OREMS) [Rathi and Solanki (1993), ORNL (1995, 1998, 1999)] which uses TRAF simulation tools to estimate evacuation time. OREMS identifies traffic operational characteristics such as average speed and bottlenecks, to aid in developing effective evacuation plans. MOEs may be reported at any spatial or temporal level. The main advantage of OREMS is its capability to perform either a static or a dynamic UE assignment, depending on demand data. The model however, has had only limited application to date.

Hobeika et al. (1994, 2002) have developed the Transportation Evacuation Decision Support System (TEDSS) Model to target man-made and natural disaster evacuations while accounting for weather conditions, and time of day. MASSVAC constitutes the simulation core for TEDSS, which works in real-time and outputs the evacuation times and routes, and the expected bottlenecks in the network. The model allows the user to specify one of the several built-in assignment rules and interactively decide on the best evacuation strategy. TEDSS has been updated in 2002 following the upgrade of MASSVAC in 1998.

Pidd et al. (1996) have combined GIS and simulation modeling to develop the Configurable Emergency Management and Planning Simulator (CEMPS) decision support system. CEMPS allows the user to specify weather information, incidents, closures, and route choice scenarios. However, the simulation module does not support dynamic traffic assignment.

Cova and Church (1997) and Church and Cova (2000) have developed the Critical Cluster

Model (CCM) to identify neighborhoods that might be of particular concern during an evacuation due to a fast moving hazard, such as a wildfire. The model has been embedded in a GIS-based platform and a case study has been conducted in Santa Barbara, California.

Alam and Goulias (1999) have employed a database management system and GIS software to develop an evacuation management system with special emphasis on traveler behavior and land use patterns. Li and Wang (2004) have developed a prototype of a GIS-based evacuation simulation system that integrates information on evacuee behavioral patterns, the transportation network and regional land-use for evacuation planning. Wilmot and Meduri (2005) also used GIS to establish evacuation zones.

Franzese and Han (2001) have developed a traffic modeling framework for hurricane evacuation called the Incident Management Decision Aid System (IMDAS). In their framework, hurricane evacuation analysis is conducted in two phases. In the first phase, the time-dependent O-D demand is estimated by 1) delineating the area to be evacuated; 2) determining the population at risk; and 3) computing the number of people that will actually evacuate using behavioral analysis and evacuation departure curves. In the second phase, the traffic simulation model embedded in OREMS loads this O-D table to evaluate the effectiveness of evacuation.

Another recent macro-level evacuation modeling and analysis system that is developed specifically for hurricane evacuation is the Evacuation Traffic Information System (ETIS) by PBS&J (2001). This system has been developed in the aftermath of Hurricane Floyd, driven by the need for a capability to forecast and anticipate large cross-state traffic volumes. At the heart of the model is a web-based travel demand forecasting system that estimates evacuation traffic congestion and cross-state travel flows for North Carolina, South Carolina, Georgia, and Florida. Based on the category of hurricane, expected participation rate, tourist occupancy, and destination choices for affected counties, ETIS outputs the level of

congestion on major highways and the expected cross-state volumes by direction. The model has been recently extended to include the Gulf States of Alabama, Mississippi, Louisiana, and Texas.

All models discussed thus far are for planning purposes – used to estimate conditions and analyze alternative strategies prior to the occurrence of an extreme event. In contrast, operational models are used to assist in decision making during an event. An example of an operational model is HURREVAC (HURRicane EVACuation) (Townsend 2003), which draws information from a wide variety of sources, including the National Hurricane Center to estimate the evacuation time.

Another model designed to work in real-time is the Smart Traffic Evacuation Management System (STEMS) [Hamza-Lup et al. (2005)]. STEMS is designed to employ ITS technologies to detect incidents through sensors and accordingly generate evacuation and traffic control plans. The model works by first delineating the evacuation zone boundaries, and specifying nodes outside the evacuation zone boundary as evacuation exit points. There are two approaches to evacuate traffic, namely the all-links and fastest-links. In the all links approach, traffic is spread across all links in the evacuation zone with an evacuation direction enforced on all links. The fastest-links approach employs a multicast routing approach to construct the evacuation routes from the incident to all the exit nodes. While the model looks fancy and promising, it suffers from a serious shortcoming. Links are assumed to have a constant speed throughout the evacuation process, which defies the fact that travel times are density-dependent let alone during evacuations where demand overloads supply.

2.2 ROUTE CHOICE AND EVACUATION

Efficient routing of vehicles to safety is a crucial aspect of any evacuation plan. The choice of evacuation routes is the reason why an evacuation plan is successful or not. Early models used static shortest-path type of algorithms to route evacuees to safety. For example, Hobeika

and Jamei (1985) use Dial's algorithm to stochastically route evacuees to shortest paths. Fahy (1991) uses the shortest path to evacuate residents in a high-rise building. Stern and Sinuany-Stern (1989) investigate the effect of route choice, whether shortest path or myopic behavior, on network clearance times in a radiological setting.

A variation of the shortest path problem is the quickest path problem [Chen and Chin (1990), Chen and Hung (1993), Kagaris et al. (1999)], whose objective is to send flow from source to sink along a single path as quickly as possible. Flows are sent repeatedly, also referred to as chain flows, along the quickest path, which is determined based on travel time and flow capacity as opposed to travel time only in the classical shortest path problem. Evidently, such a model is of special interest in the evacuation of spectators in concerts or sport events where a single path exists towards the parking lot or metro stop.

Another static network flow model of interest in evacuation is the minimum cost flow model, which aims at sending flow from a super source to a super sink in the least possible cost, resembling the SO approach in traffic assignment. For example, Yamada (1996) used the minimum-cost network flow problem to assign pedestrian evacuees to shelters at the city scale. Yamada defined the shortest evacuation plan as one where the total distance from all evacuees to all shelters is minimized. This approach can also be used in a road network context, where each vehicle is routed to its nearest evacuation zone exit under a shortest network-distance assumption.

However, despite the robustness and efficiency of their solution algorithms, static network flow models are not suitable to tackle real evacuation problems as they cannot capture the time dimension. In contrast, flows must be dynamic (time-dependent) to express the movements of particles as they reach safety (super sink). Therefore, evacuation problems are best modeled using dynamic network flow models, which can be regarded as a time-expanded static network flow model.

Dynamic network flow modeling has been extensively applied for building evacuation problems. Chamlet et al. (1982), Choi et al. (1984) and Kisko and Francis (1985) have all modeled building evacuation problems as dynamic networks with side constraints where the objective is to minimize the turnstile cost. Choi et al. (1984, 1988) in their model account for the fact that link capacities are not constant but rather are flow-dependent. An excellent survey of dynamic mathematical models for evacuation is given in Hamacher and Tjandra (2002).

Dunn (1992) proposes two algorithms for finding optimal evacuation routes, where the objective is to maximize the flow through a capacity-constrained network, i.e. the problem is modeled as a maximum-flow problem. Hobeika and Kim (1998) compares different static traffic assignment procedures in evacuation modeling using a traffic simulator and concludes that UE assignment produces better results than a shortest path algorithm in terms of minimizing evacuation time.

Novel assignment ideas for traffic assignments in the context of evacuations have also been proposed. For example, Campos et al. (1999) proposes a method to allocate traffic to k-optimal independent paths (no overlap) to reduce crashes and facilitate continuous traffic flow during evacuations. Cova and Johnson (2003) proposes a lane-based evacuation routing approach to reduce traffic delays at intersections by limiting conflicts. It is worth noting that while such an approach will reduce interactions at the intersections, the total distance traveled is likely to increase. The approach is illustrated on a representation of Salt Lake City, Utah.

The study by Sheffi et al. (1982a, 1982b) indirectly highlights the need to provide route information that captures the expected travelers' behavior and is consistent with experienced network conditions. Otherwise, travelers could ignore the supplied information if this information is not accurate or reliable. As such, a desirable evacuation route advisory strategy must be: (1) normative in nature in order to improve overall system performance,

and (2) consistent with the predicted network conditions and travelers' behavior. To achieve these two objectives, one must be able to model the evolution of traffic in a transportation network, a capability only available in DTA models.

Barrett et al. (2000) proposes a framework in which a dynamic traffic management model for hurricane evacuation can be used for long-term and short-term planning purposes as well as for real-time operational purposes. However, neither model nor numerical results are provided.

While UE assignment has been used extensively to model the expected behavior of travelers in normal situations, there is mounting evidence that in case of emergency and other extreme events; travelers may not have perfect information regarding the state of the network (a basic assumption for UE concept) and hence may be willing to follow an SO-based routing advice [Tuydes (2005)] so long as evacuees have had a positive experience in the past [Dash and Morrow (2001)].

One of the first studies to use an SO objective in the evacuation context is that of Sattayhatewa and Ran (2000), who use an analytical DTA model to either 1) minimize the total evacuation travel time of the disaster zone (without pre-defining a target evacuation time), or 2) minimize travel time for each origin destination pair. However, the model has been only tested on a three-link network.

Recently, the trend has been to incorporate traffic simulation with optimization techniques. For example, Liu et al. (2005a, 2005b) present an integrated optimization-simulation evacuation model for real-time operations. The model employs a bi-level optimization module to solve a generalized CTM-based network flow problem. The upper level program essentially solves the maximum dynamic flow problem (maximum flow for a given $\overline{W}$) and the lower level program minimizes total system travel time (SO). The extension to real-time applications requires a feedback process for gathering actual field conditions and adjusting

control strategies appropriately.

Yuan et al. (2006) use DYNASMART-P to solve an SO-based simultaneous optimization of destination and route assignment for the evacuation problem. They utilize the super zone feature in DYNASMART-P to connect the destinations to a super sink and effectively convert the problem to a single-destination evacuation problem. Their experiments show huge savings over the base case. Other similar studies that use an SO objective include Tuydes (2005b) and Liu et al. (2006), and Chiu et al. (2007).

An interesting study is the one conducted by Sbayti and Mahmassani (2006), which accounts for background traffic during partial network evacuations. In their study, the general assumption that networks are empty at time zero is not used. Instead, extreme events that warrant evacuation are modeled to occur midway through the day. Vehicles impacted by the event are identified and re-routed to safety in such a way to minimize their overall clearance time. Remaining (non-impacted) vehicles are assumed to retain their paths.

2.3 EVACUATION DEMAND

Human behavior is the most critical variable in evacuation planning and modeling. Many an evacuation plans have gone awry due to improper accounting for evacuees' behavior during an evacuation [Petruccelli (2003)]. Human behavior affects two aspects in evacuation models. First, it determines the population (evacuation demand) that will effectively comply with the evacuation order, and then it determines how evacuees choose and update their paths. While the latter is typically handled by the assignment principle, the former is much harder to account for.

Generally, the temporal evacuation demand is estimated using participation rates and mobilization curves established from observing past evacuations [Lewis (1985), Stern and Sinuany-Stern (1989), PBS&J (2000a, 2000b, 2001)]. The process is done in two phases

where in the first phase, participation rates are used to estimate the total demand; and in the second phase, the total demand is distributed to time intervals using a mobilization curve, such as the S-shaped logit-based function proposed by Sheffi (1985).

Irwin and Hurlbert (1995) develop a model using data from Hurricane Andrew that depends on variables such as the respondent's perception of getting hurt if staying, the perceived ability of the house to withstand the storm, prior hurricane experience, gender, marital status, education, age, and race of the owner.

Another study [RDS (1999)], using data from Hurricane Bonnie, finds that the most influential variables are whether an evacuation order had been issued or not, the risk of flooding, whether the neighbors evacuated or not, and type of structure of the home. Dow and Cutter (2002) have used a survey of coastal South Carolina, to investigate the impact of household decisions such as the number of vehicles used per household, departure time, distance traveled, and the role of information in the selection of specific evacuation routes on evacuation demand during Hurricane Floyd.

A model package that estimates total evacuation demand is ETIS [PBS&J (2001), Lewis (2001)]. ETIS uses default evacuation participation rates to provide graphical output in the form of maps, diagrams, and tables. The model is proprietary and is developed specifically for the Southeastern United States (Florida, Georgia, South Carolina, and North Carolina). The model is currently being expanded to include other neighboring states.

The common practice in determining evacuation demand is to include some subjective perceptions as independent variables because of their statistical significance. However, it must be recognized that while these variables may contribute to explaining evacuation behavior, they are not good variables for forecasting because they cannot be measured and as such cannot be used in hypothetical tests. An alternative albeit less commonly used form of trip generation is logistic regression [Irwin and Hurlbert (1995), RDS (1999)]. Logistic

regression is used in place of regular linear regression in evacuation because the dependent variable (to evacuate or not) is a binary variable which introduces violations of some of the assumptions underlying regular linear regression analysis. A study using data from Hurricane Andrew revealed that logistic regression model provides better estimates of evacuation than the linear-regression model developed for that region [Wilmot and Mei (2003)]. Fu and Wilmot (2004) propose a sequential logit choice model to estimate the probability of a household evacuating in a given time period.

Another issue in modeling human behavior is the impact of experience on future evacuation decisions, i.e. whether or not to evacuate. For example, people who have been stuck in long delays in response to previous evacuation orders are less likely to heed future evacuation orders than those who learned second-hand of the delays [Dash and Morrow (2001)]. Similarly, evacuees may not follow evacuation route advisory if they have experienced first-hand their ineffectiveness in previous evacuations. Therefore, planners must exercise extra caution when issuing evacuation orders or route advisory for that matter. A study that recognizes the fact that evacuees may not comply with evacuation route advisory is the one conducted by Chiu et al. (2005), who have tested the impact of human behavior, modeled as boundedly rational [Simon (1953), Mahmassani and Chang (1987)], on the compliance of motorists to off-line evacuation advisory plans.

2.4 EVACUATION MANAGEMENT STRATEGIES

Several management strategies have been proposed or investigated in the past. For example, Zaragoza and Burris (1998) advocate the importance of advanced technologies, specifically traffic surveillance cameras for emergency management. Baxter (2001) evaluates the potential real-time use of ITS technologies to improve safety and efficiency during hurricane evacuation in Florida. Similarly, Morrow (2002) investigates the implementation of ITS technologies to reduce the evacuation time when major storms threaten Florida. Urbina and

Wolshon (2003) also discuss the benefits of using ITS during hurricane evacuation.

Another study to investigate the effect of various traffic management measures on evacuation times is the one conducted by Church and Sexton (2002), who use agent-based simulation techniques to examine the sensitivity of evacuation time under a set of measures such as having an additional exit, vehicle occupancy levels per household and traffic controls. While there is a plethora of studies in this regard, the focus in this section is on two specific strategies, one pertaining for demand management, and the other for supply management.

2.4.1 Demand Staging and Flow Scheduling

As mentioned in Chapter 1, one option to manage traffic during evacuations is to spread the evacuation demand over a longer period to alleviate the loads on the network and delay network degradation. Such a process is referred to in the literature as staging or flow scheduling. By convincing some of the evacuees that it is "faster to wait", it is possible to move closer to an SO state and therefore reduce the minimum network clearance time as well as average trips times.

There are two general forms of staging evacuation operations: zone scheduling and flow scheduling. In zone scheduling, zones are sequentially evacuated starting with the most urgent. You can have strict staging where subsequent zones will not be allowed to evacuate until the current zone is fully evacuated or staggered staging where each zone has its own evacuation start time. Flow scheduling, On the other hand, is vehicle-based, that is each vehicle will have its own evacuation start time.

The study by Chen and Zhan (2004) is one of the first documented studies on the staging of evacuation operations. They use microscopic simulation to compare the effect of staging versus simultaneous evacuation. The study concludes that staging is not effective when congestion is near free-flow conditions. The staging strategies considered in this study,

however, have been identified a priori and are not generated to satisfy specific system level objectives.

Both Tuydes (2005b) and Liu et al. (2006) use the Linear Programming (LP) formulation by Ziliaskopoulos (2000) for the Cell Transmission Model (CTM) [Daganzo (1994, 1995)] to find the optimal staged evacuation strategy. Their motive behind staging is the assumption that there exist different regions in the network with different safety time windows (time during which it is safe to be exposed). The model uses a SO approach and assumes exogenous evacuation demand response and mobilization rates and safety time-windows. The main decision variables in this model are the zonal evacuation order times; however, both models have been tested on a small network. Tuydes (2005b) develops a tabu-based heuristic to solve the staging problem for large networks.

Sbayti and Mahmassani (2006) use an MSA-based heuristic to solve for the joint optimal evacuation destination-route-flow-staging problem that minimizes the network clearance time. The procedure is applied for a subset of vehicles, referred to as impacted vehicles, while remaining (background) traffic is assumed to follow their original prescribed paths. The traffic simulator within DYNASMART-P is used to estimate the link travel times and turning penalties.

Chiu et al (2007) have also used the linear programming formulation of the CTM to solve the joint optimal evacuation destination-route-flow-staging problem. The problem is formulated as a SO DTA problem for which interior point method techniques are used to solve. The flow staging results are obtained by computing the difference in cell (link) occupancies for two successive time periods.

2.4.2 Capacity Redistribution or Contraflow

Another option to manage evacuation is to tackle the supply side of the problem, which

experience suggests that routes have insufficient in capacity to handle the unusual surge in demand [Alsnih and Stofer (2004)]. While there is no time to build new roads during evacuations, one can always reverse the direction on some selected lanes in the networks in a process known as contraflow. This can lead to a temporary increase in the outbound operational capacity without major infrastructure changes.

Contraflow involves reversing one or more lanes on a divided roadway in the inbound direction in order to create more capacity for outbound traffic. Crossover sections are normally used to channel traffic to these lanes with incoming traffic usually blocked until the end of the contraflow program. Contraflow plans have been used for decades in everyday scenarios such as sporting events, work zones, bridge construction projects, tunnels, and along major arterials. For example, the center turn lanes of roads around a stadium may be used to accommodate sporting event traffic. During freeway work zones, when traffic is rather heavy, one or more lanes may be reversed in the inbound via crossover.

The same thing can also be done for a work zone on an arterial, where a lane needs to be completely blocked. If the traffic is heavy, a lane may be borrowed (and reversed) from the other direction until work is finished. In this case, no cross over is needed as arterials are usually not grade-separated. Lane reversal is also used during bridge construction projects or any situation where a lane must be closed during times when construction crews are not at work as in the case of the Woodrow Wilson Bridge project in Washington, DC. While construction is in progress on a parallel twin span, the recently completed first span accommodates both directions (three lanes each way).

That being said, lane reversals are still a new and relatively untested system for evacuations. Unlike in every day lane reversals, drivers are typically unaware of reversible lanes as well as their reversal times in an emergency setting. This can become a source of confusion and a huge safety concern due to the lack of proper signage and control. In fact, Wolshon (2001)

argues that the costs and benefits of lane reversals for evacuations remain largely unknown. Therefore, the general approach has been to avoid contraflow strategies unless it is really warranted.

There are several issues relating to contraflow operations. First, there is the issue of when to start and when to shutdown the contraflow procedure. For example, most states will not utilize contraflow in darkness. The need for proper lighting conditions cannot be more critical than in evacuations where proper signage and directions may be lacking. Therefore, contraflow must be ordered in a manner that will allow all evacuation traffic to clear the highway before darkness.

Another critical issue regarding contraflow is its starting and ending point. The ability to adequately load contraflow lanes (by crossovers for example) is very important to avoid bottlenecks. A study by Theodoulou and Wolshon (2004) on the adequacy of the lane reversal plan for traffic headed westbound out of New Orleans, Louisiana, on Interstate 10 indicates that the contraflow system is not being fully utilized due to limited loading points. Therefore, an inadequate loading capacity may lead to a "cry wolf" scenario, where residents will be reluctant to evacuate in the future [Wolshon (2005a, 2005b)].

An even more critical issue is the downstream capacity at the termination point of a contraflow plan. Any premature termination and traffic could back up for miles. Therefore, the contraflow operation must terminate at an interchange with another controlled-access facility where enough capacity is available. Finally, to ensure a successful contraflow plan, there should be ample coordination and communication among all concerned agencies as well as public outreach strategies to inform the public of existing evacuation plans and what to do or expect during evacuations. However, all these issues have not stopped researchers and planners from investigating the impact of contraflow during emergency evacuations.

For example, Zhou et al. (1993) applies sensitivity analysis to find the optimal 1-shift (a shift

is a single reversal operation) contraflow schedule that would minimize the total expected delay for a tunnel facility. Their algorithm, however, is not efficient and needs to perform an exhaustive enumeration of candidate solutions to select the best option.

Dong and Xue (1997) and Xue and Dong (2000) use multi-level constrained optimization techniques to minimize total traffic delay in order to find the optimal contraflow control for an n-shift schedule. They have implemented their control system on the George Massey Tunnel to find the optimal contra-flow schedule in response to sensed and predicted (real-time) traffic conditions.

Franzese and Han (2001) proposes a computer-based system to simulate traffic flow and evaluate the impacts of different traffic management alternatives on emergency evacuation. They conclude that traffic management such as contraflow operations could have a significant impact in the effectiveness of evacuation plans.

Tuydes and Ziliaskopoulos (2004) propose a linear program system-optimal DTA model with capacity-reversibility (contraflow) capability based on the CTM. In their model, however, the capacity is treated as a continuous variable rather than discrete. Another shortcoming is the high computation costs associated with this model.

Theodoulou and Wolshon (2004) have used the microscopic simulation model CORSIM to conclude that existing contraflow plans for New Orleans are likely to result in underutilization of the reversed lanes. The study also identifies simple inexpensive modifications to improve existing plans.

2.5 DYNAMIC TRAFFIC ASSIGNMENT PROBLEM

Network flow models generally treat link travel times as either constant or time-dependent. While assuming constant link travel times may be justifiable in building evacuations, this is generally not the case in congested transportation networks, where the speed will diminish

with higher densities, until queues start to form. An evacuation model where link travel times are flow-dependent is more realistic but also much more difficult to handle from a mathematical point of view due to the nonlinearity of link travel times [Janson (1991b), Ran and Boyce (1996)]. A class of mathematical problems that can handle density-dependent travel times is DTA [Jayakrishnan and Tsai (1995), Carey and Subrahmanian (2000)].

DTA has been conceived in response to the recent developments in Advanced Transportation Management System (ATMS) and Advanced Traveler Information System (ATIS). DTA models overcome the limitations inherent in SA models such as the failure to capture the dynamics of traffic operations, trip chaining and the effect of intersection delay on the calculation of shortest paths. The DTA problem is to solve for a dynamic traffic flow pattern as a result of supply and demand interactions. DTA models have a plethora of applications ranging from real-time management to offline planning and evaluations, and it is by far the tool most suited for evacuation modeling. DTA models are characterized by the traffic assignment principle used and the embedded traffic flow model.

2.5.1 Traffic Assignment Principles

There are two basic traffic assignment principles corresponding to Wardop's first and second principles [Wardrop (1952)], namely the UE and the SO principles. Other variants of the UE principle such as stochastic UE and tolerance-based UE [Szeto and Lo (2005)] have been proposed in the past; however their use is not as common. Sheffi (1985) has summarized the UE conditions for static networks as such:

> *"for each O-D pair, the travel cost on all used paths is equal and less than or equal to the travel cost that would be experienced by a single vehicle on any unused path "*

Ran and Boyce (1996) have extended this condition to the dynamic case by providing a time-

dependent generalization of Wardrop's first principle:

> *"for each O-D pair at each interval of time, if the actual travel times experienced by travelers departing at the same time are equal and minimal, then the dynamic flow over the network is in a travel time-based ideal dynamic user-optimal state"*

The UE conditions can be mathematically stated as follows:

$$\boldsymbol{C} - \boldsymbol{\pi} \geq 0 \tag{2.1a}$$

$$\boldsymbol{f}\left(\boldsymbol{C} - \boldsymbol{\pi}\right) = 0 \tag{2.1b}$$

$$\boldsymbol{f} \geq 0 \tag{2.1c}$$

Where $\boldsymbol{f}$ is the vector of path assignments, $\boldsymbol{C}$ is the vector of path trip times, and $\boldsymbol{\pi}$ is the vector of minimum path travel times. Conditions (2.1) state that if the vector of path flow assignments $\boldsymbol{f}$ is positive, then the corresponding path travel times vector $\boldsymbol{C}$ should be equal to the minimum path travel times vector $\boldsymbol{\pi}$. Inherent in these conditions is the assumption that each trip-maker is rational and chooses the path that minimizes his travel cost. Equivalently, the UE-DTA problem is to find a feasible time-varying path flow pattern $\boldsymbol{f}$ satisfying conditions (2.1).

An alternative route choice behavior, though less commonly adopted, is the SO assignment, which is based on Wardrop's second principle and states that travelers will behave cooperatively when choosing their departure times and routes in order to minimize the total cost of the system. The SO conditions can be mathematically stated as follows:

$$\tilde{\boldsymbol{C}} - \tilde{\boldsymbol{\pi}} \geq 0 \tag{2.2a}$$

$$\boldsymbol{f}(\tilde{\boldsymbol{C}} - \tilde{\boldsymbol{\pi}}) = 0 \tag{2.2b}$$

$$\boldsymbol{f} \geq 0 \tag{2.2c}$$

Where $\tilde{\boldsymbol{C}}$ is the vector of path marginal trip times, and $\tilde{\boldsymbol{\pi}}$ is the vector of minimum path marginal travel times. Conditions (2.2) state that if the vector of path flow assignments $\boldsymbol{f}$ is positive, then the corresponding path marginal travel times vector $\tilde{\boldsymbol{C}}$ should be equal to the minimum path travel times vector $\tilde{\boldsymbol{\pi}}$. the SO-DTA problem is to find a feasible time-varying path flow pattern $\boldsymbol{f}$ satisfying conditions (2.2).

Inherent in this formulation is the assumption that the complete time-varying O-D demand information for the entire planning horizon is available, a priori, to the (single) central controller, whose objective is minimize total system travel time. The key behavioral assumption for the path choice decisions of network users is that all vehicles comply fully with the path assignment instructions given by the central controller, and no en-route path-switching is made after departure from the origins. Four traffic flow propagation models have been commonly used in DTA: 1) link performance functions, 2) link exit functions, 3) CTM, and 4) simulation.

2.5.1.1 ***Link Performance Functions***

Link performance functions relate link travel times to link volumes and have been used in the past [Janson (1991b), Ran et al. (1996), Chen and Hsueh (1998)]. The most common of link performance functions is the BPR volume-delay functions (1964) commonly used in static traffic assignment. The general form of the BPR function is:

$$c_a(t) = c_a^{\min}\left(1+\frac{x_a(t)}{N_a(t)}\right)^{\alpha_a} \tag{2.3}$$

Where $c_a(t)$ is the link travel time on link a at time step t, $c_a^{\min}$ is the minimum travel time on link a corresponding to free-flow conditions, $x_a(t)$ is the volume on link a at time step t, $N_a(t)$ is the physical capacity of link a at time step t, and α_a is the shape parameter associated with link a.

BPR functions are designed to model a steady degradation of highway speeds as the volume of traffic approaches capacity. However there is evidence to indicate that at low congestion, speeds tend to remain much more consistent as volume increases. As a matter of fact, the use of BPR functions results in unrealistic assignments – volume-to-capacity values greater than one are sometimes necessary in calculations to converge to an equilibrium trip assignment.

Another popular link performance model is Greenshields, which has been conceived after extensive analysis of traffic data, relates link speed (and hence link travel time) with link density, up to an appropriately specified jam density. The Greenshields model is mathematically expressed as follows:

$$\vartheta_a(t) = \vartheta_a^{\max}\left(1 - \frac{\kappa_a(t)}{\kappa_a^{\text{jam}}}\right)^{\alpha_a} \tag{2.4}$$

where $\vartheta_a(t)$ is the average speed on link a at time step t, and $\vartheta_a^{\max}$ is the maximum speed on link a. $\kappa_a(t)$ is the average density on link a at time step t, and κ_a^{jam} is the jam density on link a.

While this model has been found to be in accord with real traffic conditions for moderate congestion levels, it is not adequate for both low and high congestion levels. To improve on its performance in congested levels, Jayakrishnan and Tsai (1995) added a minimum speed term $\vartheta_a^{\min}$ to the original Greenshields model to ensure that the outflow volume does not reach zero. They dubbed their model as the Modified Greenshields Model (Figure 2.1), which has the following form:

$$\vartheta_a(t) = \vartheta_a^{\min} + \left(\vartheta_a^{\max} - \vartheta_a^{\min}\right)\left(1 - \frac{\kappa_a(t)}{\kappa_a^{\text{jam}}}\right)^{\alpha_a} \tag{2.5}$$

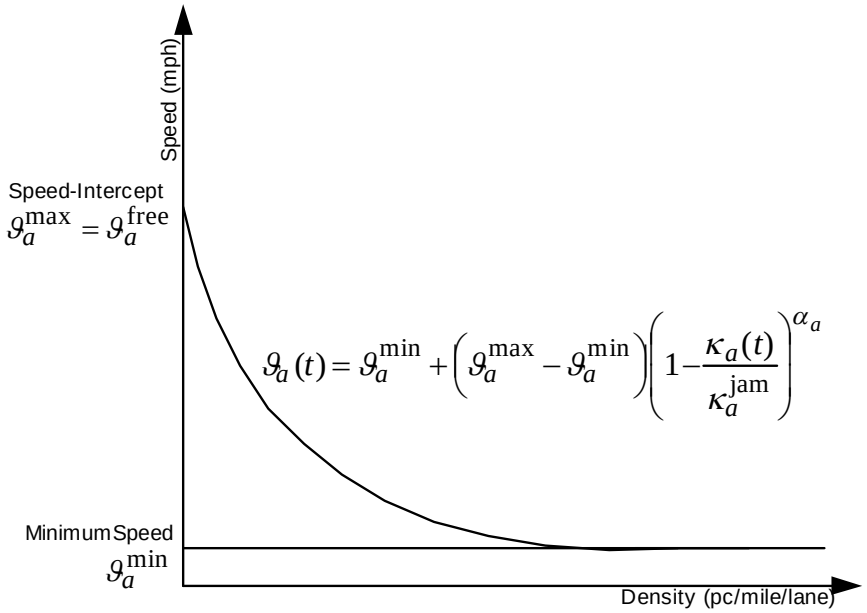

Figure 2.1 Single regime modified Greenshields model

Note that, the maximum speed is a mathematical construct which may or may not correspond to the free-flow speed, as it will become obvious later. While the modified Greenshields model has been found to be adequate for congested conditions, it did not adequately describe free-flow conditions on freeways, where traffic speeds did not decrease with increasing densities. It was observed that free-flow speeds are attained in general up to a certain cut-off density κ_a^{cutoff}, after which speeds started to decrease in accordance to (2.5). This led to the introduction of another traffic regime and resulted in a dual-regime modified Greenshields model (Figure 2.2):

$$\vartheta_a(t) = \begin{cases} \vartheta_a^{\text{free}}, & \kappa_a \le \kappa_a^{\text{cutoff}} \\ \vartheta_a^{\min} + \left(\vartheta_a^{\max} - \vartheta_a^{\min}\right)\left(1 - \dfrac{\kappa_a(t)}{\kappa_a^{\text{jam}}}\right)^{\alpha_a}, & \kappa_a > \kappa_a^{\text{cutoff}} \end{cases} \tag{2.6}$$

where $\vartheta_a^{\text{free}}$ is the free-flow speed on link a.

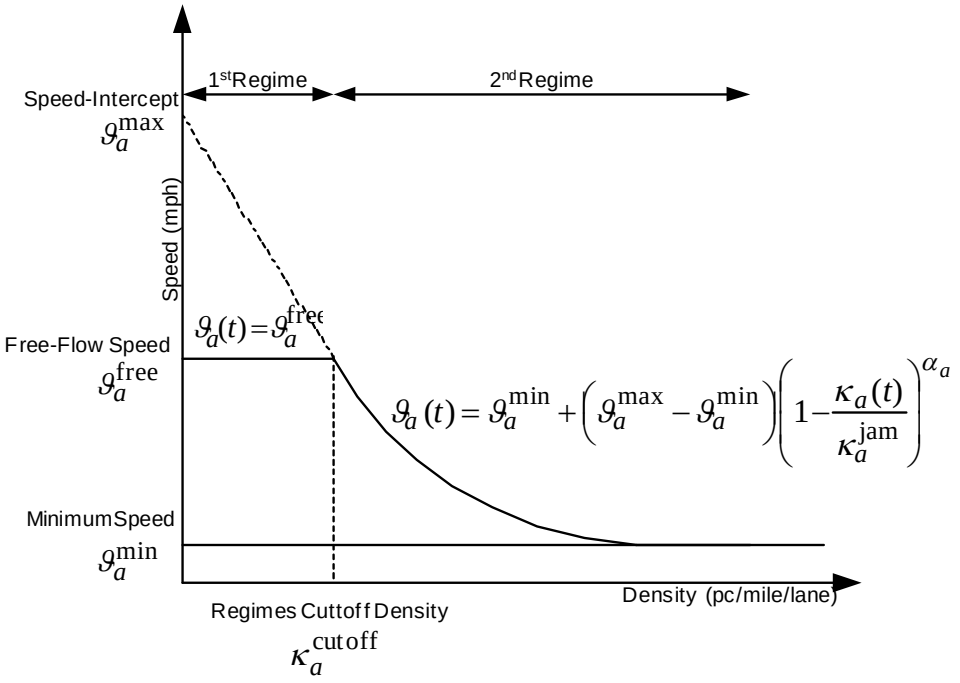

Figure 2.2 Dual regime modified Greenshields model

Dual-regime models are generally applicable to freeways since they typically have more capacity (higher service flow rates) than arterials, and can accommodate dense traffic (up to 2300 pc/hour/lane) at near free-flow speeds. On the other hand, single regime models apply to arterials due to the presence of signalized intersections where a slight increase in traffic would elicit more deterioration in prevailing speeds than in the case of freeways.

2.5.1.2 ***Link Exit Functions***

Merchant and Nemhauser (1978a, 1978b) are the first to introduce the concept of an exit function to regulate the outflow of a link given the number of vehicles on it. Since then, it has been used extensively in analytical DTA models [Carey (1987), Friesz et al. (1989), Wie et al. (1995)]. Carey (1987) actually used the exit function as an upper bound for the link outflow instead of specifying the exact value of the outflow and thus allowed flow control on the links. The major drawback of an exit function is that it implicitly assumes that changes in density propagates instantaneously across the link and therefore fails to capture queue

formation phenomenon [Boyce et al. (2001), Carey and McCartney (2002)].

2.5.1.3 ***Cell Transmission Model***

The cell transmission model has been developed by Daganzo (1994) as a discrete approximation to the hydrodynamic theory of traffic flow. It is capable of automatically tracking shocks and acceleration waves and thus capturing the formation, propagation, and dissipation of queues. CTM has been sufficiently validated by field data in Lin and Daganzo (1994) and Lin and Ahanotu (1995). Daganzo's model divides the transportation network into small homogeneous and interconnected cells and assumes piecewise linear relationships between flow and density at the cell level. Despite its simplicity, the cell-transmission model (CTM) is able to describe and accurately capture traffic propagation phenomena such as disturbances and shockwaves in traffic networks. CTM is relatively easy to be transformed into a mesoscopic model, where vehicles can be individually tracked between origins and destinations for possible dynamic traffic assignment applications. More recently, Ziliaskopoulos (2000) linearized the CTM model when developing a linear programming formulation of the SO-DTA problem.

2.5.1.4 ***Simulation-based Models***

The use of simulation techniques is the method of choice for propagating traffic within the context of dynamic traffic assignment models. This approach has the merit of closely approximating the travel behavior of individual drivers and easily incorporating all kinds of control measures. Simulation precludes the holding of traffic, enforces FIFO conditions, and circumvents the need for link performance/exit functions, but they are mathematically intractable.

Simulation techniques are ideally suited for microscopic models but they are tricky to validate because human behavior is difficult to observe and model. Moreover, microscopic

traffic simulation models such as AIMSUN, PARAMICS or VISSIM, require a huge number of input parameters to accurately model vehicle behavior in the network. On the other hand, macroscopic simulation-based DTA models follow the hydrodynamic theory of traffic flow [Lighthill and Whitham (1955), Richards (1956)] and therefore require much less processing power and only a handful of simple parameters in order to work reasonably well. A third approach that is gaining popularity is the mesoscopic approach, where a macroscopic traffic flow model is used but vehicles are tracked individually in the network to maintain a higher level of detail.

One of the earliest mesoscopic simulation platforms is CONTRAM [Leonard et al. (1989)], which is used in predicting traffic routes, link flows, queues, and delays at junctions. Another pioneer model is INTEGRATION [Van Aerde and Yagar (1988)], which models the behavior of individual vehicles and is capable of assignment. Ghali and Smith (1992) have proposed a simulation-based solution procedure to the SO-DTA problem where congestion is assumed to arise at bottlenecks modeled as deterministic queues. The SO assignment is accomplished by assigning individual vehicles onto paths using link marginal costs determined using CONTRAM.

DYNASMART (Dynamic Network Assignment-Simulation Model for Advanced Road Telematics) is perhaps the most well-known simulation-based DTA system. It is built around the mesoscopic traffic simulation model proposed by Jayakrishnan et al. (1994) and the generalized least-cost shortest path algorithm developed by Ziliaskopoulos and Mahmassani (1993, 1996). The assignment procedure is based on the iterative algorithm developed by Mahmassani and Peeta (1992), Mahmassani et al. (1993), Peeta (1994), and Peeta and Mahmassani (1995a, 1995b). There are two versions of DYNASMART: P and X. DYNASMART-P is designed for off-line planning applications, whereas DYNASMART-X is designed for estimating and predicting current and future states of the network in real-time. The computational issues for the real-time version have been addressed by using a rolling

horizon framework [Peeta and Mahmassani (1995b)], and distributed computing [Mahmassani (1997), Hawas and Mahmassani (1997)]. DYNASMART is perfectly suitable for ITS/ATIS applications and supports five classes of users: UE, SO, pre-trip, Variable Message Signs (VMS) responsive, and boundedly-rational users [Mahmassani and Chang (1987)]. A comprehensive review of the simulation-based approach is presented by Mahmassani (2001).

Another well-known simulation-based DTA system is DYNAMIT (Dynamic Network Assignment for the Management of Information Travelers) by Ben-Akiva et al. (1997, 1998), and Bottom (2000). DYNAMIT estimates and predicts in real-time current and future traffic conditions and is organized around two main modules: state estimation and prediction-based guidance generation. DYNAMIT consists of a demand and a supply simulator that interact to generate optimal route guidance under a rolling horizon framework. The demand simulator utilizes historical and real-time data, to estimate and predict O-D flows. The supply simulator uses a mesoscopic traffic model in which links are divided into segments that include a moving part and a queuing part. Basic explanations of the framework and logics are presented in Ben-Akiva et al. (2000). Another simulation-based DTA model that is gaining popularity is VISTA [Ziliaskopoulos and Waller (2000)], which operates within an internet-based GIS environment. VISTA integrates data and models into one framework and uses RouteSim [Ziliaskopoulos and Lee (1996)], a mesoscopic traffic model based on CTM to propagate vehicles in the network.

3 EFFICIENT SOLUTION HEURISTIC FOR THE SYSTEM-OPTIMAL DYNAMIC TRAFFIC ASSIGNMENT PROBLEM

Chapter 1 has briefly alluded to the fact that the evacuation problems to be addressed in this dissertation are variations of the classical SO-DTA problem, which has been studied extensively in the literature [Merchant and Nemhauser (1978a, 1978b), Carey (1986, 1987), Ho (1980), Peeta (2004)]. The enormity of the computational cost of analytical models and the failure to capture traffic dynamics through side constraints have led to the development of simulation-based DTA models, which while able to handle larger networks and realistically capture traffic dynamics, the quality of their solution has long been questioned due to the use of averaging heuristics such as the MSA.

MSA remains by far the most widely used solution heuristic in the context of simulation-based DTA. Its simplicity and non-requirement of derivative information for the flow-cost mapping function are the main reasons for its widespread use. However, its convergence properties in real-life networks has been inconclusive, especially because (1) simulation-based models are typically not well-behaved mathematically, and therefore their solution properties are not guaranteed, and (2) pre-determined step sizes do not exploit local information in searching for a solution, and therefore lack a proper decent direction [Bertsekas 1995].

This chapter focuses on the development of an efficient simulation-based solution heuristic for the SO-DTA model that exceeds MSA-based heuristics performance wise while not requiring excessive memory requirements. In this regard, the work of Lu (2007) on developing a theoretically sound simulation-based UE-DTA model and its solution heuristic is extended to the SO-DTA case along with the necessary modifications. Shortcomings of the solution heuristic by Lu (2007) are identified and addressed as well. The resulting SO-DTA solution heuristic is then tested and compared against MSA towards the end of the chapter.

3.1 INTRODUCTION

Several SO-DTA formulations have been proposed in the past including mathematical programming, control theory, nonlinear complimentarity problems, and VI problems. However, a major issue in these models is the modeling of traffic dynamics using link performance functions or link exit functions, which are not realistic and do not uphold FIFO conditions. Recently, researchers have formulated DTA problems as linear programs (LPs) following Ziliaskopoulos (2000). However, the LP nature of such models coupled with the cellular nature of the CTM model limits the applicability of such a model to real-life networks [Tuydes 2005].

Instead, simulation-based heuristics have been used to solve SO-DTA models. The most widely adopted heuristic is the MSA, which, while not computationally intensive and easy to implement, suffers from a similar deficiency to that of the Frank-Wolfe algorithm, where the step sizes are pre-determined and fixed across-the-board regardless of the degree of inferiority of paths. This leads to the slow convergence rates in later iterations due to "zigzagging" around the optimal solution. Nonetheless, satisfactory computational experience has been reported with the MSA in some simulation-based models [Janson (1991a, 1991b), Mahmassani et al. (1993a), Ran and Boyce (1996), Mahmassani (1998), Tong and Wong (2000), Liu et al. (2005c)].

More recently, Sbayti et al. (2007) have proposed an efficient vehicle-based implementation of the MSA that relaxes the across-the-board step size rule while maintaining the total number of vehicles to update their paths in accordance with the MSA rule. In this heuristic, vehicles are sorted according to experienced travel time (or any other user-selected criterion) and the most expensive $1/k$ vehicles, where k is the iteration number, are shifted to the cheapest path (from shortest path) for that iteration. The method retains the nice features of the MSA while providing for a better search direction than the classical MSA implementation.

Currently, the general approach has been to formulate simulation-based models as a VI problem after the pioneering work of Smith (1993) who showed that solving the VI problem

$$\boldsymbol{C}(\boldsymbol{f}^*)\cdot(\boldsymbol{f}-\boldsymbol{f}^*)\geq 0 \tag{3.1}$$

is equivalent to solving the UE-DTA problem, where $\boldsymbol{C}(\boldsymbol{f})$ is the path travel time vector evaluated at flow pattern $\boldsymbol{f}$, and $\boldsymbol{f}^*$ is the optimal flow pattern. Similarly, without loss of generality, solving the VI problem:

$$\tilde{\boldsymbol{C}}(\boldsymbol{f}^*)\cdot(\boldsymbol{f}-\boldsymbol{f}^*)\geq 0 \tag{3.2}$$

is equivalent to solving the SO-DTA problem, where $\tilde{\boldsymbol{C}}(\boldsymbol{f})$ is the path marginal travel time vector evaluated at flow pattern $\boldsymbol{f}$.

VI easily handles the asymmetrical cost functions typical of DTA problems and provides an easier platform to verify existence and uniqueness of solutions. Studies that formulate DTA problems as VI include, but are not limited to, Smith and Winsten (1995), Ran and Boyce (1996), Chen and Hsueh (1998), Lo and Szeto (2002), Jang et al. (2005), Ziliaskopoulos and Chang (2005), and Lu (2007). A comprehensive review on VI formulations for DTA problems can be found in Nagurney (1998), Patriksson (1999), and Peeta and Ziliaskopoulos (2001). The VI problems are generally reformulated to an NMP that are iteratively solved using descent methods.

This chapter focuses on developing and solving a simulation-based SO-DTA model with time-varying O-D demands that is capable of realistically capturing traffic dynamics while satisfying SO-DTA conditions. The SO-DTA model presented in this chapter follows the same steps of the VI formulation and its reformulation as the NMP by Lu (2007) for the UE-DTA case with the required modifications.

3.2 NOTATIONS AND DEFINITION OF VARIABLES

Consider a transportation network represented by a directed graph with multiple origins (source nodes) and destinations (sink nodes). Let $r \in R \subset N$ and $s \in S \subset N$ denote an origin node and a destination node, respectively. Note that any node may be both an origin and a destination node at the same time, i.e. sets R and S are not mutually exclusive. Let $a \in A$ denote a directed arc in the network represented by the graph $G(N, A)$ with $|N|$ nodes and $|A|$ directed arcs.

In the context of DTA, we distinguish between two types of periods: the study period and the demand assignment period. The study period $[0, W]$ is discretized into T time steps of length Δ such that $W = T \cdot \Delta$. Associated with the study period is the time index $t = 1, ..., T$, which is primarily used to keep track of the trip time of vehicles in the network. Similarly, the demand assignment period, $[0, W_\tau]$ is discretized into T_τ departure periods of length $\Delta_\tau \geq \Delta$ such that $T_\tau = W_\tau \cdot \Delta_\tau$. Associated with the demand assignment period is the departure time index $\tau = 1, ..., T_\tau$. Assume that W is long enough for all the traffic to clear the network, i.e. $W > W_\tau$.

Let $f^\tau_{r,s,p}$ be the flow leaving origin r going to destination s assigned to path $p \in P^\tau_{r,s}$ during departure period τ, where $P^\tau_{r,s}$ is the set of all possible paths between r and s at departure time τ. Let $\boldsymbol{f}$:

$$\boldsymbol{f} = \left\{ f^\tau_{r,s,p} \mid \exists\, p \in P^\tau_{r,s} \forall r \in R, s \in S, \tau = 1, ..., T_\tau \right\}$$

be the vector of dynamic flow assignments $f^\tau_{r,s,p}$ in $G(N, A)$. Associated with $\boldsymbol{f}$ is a vector of path travel times $\boldsymbol{C}(\boldsymbol{f})$:

$$\boldsymbol{C}(\boldsymbol{f}) = \left\{ C^\tau_{r,s,p}(\boldsymbol{f}) \mid \exists\, p \in P^\tau_{r,s} \forall r \in R, s \in S, \tau = 1, ..., T_\tau \right\}$$

and a vector path marginal travel times (or simply marginals) $\tilde{\boldsymbol{C}}(\boldsymbol{f})$:

$$\tilde{\boldsymbol{C}}(\boldsymbol{f}) = \left\{ \tilde{C}^{\tau}_{r,s,p}(\boldsymbol{f}) \mid \exists\, p \in P^{\tau}_{r,s} \forall r \in R, s \in S, \tau = 1,...,T_{\tau} \right\}$$

Equivalently, one can also think in terms of link travel times and link marginal travel times. Let $c_a(t)$ and $\tilde{c}_a(t)$ denote the travel time and marginal travel time for link a at time step t, respectively. Define $\boldsymbol{c}$ as the vector of link travel times:

$$\boldsymbol{c} = \{c_a(t) \mid a \in A\}$$

and $\tilde{\boldsymbol{c}}$ as the vector of link marginal travel times:

$$\tilde{\boldsymbol{c}} = \{\tilde{c}_a(t) \mid a \in A\}$$

Furthermore, in the context of DTA, we differentiate among three link flow variables associated with link a: 1) capacity (maximum physical storage or occupancy) $y_a(t)$; 2) inflow volume $u_a(t)$; and 3) outflow volume $v_a(t)$. The associated link flow vectors are defined as follows:

$$\boldsymbol{y} = \{y_a(t) \mid a \in A\}$$

$$\boldsymbol{u} = \{u_a(t) \mid a \in A, t = 1,...,T\}$$

$$\boldsymbol{v} = \{v_a(t) \mid a \in A, t = 1,...,T\}$$

Therefore, the volume present on link a at time step t, $x_a(t)$ may be computed as:

$$x_a(t) = u_a(t) - v_a(t) \qquad \forall a, t$$

Define the vector of time-dependent link volume $\boldsymbol{x}$ as follows:

$$\boldsymbol{x} = \{x_a(t) \mid a \in A, t = 1,...,T\}$$

One can also define inflow and outflow volumes for a given node in the network. Define $I_n(t)$ as the total flow entering a node n in time step t and similarly define $O_n(t)$ as the total flow exiting a node n in time step t. Finally, O-D demand is also time-dependent. Let $\boldsymbol{d}$ be the O-D demand time dependent vector defined as:

$$\boldsymbol{d} = \left\{ d_{r,S}^{\tau} \mid r \in R, s \in S, \tau = 1,...,T_{\tau} \right\}$$

where $d_{r,S}^{\tau}$ is the traffic demand associated with $r-s$ at departure time τ. In the context of evacuations, one can also define the total demand d_r at an origin r to be evacuated.

3.3 TYPICAL PATH-BASED SO-DTA FORMULATION

3.3.1 Problem Statement and Formulation

Consider an urban traffic network represented by the directed graph $G(N, A)$ with multiple origins r and multiple destinations s. Furthermore, assume the time-dependent O-D trip desires $d_{r,S}^{\tau}$ are known a priori. The SO-DTA problem is therefore to determine the time-dependent path-flow pattern $\boldsymbol{f}$ so as to minimize the total system trip time subject to DTA constraints.

3.3.1.1 *Objective Function:*

The objective of the SO-DTA model is to minimize the total system trip time, that is:

$$\text{Min } Z(\boldsymbol{f}) = \sum_{\tau}\sum_{r}\sum_{s}\sum_{p} C_{r,s,p}^{\tau} \cdot f_{r,s,p}^{\tau} \tag{3.3}$$

The constraints of the model include flow conservation, flow propagation, non-negativity and boundary constraints as described below:

3.3.1.2 *Supply-Demand Conservation Constraints:*

The total path flows originating from origin r going to destination s at departure time τ must be equal to the demand at origin r going to destination s at departure time τ:

$$\sum_{p} f_{r,s,p}^{\tau} = d_{r,s}^{\tau} \qquad \forall r, s, \tau \tag{3.4}$$

3.3.1.3 ***Flow Conservation Constraints:***

Flow leaving an origin node r in time step t must be equal to the total flow entering the links incident from node $r \in R$:

$$\sum_a v_a(t) = O_r(t) \qquad \forall r,t,a \in \Gamma(r) \tag{3.5}$$

where $\Gamma(n)$ denote the set of links that are downstream of node n, respectively. Similarly, flow entering a destination node $s \in S$ in time step t must be equal to the total flow leaving the links incident to node $s \in S$:

$$\sum_a u_a(t) = I_s(t) \qquad \forall s,t,a \in \Gamma^{-1}(s) \tag{3.6}$$

where $\Gamma^{-1}(n)$ denote the set of links that are upstream of node n.

Moreover, since holding of traffic is not allowed at origin nodes, the total flow entering a node $n \notin R,S$ in time step t must also leave node n at time t:

$$\sum_a v_a(t) - \sum_b u_b(t) = O_n(t) - I_n(t) = 0 \qquad \forall t,\ a \in \Gamma(n), b \in \Gamma^{-1}(n), n \notin R \tag{3.7}$$

3.3.1.4 ***Flow Propagation Constraints:***

For a given link a, the existing volume (link occupancy) at time $t+1$ is equal to the existing volume at time t plus the net difference between the inflow and outflow volumes at time t, as follows:

$$x_a(t+1) = x_a(t) + u_a(t) - v_a(t) \qquad \forall a,t \tag{3.8}$$

3.3.1.5 ***Arc-path Dynamic Constraints:***

Let $\xi_{r,s,p}^{\tau,a}(t)$ be the time-dependent link-path index, equal to 1 if vehicles going from origin r to destination s during departure time τ are assigned to path τ are on link a during time

step t; and 0 otherwise. That is:

$$\xi_{r,s,p}^{\tau,a}(t) = \begin{cases} 1 & \text{if } f_{r,s,p}^{\tau} \text{ enters arc } a \text{ at time step } t \\ 0 & \text{otherwise} \end{cases} \tag{3.9}$$

Therefore, the link volumes and path travel times may be obtained as follows:

$$x_a(t) = \sum_{\tau}\sum_{r}\sum_{s}\sum_{p} f_{r,s,p}^{\tau} \cdot \xi_{r,s,p}^{\tau,a}(t) \qquad \forall a,t \tag{3.10}$$

$$C_{r,s,p}^{\tau} = \sum_{t}\sum_{a} \xi_{r,s,p}^{\tau,a}(t) \bullet \Delta \qquad \forall r,s,p,\tau \tag{3.11}$$

3.3.1.6 ***Non-negativity Constraints:***

All variables must be non-negative, especially the link flow variables since negative values may imply that FIFO conditions are not adhered to:

$$\xi_{r,s,p}^{\tau,a}(t) = 0 \text{ or } 1 \qquad \forall r,s,a,p,\tau,t \tag{3.12}$$

$$x_a(t), u_a(t), v_a(t) \geq 0 \qquad \forall a,t \tag{3.13}$$

$$f_{r,s,p}^{\tau} \geq 0 \qquad \forall r,s,p,\tau \tag{3.14}$$

3.3.1.7 ***Boundary Constraints:***

No traffic is assumed on the network at time $t = 0$, therefore:

$$x_a(0), u_a(0), v_a(0) = 0 \qquad \forall a,t \tag{3.15}$$

Constraints (3.10) and (3.11) are the hardest to evaluate and result from the need to capture correctly the complex flow interactions in a dynamic setting. While they lack the convexity and tractability of simple analytical constraints, they force the system to adhere to traffic flow principles such as the satisfaction of FIFO conditions, preclusion of holding of vehicles, and

the representation of link interactions and other dynamic traffic phenomena. These variables are a function of the flow assignments $f_{r,s,p}^{\tau}$, which are in turn a function of time-dependent link-path index $\xi_{r,s,p}^{\tau,a}(t)$, and this leads to a very complex fixed-point problem [Peeta (1994)]:

$$\boldsymbol{\xi} = \aleph\left(\boldsymbol{f}(\boldsymbol{\xi})\right) \tag{3.16}$$

where $\boldsymbol{\xi}$ is a vector of $\xi_{r,s,p}^{\tau,a}(t)$. Since the properties of $\aleph(\bullet)$ are not well understood, it can only be realistically evaluated via simulation techniques, which circumvents the use of unrealistic side constraints such exit functions or link performance functions. To reflect the use of simulation techniques, constraints (3.10) and (3.11) will be replaced by the following equations throughout this dissertation:

$$x_a(t) = \Omega_a(t, \boldsymbol{f}) \qquad \forall a,t \tag{3.17}$$

$$C_{r,s,p}^{\tau} = \Phi_{r,s,p}^{\tau}(\boldsymbol{f}) \qquad \forall r,s,p,\tau \tag{3.18}$$

where $\Omega_a(t, \boldsymbol{f})$ and $\Phi_{r,s,p}^{\tau}(\boldsymbol{f})$ are unique link flow-cost and path flow-cost mapping functions evaluated through simulation. To summarize, the SO-DTA problem is formulated as follows:

Given: $d_{r,s}^{\tau}$

Find: $f_{r,s,p}^{\tau}$

To:
$$\text{Min } Z(\boldsymbol{f}) = \sum_{\tau}\sum_{r}\sum_{s}\sum_{p} C_{r,s,p}^{\tau} f_{r,s,p}^{\tau} \tag{3.19}$$

Subject to:
$$\sum_{p} f_{r,s,p}^{\tau} = d_{r,s}^{\tau} \qquad \forall r,s,\tau \tag{3.19a}$$

$$\sum_{a} v_a(t) = O_r(t) \qquad \forall r,t,a \in \Gamma(r) \tag{3.19b}$$

$$\sum_a u_a(t) = I_s(t) \qquad \forall s,t,a \in \Gamma^{-1}(s) \tag{3.19c}$$

$$\sum_a v_a(t) - \sum_b u_b(t) = O_n(t) - I_n(t) = 0 \qquad \forall t,\ a \in \Gamma(n), b \in \Gamma^{-1}(n), n \notin R \tag{3.19d}$$

$$x_a(t) = \Omega_a(t, \boldsymbol{f}) \qquad \forall a,t \tag{3.19e}$$

$$C^{\tau}_{r,s,p} = \Phi^{\tau}_{r,s,p}(\boldsymbol{f}) \qquad \forall r,s,p,\tau \tag{3.19f}$$

$$x_a(t), u_a(t), v_a(t) \geq 0 \qquad \forall a,t \tag{3.19g}$$

$$x_a(0), u_a(0), v_a(0) = 0 \qquad \forall a,t \tag{3.19h}$$

$$f^{\tau}_{r,s,p} \geq 0 \qquad \forall r,s,p,\tau \tag{3.19i}$$

3.3.2 Optimality Conditions

The optimality conditions of program (3.19) are studied to investigate the underlying assignment principle, which in turn will help shape the solution algorithm. Let $\boldsymbol{L}(\boldsymbol{f}, \tilde{\boldsymbol{\pi}})$ be the Lagrangian of the SO-DTA formulation, where $\tilde{\boldsymbol{\pi}}$ denote the vector of Lagrangian variables (or dual variables) associated with constraint (3.19a). Remaining constraints are either definition constraints or are internally conserved (not an explicit function of the path-flow assignments) and hence adding them to $\boldsymbol{L}(\boldsymbol{f}, \tilde{\boldsymbol{\pi}})$ will result in the same set of constraints. Therefore, the Lagrangian of the SO-DTA formulation can be expressed as:

$$\text{Min } \boldsymbol{L}(\boldsymbol{f}, \tilde{\boldsymbol{\pi}}) = Z(\boldsymbol{f}) + \sum_{\tau}\sum_{r}\sum_{s} \tilde{\pi}^{\tau}_{r,s} \left(d^{\tau}_{r,s} - \sum_{p} f^{\tau}_{r,s,p} \right) \tag{3.20}$$

Subject to: DTA constraints (3.20j)

where constraints (3.19b) – (3.19h) collectively represent DTA constraints. The necessary conditions for a minimum of this program are given by the first-order conditions for a stationary point of program (3.20).

$$\frac{\partial \mathcal{L}(\boldsymbol{f}, \tilde{\boldsymbol{\pi}})}{\partial f_{r,s,p}^{\tau}} \geq 0 \qquad \forall r, s, p, \tau \tag{3.21a}$$

$$f_{r,s,p}^{\tau} \frac{\partial \mathcal{L}(\boldsymbol{f}, \tilde{\boldsymbol{\pi}})}{\partial f_{r,s,p}^{\tau}} = 0 \qquad \forall r, s, p, \tau \tag{3.21b}$$

$$\frac{\partial \mathcal{L}(\boldsymbol{f}, \tilde{\boldsymbol{\pi}})}{\partial \tilde{\pi}_{r,s}^{\tau}} = 0 \qquad \forall r, s, \tau \tag{3.21c}$$

$$f_{r,s,p}^{\tau} \geq 0 \qquad \forall r, s, p, \tau \tag{3.21d}$$

DTA constraints (3.21e)

Keeping in mind that

$$\frac{\partial f_{r,s,p}^{\tau}}{\partial f_{\dot{r},\dot{s},\dot{p}}^{\dot{\tau}}} = \begin{cases} 1 & \text{if } r = \dot{r}, s = \dot{s}, \tau = \dot{\tau} \\ 0 & \text{otherwise} \end{cases}$$

the term $\frac{\partial \mathcal{L}(\boldsymbol{f}, \tilde{\boldsymbol{\pi}})}{\partial f_{r,s,p}^{\tau}}$ may be evaluated for a particular path-flow variable $f_{\dot{r},\dot{s},\dot{p}}^{\dot{\tau}}$:

$$\frac{\partial \mathcal{L}(\boldsymbol{f}, \tilde{\boldsymbol{\pi}})}{\partial f_{\dot{r},\dot{s},\dot{p}}^{\dot{\tau}}} = \underbrace{C_{\dot{r},\dot{s},\dot{p}}^{\dot{\tau}} + \frac{\partial \sum_{\tau}\sum_{r}\sum_{s}\sum_{p} C_{r,s,p}^{\tau}}{\partial f_{\dot{r},\dot{s},\dot{p}}^{\dot{\tau}}}}_{\tilde{C}_{\dot{r},\dot{s},\dot{p}}^{\dot{\tau}}} - \tilde{\pi}_{\dot{r},\dot{s}}^{\dot{\tau}} \tag{3.22}$$

therefore, the first order optimality conditions for the SO-DTA problem are:

$$\tilde{C}_{r,s,p}^{\tau} - \tilde{\pi}_{r,s,p}^{\tau} \geq 0 \qquad \forall r, s, p, \tau \tag{3.23a}$$

$$f_{r,s,p}^{\tau} \left[\tilde{C}_{r,s,p}^{\tau} - \tilde{\pi}_{r,s}^{\tau} \right] = 0 \qquad \forall r, s, p, \tau \tag{3.23b}$$

$$f_{r,s,p}^{\tau} \geq 0 \qquad \forall r, s, p, \tau \tag{3.23c}$$

DTA constraints (3.23d)

where $\tilde{\boldsymbol{\pi}}(\boldsymbol{f})$ denotes the vector of minimum O-D marginal travel times:

$$\tilde{\boldsymbol{\pi}}(\boldsymbol{f}) = \left\{ \tilde{\pi}^{\tau}_{r,s,p}(\boldsymbol{f}) \mid \exists\, p \in P^{\tau}_{r,s} \forall r \in R, s \in S, \tau = 1,...,T' \right\}$$

3.4 REFORMULATION VIA A GAP FUNCTION

The flow pattern $\boldsymbol{f}^*$ is a solution to the SO-DTA problem if it satisfies conditions (3.23), which collectively state that if the path flow $\boldsymbol{f}^*$ is positive, then the experienced path travel time marginals $\tilde{\boldsymbol{C}}(\boldsymbol{f}^*)$ should be equal to the minimum path travel time marginals $\tilde{\boldsymbol{\pi}}(\boldsymbol{f})$ for the same (r,s,τ) combination. Inherent in this formulation is the assumption that the complete time-varying O-D demand information $\boldsymbol{d}$ for the entire planning horizon is known a priori, to the (single) central controller, whose objective is minimize total system trip time.

The asymmetry in the Jacobian matrix and the complexity of the dynamic network loading functions greatly reduces the choice of algorithms available to solve a program such as (3.19) since existence and uniqueness cannot be guaranteed. Therefore, researchers generally formulate the DTA problems as VI problems. Analogous to path-based VI formulation by Smith (1993) for the UE-DTA problem, the SO-DTA problem may be formulated as a VI as follows: find a time-varying path-flow pattern $\boldsymbol{f}^*$ such that

$$\sum_{\tau}\sum_{r}\sum_{s}\sum_{p} f^{\tau}_{r,s,p}\left[\tilde{C}^{\tau}_{r,s,p} - \tilde{\pi}^{\tau}_{r,s}\right] \geq 0 \qquad \forall r, s, p, \tau \tag{3.24}$$

The equivalence to the SO-DTA program (3.19) is given by Smith (1979). Assuming the path travel times and path marginal travel times are continuous and strictly monotone, it can be established that a solution for the above VI problem exists and is unique [Smith (1993), Nagurney (1998)]. However, while commonly made in the literature, these assumptions cannot be expected to hold in a realistic traffic network with signalized junctions and as such it is unlikely that the VI problem will have a unique solution in a simulation-based model.

Following Lu (2007) treatment of the UE-DTA problem, the VI problem (3.24) will be

reformulated via a gap function, to an equivalent NMP whose global minima coincide with those of program (3.19). Define a gap function as follows:

$$G_{\mathrm{SO}} = \sum_{\tau}\sum_{r}\sum_{s}\sum_{p} f_{r,s,p}^{\tau}\left(\tilde{C}_{r,s,p}^{\tau} - \tilde{\pi}_{r,s}^{\tau}\right) \tag{3.25}$$

G_{SO} provides a measure of the violation of the SO-DTA conditions in terms of the difference between the actual path marginal travel times and the least-cost path marginal travel time evaluated at $\boldsymbol{f}$. It is evident that the difference vanishes when the time-varying path flow vector $\boldsymbol{f}^*$ satisfies the SO-DTA conditions. Thus, solving the SO-DTA problem can be viewed as a process of finding the path flow vector $\boldsymbol{f}^*$ such that $G_{\mathrm{SO}}(\boldsymbol{f}^*) = 0$. Therefore, an equivalent problem would be to

$$\text{Min } Z = G_{\mathrm{SO}} = \sum_{\tau}\sum_{r}\sum_{s}\sum_{p} f_{r,s,p}^{\tau}\left(\tilde{C}_{r,s,p}^{\tau} - \tilde{\pi}_{r,s}^{\tau}\right) \tag{3.26}$$

Subject to:

$$\tilde{C}_{r,s,p}^{\tau} - \tilde{\pi}_{r,s,p}^{\tau} \geq 0 \qquad \forall r, s, p, \tau \tag{3.26e}$$

$$\sum_{p} f_{r,s,p}^{\tau} = d_{r,s}^{\tau} \qquad \forall r, s, \tau \tag{3.26f}$$

$$f_{r,s,p}^{\tau} \geq 0 \qquad \forall r, s, p, \tau \tag{3.26g}$$

DTA constraints (3.26h)

3.5 PROPOSED METHODOLOGY AND SOLUTION ALGORITHM

3.5.1 Solution Framework

This study adopts a hybrid approach for solving the reformulated SO-DTA problem. The hybrid approach integrates a mesoscopic traffic simulator (DYNASMART in this case) to estimate the state of the system (paths travel times and marginals) and an appropriate optimization technique (projected gradient method in this case) to solve an analytic SO-DTA

model, i.e. minimize G_{SO}. The solution framework is essentially an iterative bi-level framework where a Dynamic Network Loading Problem (DNLP) is solved in the upper level to estimate the state of the system, and an analytical model (NMP) is solved in the lower level to determine the path-flow assignments that minimize G_{SO}.

Traditionally, a pure analytical SO-DTA model will normally compute the path travel time as a summation of corresponding link travel times, where the later are usually represented by certain volume-delay functions. However, these functions take a simplistic view of congestion and do not incorporate network or traffic characteristics such as intersection control, ITS strategies, and different user types, etc. The SO-DTA model in this study utilizes the link and path travel times evaluated from the DNLP (or DYNASMART in this study). In other words, while solving the analytical SO-DTA, the link and path marginal travel times are fixed using the results from the traffic simulator. Consequently, the SO-DTA problem will reduce to a time-dependent least marginal path search for each O-D pair at each departure time period.

The process will iterate until a stable solution is attained. The solution stability is based on the comparison of path assignments over successive iterations, as proposed by Peeta (1994). For each (r,s,τ,p) combination, the flow $f_{r,s,p}^{\tau}{}^{(k)}$ in current iteration k is compared with that of the next iteration $f_{r,s,p}^{\tau}{}^{(k+1)}$. The number of cases, in which the absolute difference $\left| f_{r,s,p}^{\tau}{}^{(k)} - f_{r,s,p}^{\tau}{}^{(k+1)} \right|$ is greater than the predetermined path convergence threshold ε, is recorded as $V(\varepsilon)$ and referred to as the number of violations. That is the process terminates with the path assignments $f_{r,s,p}^{\tau}{}^{(k+1)}$ as the final solution if and only if $V(\varepsilon) \le \overline{V}(\varepsilon)$, where $\overline{V}(\varepsilon)$ is a predetermined user-specified upper bound, otherwise the process keeps iterating.

This convergence criterion serves as a proxy for another convergence criterion commonly used in static assignment, which is the number of newly generated paths. In static assignment, the solution algorithm would terminate when no new paths can be added to the

restricted network [Larsson and Patriksson (1992), Ziliaskopoulos et. al. (2004)]; however, when the time dimension is incorporated, attaining such a condition is not practical. One can always show that the number of newly added paths in a DTA setting is decreasing, but up to a certain point where the number of paths fluctuates. Therefore, what this convergence criterion reflects is achievement of a stable solution. However, it does not say anything about the quality of the solution (proximity to ideal SO conditions). In this regard, the relative (duality) gap as defined by Janson (1991b) is used:

$$\tilde{G}_{\mathrm{SO}}^{(k)} = \frac{\sum_r \sum_s \sum_\tau \sum_p f_{r,s,p}^{\tau\,(k)} \left| \tilde{C}_{r,s,p}^{\tau\,(k)} - \tilde{\pi}_{r,s}^{\tau\,(k)} \right|}{\sum_r \sum_s \sum_\tau d_{r,s}^{\tau} \tilde{\pi}_{r,s}^{\tau\,(k)}} = \frac{G_{\mathrm{SO}}(\boldsymbol{f})^{(k)}}{\sum_r \sum_s \sum_\tau d_{r,s}^{\tau} \tilde{\pi}_{r,s}^{\tau\,(k)}} \qquad (3.27)$$

The numerator in (3.27) represents the total gap (slackness) and is related directly to SO-DTA optimality conditions (3.23). If the total slackness is zero, it means that an exact SO-DTA solution is found, otherwise $\tilde{G}_{\mathrm{SO}}^{(k)}$ measures the relative distance to the exact solution. Finally, the average system trip time, which represents the objective of the original SO-DTA problem (3.19) is also used in the analysis to assess the quality of the solution.

The proposed solution framework is applicable for the case vehicles are equipped for communication with the central controller. The key behavioral assumption for path choice decisions is that all vehicles comply fully with the path assignments given by the central controller, and no en-route path-switching is made after departing. The solution framework operates as follows. At each iteration k, the algorithm: (1) evaluates current path assignments by an embedded simulation-based dynamic network loading model – DYNASMART; (2) determines a search direction by solving a time-dependent least cost path problem; and (3) updates path assignments for iteration $k+1$ by applying a suitable step size along the search direction. The solution framework is presented in Figure 3.1.

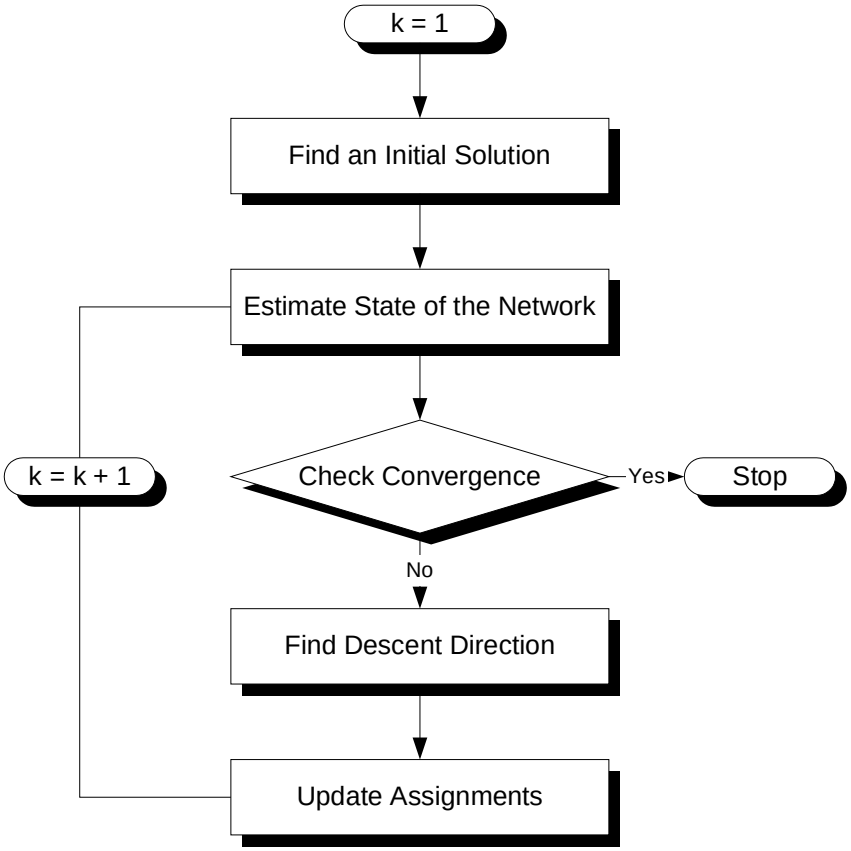

Figure 3.1 Solution framework of the SO-DTA problem

3.5.2 Updating Path Assignments

Most simulation-based algorithms in the literature have a similar solution framework. The main difference lies in how the assignments are updated for the next iteration. The calculation of $\boldsymbol{f}^{(k+1)}$ from $\boldsymbol{f}^{(k)}$ can be written in mathematical form as follows [Bertsekas and Gafni 1983]:

$$\boldsymbol{f}^{(k+1)} = \boldsymbol{f}^{(k)} + \rho^{(k)} \times h^{-1(k)} \times \theta^{(k)} \tag{3.28}$$

where $\theta^{(k)}$ is the descent direction and $\rho^{(k)} \in [0,1]$ is the step size along $\theta^{(k)}$ and $h^{-1(k)}$ is a scaling matrix. The decent direction is generally taken to be the negative of the gradient of the gap function. Ignoring the partial derivatives of the path cost with respect to path flow, the decent direction becomes:

$$\theta = -\nabla G_{SO} = -\frac{\partial G_{SO}}{\partial \boldsymbol{f}} = \tilde{\boldsymbol{\pi}}(\boldsymbol{f}) - \tilde{\boldsymbol{C}}(\boldsymbol{f}) \tag{3.29}$$

The resulting flow assignments are typically projected onto feasible space:

$$\boldsymbol{f}^{(k+1)} = \left[\boldsymbol{f}^{(k)} - \rho^{(k)} \times h^{-1(k)} \times \left(\tilde{C}(\boldsymbol{f}^{(k)}) - \tilde{\pi}(\boldsymbol{f}^{(k)}) \right) \right]^{+} \tag{3.30}$$

where $[\ ]^{+}$ denotes the unique projection onto the positive orthant. We can rewrite (3.30) as:

$$\boldsymbol{f}^{(k+1)} = \boldsymbol{f}^{(k)} - \boldsymbol{\delta}^{(k)} \tag{3.31}$$

where $\boldsymbol{\delta}^{(k)}$ is the amount of flow shifted from non-optimal routes to optimal routes and is proportional to the difference in the route marginal time and the current least marginal time path:

$$\boldsymbol{\delta}^{(k)} = \left[\rho^{(k)} \times \boldsymbol{h}^{-1(k)} \times \left(\tilde{\boldsymbol{C}}(\boldsymbol{f}^{(k)}) - \tilde{\boldsymbol{\pi}}(\boldsymbol{f}^{(k)}) \right) \right]^{+} \tag{3.32}$$

For the units in (3.32) to be consistent, the scaling matrix term, $\boldsymbol{h}^{-1}$ must have units of vehicles/time. In other words, $\boldsymbol{h}^{-1}$ transforms the difference in the route marginal time and the least marginal time path into flow (or vehicles). Jayakrishnan et al. (1994) adapted the projection method by [Bertsekas and Gafni (1983)] into solving the traffic assignment problem. In their method, the basic assignments update equation:

$$f_{r,s,p}{}^{(k+1)} = f_{r,s,p}{}^{(k)} - \rho^{(k)} \times h^{-1(k)} \times \left(C_{r,s,p}{}^{(k)} - \pi_{r,s}{}^{(k)} \right) \tag{3.33}$$

where

$$h = \sum_{p \in P_{r,s}} \frac{\partial \left(C_{r,s,p}{}^{(k)} f_{r,s,p}{}^{(k)} \right)}{\partial f} = \sum_{p \in P_{r,s}} \tilde{C}_{r,s,p}{}^{(k)} \tag{3.34}$$

and $\rho^{(k)} = 1$. In other, the scaling matrix is in fact the Hessian matrix approximated by its

diagonal terms. However, the determination of the scaling term h^{-1} has been the most problematic in the general absence of derivative information in simulation-based models. Therefore, the typical approach has been to approximate the scaling matrix $\boldsymbol{h}^{-1}$ with the flow pattern $\boldsymbol{f}$ and re-write (3.33) as follows:

$$\delta^{(k)} = \left[\rho^{(k)} \times \boldsymbol{f}^{(k)} \times \left(\tilde{C}(\boldsymbol{f}^{(k)}) - \tilde{\pi}(\boldsymbol{f}^{(k)}) \right) \right]^{+} \tag{3.35}$$

The problem then reverts to a simple shortest path problem to determine the least-cost path tree $\tilde{\boldsymbol{\pi}}(\boldsymbol{f}^{(k)})$ and hence the decent direction $[\tilde{\boldsymbol{C}}(\boldsymbol{f}^{(k)}) - \tilde{\boldsymbol{\pi}}(\boldsymbol{f}^{(k)})]$. A simple line search problem is then solved to determine the optimal step-size $\rho^{(k)}$. A simpler approach would be to use a predetermined step-size scheme such as MSA instead of the line search problem.

Another variation of the above approach that also ignores derivative information is to lump the scaling term h^{-1} with the step-size ρ into a swap rate $\hat{\rho}$ that effectively converts units of time into flow. Such a technique is generally referred to as route-swapping which shift vehicles from expensive routes to cheapest routes [Smith and Winsten (1995), Cybis (1995), Huang and Lam (2002), and Szeto and Lo (2005)]:

$$\delta^{(k)} = \left[\hat{\rho}^{(k)} \times \left(\tilde{C}(\boldsymbol{f}^{(k)}) - \tilde{\pi}(\boldsymbol{f}^{(k)}) \right) \right]^{+} \tag{3.36}$$

Still, the determination of the swap rate $\hat{\rho}^{(k)}$ is problematic. A small swap rate and convergence will take forever to reach, and a large swap rate and oscillations will occur [Szeto and Lo (2005)]. The general approach has been to parametrically solve for the optimal swap rate, however, often than not, the resulting optimal swap rate is rather network specific (non-transferable to other networks), flow-specific, and is very time consuming to find.

To circumvent such a time-consuming process, Lu (2007) sets the swap rate to the inverse of the path cost $\tilde{C}^{-1}(\boldsymbol{f})$ as follows:

$$\delta^{(k)} = \left[\boldsymbol{f}^{(k)} \times \tilde{\boldsymbol{C}}^{-1}(\boldsymbol{f}^{(k)}) \times \left(\tilde{\boldsymbol{C}}(\boldsymbol{f}^{(k)}) - \tilde{\pi}(\boldsymbol{f}^{(k)}) \right) \right]^{+} \tag{3.37}$$

Such an approach is designed to take care of the inherent deficiency in traditional route-swap methods, where the fraction of traffic to be swapped is determined solely on the absolute path-cost differences, i.e. $\left(\tilde{\boldsymbol{C}}(\boldsymbol{f}) - \tilde{\pi}(\boldsymbol{f})\right)$, regardless of the distance to optimality. Therefore shifting flow in proportion to the relative difference in path costs, i.e. $\left(\tilde{\boldsymbol{C}}(\boldsymbol{f}) - \tilde{\pi}(\boldsymbol{f})\right) / \tilde{\boldsymbol{C}}(\boldsymbol{f})$, provides a better measure for the distance to optimality since paths further away from optimally (higher relative cost difference) will have to shift more flow than paths closer to optimality despite having the same absolute difference in costs. Yet, this method has some drawbacks and is dependent on the starting solution. For example, consider the following two-path static network:

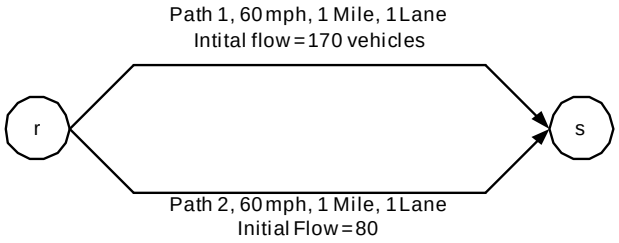

Figure 3.2 Two-path network example

Assume that each path is 1 mile long and that the free-flow speed is 60 mph (or 1 mile/min). Assume that paths speed is given by the commonly accepted Greenshields model [see (2.4)] with shape parameter $\alpha_a = 1$ and jam density $\kappa_a^{\text{jam}} = 250$ veh/lane-mile. The path travel times are therefore given by the following relation:

$$C_a = \frac{L_a}{a} = \frac{1}{\left(1 - \frac{f_a}{250}\right)} \tag{3.38}$$

where L_a is the length of link a. We are interested in moving 250 vehicles from r to s under a static UE assignment principle. The solution quality will be assessed by the UE gap

function for static conditions as follows:

$$G_{\mathrm{UE}}(\boldsymbol{f}) = \sum_{r}\sum_{s}\sum_{p} f_{r,s,p}\left(C_{r,s,p} - \pi_{r,s}\right) \tag{3.39}$$

Starting with initial path flows of 170 vehicles and 80 vehicles for paths 1 and 2, respectively, the path times for the first iteration are $C_1^{(1)} = 3.125\,\text{min}$ and $C_2^{(1)} = 1.471\,\text{min}$ with a corresponding $G_{\mathrm{UE}}(\boldsymbol{f})^{(1)} = 281.18\,\text{min}$. According to (3.37) and replacing path marginals $\tilde{\boldsymbol{C}}(\boldsymbol{f})$ with path travel times $\boldsymbol{C}(\boldsymbol{f})$, path 1 will have to shift 90[1] vehicles of its flow to path 2. The assignments for the next iteration become $f_1^{(2)} = 80\,\text{veh}$[2] and $f_1^{(2)} = 170\,\text{veh}$[3], i.e. the assignments are reversed from initial conditions. This will create an infinite cycle of updates without converging to a stationary point.

3.5.3 Optimal Route Swap Calculations

3.5.3.1 *Pair-wise Route Swapping Example*

So exactly how much flow should $\delta^{(1)}$ we shift from path 1 to path 2 to achieve user equilibrium? Let $\delta^{(1)}$ be the optimal number if vehicles to shift from path 1 to path 2. Therefore, at equilibrium, we must have:

$$C_1^{(1)} - \delta^{(1)} \times \frac{\partial C_1^{(1)}}{\partial f} = C_2^{(1)} + \delta^{(1)} \times \frac{\partial C_2^{(1)}}{\partial f} \tag{3.40}$$

or equivalently,

$$\delta^{(1)} = \frac{C_1^{(1)} - C_2^{(1)}}{\left(\dfrac{\partial C_1^{(1)}}{\partial f} + \dfrac{\partial C_2^{(1)}}{\partial f}\right)} \tag{3.41}$$

---

[1] $\delta^{(1)} = 170 \times (3.125 - 1.471)/3.125 = 90\ \text{veh}$

[2] $f_1^{(2)} = f_1^{(1)} - \delta^{(1)} = 170 - 90 = 80\ \text{veh}$

[3] $f_2^{(2)} = f_2^{(1)} + \delta^{(1)} = 80 + 90 = 170\,\text{veh}$

The appropriate swap rate (or conversion factor) is therefore sum of route cost derivatives. In other words, the conversion factors correspond to objective function second-order derivatives, i.e. to the diagonal elements of the Hessian matrix. The desirable flow shift can therefore be viewed as the product of the objective function's inverse Hessian (approximated by its diagonal terms) by its gradient. This provides an intuitive insight to the gradient projection method as proposed by Bertsekas and Gafni (1983) and adapted by Jayakrishnan et al. (1994) for the case of pair-wise route swap.

Equation (3.41) requires the computation of the path derivatives. In this regard, the path derivatives will be computed as follows:

$$\frac{\partial C_a}{\partial f_a} = \frac{1}{250}\left(1 - \frac{f_a}{250}\right)^{-2} \tag{3.42}$$

Going back to the two-path problem and using (3.41) results in path-cost derivatives $\partial C_1^{(1)} / \partial f \quad = 0.03906$ and $\partial C_2^{(1)} / \partial f = 0.00865$. This yields an optimal swap rate $\delta^{(1)} \approx 35$ veh. The assignments for the next iteration become $f_1^{(2)} = 135$ veh [4] and $f_2^{(2)} 110$ veh [5]. The with corresponding travel times are $C_1^{(2)} = 2.17$ min and $C_2^{(2)} = 1.85$ min. The gap at this assignment level is $G_{\mathrm{UE}}(\boldsymbol{f})^{(2)} = 43.48$ min. The path-cost derivatives for the second iteration are $\partial C_1^{(2)} / \partial f = 0.0189$, $\partial C_2^{(2)} / \partial f = 0.0137$ and consequently $\delta^{(2)} \approx 10$ veh. The assignments for the third iteration become $f_1^{(3)} = f_2^{(3)} = 125$ veh, with corresponding travel times of $C_1^{(3)} = C_2^{(3)} = 2$ min and $G_{\mathrm{UE}}(\boldsymbol{f})^{(3)} = 0$ min.

The same approach can be extended to SO case by replacing the path costs $\boldsymbol{C}$ with the path travel time marginals $\tilde{\boldsymbol{C}}$. The SO optimality conditions will hold if and only if the path marginal travel times are equal. Evaluating these conditions under the initial assignments, we

[4] $f_1^{(2)} = f_1^{(1)} - \delta^{(1)} = 170 - 35 = 135$ veh

[5] $f_2^{(2)} = f_2^{(1)} + \delta^{(1)} = 80 + 35 = 110$ veh

get $\tilde{C}_1^{(1)} = 9.76\,\text{min}$ [6] and $\tilde{C}_2^{(1)} = 2.163\,\text{min}$ [7], resulting in $G_{\text{SO}}(\boldsymbol{f})^{(1)} = 1292.51\,\text{min}$. Such an assignment pattern also suggests shifting vehicles from path 1 to 2. At optimality, we must have both path marginal travel times to be equal, i.e.

$$\tilde{C}_1^{(1)} - \delta^{(1)} \times \frac{\partial \tilde{C}_1^{(1)}}{\partial f} = \tilde{C}_2^{(1)} + \delta^{(1)} \times \frac{\partial \tilde{C}_2^{(1)}}{\partial f} \tag{3.43}$$

or equivalently,

$$\delta^{(1)} = \frac{\tilde{C}_1^{(1)} - \tilde{C}_2^{(1)}}{\frac{\partial \tilde{C}_1^{(1)}}{\partial f} + \frac{\partial \tilde{C}_2^{(1)}}{\partial f}} \tag{3.44}$$

where

$$\frac{\partial \tilde{C}_a}{\partial f_a} = \frac{\partial\left(C_a + f_a \frac{\partial C_a}{\partial f_a}\right)}{\partial f_a} = 2\frac{\partial C_a}{\partial f_a} + x_a \frac{\partial^2 C_a}{\partial {f_a}^2} \tag{3.45}$$

and

$$\frac{\partial^2 C_a}{\partial {f_a}^2} = 2\left(\frac{1}{250}\right)^2 \left(1 - \frac{f_a}{250}\right)^{-3} \tag{3.46}$$

Using (3.44), we get $\delta^{(1)} \approx 30\,veh$ which leads to next iteration path assignments of $f_1^{(2)} = 140\,veh$, $f_2^{(2)} = 110\,veh$. The corresponding travel times of at this assignment level are $C_1^{(2)} = 2.27\,\text{min}$, $C_2^{(2)} = 1.79\,\text{min}$ with an SO gap $G_{\text{SO}}(\boldsymbol{f})^{(2)} = 276.71\,\text{min}$. The shift size for the next iteration is $\delta^{(2)} \approx 15\,veh$, hence the assignments for the third iteration are $f_1^{(3)} = f_2^{(3)} = 125\,veh$, with corresponding travel times of $C_1^{(3)} = C_2^{(3)} = 2\,\text{min}$ and an SO gap $G_{\text{SO}}(\boldsymbol{f})^{(3)} = 0\,\text{min}$.

---

[6] $\tilde{C}_1^{(1)} = C_1^{(1)} + f_1^{(1)}[\partial C_1^{(1)} / \partial f] = 3.125 + 170 \times 0.03906 = 9.76\,\text{min}$

[7] $\tilde{C}_2^{(1)} = C_2^{(1)} + f_2^{(1)}[\partial C_2^{(1)} / \partial f] = 1.471 + 80 \times 0.00865 = 2.163\,\text{min}$

3.5.3.2 ***General Case***

In real cases, there will be more than two paths between a given $r-s$ pair. Assume that the shift vector $\boldsymbol{\delta}$, is algebraic. Assume that if δ_p is negative, then path p will shift $|\delta_p|$ of its flow to other cheaper paths, and if δ_p is positive, then an extra flow of $|\delta_p|$ will be shifted to path p from more expensive paths. We will now derive the SO route swap conditions for a three-path network and later for the general case. For simplicity, the iteration number is dropped from the subsequent derivation. Assume now there are three paths between A and B. Define $\tilde{C}' \equiv \partial \tilde{C} / \partial f$, then, the SO conditions for the three-path problem become:

$$\tilde{C}_1 + \delta_1 \times \tilde{C}_1' = \tilde{C}_2 + \delta_2 \times \tilde{C}_2' = \tilde{C}_3 + \delta_3 \times \tilde{C}_3' \tag{3.47}$$

and

$$\delta_1 + \delta_2 + \delta_3 = 0 \tag{3.48}$$

Expressing δ_1 and δ_2 in terms of δ_3, we have

$$\delta_1 = \frac{\left(\tilde{C}_3 - \tilde{C}_1\right)}{\tilde{C}_1'} + \frac{\tilde{C}_3'}{\tilde{C}_1'} \times \delta_3 \tag{3.49}$$

and

$$\delta_2 = \frac{\left(\tilde{C}_3 - \tilde{C}_2\right)}{\tilde{C}_2'} + \frac{\tilde{C}_3'}{\tilde{C}_2'} \times \delta_3 \tag{3.50}$$

Substituting δ_1 and δ_2 values in (3.49) and (3.50) back to (3.48), we get

$$\delta_3 = \frac{\left[\frac{\left(\tilde{C}_1 - \tilde{C}_3\right)}{\tilde{C}_1'} + \frac{\left(\tilde{C}_2 - \tilde{C}_3\right)}{\tilde{C}_2'}\right]}{1 + \left(\frac{\tilde{C}_3'}{\tilde{C}_1'} + \frac{\tilde{C}_3'}{\tilde{C}_2'}\right)} \tag{3.51}$$

Once δ_3 is determined, δ_1 and δ_2 are easily calculated from (3.49) and (3.50), respectively. In general, there will be many more paths for a given (r,s,τ) combination. Let $\bar{P}_{r,s}^{\tau} \subset P_{r,s}^{\tau}$ be the set of active (non-zero flow) paths for a given (r,s,τ) combination and denote by

$\left|\overline{P}_{r,s}^{\tau}\right|$ the number of paths in $\overline{P}_{r,s}^{\tau}$. Extending the derivation to the general case of $\left|\overline{P}_{r,s}^{\tau}\right|$ paths, the optimal shifts under an SO assignment will be:

$$\delta_{r,s,p}^{\tau} = \frac{\left(\tilde{C}^{\tau}_{r,s,\left|\overline{P}_{r,s}^{\tau}\right|} - \tilde{C}_{r,s,p}^{\tau}\right)}{\tilde{C}'^{\tau}_{r,s,p}} + \frac{\tilde{C}'^{\tau}_{r,s,\left|\overline{P}_{r,s}^{\tau}\right|}}{\tilde{C}'^{\tau}_{r,s,p}} \times \delta^{\tau}_{r,s,\left|\overline{P}_{r,s}^{\tau}\right|} \qquad \forall p \neq \left|\overline{P}_{r,s}^{\tau}\right| \tag{3.52}$$

where

$$\delta^{\tau}_{r,s,\left|\overline{P}_{r,s}^{\tau}\right|} = \frac{\left[\sum_{p} \frac{\tilde{C}^{\tau}_{r,s,p} - \tilde{C}^{\tau}_{r,s,\left|\overline{P}_{r,s}^{\tau}\right|}}{\tilde{C}'^{\tau}_{r,s,p}}\right]}{1 + \sum_{p} \frac{\tilde{C}'^{\tau}_{r,s,\left|\overline{P}_{r,s}^{\tau}\right|}}{\tilde{C}'^{\tau}_{r,s,p}}} \tag{3.53}$$

The flow-shift matrix $\boldsymbol{\delta}$ must be adjusted for feasibility before being used to update the assignments for the next iteration. A path p cannot possibly shift more flow than what it has and similarly, a path p cannot accept more flow than what is physically available (mass-balance). Bearing these 2 conditions in mind, the adjusted shifts may be computed as follows:

$$\tilde{\delta}_{r,s,p}^{\tau} = \max_{\delta_{r,s,p}^{\tau}<0}\left(\delta_{r,s,p}^{\tau}, -f_{r,s,p}^{\tau}\right) \qquad \forall r,s,p,\tau \tag{3.54}$$

To preserve mass-balance, the sum of the negative flow-shifts must be equal to the sum of the positive flow shifts, i.e. the positive flow-shifts must be adjusted as such:

$$\tilde{\delta}_{r,s,p}^{\tau} = \frac{\sum_{\dot{p},\delta_{r,s,\dot{p}}^{\tau}<0} \hat{\delta}_{r,s,\dot{p}}^{\tau}}{\sum_{\ddot{p},\delta_{r,s,\ddot{p}}^{\tau}>0} \delta_{r,s,\ddot{p}}^{\tau}} \delta_{r,s,p}^{\tau} \qquad \forall r,s,p,\tau \tag{3.55}$$

Therefore, the assignments for the next iteration become:

$$f_{r,s,p}^{\tau\,(k+1)} = f_{r,s,p}^{\tau\,(k)} + \tilde{\delta}_{r,s,p}^{\tau\,(k)} \qquad \forall r, s, p, \tau \tag{3.56}$$

where $\tilde{\delta}_{r,s,p}^{\tau}$, is algebraic.

3.5.4 Solution Algorithm

The path-based formulation of the SO-DTA problem necessitates the enumeration of all the paths in the network, which is impractical even for reasonably small networks. Therefore, this study adopts a column-generation approach to minimize storage requirements. At the heart of such a method, is the notion of active path set $\overline{P}_{r,s}^{\tau}$, which denotes the set of non-zero flow paths. At every iteration k, the column generation approach identifies an efficient solution (i.e. least marginal travel time path) $\hat{p} \in P_{r,s}^{\tau}$ for each (r,s,τ) combination and adds it to $\overline{P}_{r,s}^{\tau}$ if $\hat{p} \notin \overline{P}_{r,s}^{\tau}$. The set $\overline{P}_{r,s}^{\tau}$ forms a restricted network for which an analytical SO-DTA problem may be solved (paths marginal travel times are known and fixed from previous iteration) in much the same way as the simplicial decomposition technique of Larsson and Patriksson (1992). However, in this study, the restricted problem will not be solved to optimality since simulation experiments and earlier studies [Mahmassani and Mouskos (1988), Lu (2007)] have concluded that such a requirement is not necessary for overall solution quality. Therefore, one (inner) iteration of the proposed optimal route swap (ORS) method will be performed for each simulation (outer) iteration and as such, the notion of a restricted network there will be no further mention of a restricted network or a restricted MNP throughout this thesis.

The solution algorithm represents a heuristic iterative procedure where the objective function is evaluated and constraints are satisfied through a simulation model. The simulation model is used to move vehicles along their assigned departure times and paths until they reach their destinations, capturing the state of the system in the process. Traffic flow dynamics in the

simulator are represented using a mesoscopic approach where vehicles are microscopically tracked but moved in packets according to a macroscopic traffic flow model. At each iteration, the heuristic defines a search direction (vector) along which the objective function is expected to improve. The descent direction is taken to be the projection of gradient vector onto the feasible space (positive orthant) with a step size vector given by the ORS procedure. The steps of the simulation-based SO-DTA algorithm are explained in detail below:

Step 1: Initialization

- Set iteration counter $k = 1$.
- Solve for the time-dependent least-marginal time path tree for all (r, s, τ) combinations assuming free-flow link travel times (i.e. time-dependent link marginal travel time are equal to the time-dependent link travel times).
- Perform an all-or-nothing assignment (AON) of the O-D demand ($d_{r,s}^{\tau}$) onto the least-cost marginal travel time tree to obtain path assignments $f_{r,s,p}^{\tau\ (k)}$ for all (r, s, τ) combinations.

Step 2: Dynamic Network Loading Problem

- Use DYNASMART to simulate path assignments $f_{r,s,p}^{\tau\ (k)}$.
- Estimate time-dependent link travel times $c(\boldsymbol{f}^{(k)})$ and time-dependent link marginal travel times $\tilde{c}(\boldsymbol{f}^{(k)})$ from simulation results.

Step 3: Update Objective Function

- Compute relative gap $\tilde{G}_{\mathrm{SO}}(\boldsymbol{f}^{(k)})$ according to (3.27).
- Compute average system trip time, which is a proxy for SO-DTA objective (3.26): $ATT = \left(\sum_{\tau} \sum_{r} \sum_{s} \sum_{p} C_{r,s,p}^{\tau} \cdot f_{r,s,p}^{\tau} \right) / \sum_{\tau} \sum_{r} \sum_{s} \sum_{p} f_{r,s,p}^{\tau}$.

Step 4: Check Convergence

- Count the number of times the condition $\left| f_{r,s,p}^{\tau\ (k+1)} - f_{r,s,p}^{\tau\ (k)} \right| > \varepsilon$ is satisfied for all (r, s, τ, p) combinations and denote that number by $V(\varepsilon)$.

- If $V(\varepsilon) \le \bar{V}(\varepsilon)$ or $k \le \bar{k}$ stop, otherwise set $k = k+1$ and go to step 5.

Step 5: Time-Dependent Marginal Time Shortest Path Problem

- Solve for the time-dependent least-marginal time path $\hat{p}^{(k)}$ and add it to the active path, $\bar{P}_{r,s}^{\tau\,(k)}$ for all (r,s,τ) combinations using link travel times $c(\boldsymbol{f}^{(k)})$ and link marginal travel times $\tilde{c}(\boldsymbol{f}^{(k)})$ from simulator.

Step 6: Update of Path Assignments

- Find the adjusted (feasible) optimal shifts $\tilde{\delta}_{r,s,p}^{\tau\,(k)}$ using (3.54) and (3.55).
- Update the assignments $f_{r,s,p}^{\tau\,(k+1)}$ for the next iteration using for each (r,s,τ,p) using (3.56) and go to step 2

3.5.5 Column Generation and Vehicle-based Solution Implementation

The solution algorithm for the SO-DTA problem presented in the previous section is flow-based and requires the storage of paths and corresponding assignments for each (r,s,τ,p) combination. While this implementation is straightforward and directly applicable in any (analytical or simulation-based) DTA algorithms, and is not restricted by the choice of traffic simulation model used for flow propagation (macroscopic, microscopic, or mesoscopic), the associated memory requirements can be huge since they grow dramatically with the size of the network. Memory also grows with additional iterations when new paths are added. Therefore, despite being the "correct" way to represent the solution algorithm, the memory requirements of the flow-based implementation could seriously hinder its deployment in large-scale road networks.

To alleviate the memory requirements of the flow-based technique and pursue successful deployments of large-scale simulation-based DTA models, a vehicle-based implementation technique for the solution algorithm is utilized. Such an implementation takes advantage of the mesoscopic properties of the simulation model (ability to track vehicles individually) to extract the active paths set (with positive flow) and assignments from the vehicle trajectories

without the need to explicitly store them. This is particularly advantageous for large-scale DTA applications, as the total number of feasible paths could significantly out-grow the total number of vehicles. Furthermore, the memory requirements for storing paths are invariant from iteration to iteration because the number of vehicles in the network is fixed a priori.

Let J^{-} be the set that includes the vehicles that will be switching their paths to cheaper ones. The column generation and vehicle-based implementation for the solution algorithm is presented below. Note that adding the least marginal travel time path $\hat{p}$ to the active path set $\overline{P}_{r,s}^{\tau}{}^{(k)}$ should not alter the definition of is $\overline{P}_{r,s}^{\tau}{}^{(k)}$ since $\hat{p}$ will definitely be having some flow shifted to it, i.e. it will be active in the subsequent iteration.

DO for every (r,s,τ) combination

  Set $J^{-} = \{0\}$

  Scan all vehicles $j \in d_{r,s}^{\tau}{}^{(k)}$ and extract active path set $\overline{P}_{r,s}^{\tau}{}^{(k)}$

  Find least marginal path $\hat{p} \in P_{r,s}^{\tau}{}^{(k)}$ and add it to the active path, $\overline{P}_{r,s}^{\tau}{}^{(k)} = \overline{P}_{r,s}^{\tau}{}^{(k)} \cup \hat{p}$

  Compute the adjusted algebraic flow shift vector $\tilde{\delta}_{r,s,p}^{\tau}{}^{(k)}, \forall p \in \overline{P}_{r,s}^{\tau}{}^{(k)}$

  DO for each path $p \in \overline{P}_{r,s}^{\tau}{}^{(k)}$

    IF $\tilde{\delta}_{r,s,p}^{\tau}{}^{(k)} < 0$ THEN

      Randomly select $|\tilde{\delta}_{r,s,p}^{\tau}{}^{(k)}|$ vehicles from path p and add them to set J^{-}

    ENDIF

  ENDDO

  DO for each path $p \in \overline{P}_{r,s}^{\tau}{}^{(k)}$

    IF $\tilde{\delta}_{r,s,p}^{\tau}{}^{(k)} > 0$ THEN

      Randomly select $\tilde{\delta}_{r,s,p}^{\tau}{}^{(k)}$ vehicles from J^{-} and assign them to p

      Remove selected vehicles from J^{-}

    ENDIF

  ENDDO

ENDDO

Figure 3.3 Vehicle-based implementation of the ORS solution heuristic

3.5.6 Determination of the Time-dependent Path Marginal Travel Times

The main component of the SO-DTA algorithm is the determination of the marginal travel time for a path, which corresponds to the additional time incurred by the system due to an additional vehicle on this path. Two types of marginal travel times may be defined global marginals and local marginals [Peeta (2004)]. The computation of global path marginal travel time is theoretically simple but computationally exhaustive, one can always assign an extra vehicle on a certain path at a given departure time and keep the rest of the network assignment the same and measure the change in system cost via simulation. However, when the link interactions are insignificant, the global marginal and the local marginal values are expected to be relatively close and the latter can be substituted for the former [Peeta and Mahmassani (1995a)]. Similar simplifications are assumed in other studies as well.

With the assumption above, the computation of local path marginal travel times includes the determination of the increase in the path travel times that can be approximated by the summation of the link marginal travel times on each path, as follows:

$$\tilde{C}^{\tau}_{r,s,p} = \sum_{t}\sum_{a} \tilde{c}_a(t).\xi^{\tau,a}_{r,s,p}(t) \qquad \forall a, r, s, p, \tau, t \tag{3.57}$$

The common approach in computing link marginal travel time is to plot the link travel times versus the number of vehicles for different periods of time and compute $\partial c(x)/\partial x$ numerically according to the method by Peeta and Mahmassani (1995a), who suggested a 3-point quadratic fit using simulation results for three consecutive time steps, with the $\partial c(x)/\partial x$ evaluated at the middle interval. However, computing the travel time marginals numerically from plots have been prone to instability and discontinuity of the in the curves due to sudden jumps between short time periods. Peeta (1994) has discussed these shortcomings and addressed them by using averaging techniques. Tuydes (2005) extends the 3-point quadratic fit into an (n+1) quadratic fit, though no numerical comparison has been provided to substantiate the claims of better performance.

This study implements an analytical approach to estimating the marginals to overcome the discontinuity in the travel time plots. It utilizes the differentiability of the modified Greenshields traffic flow model embedded in DYNASMART. Greenshields relates the link speed to density as follows:

$$\vartheta_a(t) = \begin{cases} \vartheta_a^{\text{free}} & \kappa_a(t) \le \kappa_a^{\text{cutoff}} \\ \vartheta_a^{\min} + \left(\vartheta_a^{\max} - \vartheta_a^{\min}\right)\left(1 - \dfrac{\kappa_a(t)}{\kappa_a^{\text{jam}}}\right)^{\alpha} & \kappa_a(t) > \kappa_a^{\text{cutoff}} \end{cases} \tag{3.58}$$

The link density $\kappa_a(t)$ can be expressed as:

$$\kappa_a(t) = \frac{x_a(t)}{L_a \times l_a} \tag{3.59}$$

where l_a is the number of lanes of link a. The link travel time $c_a(t)$ can then be computed as follows:

$$c_a(t) = \frac{L_a}{\vartheta_a(t)} \tag{3.60}$$

The link marginal travel time, by definition, is the additional cost incurred by the system due to an additional vehicle at time t, i.e.

$$\tilde{c}_a(t) = c_a(t) + \frac{\partial c_a(t)}{\partial x_a(t)} \tag{3.61}$$

The term $\partial c_a(t) / \partial x_a(t)$ can be computed as:

$$\frac{\partial c_a(t)}{\partial x_a(t)} = \frac{\partial\left(\dfrac{L_a}{\vartheta_a(t)}\right)}{\partial x_a(t)} \tag{3.62}$$

Differentiating (3.62) we get:

$$\frac{\partial c_a(t)}{\partial x_a(t)} = \alpha_a \frac{L_a}{\underset{a}{\text{free}}} \frac{1}{l_a \cdot L_a . \kappa_a^{\text{jam}}} \left(1 - \frac{x_a(t)}{l_a \cdot L_a . \kappa_a^{\text{jam}}} \right)^{-\alpha_a - 1}, \quad \kappa_a(t) > \kappa_a^{\text{cutoff}} \tag{3.63}$$

Note that $\partial c_a(t) / \partial x_a(t)$ is non-zero if and only if $\kappa_a(t) > \kappa_a^{\text{cutoff}}$. Simulation results have shown that using link marginals according to (3.63) yields a lower system travel time and consequently lower SO gaps than the method by Peeta and Mahmassani (1995a). Furthermore, the second link cost derivative is easily calculated as:

$$\frac{\partial^2 c_a}{\partial {x_a}^2} = \alpha_a (\alpha_a + 1) \frac{L_a}{\vartheta_a^{\text{free}}} \left(\frac{1}{l_a \cdot L_a . \kappa_a^{\text{jam}}} \right)^2 \left(1 - \frac{x_a}{l_a \cdot L_a . \kappa_a^{\text{jam}}} \right)^{-\alpha_a - 2}, \kappa_a(t) > \kappa_a^{\text{cutoff}} \tag{3.64}$$

3.6 EXPERIMENTAL DESIGN AND MODEL RESULTS

Three sets of numerical experiments are conducted to test the optimal route-swap (ORS) algorithm. The first set of experiments aims to validate the use of analytical marginals as computed by equation (3.63) instead of numerical marginals as computed by Peeta (1994) in SO DTA solution heuristics. To this end the both the MSA and ORS algorithms are applied to a very small network typical of what is normally found in research papers. The second set of experiments is conducted on a relatively small network in terms of the overhead associated in solving for the time-dependent least marginal travel time paths, yet reasonably sized to draw conclusions regarding the performance of the ORS algorithm in comparison to the MSA. The final set is conducted on a regional network and is intended to showcase the ORS performance on a large real-life urban road network.

The ORS and MSA algorithms are implemented using the vehicle-based approach, which uses the vehicle path set as a proxy for keeping track of the path assignments. The algorithms are coded and compiled by using the Compaq Visual FORTRAN 6.6 and evaluated on a Windows XP machine with an Intel Pentium IV 2.8 GHz CPU and 4GB RAM.

In all experiments conducted, the following parameter settings are applied. The simulation time step is 6 sec, the resolution (aggregation interval) of the time-dependent least marginal travel time path tree calculation is 1 minute, which is the same as O-D demand assignment interval τ. The origins and destinations are regular nodes and are uniformly distributed over the whole network. Freeways are shown in blue whereas remaining arterials and surface roads are shown in white. The free mean speed on freeway links is 70 mph, on major arterials is 50 mph, and on ramps and local streets is 40 mph. The jam density is 220 veh/lane-mile for freeways and 120 veh/lane-mile for other road types. The corresponding minimum speeds for all link types are to set to 3 mph. All intersections are either signalized or sign controlled (stop or yield), except on freeways. The service flow rate is set at 2200 veh/hour-lane for freeways and 1800 veh/hour-lane for non-freeway links.

In each experiment, a 2-hour time-varying O-D demand table is loaded (Figure 3.4) with the (simulation) planning horizon set long enough to allow vehicles to clear the network. The initial solutions of the experiments are obtained by performing an AON assignment of the demand onto the least marginal travel time path tree computed using free-flow travel times.

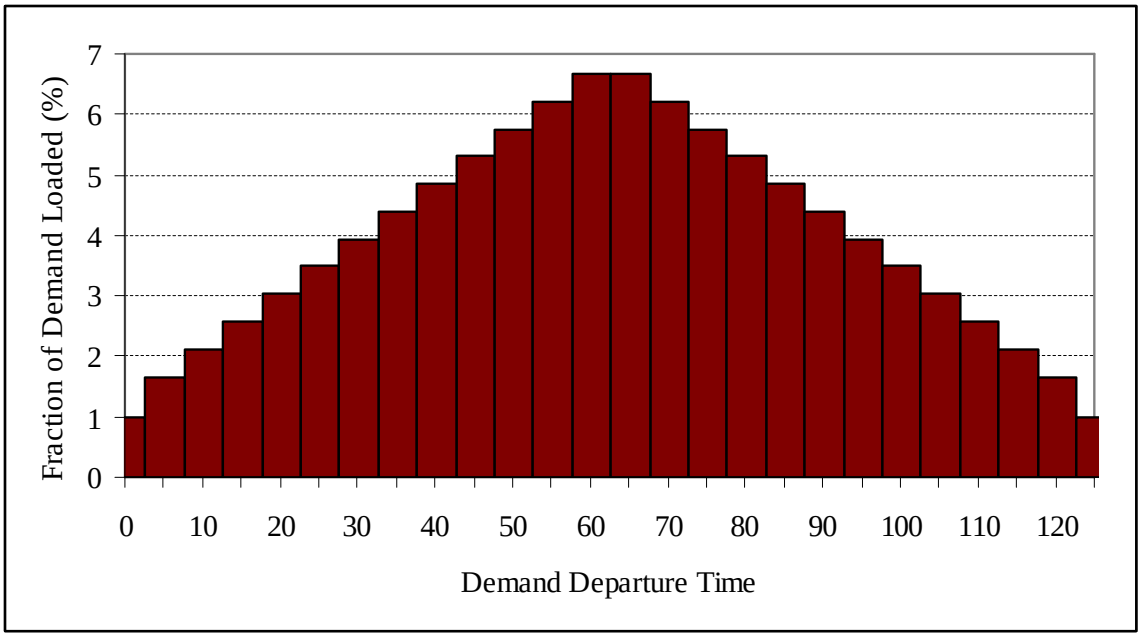

Figure 3.4 Demand temporal profile for all O-D pairs

Given a set of path flows $\boldsymbol{f}$, DYNASMART is used to push the flow through the network and determine experienced link travel times $\boldsymbol{c}(\boldsymbol{f})$ and volumes $x(\boldsymbol{f})$. The first and second link travel time derivatives with respect to flow are then calculated according to equations (3.63) and (3.64), respectively. Two measures of effectiveness are calculated namely, percent relative experienced gap $\tilde{G}_{SO}$ and average vehicle experienced trip time ATT. The algorithm terminates if any of the following three stopping criteria are satisfied: 1) number of violations is less than 50; 2) if iteration is 50; or 3) objective function does not change more than 1% over three consecutive iterations.

3.6.1 The Method of Successive Averages

Before reporting experimental results, we first briefly describe the MSA heuristic. For the MSA to "theoretically" converge, the sequence of step sizes has to satisfy the following two conditions [Robins and Monro (1951); Blum (1954)]:

$$\sum_{k=1}^{\infty} \rho^{(k)} = \infty \tag{3.65}$$

$$\sum_{k=1}^{\infty} \left(\rho^{(k)} \right)^2 < \infty \tag{3.66}$$

A convenient move size sequence satisfying the above two conditions is the reciprocal of the iteration number; i.e. $\rho^{(k)} = 1/k$. With this move size, path assignments $\boldsymbol{f}^{(k)}$ for iteration k may be updated, using the convex combination method, to obtain the path assignments $\boldsymbol{f}^{(k+1)}$ for iteration $(k+1)$ as follows:

$$\boldsymbol{f}^{(k+1)} = \boldsymbol{f}^{(k)} + \frac{1}{k}\left(\boldsymbol{g}^{(k)} - \boldsymbol{f}^{(k)} \right) = \left(1 - \frac{1}{k} \right) \boldsymbol{f}^{(k)} + \frac{1}{k} \boldsymbol{g}^{(k)} \tag{3.67}$$

where $\boldsymbol{g}^{(k)}$ is the auxiliary path assignments obtained by an AON assignment on least-cost paths for iteration k and $(\boldsymbol{g}^{(k)} - \boldsymbol{f}^{(k)})$ is the search direction for iteration k. Equation (3.67) can be alternatively expressed as:

$$f_{r,s,p}^{\tau\,(k+1)} = \begin{cases} \dfrac{k-1}{k} f_{r,s,p}^{\tau\,(k)} & \text{if } p \neq \hat{p} \\ \dfrac{1}{k} g_{r,s,p}^{\tau\,(k)} & \text{if } p = \hat{p} \text{ is a new auxiliary path} \\ \dfrac{k-1}{k} f_{r,s,p}^{\tau\,(k)} + \dfrac{1}{k} g_{r,s,p}^{\tau\,(k)} & \text{if } p = \hat{p} \text{ is an old auxiliary path} \end{cases} \tag{3.68}$$

where $\hat{p}$ is the least-marginal travel time path between $r-s$.

Equation (3.68) makes it clear that what the MSA essentially does is shifting vehicles from inferior (expensive) paths to current optimal (auxiliary) paths for each (r,s,τ) combination at the constant rate of $1/k$. This helps a lot in preventing the allocation of too much traffic to a single path; however, such a constant swap rate, especially in a dynamic setting, penalizes all inferior paths equally regardless of the degree of inferiority relative to the current optimal solution. The MSA method presented above is flow-based. A vehicle-based implementation of the MSA is made possible by recognizing that each vehicle on a non-optimal path p will switch to an optimal (auxiliary) path $\hat{p}$ with a probability $P(p) = 1/k$. The assignment update step can then be expressed as follows:

DO for every (r,s,τ) combination

  Scan all vehicles $j \in (r,s,\tau)$ and extract active path set $\bar{P}_{r,s}^{\tau\,(k)}$

  Find least-cost marginal path $\hat{p} \in P_{r,s}^{\tau\,(k)}$ and add it to the active path, $\bar{P}_{r,s}^{\tau\,(k)} = \bar{P}_{r,s}^{\tau\,(k)} \cup \hat{p}$

  DO for each path $p \in \bar{P}_{r,s}^{\tau\,(k)}, p \neq \hat{p}$

    Compute the switching probability $P(p) = 1/k$

    DO for each vehicle $j \in p \neq \hat{p}$

      Draw a random number $r \in (0,1)$

      IF $r < P(p)$ THEN

        Switch vehicle j to path $\hat{p}$

      ENDIF

    END DO

  END DO

END DO

Figure 3.5 Vehicle-based implementation of the MSA solution heuristic

3.6.2 Experiments on a Small-Size Network – Nine-node Network

This set of experiments is done to primarily test the effect of using analytical marginals instead of numerical marginals. The experiments are conducted on the Nine-node (all actuated) network shown in Figure 3.6. The links are two-way lanes with a length of 0.5 miles. We are interested in sending 9250 vehicles flow from node 1 to node 9 under an SO-DTA assignment rule. Figure 3.7 presents the results of the vehicle-based MSA procedure for both analytical and numerical marginals at convergence.

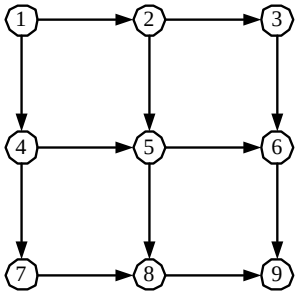

Figure 3.6 Nine-node network

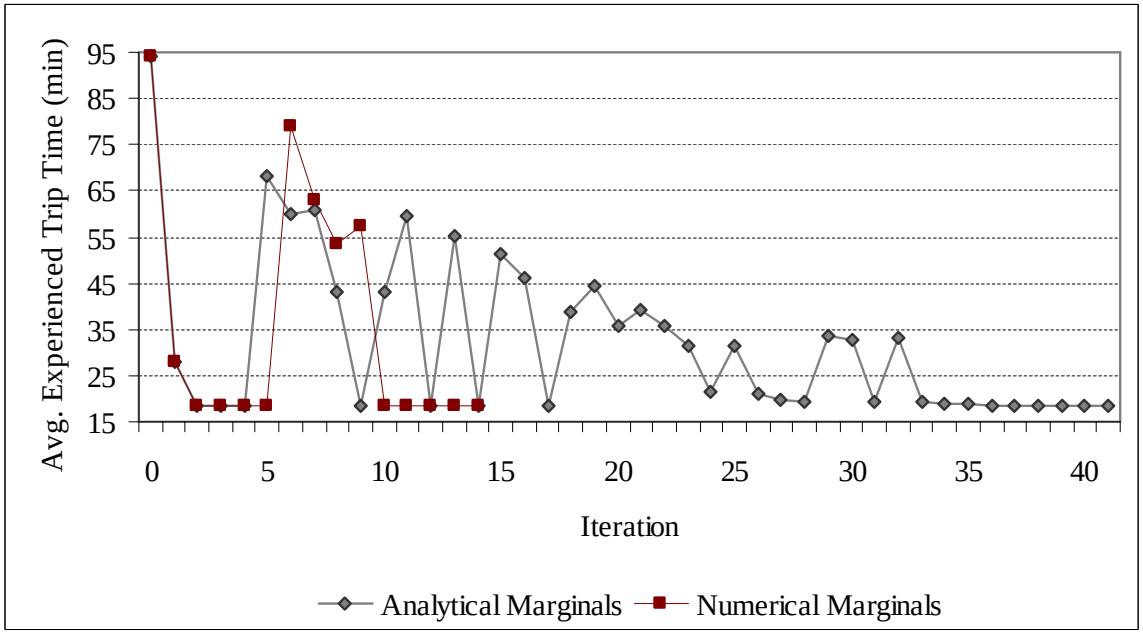

Figure 3.7 Average experienced trip time convergence pattern using MSA

The minimum average experienced trip time is 18.57 min for both marginal calculation methods. The numerical method required 15 iterations to converge (as per the stopping

criteria listed above) compared with 41 iterations for the analytical method. The convergence pattern of the relative gap $\tilde{G}$ (Figure 3.8) also gives the (false) impression that numerical marginals leads to better solution quality. However, if we let both algorithms to run for 50 iterations (Figure 3.9), one can no longer make the same conclusion. Analytical marginals clearly resulted in a stable solution whereas numerical marginals resulted in more fluctuations. Similarly, analyzing the extended convergence pattern for the relative gap (Figure 3.10) also shows that analytical marginals results in a stable solution while numerical marginals caused the relative gap to fluctuate and never stabilize.

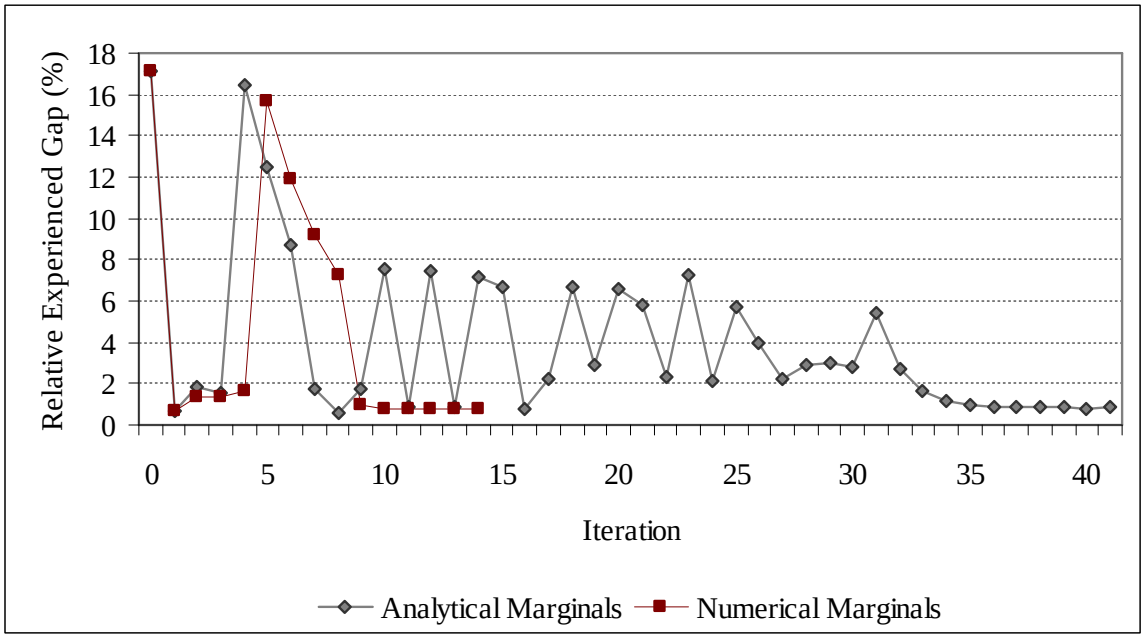

Figure 3.8 Relative experienced gap convergence pattern using MSA

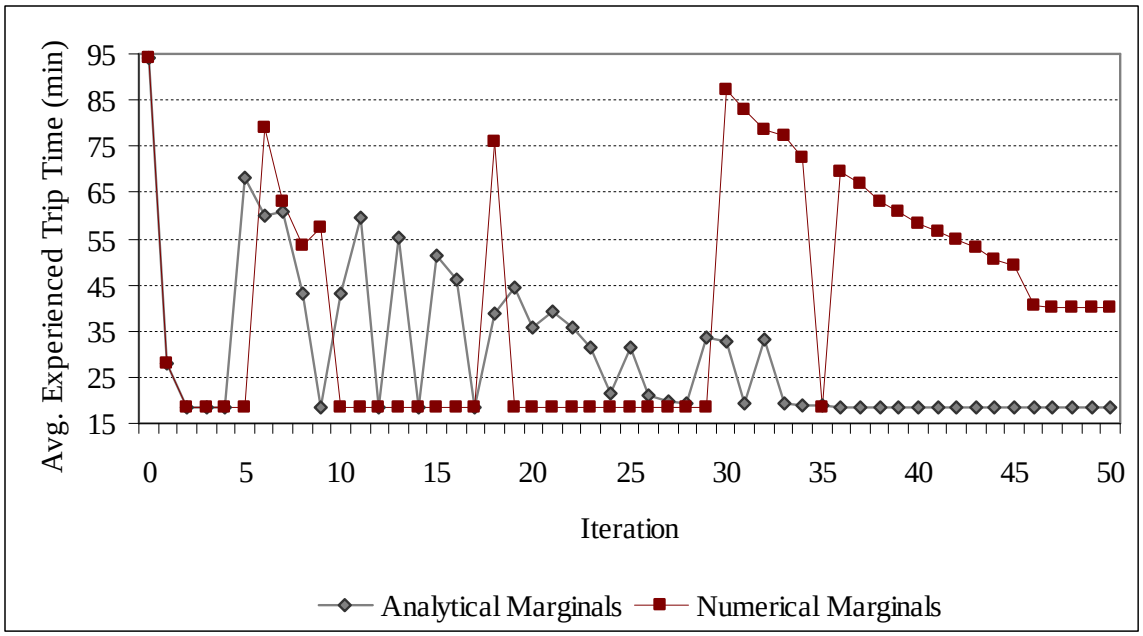

Figure 3.9 Average experienced trip times extended convergence pattern using MSA

The previous results have demonstrated that MSA fluctuates considerably before stabilizing. In fact, Figure 3.10 provides an example where the automatic step size selection used by the MSA is uninformative enough to guarantee descent in objective function, even when applied to a very small network. On the contrary, ORS almost guarantees descent at every iteration due to the exploitation of local information and derivative information (Figure 3.11). ORS method resulted in 18.6 min with a relative gap of 0.56%. Figure 3.12 actually validates the way ORS heuristic works, which aims at equilibrating (in terms of travel time marginals) flows at every iteration by calculating the optimal shifts for all active paths simultaneously. It should be noted that, due to column generation techniques, the gap measure cannot be considered solely as the measure of proximity to optimality since we did not enumerate all the paths in the network. Therefore, the gap measure reported in these figures represents the gap across all active paths only and not the theoretical gap across the network. Hence, when making conclusions regarding optimality conditions in this thesis, it will be made after jointly considering average travel times and relative gaps.

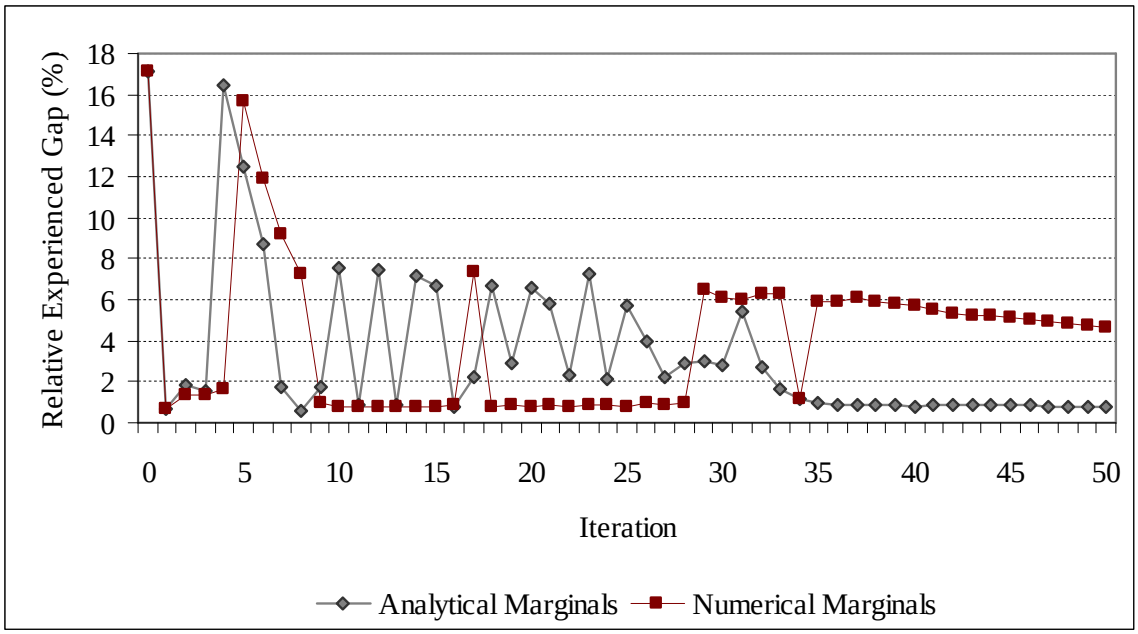

Figure 3.10 Relative experienced gap extended convergence pattern using MSA

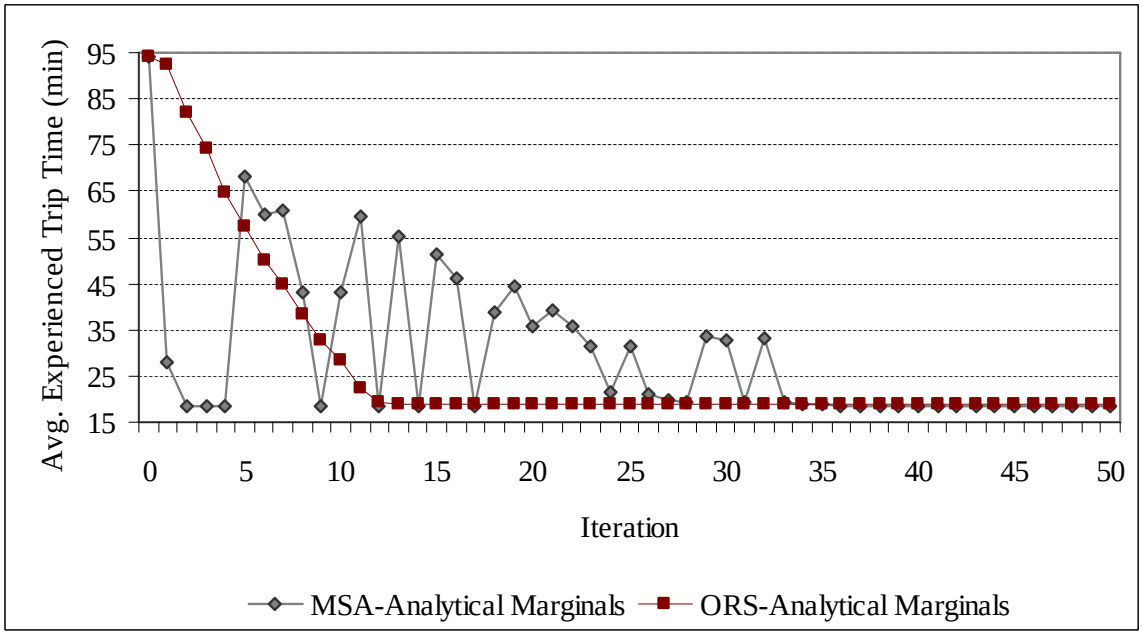

Figure 3.11 Comparison of the experienced average trip time
extended convergence patterns for MSA and ORS

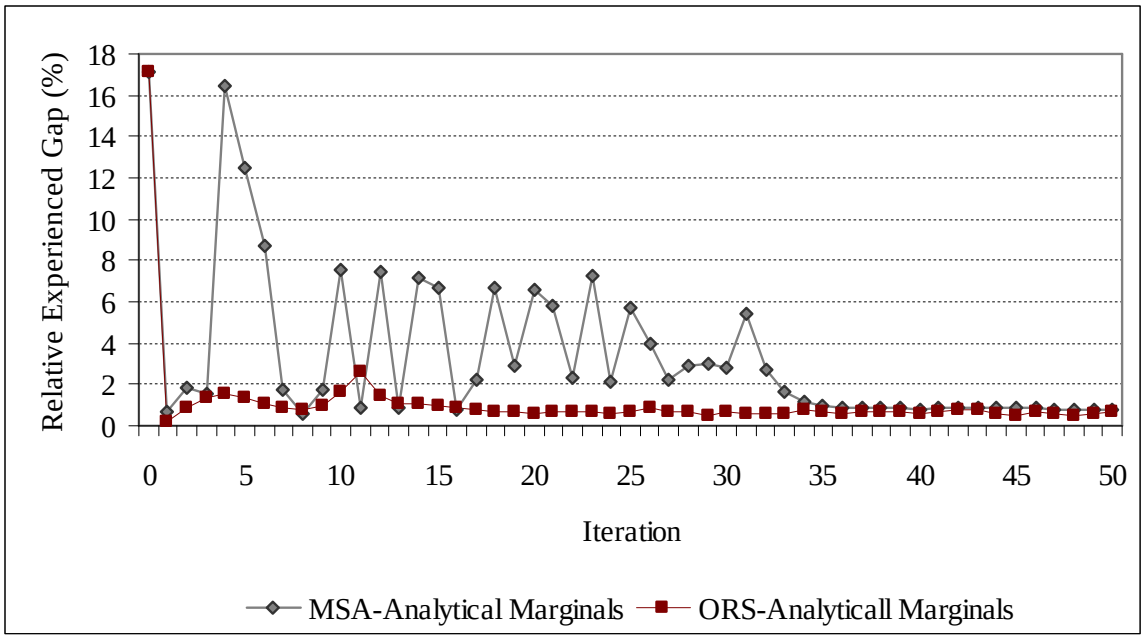

Figure 3.12 Relative experienced gap extended convergence patterns for MSA and ORS

3.6.3 Experiments on a Medium-sized Network – Fort Worth

The second set of experiments is conducted on the Fort Worth network (Figure 3.13), which is extracted from the Texas network and corresponds to one sector of Interstate Highway I-35W between I-20 and I-30, with a surrounding network of signalized arterials and stop/yield controlled local streets on both sides of the freeway. The network consists of 191 nodes, 573 links and 13 traffic analysis zones. The zonal layout and its corresponding O-D trip flows are depicted in (Figure 3.14). The objective of these experiments is to compare the ORS heuristic with the MSA heuristic under an SO-DTA assignment.

Analytical marginals are used in these experiments and for the remainder of this dissertation. The comparison is made for three levels of two-hour time-varying demands: 1) 45k vehicles (light congestion); 2) 75k vehicles (moderate congestion), and 3) 105k vehicles (high congestion). Therefore, six simulation runs are generated. Both heuristics are executed for 50 iterations in order to examine whether the solution is following a proper descent direction over these iterations. The solution quality is evaluated primarily according to the average

experienced trip time, with the relative gap measure used as a secondary check due to the use of column generation. Moreover, the relative gap can be misleading for low demand, since small gaps are easily obtained in the first few iterations without exhausting all the possible solutions (paths), and hence the algorithm might stop prematurely.

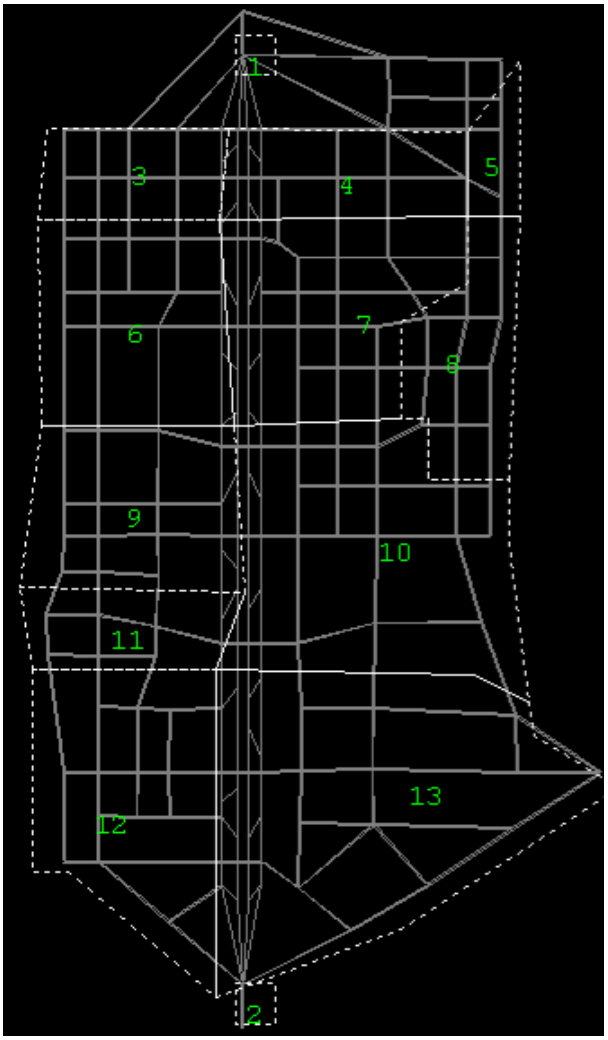

Figure 3.13 Fort Worth network

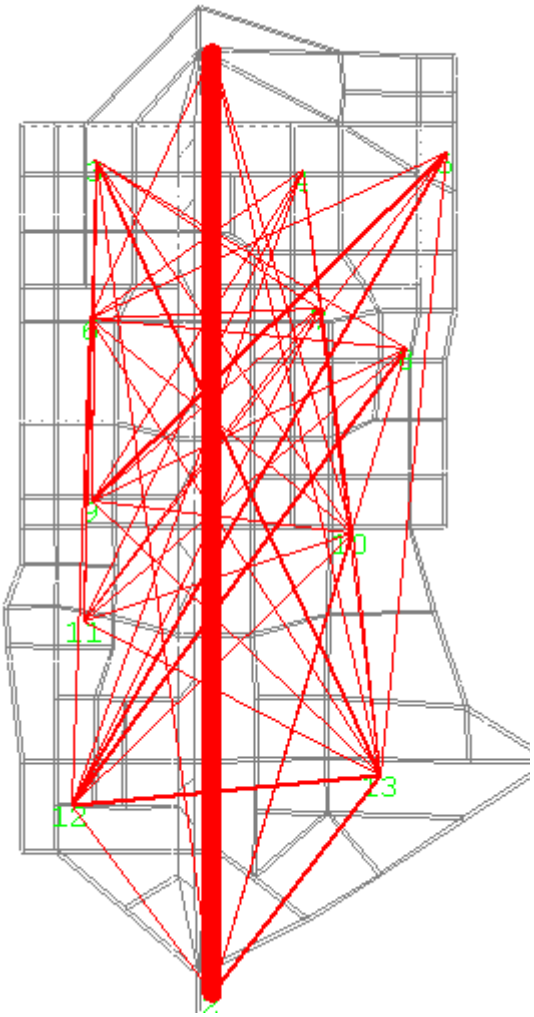

Figure 3.14 O-D flows in Fort Worth network

Figure 3.15 and Figure 3.16 depict the results of performing 50 iterations of the MSA and ORS heuristics on the Fort Worth network. Both heuristics showed nice convergence properties and achieved very similar results. The minimum average trip time under MSA is 4.53 min and is achieved at iteration 50 with a corresponding relative gap of 5.4%, which

suggests that descent is being achieved, on average. While such a conclusion contradicts the observations made earlier (i.e. MSA fluctuations) for the Nine-node network, the descent is mainly attributed to the light traffic conditions in the network as becomes apparent under heavier demand conditions. The ORS procedure, on the other hand, converged faster to its optimal solution of 4.56 min, achieved after 24 iterations, and a relative gap of 5.02%.

Figure 3.17 and Figure 3.18 depict similar results as above, for the two-hourly demand level of 75k vehicles. In this experiment, MSA starts to show its brittle nature, as can be seen from the fluctuations in both average trip times and relative gaps. For example, the minimum average trip time under MSA is 5.14 min and is achieved after 43 iterations with a corresponding relative gap of 9.86%. The average trip time is 5.43 min after 50 iterations, or a 10% increase. Still the performance can be deemed satisfactory. On the other hand, ORS heuristic retains its nice convergence pattern despite the 66% increase in demand level. The minimum trip time is achieved after 23 iterations with a relative gap of 7.07% and the trip time is still at 4.99 min after 50 iterations, despite a slight increase in the relative gap.

Figure 3.19 and Figure 3.20 depict the results for the two-hourly demand level of 105k vehicles. It is at high congestion levels that MSA fails to perform adequately. For example, the minimum average trip time under MSA is 6.99 min and is achieved after 27 iterations with a corresponding relative gap of 14.18%. The average trip time increases by 34% to 9.39 min after 50 iterations, despite a reduction in relative gap to 8.62%. The ORS heuristic, in contrast, retains its faster and smoother convergence pattern. The minimum trip time of 6.39 min is achieved after 38 iterations with a corresponding relative gap of 4.94%. After 50 iterations, the average trip time only increased by 0.5% to 6.43 min and the relative gap only increased by 4% to 5.17%.

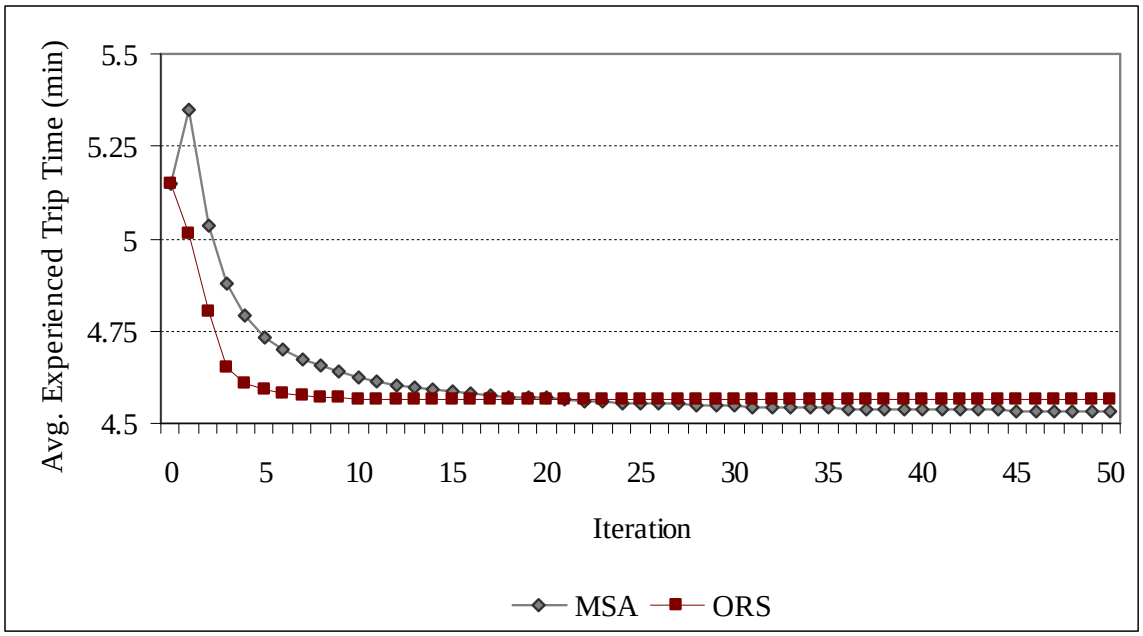

Figure 3.15 Average experienced trip time extended convergence pattern for MSA and ORS – light demand

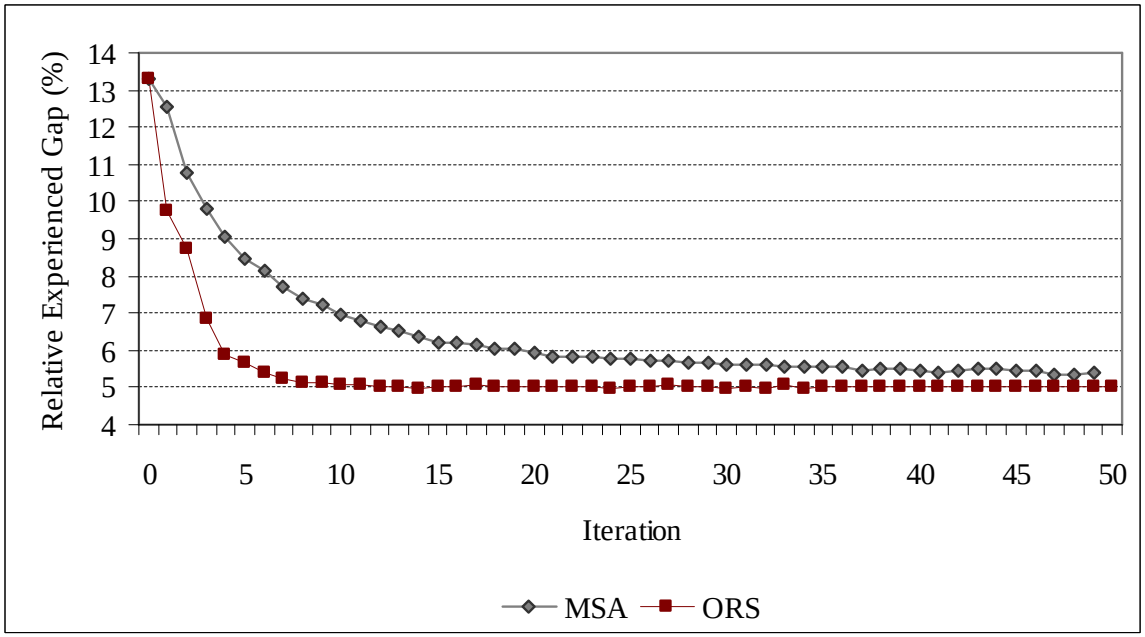

Figure 3.16 Relative experienced gap extended convergence pattern for MSA and ORS – light demand

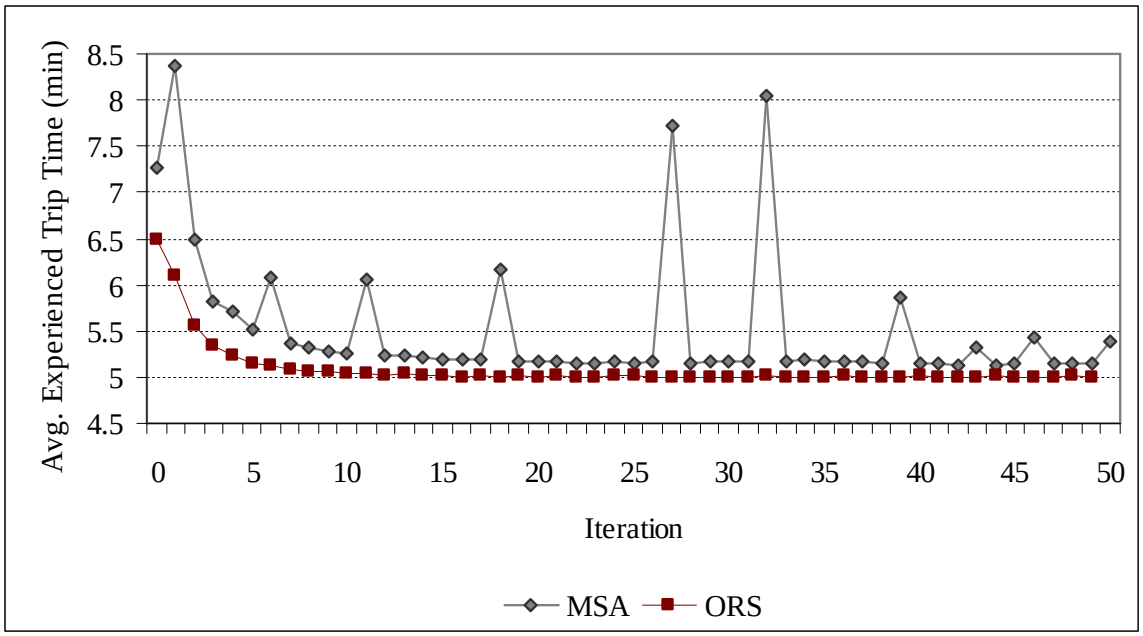

Figure 3.17 Average experienced trip time extended convergence pattern for MSA and ORS – medium demand

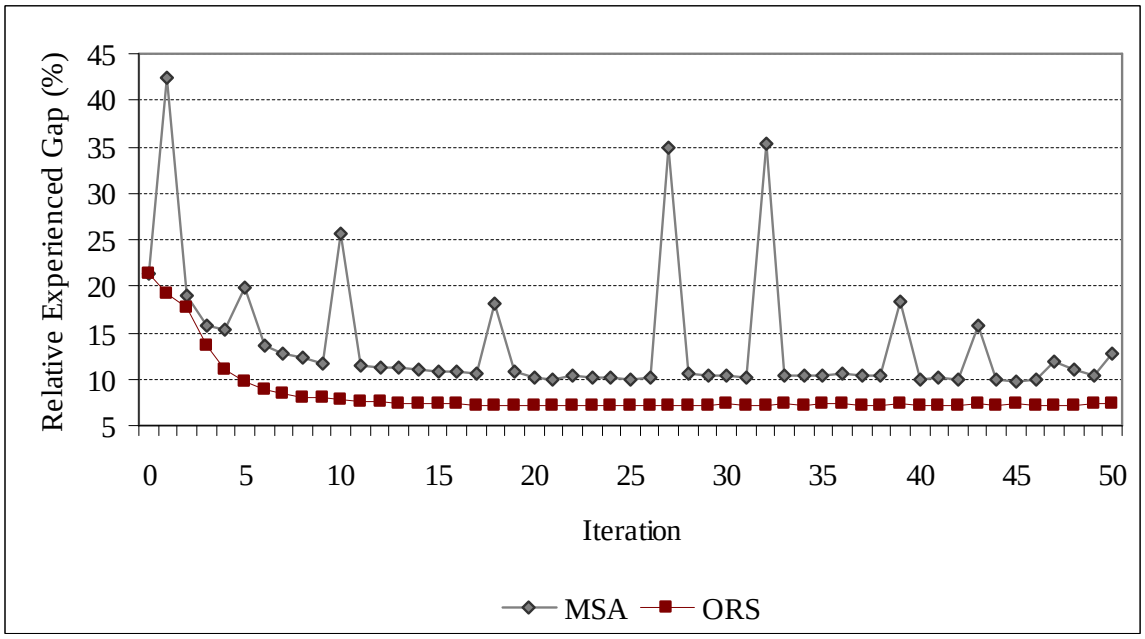

Figure 3.18 Relative experienced gap extended convergence pattern for MSA and ORS – medium demand

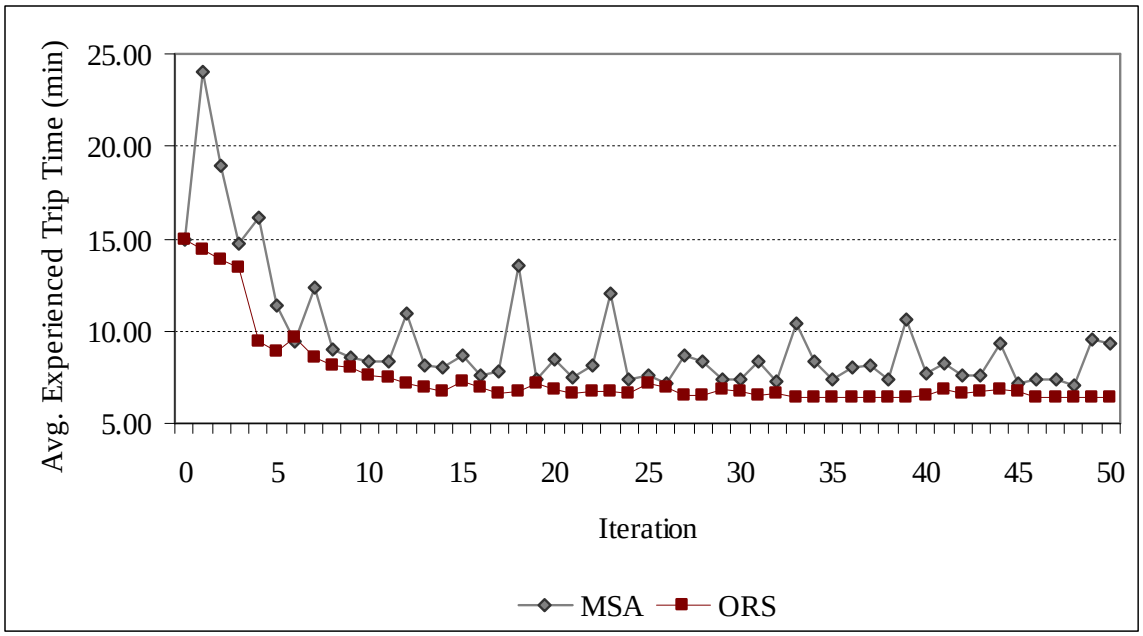

Figure 3.19 Average experienced trip time extended convergence pattern for MSA and ORS – heavy demand

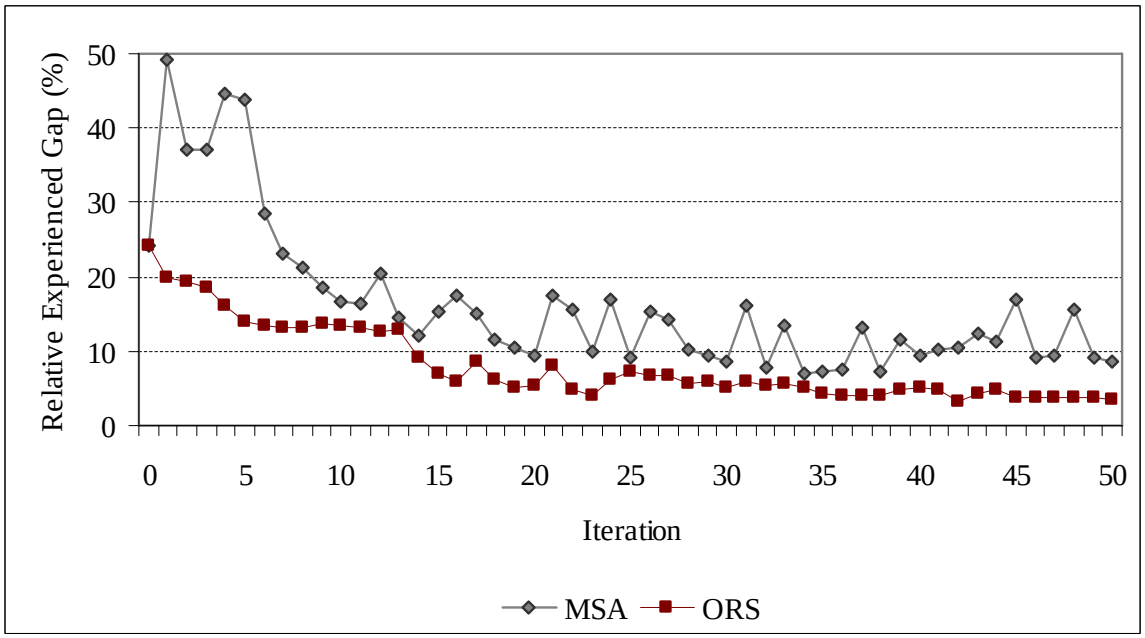

Figure 3.20 Relative experienced gap extended convergence pattern for MSA and ORS – heavy demand

The results for all the experiments in this section are presented in Table 3.1. The ORS heuristic easily outperformed MSA under the three levels of time-varying O-D demand. Unlike the MSA heuristic, the ORS heuristic showed consistent convergence properties at all of demand levels considered. Nonetheless, MSA has been shown to perform satisfactorily under light to moderate congestion levels, above which fluctuations take over.

Table 3.1 Summary of simulation results for Fort Worth network

Demand Level (Vehicles)	*Solution Heuristic*	*Optimal Results*		*Results at Iteration 50*	
		Average Trip Time (min)	*Relative Gap (%)*	*Average Trip Time (min)*	*Relative Gap (%)*
45,000	MSA	4.53 @ iteration 50	5.40	4.53	5.40
	ORS	4.56 @ iteration 24	5.02	4.56	5.05
75,000	MSA	5.14 @ iteration 43	9.86	5.43	10.04
	ORS	4.99 @ iteration 23	7.07	4.99	7.27
105,000	MSA	6.99 @ iteration 27	14.18	9.39	8.62
	ORS	6.39 @ iteration 38	4.94	6.42	5.07

3.6.4 Experiments on a Large-sized Network – Knoxville

While the performance of the ORS procedure is quite impressive for the Nine-node and Fort Worth networks, it is important to test it on an actual large-scale network. The Knoxville, TN network is considered for this third set of experiments. The network consists of 1347 nodes, 3004 links and 356 traffic analysis zones (Figure 3.21). About 200k vehicles are loaded in two hours in this experiment. A schematic of the O-D flows is shown in Figure 3.22.

Figure 3.21 Knoxville, TN network

Figure 3.22 O-D flows in Knoxville network

The results showed in Figure 3.23 and Figure 3.24, confirmed that even on larger more congested networks, the ORS heuristic exhibits similar convergence characteristics as in the earlier experiments. The average network experienced trip time improved with almost every iteration of the heuristic, reducing the average experienced trip time from 22.49 min to 10.74 in 43 iterations (at convergence) with the average trip time remaining virtually unchanged (10.8 min) after 50 iterations (Figure 3.23). In contrast, MSA only managed to reduce the trip time to 12.22 min (after 42 iterations), which got worse to 14.19 min after 50 iterations.

The relative gap also exhibited similar convergence properties, reaching 4.38% after 43 iterations (at convergence) and remaining virtually unchanged after 50 iterations (Figure 3.24). In contrast, MSA could only reduce relative gap to 7.4% after 42 iterations (at convergence), which got worse to 9.2% after 50 iterations.

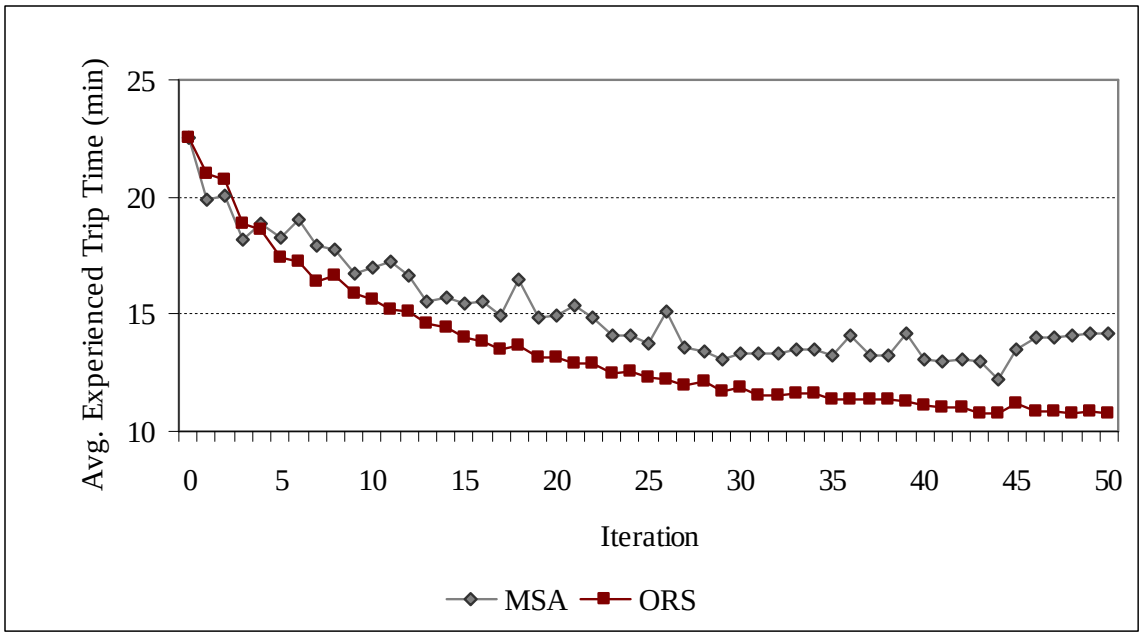

Figure 3.23 Convergence pattern of ORS for the Knoxville, TN network.

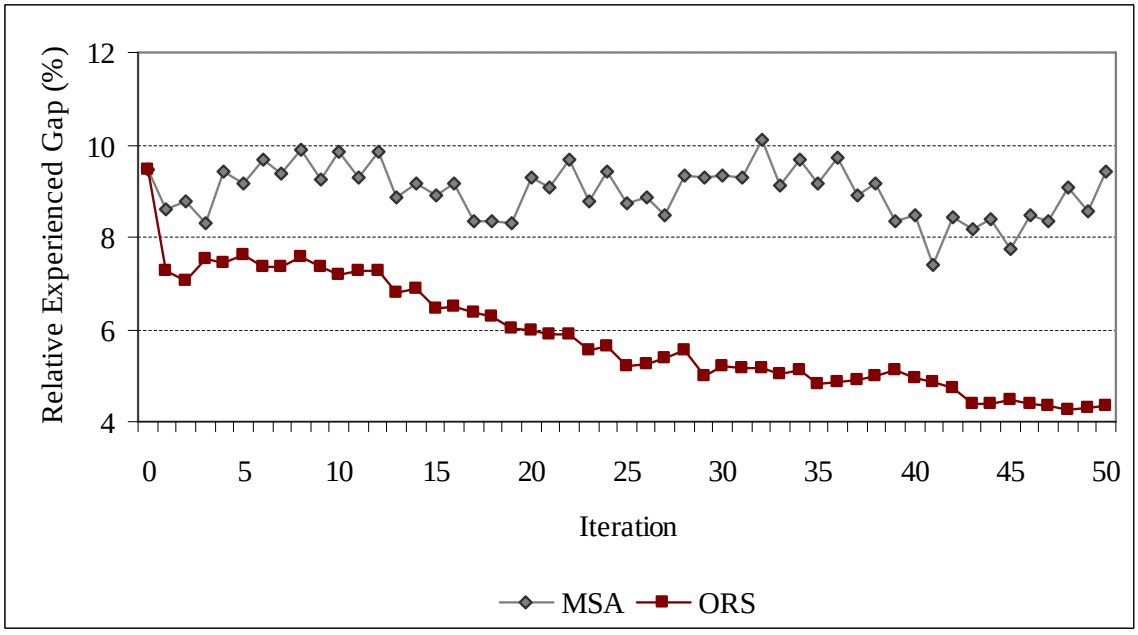

Figure 3.24 Convergence pattern of ORS for the Knoxville, TN network.

4 OPTIMAL DEMAND-SCHEDULING PROBLEM

This chapter formulates the evacuation models that incorporate demand-scheduling strategies, which aim at spreading the demand over a longer period to prevent network breakdown and facilitate mobility to safety. There are two basic types of evacuation: no-notice and advance-notice. For no-notice evacuations, the approach is to formulate the problem as an MNCT-DTA problem. For advance-notice evacuations, the approach is to formulate the problem as an LNCT-DTA problem, which is a special case of the Fixed Arrival Time (FAT) SO-DTA model introduced by Li (1999). Both approaches involve solving for the joint-optimal departure time, destination, and route choices for evacuees to satisfy the objective at hand. Models that constrain (fix) the departure time and destination choices reduce the evacuation problem to the classical SO-DTA problem, which has been extensively addressed in the literature and briefly in chapter 3.

4.1 INTRODUCTION

In the context of evacuation models, we distinguish between two time measures associated with a vehicle: 1) trip time and 2) evacuation time. The trip time is the time incurred by the vehicle along its journey from origin to destination. The evacuation time, on the other hand, is the total amount of time incurred by a vehicle from the instance an evacuation order is given until it reaches its destination. It is combines wait time at the origin and the actual trip time on the network. To illustrate the difference, assume that an evacuation order has been issued at 10:00 AM. A vehicle that departs at 12:00 PM and reaches its (safety) destination at 6:00 PM incurs a travel time of 6 hours, whereas its evacuation time is 8 hours. The former time measure is generally used in classical SO-DTA models, whereas the latter time measure will be used in the MNCT-DTA model, as will become evident shortly.

The MNCT-DTA and LNCT-DTA problems formulated in this chapter will be transformed, via an appropriate path cost function, to the same structural form of the SO-DTA problem

described in chapter 3. The solution heuristic of the SO-DTA problem developed in chapter 3 will be adapted to solve the "transformed" SO-DTA problems of this chapter. In these two models, evacuees (vehicles) are assumed to adhere to the evacuation guidance information at all times and not switch on their own to different departure times, destinations, and paths.

Ideally, the goal of an evacuation model is to evacuate the network in the least amount of time with evacuees incurring the least amount of actual travel time. These two objectives are somewhat conflicting due to the nonlinear and non-unique solutions of path-based DTA models[8]. The first objective, which is equivalent to the MNCT-DTA objective, tends to force evacuees to depart earlier to reach safety faster, whereas the second objective, which is equivalent to the SO-DTA objective, tends to force the evacuees to depart later to avoid congestion and consequently minimize their trip times. This translates into a bi-objective problem however, instead of solving for the efficient frontier (pareto-optimal), we are interested in one specific point on the frontier. This point corresponds to minimizing the second objective (minimize system trip time) given that the first objective (minimize network clearance time) is optimal. That is, of all the (non-unique) DTA solutions that clear the network at the minimum possible time, we are interested in the solution that incurs the least amount of actual travel time. We refer to this bi-objective problem as the Optimal Demand-Scheduling (ODS) DTA problem.

4.2 MINIMUM NETWORK CLEARANCE TIME PROBLEM

The main objective of an evacuation model is to minimize the network clearance time W, i.e. the time required for the last evacuee to reach safety. However, minimizing the network clearance time is not trivial. Let $\eta(t)$ be the cost incurred by the system when a vehicle exits the network in time step t. Assuming that $\eta(1) \le \cdots \le \eta(t) \le \cdots \le \eta(T)$ and $\eta(t) = t$, the

[8] Jarvis and Ratliff (1982) prove that the flow pattern that minimizes the average evacuation time also minimizes the network clearance time and the average network trip time. This is known as the triple optimization theory and is based on the LP nature of network flows.

minimum network clearance time can be found by minimizing the average evacuation time for all evacuees in the system [Hamacher and Tjandra (2002)], i.e.

$$\text{Min } (W) = \text{Min } (T) = \text{Min} \sum_{t=1}^{T} \sum_{s \in \bar{S}} t \cdot I_S(t) \tag{4.1}$$

For a path-based formulation, the objective function in (4.1) becomes:

$$\text{Min } Z(\boldsymbol{f}) = \sum_{\tau} \sum_{s \in \bar{S}} \sum_{r} \sum_{p} \left(\tau + C^{\tau}_{r,s,p} \right) f^{\tau}_{r,s,p} \tag{4.2}$$

The objective function in (4.2) is a modified version of the classical SO-DTA objective and represents the minimization of the total system evacuation time as opposed to the total system time. The term $(\tau + C^{\tau}_{r,\bar{s},p})$ represents the number of departure (or assignment) periods τ, measured from the start of evacuation plus the path trip time $C^{\tau}_{r,\bar{s},p}$, for a given vehicle. Therefore (4.2) essentially measures the total system evacuation time and not the total system trip time as in classical SO-DTA formulations.

Relative to the SO-DTA case, (4.2) has the extra term τ added to the path cost. Defining a new path cost term $\chi^{\tau}_{r,s,p}$ as follows:

$$\chi^{\tau}_{r,s,p} = \left(\tau + C^{\tau}_{r,s,p} \right) \qquad \forall r, s, p, \tau \tag{4.3}$$

transforms (4.2) into an SO-DTA type objective:

$$\text{Min } Z(\boldsymbol{f}) = \sum_{\tau} \sum_{r} \sum_{p} \chi^{\tau}_{r,\bar{s},p} f^{\tau}_{r,\bar{s},p} \tag{4.4}$$

4.2.1 Problem Statement and Formulation

Consider an urban setting represented by the directed graph $G(N, A)$ with multiple origins $r \in R$ and a set of shelter destinations $s \in \bar{S}$ requires evacuation. Assume that the total

demand to be evacuated at each origin, d_r , is known a priori and that the network is empty at start of evacuation. Therefore, the MNCT-DTA problem is to determine the time-dependent path-flow pattern $\boldsymbol{f}^*$ to minimize the network clearance time. In contrast to the classical SO-DTA problem, this model relaxes departure time and destination choice constraints to minimize the network clearance time.

The destination choice in MNCT-DTA model is easily addressed by connecting all safety destinations $s \in \bar{S}$ to a super sink $\bar{s}$ via zero-cost infinite capacity links, effectively transforming the problem to a single destination problem. The actual destination choices for travelers can be inferred from $f^{\tau}_{r,\bar{s},p}$ variables by tracing the node sequence along path p from r to $\bar{s}$ and labeling the penultimate (second to last) node as the actual destination s. The problem is formulated as follows:

Given: $d_r, \bar{s}$

Find: $f^{\tau}_{r,\bar{s},p}$

To:
$$\text{Min } Z(\boldsymbol{f}) = \sum_{\tau}\sum_{r}\sum_{p} \chi^{\tau}_{r,\bar{s},p} f^{\tau}_{r,\bar{s},p} \tag{4.5}$$

Subject to:
$$\sum_{\tau}\sum_{p} f^{\tau}_{r,\bar{s},p} = d_r \qquad \forall r \tag{4.5a}$$

$$f^{\tau}_{r,\bar{s},p} \geq 0 \qquad \forall r, p, \tau \tag{4.5b}$$

$$\text{DTA Constraints} \tag{4.5c}$$

4.2.2 Optimality Conditions

The optimality conditions of program (4.5) are studied to investigate the underlying assignment principle, which in turn will shape the solution algorithm. Let $\boldsymbol{L}(\boldsymbol{f}, \hat{\boldsymbol{\pi}})$ be the Lagrangian of program (4.5), where $\hat{\boldsymbol{\pi}}$ denote the vector of Lagrangian variables (or dual

variables) associated with the constraint (4.5a). Remaining constraints will not be part of $\boldsymbol{\Lambda}(\boldsymbol{f}, \hat{\boldsymbol{\pi}})$ since they are definitional constraints and are not an explicit function of the path-flow assignments.

$$\text{Min}\,\boldsymbol{\Lambda}(\boldsymbol{f}, \hat{\boldsymbol{\pi}}) = \sum_{\tau}\sum_{r}\sum_{p} \chi^{\tau}_{r,\bar{s},p} f^{\tau}_{r,\bar{s},p} + \sum_{r} \hat{\boldsymbol{\pi}}_{r,\bar{s}} \left(d_r - \sum_{\tau}\sum_{p} f^{\tau}_{r,\bar{s},p} \right) \tag{4.6}$$

Subject to: $$f^{\tau}_{r,\bar{s},p} \geq 0 \qquad \forall r, p, \tau \tag{4.6a}$$

$$\text{DTA Constraints} \tag{4.6b}$$

The necessary conditions for a minimum of this program are given by the first-order conditions for a stationary point of the Lagrangian program (4.6). The first order optimality conditions for this system are:

$$\frac{\partial \boldsymbol{\Lambda}(\boldsymbol{f}, \hat{\boldsymbol{\pi}})}{\partial f^{\tau}_{r,\bar{s},p}} \geq 0 \qquad \forall r, p, \tau \tag{4.7a}$$

$$f^{\tau}_{r,\bar{s},p} \frac{\partial \boldsymbol{\Lambda}(\boldsymbol{f}, \hat{\boldsymbol{\pi}})}{\partial f^{\tau}_{r,\bar{s},p}} = 0 \qquad \forall r, p, \tau \tag{4.7b}$$

$$\frac{\partial \boldsymbol{\Lambda}(\boldsymbol{f}, \hat{\boldsymbol{\pi}})}{\partial \hat{\pi}_{r,\bar{s}}} = 0 \qquad \forall r \tag{4.7c}$$

$$f^{\tau}_{r,\bar{s},p} \geq 0 \qquad \forall r, p, \tau \tag{4.7d}$$

$$\text{DTA Constraints} \tag{4.7e}$$

The term $\partial \boldsymbol{\Lambda}(\boldsymbol{f}, \hat{\boldsymbol{\pi}}) / \partial f^{\tau}_{r,\bar{s},p}$ may be derived further with respect to a random flow variable $f^{\dot{\tau}}_{\dot{r},\bar{s},\dot{p}}$ as follows:

$$\frac{\partial \boldsymbol{\Lambda}(f, \hat{\boldsymbol{\pi}})}{\partial f^{\dot{\tau}}_{\dot{r},\bar{s},\dot{p}}} = \dot{\tau} + \underbrace{C^{\dot{\tau}}_{\dot{r},\bar{s},\dot{p}} + \frac{\partial}{\partial f^{\dot{\tau}}_{\dot{r},\bar{s},\dot{p}}} \sum_{\tau}\sum_{r}\sum_{p} C^{\tau}_{r,\bar{s},p}}_{\tilde{C}^{\dot{\tau}}_{\dot{r},\bar{s},\dot{p}}} - \hat{\pi}_{\dot{r},\bar{s}} \tag{4.8}$$

Define $\tilde{\chi}^{\tau}_{r,\bar{s},p}$ as:

$$\tilde{\chi}^{\tau}_{r,\bar{s},p} = \tau + \tilde{C}^{\tau}_{r,\bar{s},p} \tag{4.9}$$

The term $\tilde{\chi}^{\tau}_{r,s,p}$ may be interpreted as the marginal cost incurred by the MNCT-DTA system due to an additional vehicle departing from r to s along path p at departure time τ. We will refer to the term $\tilde{\chi}^{\tau}_{r,\bar{s},p}$ as MNCT-DTA marginal cost from this point onwards. Therefore, the optimality conditions for the Lagrangian program (4.6) are:

$$f^{\tau}_{r,\bar{s},p}\left(\tilde{\chi}^{\tau}_{r,\bar{s},p} - \hat{\pi}_{r,\bar{s}}\right) = 0 \qquad \forall r, p, \tau \tag{4.10a}$$

$$\tilde{\chi}^{\tau}_{r,\bar{s},p} - \hat{\pi}_{r,\bar{s}} \geq 0 \qquad \forall r, p, \tau \tag{4.10b}$$

$$\sum_{\tau}\sum_{p} f^{\tau}_{r,\bar{s},p} = d_r \qquad \forall r \tag{4.10c}$$

$$f^{\tau}_{r,\bar{s},p} \geq 0 \qquad \forall r, p, \tau \tag{4.10d}$$

DTA Constraints (4.10e)

4.2.3 Reformulation via a Gap Function

Smith (1979) showed that solving a program like (4.5) is equivalent to finding a flow pattern $\boldsymbol{f}$ that satisfies optimality conditions (4.10):

Given: $d_r, \bar{s}$

Find: $f^{\tau}_{r,\bar{s},p}$

Such that:
$$\sum_{\tau}\sum_{r}\sum_{p} f^{\tau}_{r,\bar{s},p}\left(\tilde{\chi}^{\tau}_{r,\bar{s},p} - \hat{\pi}_{r,\bar{s}}\right) \geq 0 \qquad \forall r, p, \tau \tag{4.11a}$$

$$\sum_{\tau}\sum_{p} f^{\tau}_{r,\bar{s},p} = d_r \qquad \forall r \tag{4.11b}$$

$$f^{\tau}_{r,\bar{s},p} \geq 0 \qquad \forall r, p, \tau \tag{4.11c}$$

DTA Constraints (4.11d)

As in chapter 3, the VI problem in (4.11) will be reformulated, via a gap function, as an equivalent NMP whose global minima coincide with those of program (4.5). In this regards, define a gap function for the MNCT-DTA problem as follows:

$$G_{\text{MNCT}} = \sum_{\tau}\sum_{r}\sum_{p} f^{\tau}_{r,\bar{s},p}\left(\tilde{\chi}^{\tau}_{r,\bar{s},p} - \hat{\pi}_{r,\bar{s}}\right) \tag{4.12}$$

G_{MNCT} provides a measure of the violation of the MNCT-DTA optimality conditions in terms of the difference between the actual path marginal travel times and the least-cost path marginal travel time evaluated at any given time-varying path flow pattern $\boldsymbol{f}$. It is evident that the difference vanishes when the time-varying path flow vector $\boldsymbol{f}$ satisfies optimality conditions (4.10). Thus, solving the MNCT-DTA problem can be also viewed as a process of finding the path flow vector $\boldsymbol{f}^*$ such that $G_{\text{MNCT}}(\boldsymbol{f}^*) = 0$. Therefore, an equivalent NMP problem is

Given: $d_r, \bar{s}$

Find: $f^{\tau}_{r,\bar{s},p}$

To: $$\text{Min } G_{\text{MNCT}}(\boldsymbol{f}) = \sum_{\tau}\sum_{r}\sum_{p} f^{\tau}_{r,\bar{s},p}\left(\tilde{\chi}^{\tau}_{r,\bar{s},p} - \hat{\pi}_{r,\bar{s}}\right) \tag{4.13}$$

Subject to: $$\left(\tilde{\chi}^{\tau}_{r,\bar{s},p} - \hat{\pi}_{r,s}\right) \geq 0 \qquad \forall r, p, \tau \tag{4.13a}$$

$$\sum_{\tau}\sum_{p} f^{\tau}_{r,\bar{s},p} = d_r \qquad \forall r \tag{4.13b}$$

$$f^{\tau}_{r,\bar{s},p} \geq 0 \qquad \forall r, p, \tau \tag{4.13c}$$

DTA Constraints (4.13d)

Associated with G_{MNCT} is the relative gap for this model $\tilde{\tilde{G}}_{\text{MNCT}}$:

$$\tilde{\tilde{G}}_{\text{MNCT}} = \frac{G_{\text{MNCT}}}{\sum_r \left[\left(\sum_\tau \sum_p f_{r,\bar{s},p}^{\tau} \right) \hat{\pi}_{r,\bar{s}} \right]} \tag{4.14}$$

4.2.4 MNCT-DTA Solution Algorithm

The transformed MNCT-DTA problem is analogous in structure to the SO-DTA problem, which means that the efficient ORS algorithm developed for the SO-DTA problem in chapter 3 can be adapted to solve the MNCT-DTA problem. The algorithm still needs to address the departure time choice before being suitable for solving the MNCT-DTA problem.

The departure time choice is reflected in constraint (4.13.b). Hence, the ORS procedure must be able to find the optimal shifts across paths and departure times jointly. In other words, ORS needs to consider all feasible path-departure time combinations when computing the optimal shifts. Define the active path-departure time set $\overline{P}_{r,s}$ as:

$$\overline{P}_{r,s} = \left\{ (p,\tau) \mid p \in \overline{P}_{r,s}^{\tau},\ f_{r,s,p}^{\tau} > 0, \forall p,\tau \right\}$$

Let $\left|\overline{P}_{r,s}\right|$ represent the total number of path-departure time combinations within $\overline{P}_{r,s}$. Assume that the paths-departure time (p,τ) combinations within $\overline{P}_{r,s}$ are sequentially numbered from 1 to $\left|\overline{P}_{r,s}\right|$. Let $H(\bullet)$ be a function that maps a given active path-departure-time combination (p,τ) in $\overline{P}_{r,s}$ to a unique index i such that:

$$H(p,\tau) = \left\{ i \mid (p,\tau) \in \overline{P}_{r,s}, 1 \le i \le \left|\overline{P}_{r,s}\right|, H(p_1,\tau_1) \ne H(p_2,\tau_2); \forall (p,\tau), (p_1,\tau_1) \ne (p_2,\tau_2) \right\}$$

Therefore, the optimal shifts under an MNCT-DTA assignment will be:

$$\delta^{\tau}_{r,\bar{s},p} = \frac{\left(\tilde{\chi}^{\dot{\tau}}_{r,\bar{s},\dot{p}} - \tilde{\chi}^{\tau}_{r,\bar{s},p}\right)}{\tilde{\chi}'^{\tau}_{r,\bar{s},p}} + \frac{\left(\tilde{\chi}^{\dot{\tau}}_{r,\bar{s},\dot{p}}\right)}{\tilde{\chi}'^{\tau}_{r,\bar{s},p}} \times \delta^{\dot{\tau}}_{r,\bar{s},\dot{p}} \quad \forall H(p,\tau) \neq \left|\overline{P}_{r,\bar{s}}\right|, H(\dot{p},\dot{\tau}) = \left|\overline{P}_{r,\bar{s}}\right| \quad (4.15)$$

where

$$\delta^{\dot{\tau}}_{r,\bar{s},\dot{p}} = \frac{\left[\sum_{\tau}\sum_{p}\left(\frac{\tilde{\chi}^{\tau}_{r,\bar{s},p} - \tilde{\chi}^{\dot{\tau}}_{r,\bar{s},\dot{p}}}{\tilde{\chi}'^{\tau}_{r,\bar{s},p}}\right)\right]}{1 + \sum_{\tau}\sum_{p}\left(\frac{\tilde{\chi}'^{\dot{\tau}}_{r,\bar{s},\dot{p}}}{\tilde{\chi}'^{\tau}_{r,\bar{s},p}}\right)} \qquad \forall H(p,\tau) \neq \left|\overline{P}_{r,\bar{s}}\right|, H(\dot{p},\dot{\tau}) = \left|\overline{P}_{r,\bar{s}}\right| \qquad (4.16)$$

and

$$\tilde{\chi}'^{\tau}_{r,\bar{s},p} = \frac{\partial \tilde{\chi}^{\tau}_{r,\bar{s},p}}{\partial f^{\tau}_{r,\bar{s},p}} = \frac{\partial\left(\tau + \tilde{C}^{\tau}_{r,\bar{s},p}\right)}{\partial f^{\tau}_{r,\bar{s},p}} = \overline{C}'^{\tau}_{r,\bar{s},p} \quad \forall r,p,\tau \qquad (4.17)$$

The flow-shift matrix $\boldsymbol{\delta}$ must be adjusted for feasibility. The negative flow-shifts will be adjusted first:

$$\tilde{\delta}^{\tau}_{r,\bar{s},p} = \max\left(\delta^{\tau}_{r,\bar{s},p}, -f^{\tau}_{r,\bar{s},p}\right) \quad \forall r,p,\tau; \delta^{\tau}_{r,\bar{s},p} < 0 \qquad (4.18)$$

then the positive flow-shits will be adjusted as follows:

$$\tilde{\delta}^{\tau}_{r,\bar{s},p} = \frac{\sum_{\dot{\tau}}\sum_{\dot{p}} \tilde{\delta}^{\dot{\tau}}_{r,\bar{s},\dot{p}}}{\sum_{\ddot{\tau}}\sum_{\ddot{p}} \delta^{\ddot{\tau}}_{r,\bar{s},\ddot{p}}} \delta^{\tau}_{r,\bar{s},p} \qquad \forall r,p,\tau; \hat{\delta}^{\dot{\tau}}_{r,\bar{s},\dot{p}} < 0; \delta^{\ddot{\tau}}_{r,\bar{s},\ddot{p}} > 0 \qquad (4.19)$$

therefore, the assignments for the next iteration become:

$$f^{\tau}_{r,\bar{s},p}{}^{(k+1)} = f^{\tau}_{r,\bar{s},p}{}^{(k)} + \tilde{\delta}^{\tau}_{r,\bar{s},p}{}^{(k)} \qquad \forall r,p,\tau \qquad (4.20)$$

where $\tilde{\delta}^{\tau}_{r,\bar{s},p}$, is algebraic.

The solution procedure assumes that the traffic control center has perfect information about the evacuation demand at each zone. Once an extreme event is detected requiring the evacuation of the whole network, evacuees are provided with evacuation trip guidance information in the form of when to evacuate (departure time), where to go (destination choice) and which route to take (path choice) in such a way to minimize the network clearance time. The solution algorithm is adapted from the SO-DTA solution algorithm.

The solution algorithm represents a heuristic iterative procedure where the objective function is evaluated and constraints are satisfied through a simulation model. The simulation model is used to move vehicles along their assigned departure times and paths until they reach their destinations, capturing the state of the system in the process. Traffic flow in the simulator is represented using a mesoscopic approach where vehicles are tracked individually but moved in packets according to macroscopic traffic flow relations between average speed and concentration on roadway links. At each iteration, the heuristic defines a search (descent) direction along which the objective function is expected to improve. Step sizes along search direction are determined using second order methods. The steps of the simulation-based MNCT-DTA algorithm are explained in detail below. A vehicle-based implementation is provided in Figure 4.1.

Step 1: Initialization

- Set iteration counter $k = 1$.
- Connect all safety destinations s to a super sink $\bar{s}$ with zero-time infinite capacity links.
- Solve for the time-dependent least MNCT-DTA marginal cost path tree $\hat{P}_{r,\bar{s}}^{\tau\,(k)}$ for all $(r, \bar{s}, \tau)$ combinations assuming free-flow link travel times.
- For each origin r, search across all shortest paths trees $\hat{P}_{r,\bar{s}}^{\tau\,(k)}, \forall \tau$ and select the departure time and path combination (τ^*, p^*) that results in lowest possible MNCT-DTA marginal cost. Let $\hat{p}_{r,\bar{s}}^{(k)}$ be that path, i.e.:

$$\hat{p}_{r,\bar{s}}^{(k)} = \left(p^*, \tau^*\right) \mid \tilde{\chi}_{r,\bar{s},p^*}^{\tau^*\ (k)} = \min_{\tau,p}\left(\tilde{\chi}_{r,\bar{s},p}^{\tau\ (k)}\right)$$

- Perform an AON of the demand d_r onto $\hat{p}_{r,\bar{s}}^{(k)}$ for every r to obtain path assignments $f_{r,\bar{s},p}^{\tau\ (k)}$.

Step 2: Dynamic Network Loading Problem

- Use DYNASMART to simulate path assignments $f_{r,\bar{s},p}^{\tau\ (k)}$.
- Estimate time-dependent link travel times $c(\boldsymbol{f}^{(k)})$ and time-dependent link marginal travel times $\tilde{c}(\boldsymbol{f}^{(k)})$ from simulation results.

Step 3: Update Objective Function

- Compute $\tilde{G}_{\text{MNCT}}^{(k)}$ according to (4.14).
- Compute average evacuation time (proxy for MNCT-DTA objective) as

$$AET^{(k)} = \frac{\sum_{\tau}\sum_{r}\sum_{p} \chi_{r,\bar{s},p}^{\tau\ (k)} f_{r,\bar{s},p}^{\tau\ (k)}}{\sum_{\tau}\sum_{r}\sum_{p} f_{r,\bar{s},p}^{\tau\ (k)}} \tag{4.21}$$

Step 4: Check Convergence

- Count the number of times the condition $\left| f_{r,\bar{s},p}^{\tau\ (k+1)} - f_{r,\bar{s},p}^{\tau\ (k)} \right| > \varepsilon$ is satisfied for all (r,τ,p) combinations and denote that number by $V(\varepsilon)$.
- If $V(\varepsilon) \le \bar{V}(\varepsilon)$ or $k \le \bar{k}$ then terminate the procedure, otherwise set $k = k+1$ and go to step 5.

Step 5: Time-Dependent Least MNCT-DTA Marginal Cost Path Problem

- Solve for the time-dependent least MNCT-DTA marginal cost path tree $\hat{P}_{r,\bar{s}}^{\tau\ (k)}$ for all $(r,\bar{s},\tau)$ combinations using link travel times $c(\boldsymbol{f}^{(k)})$ and link marginal travel times $\tilde{c}(\boldsymbol{f}^{(k)})$.
- Extract $\hat{p}_{r,\bar{s}}^{(k)}$ from $\hat{P}_{r,\bar{s}}^{\tau\ (k)}$ and add it to the active-path set $\bar{P}_{r,\bar{s}}^{(k)}$, for every r.

Step 6: Update of Path Assignments

- Find the optimal un-adjusted shifts $\delta_{r,s,p}^{\tau\,(k)}$ for all paths in active set $\overline{P}_{r,\bar{s}}^{(k)}$ according to equations (4.15) and (4.16).
- Find the optimal adjusted shifts $\tilde{\delta}_{r,s,p}^{\tau\,(k)}$ for all paths in $\overline{P}_{r,\bar{s}}^{(k)}$ according to equations (4.18) and (4.19).
- Update the assignments $f_{r,\bar{s},p}^{\tau\,(k+1)}$ for the next iteration $(k+1)$ using for each (r,τ,p) using (4.20) and go to step 2.

The solution algorithm described above generates only one new solution (path-departure time combination) $\hat{p}_{r,\bar{s}}^{(k)}$, per origin node in the network. While this is the exact theoretical extension of the ORS solution algorithm described in chapter 3 to the MNCT-DTA problem, simulation experiments have shown this algorithm to be rather slow to converge due to the limited number of new solutions (path-departure time combinations) added to the active path-departure time set $\overline{P}_{r,\bar{s}}^{(k)}$ at every iteration. A possible improvement is to add a new (efficient) path for all departure time combinations, resulting in up to $r \times \tau$ new solutions at each iteration. Therefore, step $5'$ will read as follows:

Step 5´: Time-Dependent Least MNCT-DTA Marginal Cost Path Problem

- Solve for the time-dependent least MNCT-DTA marginal cost path tree $\hat{P}_{r,\bar{s}}^{\tau\,(k)}$ for all $(r,\bar{s},\tau)$ combinations using link travel times $c(\boldsymbol{f}^{(k)})$ and link marginal travel times $\tilde{c}(\boldsymbol{f}^{(k)})$.
- Add $\hat{p}_{r,\bar{s}}^{\tau\,(k)}$ for all departure times τ to the active-path set $\overline{P}_{r,\bar{s}}^{(k)}$ for each r.

Set $k = 1$
DO for every r

Set $J^{-} = \{0\}$

Scan all vehicles $j \in d_r$ and extract active path set $\overline{P}_{r,\bar{s}}^{(k)}$

DO for every τ

Find least-cost MNCT-marginal path $\hat{p}_{r,\bar{s}}^{\tau\,(k)}$ and add it to the active path, $\overline{P}_{r,\bar{s}}^{(k)}$

Compute the adjusted algebraic flow shift vector $\tilde{\delta}_{r,\bar{s},p}^{\tau\,(k)}, \forall p \in \overline{P}_{r,\bar{s}}^{(k)}$

DO for each path $p \in \overline{P}_{r,\bar{s}}^{\tau\,(k)}$

IF $\tilde{\delta}_{r,\bar{s},p}^{\tau\,(k)} < 0$ THEN

Randomly select $|\tilde{\delta}_{r,\bar{s},p}^{\tau\,(k)}|$ vehicles from path p and add them to set J^{-}

ENDIF

ENDDO

DO for each path $p \in \overline{P}_{r,\bar{s}}^{\tau\,(k)}$

IF $\tilde{\delta}_{r,\bar{s},p}^{\tau\,(k)} > 0$ THEN

Randomly select $\tilde{\delta}_{r,\bar{s},p}^{\tau\,(k)}$ vehicles from J^{-} and assign them to p

Remove selected vehicles from J^{-}

ENDIF

ENDDO

ENDDO

ENDDO

Figure 4.1 Vehicle-based implementation of the MNCT-DTA solution heuristic

4.3 LATEST NETWORK EVACUATION TIME PROBLEM

The LNCT problem is best suited to the case where a network needs to be evacuated within a predetermined time. For example, it could be the case where evacuees have strict time windows to reach decontamination centers, due to an anthrax attack or a nuclear meltdown. Such a requirement imposes implicit constraints on the set of feasible departure time choices for evacuees. However, no explicit constraints regarding departure times will be specified in this formulation. The only requirement in this case would be that evacuees exit times are less

than or equal to the target network exit time.

4.3.1 Problem Statement and Formulation

Consider an urban setting represented by the directed graph $G(N, A)$ with multiple origins $r \in R$, requires evacuation due to an extreme event. Assume that a set of shelter destinations $s \in \bar{S}$ for that type of event has been identified. Furthermore, assume the total demand to be evacuated at each origin d_r is known and must be evacuated before a target time $\overline{W}$. Additionally, assume that the network is empty at the time of evacuation.

The LNCT-DTA problem is then to determine the time-dependent path-flow pattern $\boldsymbol{f}$ to minimize the total system trip time, while exiting the network by time $\overline{W}$. The destination choice is easily incorporated by connecting all the destinations s to a super-sink $\bar{s}$ via zero-cost infinite capacity links. This transforms the problem from a multi-destination to a single-destination DTA problem. The constraints for this model are similar to that of the SO-DTA model, with one additional constraint regarding network exit times. The problem is formulated as follows:

Given: $d_r, \bar{s}, \overline{W}$

Find: $f^{\tau}_{r,\bar{s},p}$

To:
$$\text{Min } Z(\boldsymbol{f}) = \sum_{\tau}\sum_{r}\sum_{p} C^{\tau}_{r,\bar{s},p} f^{\tau}_{r,\bar{s},p} \tag{4.22}$$

Subject to:
$$\sum_{\tau}\sum_{p} f^{\tau}_{r,\bar{s},p} = d_r \qquad \forall r \tag{4.22a}$$

$$C^{\tau}_{r,\bar{s},p} \le \overline{W} \qquad \forall r, p, \tau \tag{4.22b}$$

$$f^{\tau}_{r,\bar{s},p} \ge 0 \qquad \forall r, p, \tau \tag{4.22c}$$

DTA Constraints (4.22d)

The resulting flow-assignments then form a basis to compute the staging policy for each evacuation zone:

$$\Lambda_{r,\bar{s}}^{\tau} = \frac{\sum_{p} f_{r,\bar{s},p}^{\tau}}{\sum_{\tau}\sum_{p} f_{r,\bar{s},p}^{\tau}} \tag{4.23}$$

where $\Lambda_{r,\bar{s}}^{\tau}$ is the staging policy or the fraction of demand leaving origin r to destination $\bar{s}$ at departure time τ.

4.3.2 Transformation of the LNCT-DTA Problem to an Equivalent SO-DTA Model

Relative to the SO-DTA case, the LNCT-DTA problem has the additional constraint (4.22b). To be able to use the ORS algorithm, we need to remove this constraint from the constraints set. Let $\Re_{r,s}$ be the set of restricted path-departure times combinations for pair $r-s$:

$$\Re_{r,s} = \left\{ (p,\tau) \,|\, \left(\tau + C_{r,s,p}^{\tau} \right) \geq \overline{W}; \forall r,s,p,\tau \right\}$$

Vehicles belonging to $\Re_{r,s}$ must shift to unrestricted path-departure time combinations in order to exit the network before $\overline{W}$. Define a new path cost $\gamma_{r,s,p}^{\tau}$ as follows:

$$\gamma_{r,s,p}^{\tau} = \begin{Bmatrix} C_{r,s,p}^{\tau} & (p,\tau) \notin \Re_{r,s}; \forall r,s,p,\tau \\ C_{r,s,p}^{\tau} + M & (p,\tau) \in \Re_{r,s}; \forall r,s,p,\tau; M >> 0 \end{Bmatrix} \tag{4.24}$$

Where M is a large positive number. We will refer to $\gamma_{r,s,p}^{\tau}$ as the LNCT-DTA (path) cost. Using $\gamma_{r,s,p}^{\tau}$, the objective of the LNCT-DTA problem (4.22) is easily transformed into a structure analogous to an SO-DTA problem as follows:

Given: $d_r, \bar{s}, \overline{W}$

Find: $f^{\tau}_{r,\bar{s},p}$

To: $$\text{Min } Z(\boldsymbol{f}) = \sum_{\tau}\sum_{r}\sum_{p} \gamma^{\tau}_{r,\bar{s},p} f^{\tau}_{r,\bar{s},p} \tag{4.25}$$

Subject to: $$\sum_{\tau}\sum_{p} f^{\tau}_{r,\bar{s},p} = d_r \qquad \forall r \tag{4.25a}$$

$$f^{\tau}_{r,\bar{s},p} \geq 0 \qquad \forall r, p, \tau \tag{4.25b}$$

DTA Constraints (4.25c)

4.3.3 Optimality Conditions

The optimality conditions of program (4.25) are studied to investigate the underlying assignment principle, which in turn will shape the solution algorithm. Let $\boldsymbol{L}(\boldsymbol{f}, \breve{\boldsymbol{\pi}})$ be the Lagrangian of program (4.25), where $\breve{\boldsymbol{\pi}}$ denote the vector of Lagrangian variables (or dual variables) associated with the constraint (4.25a). Remaining constraints will not be part of $\boldsymbol{L}(\boldsymbol{f}, \breve{\boldsymbol{\pi}})$ since they are definitional constraints and are not an explicit function of the path-flow assignments.

Given: $d_r, \bar{s}$

Find: $f^{\tau}_{r,\bar{s},p}$

To: $$\text{Min } \boldsymbol{L}(\boldsymbol{f}, \breve{\boldsymbol{\pi}}) = \sum_{\tau}\sum_{r}\sum_{p} \gamma^{\tau}_{r,\bar{s},p} f^{\tau}_{r,\bar{s},p} + \sum_{r} \breve{\boldsymbol{\pi}}_{r,\bar{s}} \left(d_r - \sum_{\tau}\sum_{p} f^{\tau}_{r,\bar{s},p} \right) \tag{4.26}$$

Subject to: $$f^{\tau}_{r,\bar{s},p} \geq 0 \qquad \forall r, p, \tau \tag{4.26a}$$

DTA Constraints (4.26b)

The necessary conditions for a minimum of this program are given by the first-order

conditions for a stationary point of the Lagrangian program (4.26). The first order optimality conditions for this system are:

$$\frac{\partial \boldsymbol{L}\,(\boldsymbol{f},\breve{\boldsymbol{\pi}})}{\partial f^{\tau}_{r,\bar{s},p}} \geq 0 \qquad \forall r,p,\tau \tag{4.27a}$$

$$f^{\tau}_{r,\bar{s},p}\frac{\partial \boldsymbol{L}\,(\boldsymbol{f},\breve{\boldsymbol{\pi}})}{\partial f^{\tau}_{r,\bar{s},p}} = 0 \qquad \forall r,p,\tau \tag{4.27b}$$

$$\frac{\partial \boldsymbol{L}\,(\boldsymbol{f},\breve{\boldsymbol{\pi}})}{\partial \hat{\pi}_{r,\bar{s}}} = 0 \qquad \forall r \tag{4.27c}$$

$$f^{\tau}_{r,\bar{s},p} \geq 0 \qquad \forall r,p,\tau \tag{4.27d}$$

DTA Constraints (4.27e)

The term $\partial \boldsymbol{L}\,(\boldsymbol{f},\breve{\boldsymbol{\pi}})/\partial f^{\tau}_{r,\bar{s},p}$ may be derived further with respect to a random flow variable $f^{\dot{\tau}}_{\dot{r},\bar{s},\dot{p}}$ as follows:

$$\frac{\partial \boldsymbol{L}\,(f,\hat{\boldsymbol{\pi}})}{\partial f^{\dot{\tau}}_{\dot{r},\bar{s},\dot{p}}} = \begin{cases} \underbrace{M + C^{\dot{\tau}}_{\dot{r},\bar{s},\dot{p}} + \frac{\partial}{\partial f^{\dot{\tau}}_{\dot{r},\bar{s},\dot{p}}}\sum_{\tau}\sum_{r}\sum_{p} C^{\tau}_{r,\bar{s},p}}_{\tilde{C}^{\dot{\tau}}_{\dot{r},\bar{s},\dot{p}}} - \breve{\boldsymbol{\pi}}_{\dot{r},\bar{s}}; & (\dot{p},\dot{\tau}) \in \Re_{r,\bar{s}} \\ \underbrace{C^{\dot{\tau}}_{\dot{r},\bar{s},\dot{p}} + \frac{\partial}{\partial f^{\dot{\tau}}_{\dot{r},\bar{s},\dot{p}}}\sum_{\tau}\sum_{r}\sum_{p} C^{\tau}_{r,\bar{s},p}}_{\tilde{C}^{\dot{\tau}}_{\dot{r},\bar{s},\dot{p}}} - \breve{\boldsymbol{\pi}}_{\dot{r},\bar{s}}; & (\dot{p},\dot{\tau}) \notin \Re_{r,\bar{s}} \end{cases} \tag{4.28}$$

Define $\tilde{\gamma}^{\tau}_{r,\bar{s},p}$ as:

$$\tilde{\gamma}^{\tau}_{r,\bar{s},p} = \begin{cases} M + \tilde{C}^{\dot{\tau}}_{\dot{r},\bar{s},\dot{p}}; & (p,\tau) \in \Re_{r,\bar{s}};\ \forall r,p,\tau;\ M >> 0 \\ \tilde{C}^{\dot{\tau}}_{\dot{r},\bar{s},\dot{p}}; & (p,\tau) \notin \Re_{r,\bar{s}};\ \forall r,p,\tau \end{cases}$$

Analogous to the term $\tilde{\chi}^{\tau}_{r,\bar{s},p}$, the term $\tilde{\gamma}^{\tau}_{r,\bar{s},p}$ can be interpreted as the marginal cost incurred by the LNCT-DTA system due to an additional vehicle departing from r to s along path p at departure time τ. We will refer to the term $\tilde{\gamma}^{\tau}_{r,\bar{s},p}$ as LNCT-DTA (path) marginal

cost. Therefore, the optimality conditions for the Lagrangian program (4.26) are:

$$f^{\tau}_{r,\bar{s},p}\left(\tilde{\gamma}^{\tau}_{r,\bar{s},p} - \breve{\pi}_{r,\bar{s}}\right) = 0 \qquad \forall r, p, \tau \tag{4.29a}$$

$$\tilde{\gamma}^{\tau}_{r,\bar{s},p} - \breve{\pi}_{r,\bar{s}} \geq 0 \qquad \forall r, p, \tau \tag{4.29b}$$

$$f^{\tau}_{r,\bar{s},p} \geq 0 \qquad \forall r, p, \tau \tag{4.29c}$$

DTA Constraints (4.29d)

4.3.4 Reformulation to a Nonlinear Minimization Program via a Gap Function

The LNCT-DTA problem is equivalent to finding a flow pattern $\boldsymbol{f^*}$ that satisfies conditions (4.29), which may be compactly expressed as a VI:

Given: $d_r, \overline{W}, \bar{s}$

Find: $f^{\tau}_{r,\bar{s},p}$

Such that:
$$\sum_{\tau}\sum_{r}\sum_{p} f^{\tau}_{r,\bar{s},p}\left[\tilde{\gamma}^{\tau}_{r,\bar{s},p} - \tilde{\pi}^{\tau}_{r,\bar{s}}\right] \geq 0 \qquad \forall r, p, \tau \tag{4.30a}$$

$$f^{\tau}_{r,\bar{s},p} \geq 0 \qquad \forall r, p, \tau \tag{4.30b}$$

DTA Constraints (4.30c)

The equivalence to program (4.25) is obtained by adapting the proof given by Smith (1979). The VI in (4.30) will be reformulated, via a gap function, to an equivalent NMP whose global minima coincide with those of (4.30). Define a gap function for the LNCT-DTA problem as follows:

$$G_{\text{LNCT}} = \sum_{\tau}\sum_{r}\sum_{p} f^{\tau}_{r,\bar{s},p}\left[\tilde{\gamma}^{\tau}_{r,\bar{s},p} - \breve{\pi}^{\tau}_{r,\bar{s}}\right] \tag{4.31}$$

G_{LNCT} provides a measure of the violation of the optimal LNCT-DTA conditions. It is evident that the difference vanishes when the time-varying path flow vector $\boldsymbol{f}$ satisfies the LNCT-DTA optimality conditions. Thus, solving the LNCT-DTA problem can be viewed as a process of finding the path flow vector $\boldsymbol{f}^*$ such that $G_{\text{LNCT}}(\boldsymbol{f}^*) = 0$. Therefore, an equivalent problem would be to

$$\text{Min } G_{\text{LNCT}}(\boldsymbol{f}) = \sum_{\tau}\sum_{r}\sum_{p} f_{r,\bar{s},p}^{\tau}\left[\tilde{\gamma}_{r,\bar{s},p}^{\tau} - \breve{\pi}_{r,\bar{s}}\right] \tag{4.32}$$

Subject to:

$$\sum_{\tau}\sum_{p} f_{r,\bar{s},p}^{\tau} = d_r \qquad \forall r \tag{4.32a}$$

$$f_{r,\bar{s},p}^{\tau} \geq 0 \qquad \forall r,s,p,\tau \tag{4.32b}$$

$$\text{DTA constraints} \tag{4.32c}$$

Associated with G_{LNCT} is the relative gap for this model $\tilde{G}_{\text{LNCT}}$, defined as follows:

$$\tilde{G}_{\text{LNCT}} = \frac{G_{\text{LNCT}}}{\sum_{r}\left[\left(\sum_{\tau}\sum_{p} f_{r,\bar{s},p}^{\tau}\right)\breve{\pi}_{r,\bar{s}}\right]} \tag{4.33}$$

4.3.5 LNCT-DTA Solution Algorithm

The transformed LNCT-DTA problem is similar in structure to the SO-DTA, which means that the efficient ORS algorithm developed for the SO-DTA problem in chapter 3 can also be used to solve the LNCT-DTA problem. The algorithm still needs to address the departure time choice before being suitable for solving the LNCT-DTA problem.

The departure time choice is reflected in constraint (4.32a) and for the ORS procedure to handle such a requirement, it must be adapted to find the optimal shifts across paths and departure times jointly. In other words, ORS needs to consider all feasible path-departure

time combinations when computing the optimal shifts. The optimal shifts under an LNCT-DTA assignment will be:

$$\delta^{\tau}_{r,\bar{s},p} = \frac{\left(\tilde{\gamma}^{\dot{\tau}}_{r,\bar{s},\dot{p}} - \tilde{\gamma}^{\tau}_{r,\bar{s},p}\right)}{\tilde{\gamma}'^{\tau}_{r,\bar{s},p}} + \frac{\left(\tilde{\gamma}^{\dot{\tau}}_{r,\bar{s},\dot{p}}\right)}{\tilde{\gamma}'^{\tau}_{r,\bar{s},p}} \times \delta^{\dot{\tau}}_{r,\bar{s},\dot{p}} \qquad \forall H(p,\tau) \neq \left|\overline{P}_{r,\bar{s}}\right|, H(\dot{p},\dot{\tau}) = \left|\overline{P}_{r,\bar{s}}\right| \quad (4.34)$$

where

$$\delta^{\dot{\tau}}_{r,\bar{s},\dot{p}} = \frac{\left[\sum_{\tau}\sum_{p}\left(\frac{\tilde{\gamma}^{\tau}_{r,\bar{s},p} - \tilde{\gamma}^{\dot{\tau}}_{r,\bar{s},\dot{p}}}{\tilde{\gamma}'^{\tau}_{r,\bar{s},p}}\right)\right]}{1 + \sum_{\tau}\sum_{p}\left(\frac{\tilde{\gamma}'^{\dot{\tau}}_{r,\bar{s},\dot{p}}}{\tilde{\gamma}'^{\tau}_{r,\bar{s},p}}\right)} \qquad \forall H(p,\tau) \neq \left|\overline{P}_{r,\bar{s}}\right|, H(\dot{p},\dot{\tau}) = \left|\overline{P}_{r,\bar{s}}\right| \quad (4.35)$$

and

$$\tilde{\gamma}'^{\tau}_{r,\bar{s},p} = \frac{\partial \tilde{\gamma}^{\tau}_{r,\bar{s},p}}{\partial f^{\tau}_{r,\bar{s},p}} = \overline{C}'^{\tau}_{r,\bar{s},p} \quad \forall r, p, \tau \quad (4.36)$$

The flow-shift matrix $\boldsymbol{\delta}$ must be adjusted for feasibility according to equations according to equations (4.18) and (4.19) with the assignments for the next iteration computed according to (4.20). The solution algorithm assumes that the traffic control center has perfect information about the evacuation demand at each zone. Once an extreme event is detected requiring the evacuation of the whole network, evacuees are provided with evacuation trip guidance information in the form of when to evacuate (departure time), where to go (destination choice) and which route to take (path choice) in such a way to minimize average trip times while reaching safety before a target evacuation time.

The solution algorithm represents a heuristic iterative procedure where the objective function is evaluated and constraints are satisfied through a simulation model. The simulation model is used to move vehicles along their assigned departure times and paths until they reach their

destinations, capturing the state of the system in the process. Traffic flow in the simulator is represented using a mesoscopic approach where vehicles are tracked individually but moved in packets according to macroscopic traffic flow relations between average speed and density on roadway links. At each iteration, the heuristic defines a search (descent) direction along which the objective function is expected to improve. Step sizes along search direction are determined according to the ORS method. The steps of the LNCT-DTA algorithm are explained in detail below. A vehicle-based implementation is provided in Figure 4.2.

Step 1: Initialization

- Set iteration counter $k = 1$.
- Connect all safety destinations s to a super sink $\bar{s}$ with zero-time infinite capacity links.
- Solve for the time-dependent LNCT-DTA marginal cost shortest path tree $\breve{P}_{r,\bar{s}}^{\tau\,(k)}$ for all $(r, \bar{s}, \tau)$ combinations assuming free-flow link travel times.
- For each origin r, search across all shortest paths trees $\breve{P}_{r,\bar{s}}^{\tau\,(k)}, \forall \tau$ and select the departure time and path combination (τ^*, p^*) that results in the minimum LNCT-DTA marginal cost. Let $\breve{p}_{r,\bar{s}}^{(k)}$ be that path, i.e.,:

$$\breve{p}_{r,\bar{s}}^{(k)} = (p^*, \tau^*) \,|\, \tilde{\gamma}_{r,\bar{s},p^*}^{\tau^*\,(k)} = \min_{\tau,p}\left(\tilde{\gamma}_{r,\bar{s},p}^{\tau\,(k)}\right)$$

- Perform an AON of the demand d_r onto $\breve{p}_{r,\bar{s}}^{(k)}$ for every r to obtain path assignments $f_{r,\bar{s},p}^{\tau\,(k)}$.

Step 2: Dynamic Network Loading Problem

- Use DYNASMART to simulate path assignments $f_{r,\bar{s},p}^{\tau\,(k)}$.
- Estimate time-dependent link travel times $c(\boldsymbol{f}^{(k)})$ and time-dependent link marginal travel times $\tilde{c}(\boldsymbol{f}^{(k)})$ from simulation results.

Step 3: Update Objective Function

- Compute $\tilde{G}_{\text{LNCT}}^{(k)}$ according to (4.33).
- Compute average LNCT-DTA cost (proxy for LNCT-DTA objective) as

$$ALC^{(k)} = \frac{\sum_{\tau}\sum_{r}\sum_{p} \gamma_{r,\bar{s},p}^{\tau\,(k)} f_{r,\bar{s},p}^{\tau\,(k)}}{\sum_{\tau}\sum_{r}\sum_{p} f_{r,\bar{s},p}^{\tau\,(k)}} \tag{4.37}$$

Step 4: Check Convergence

- Count the number of times the condition $\left| f_{r,\bar{s},p}^{\tau\,(k+1)} - f_{r,\bar{s},p}^{\tau\,(k)} \right| > \varepsilon$ is satisfied for all (r,τ,p) combinations and denote that number by $V(\varepsilon)$.
- If $V(\varepsilon) \le \bar{V}(\varepsilon)$ or $k \le \bar{k}$ then terminate the procedure, otherwise set $k = k+1$ and go to step 5.

Step 5: Time-Dependent LNCT-DTA Marginal Cost Shortest Path Problem

- Solve for the time-dependent LNCT-DTA marginal cost shortest path tree $\breve{P}_{r,\bar{s}}^{\tau\,(k)}$ for all $(r,\bar{s},\tau)$ combinations.
- Extract $\breve{p}_{r,\bar{s}}^{(k)}$ from $\breve{P}_{r,\bar{s}}^{\tau\,(k)}$ and add it to the active-path set $\bar{P}_{r,\bar{s}}^{(k)}$, for every r.

Step 6: Update of Path Assignments

- Find the optimal un-adjusted shifts $\delta_{r,\bar{s},p}^{\tau\,(k)}$ for all paths in $\bar{P}_{r,\bar{s}}^{(k)}$ according to equations (4.15) and (4.16).
- Find the optimal adjusted shifts $\tilde{\delta}_{r,\bar{s},p}^{\tau\,(k)}$ for all paths in $\bar{P}_{r,\bar{s}}^{(k)}$ according to equations (4.18) and (4.19).
- Update the assignments $f_{r,\bar{s},p}^{\tau\,(k+1)}$ for the next iteration $(k+1)$ using for each (r,τ,p) using (4.20) and go to step 2.

The solution algorithm described above is the exact theoretical extension of the ORS solution algorithm described in chapter 3 to the LNCT-DTA problem. Simulation experiments have shown this algorithm to be rather slow to converge due to the limited number of new path-

departure time combinations (potential solutions) added to the active path set $\overline{P}_{r,\bar{s}}^{(k)}$ in every iteration. An possible improvement is to add a new (efficient) path for all departure time combinations, resulting in up to $r \times \tau$ new solutions at each iteration. Therefore, step $5'$ will read as follows:

Step 5´: Time-Dependent LNCT-DTA Marginal Cost Shortest Path Problem

- Solve for the time-dependent least LNCT-DTA marginal cost path tree $\breve{P}_{r,\bar{s}}^{\tau(k)}$ for all $(r, \bar{s}, \tau)$ combinations.
- Add $\breve{p}_{r,\bar{s}}^{\tau(k)}$ for all departure times τ to the active-path set $\overline{P}_{r,\bar{s}}^{(k)}$ for each r.

$k = 1$
DO for every r
  Set $J^{-} = \{0\}$
  Scan all vehicles $j \in d_r$ and extract active path set $\overline{P}_{r,\bar{s}}^{(k)}$
  DO for every τ
    Find least-cost LNCT-marginal path $\breve{p}_{r,\bar{s}}^{\tau(k)}$ and add it to the active path, $\overline{P}_{r,\bar{s}}^{(k)}$
    Compute the adjusted algebraic flow shift vector $\tilde{\delta}_{r,\bar{s},p}^{\tau(k)}, \forall p \in \overline{P}_{r,\bar{s}}^{(k)}$
    DO for each path $p \in \overline{P}_{r,\bar{s}}^{\tau(k)}$
      IF $\tilde{\delta}_{r,\bar{s},p}^{\tau(k)} < 0$ THEN
        Randomly select $|\tilde{\delta}_{r,\bar{s},p}^{\tau(k)}|$ vehicles from path p and add them to set J^{-}
      ENDIF
    ENDDO
    DO for each path $p \in \overline{P}_{r,\bar{s}}^{\tau(k)}$
      IF $\tilde{\delta}_{r,\bar{s},p}^{\tau(k)} > 0$ THEN
        Randomly select $\tilde{\delta}_{r,\bar{s},p}^{\tau(k)}$ vehicles from J^{-} and assign them to p
        Remove selected vehicles from J^{-}
      ENDIF
    ENDDO
  ENDDO
ENDDO

Figure 4.2 Vehicle-based implementation LNCT-DTA solution heuristic

4.4 COMBINING THE TWO PROBLEMS: OPTIMAL SCHEDULING OF EVACUATION DEMAND

The objective of the MNCT-DTA problem is to minimize the network clearance time, which may be substituted by minimizing the total turnstile costs (exit times) of individual evacuees. In other words, the model is insensitive for variations in experienced trip times as long vehicles exit at the same time. For example, a vehicle departing at 8:00 AM and reaching the safety at 8:50 AM has the same contribution to the objective function of the MNCT-DTA as a vehicle departing at 8:15 AM and reaching safety at 8:50 AM despite incurring different trip times. Whereas for the LNCT-DTA problem with a target network clearance time of 8:50 AM, the second vehicle will have a lower contribution to the objective function (better) since its trip time is shorter.

Ideally, the best solution would be to combine both problems, which due to the conflicting objectives of the MNCT-DTA and the LNCT-DTA problems, can only be achieved in a bi-objective framework whose solution is obtained in two sequential stages. In the first stage, an MNCT-DTA problem is solved to determine the minimum network clearance time W^* and in the second stage, an LNCT-DTA problem is solved with the target evacuation time. We refer to the resulting problem as optimal demand scheduling (ODS) DTA problem and the resulting time-dependent O-D path flows $\boldsymbol{f}^*$ as the optimal demand scheduling flow pattern.

4.4.1 Problem Statement and Formulation

Consider an urban setting represented by the directed graph $G(N, A)$ with multiple origins R requires evacuation due to an extreme event. Assume that a set of shelter destinations $\bar{S}$ for that type of event has been identified. Furthermore, assume the total demand to be evacuated at each origin d_r is known a priori. The ODS-DTA problem is therefore to determine the time-dependent path-flow pattern $\boldsymbol{f}$ to minimize the network clearance time, while keeping the average trip times in the network at a minimum.

Given: $d_r, \bar{s}$

Find: $f^{\tau}_{r,\bar{s},p}$

To: $$\text{Min } Z(\boldsymbol{f}) = \sum_{\tau}\sum_{r}\sum_{p} C^{\tau}_{r,\bar{s},p} f^{\tau}_{r,\bar{s},p} \tag{4.38}$$

Subject to: $$\sum_{\tau}\sum_{p} f^{\tau}_{r,\bar{s},p} = d_r \qquad \forall r \tag{4.38a}$$

$$f^{\tau}_{r,\bar{s},p}\left(\tilde{\chi}^{\tau}_{r,\bar{s},p} - \hat{\pi}_{r,\bar{s}}\right) = 0 \qquad \forall r, p, \tau \tag{4.38b}$$

$$\tilde{\chi}^{\tau}_{r,\bar{s},p} - \hat{\pi}_{r,\bar{s}} \geq 0 \qquad \forall r, p, \tau \tag{4.38c}$$

$$f^{\tau}_{r,\bar{s},p} \geq 0 \qquad \forall r, p, \tau \tag{4.38d}$$

DTA Constraints (4.38e)

The objective function in (4.38) represents minimization of the total system trip time. The remaining constraints, collectively represent the MNCT-DTA optimality constraints. This formulation ensures that the system trip time is minimized while guaranteeing that vehicles exit the network in the minimum possible time.

4.4.2 Optimality Conditions for the ODS-DTA Problem

The optimality conditions for the ODS-DTA problem are actually the collection of optimality conditions for both SO-DTA and MNCT-DTA problems. They are stated below:

$$f^{\tau}_{r,\bar{s},p}\left(\tilde{C}^{\tau}_{r,\bar{s},p} - \tilde{\pi}_{r,\bar{s}}\right) = 0 \qquad \forall r, p, \tau \tag{4.39a}$$

$$\tilde{C}^{\tau}_{r,\bar{s},p} - \tilde{\pi}_{r,\bar{s}} \geq 0 \qquad \forall r, p, \tau \tag{4.39b}$$

$$f^{\tau}_{r,\bar{s},p}\left(\tilde{\chi}^{\tau}_{r,\bar{s},p} - \hat{\pi}_{r,\bar{s}}\right) = 0 \qquad \forall r, p, \tau \tag{4.39c}$$

$$\tilde{\chi}^{\tau}_{r,\bar{s},p} - \hat{\pi}_{r,\bar{s}} \geq 0 \qquad \forall r, p, \tau \tag{4.39d}$$

$$f^{\tau}_{r,\bar{s},p} \geq 0 \qquad \forall r, p, \tau \tag{4.39e}$$

DTA Constraints (4.39f)

4.4.3 ODS-DTA Solution Algorithm

The ODS-DTA problem is a bi-objective problem, however, the primary objective is still to minimize the network clearance but it must be done at minimum cost to the system. Therefore, we are not interested in the trade-off curve between these two objectives, but rather in a single point on the pareto-optimal curve. The problem therefore can be solved in two sequential stages where an MNCT-DTA problem is solved first to determine the minimum network clearance time W^*, and an LNCT-DTA problem is solved in the second stage to minimize system trip time, with a target evacuation time equal to W^*.

The second stage can be solved in two approaches. The first approach is to solve it as standard stand-alone LNCT-DTA problem, i.e. without a feasible initial solution (the infeasibility stems form the fact that initial solutions based on AON assignments will generally not result in network clearance times less than W^*). The second approach, which will be adopted in the ODS-DTA problem, is to solve the LNCT-DTA problem using the MNCT-DTA solution (from stage I) as the initial solution. The initial solution is therefore feasible since it clears the network the minimum network clearance time and will therefore result in a much faster convergence rate.

4.5 EXPERIMENTAL RESULTS

Two sets of simulation experiments are performed in this chapter to investigate the performance of the MNCT-DTA, LNCT-DTA, and ODS-DTA algorithms. The first set is performed on the Nine-node network and the second set is conducted on the Fort Worth

network. In all these experiments, the algorithms are allowed to run well beyond the stopping point (convergence) to examine whether the algorithms are following a proper descent direction over these iterations.

The objective function of the MNCT-DTA problem is the minimization of the evacuation time, however, the desired outcome of the MNCT-DTA problem is to minimize network clearance time, which is theoretically supposed to coincide with the minimum average evacuation time. While simulation results prove that these two solution points are not always 100% identical, they nonetheless indicate that they are extremely close. In other words, the behavior of the network clearance time tracks the behavior of the average evacuation time rather exceptionally. To remove any sort of confusion, MNCT-DTA solutions will be declared "optimal" when the average evacuation time is at a minimum (this may or may not correspond to the actual minimum network clearance time, but the difference is negligible). Note that in these experiments, iteration zero represents the case for simultaneous immediate evacuation where all vehicles depart immediately (no staging or scheduling is involved) and will therefore act as a yardstick to which MNCT-DTA solutions are compared.

The objective for the LNCT-DTA is to minimize the total cost in the system as defined in program (4.25). The target evacuation time for the LNCT-DTA problem in these experiments will be the network clearance time as obtained from solving the corresponding MNCT-DTA problem. Therefore, the LNCT-DTA problem solved here is in fact equivalent to ODS-DTA problem with the exception that the initial solution is infeasible as opposed to using MNCT-DTA solution as the initial solution for the ODS-DTA algorithm.

Four measures are used to fully analyze the results of the LNCT-DTA algorithm. They are; 1) average LNCT-DTA objective value as computed by (4.37) with a penalty $M = 1000$, 2) average trip time, 3) average evacuation time, and 4) network clearance time. Finally, The ODS-DTA algorithm is analyzed in much a similar way to the LNCT-DTA algorithm, with

the exception that the initial solution is obtained from solving MNCT-DTA (Stage I). This algorithm is only tested using the Fort-Worth network.

4.5.1 Experiments on the Nine-node Network

Experiments on the Nine-node network will examine the convergence patterns of the MNCT-DTA and LNCT-DTA algorithms only (ODS-DTA algorithm will not be executed for this network). The analysis is made for three demand levels namely, 2,000 vehicles (light traffic), 5,000 vehicles (medium traffic), and 10,000 vehicles (heavy traffic). The demand is present at node 1 and is to be evacuated to node 9 [see Figure 3.6].

4.5.1.1 *Convergence Pattern Analysis for MNCT-DTA Algorithm*

Depicted in Figure 4.3 are the results of the first 50 iterations of the MNCT-DTA algorithm for an evacuation demand of 2,000 vehicles. The network clearance time at initial conditions is 64.2 min with an average evacuation time of 24.9 min. Since all vehicles depart at time zero, the average trip time at iteration zero is 24.9 min as well. The minimum average evacuation time of 19.6 min is achieved after 7 iterations, with a corresponding minimum network clearance time of 46.1 min and an average trip time of 4.2 min. These optimal values remain virtually unchanged after 50 iterations, which confirm the appropriateness of the descent direction embedded in the solution algorithm. Moreover, Figure 4.3 clearly shows that network clearance time tracks the average evacuation time exceptionally well. Overall, the MNCT-DTA algorithm managed to improve the network clearance time by 28%, the average evacuation time by 21%, and the average trip time by 83.1% from initial conditions. A summary of results for this experiment is provided in Table 4.1.

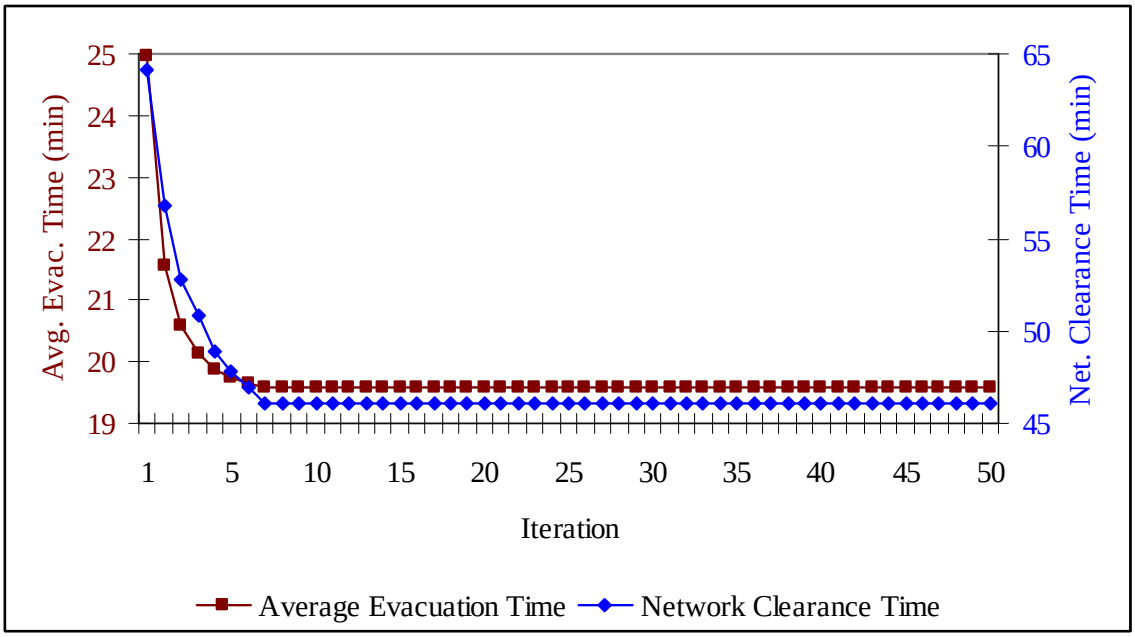

Figure 4.3 Convergence pattern for MNCT-DTA algorithm for the Nine-node network – 2000 vehicles

Table 4.1 Summary of MNCT-DTA optimality results for the Nine-node network – 2,000 vehicles

Measure of Effectiveness	*Initial Conditions*	*Results at Optimality*	*Results after 50 Iterations*
Iteration	0	7	50
Network Clearance Time (min)	64.2	46.1	47.92
Average Evacuation Time (min)	24.9	19.6	19.76
Average Trip Time (min)	24.9	4.2	3.96

The same experiment is repeated for a demand of 5,000 vehicles. The corresponding results for the first 50 iterations of the MNCT-DTA algorithm are shown in Figure 4.4. The initial conditions are a network clearance time of 162.6 min, an average evacuation time of 59.5 min, and an average trip time of 59.5 min as well. The minimum average evacuation time is 44.6 min and is achieved after 13 iterations with a corresponding minimum network clearance time of 87.8 min and average trip time of 4.6 min. These optimal values also remain virtually unchanged after 50 iterations, which confirm the appropriateness of the descent direction embedded in the solution algorithm. Moreover, Figure 4.4 clearly shows that network clearance time tracks the average evacuation time exceptionally well. Overall,

the MNCT-DTA algorithm managed to improve the network clearance time by 45%, the average evacuation time by 25%, and the average trip time by 92%. A summary of results for this experiment is provided in Table 4.2.

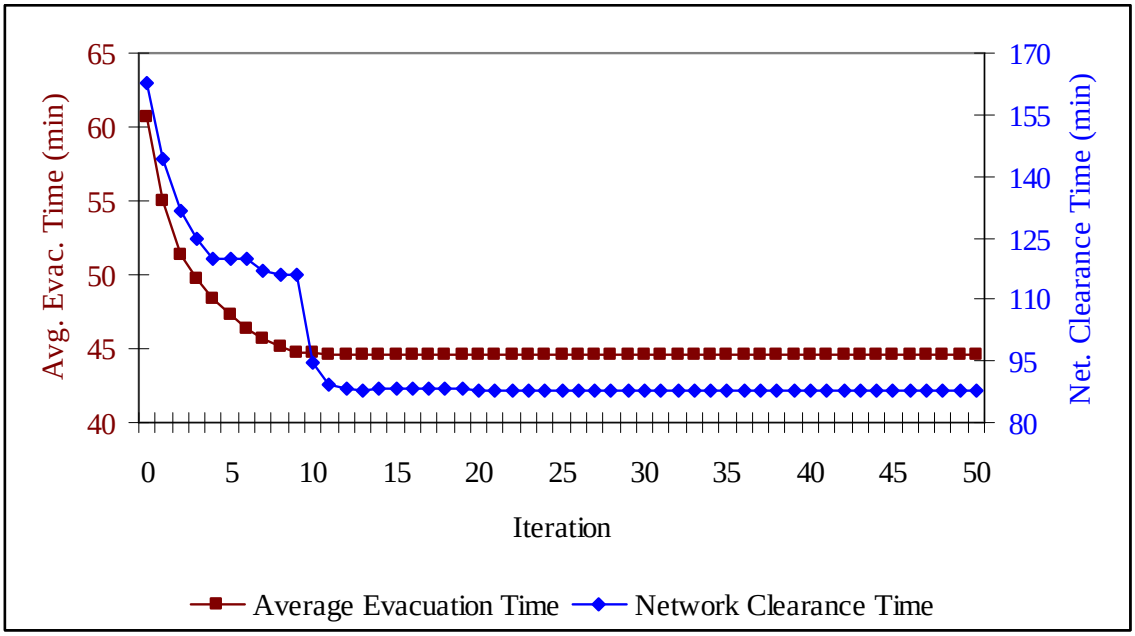

Figure 4.4 Convergence pattern for MNCT-DTA algorithm for the Nine-node network – 5000 vehicles

Table 4.2 Summary of MNCT-DTA optimality results for the Nine-node network – 5000 vehicles

Measure of Effectiveness	*Initial Conditions*	*Results at Optimality*	*Results after 50 Iterations*
Iteration	0	13	50
Network Clearance Time (min)	162.6	87.8	87.98
Average Evacuation Time (min)	59.5	44.60	44.61
Average Trip Time (min)	59.5	4.63	4.65

The same experiment is now repeated for a demand of 10,000 vehicles. The corresponding results for the first 50 iterations of the MNCT-DTA algorithm are shown in Figure 4.5. The initial conditions are a network clearance time of 324.6 min, an average evacuation time of 159.8 min, and an average trip time of 159.8 min as well. The minimum average evacuation trip time of 88.4 min is achieved after 22 iterations for corresponding minimum network

clearance time of 178.5 min and average trip time of 6.99 min. The optimal values remain virtually unchanged after 50 iterations, which again validates the appropriateness of the descent direction embedded in the solution algorithm. Overall, MNCT-DTA algorithm managed to improve the network clearance time by 45%, the average evacuation time by 45%, and the average trip time by 96%. A summary of the results is provided in Table 4.3.

Table 4.3 Summary of MNCT-DTA optimality results for the Nine-node network – 10,000 vehicles

Measure of Effectiveness	*Initial Conditions*	*Results at Optimality*	*Results after 50 Iterations*
Iteration	0	22	50
Network Clearance Time (min)	324.6	178.54	173.75
Average Evacuation Time (min)	159.8	88.42	88.66
Average Trip Time (min)	159.8	6.99	7.02

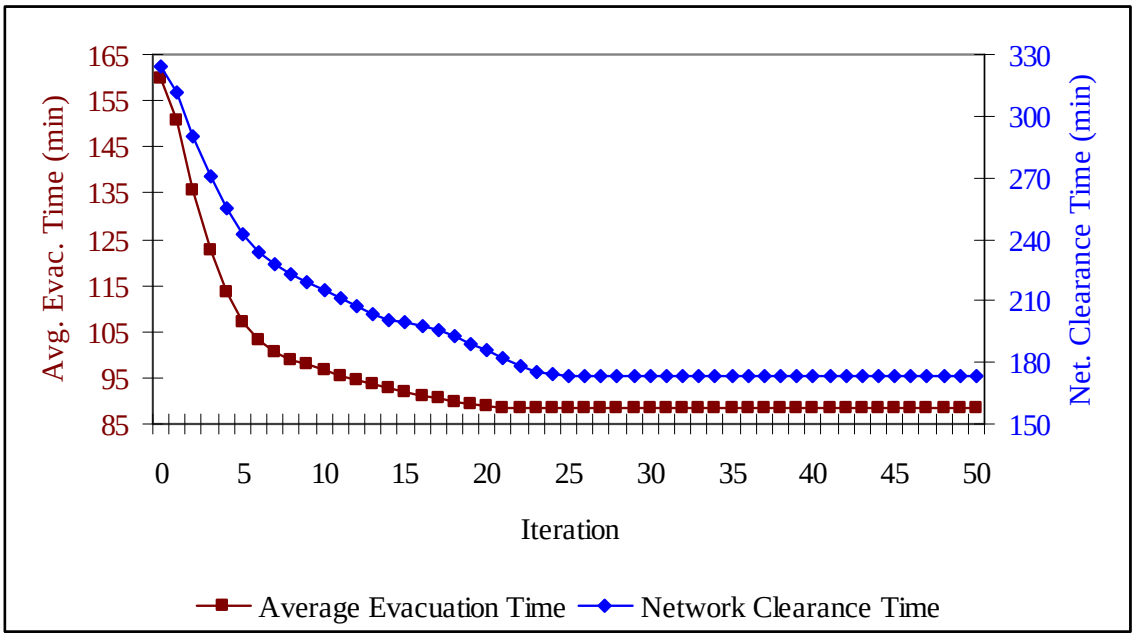

Figure 4.5 Convergence pattern for MNCT-DTA algorithm – 10000 vehicles

Figure 4.3, Figure 4.4, and Figure 4.5 showed that minimizing the total turnstile costs i.e. average network evacuation time is equivalent to minimizing the network clearance time.

Granted that these two minimums did not fully correspond to the same solution point in these experiments, however the difference is extremely small and negligible.

4.5.1.2 *Convergence Pattern Analysis for LNCT-DTA Algorithm*

The first experiment is conducted for a demand level of 2,000 vehicles and a target network evacuation time of 46.1 min. Figure 4.6 depicts the network clearance time and the (transformed) average LNCT-DTA objective results of the first 25 iterations of the algorithm. The optimal average objective value is 2.47 min and is achieved after 13 iterations. The corresponding network clearance time is 46.32 min, a 0.48% increase over the target evacuation time.

The average evacuation time at optimality is 20.71 min, a 5% increase over the optimal objective value (19.6 min) of the associated MNCT-DTA problem. The average trip time is 2.49 min, which is within 1% of the (transformed) average LNCT-DTA objective which essentially means that all vehicles managed to exit the network within the target evacuation time. Moreover, the average trip time represents a 41% improvement over the associated MNCT-DTA problem (4.2 min). Figure 4.7 shows that the behavior of the network clearance time is, as expected, very similar to that of the average evacuation time. Figure 4.8 shows that the average trip time does indeed drop with a steady the network clearance time. The results do not change much after 25 iterations as reported in Table 4.4.

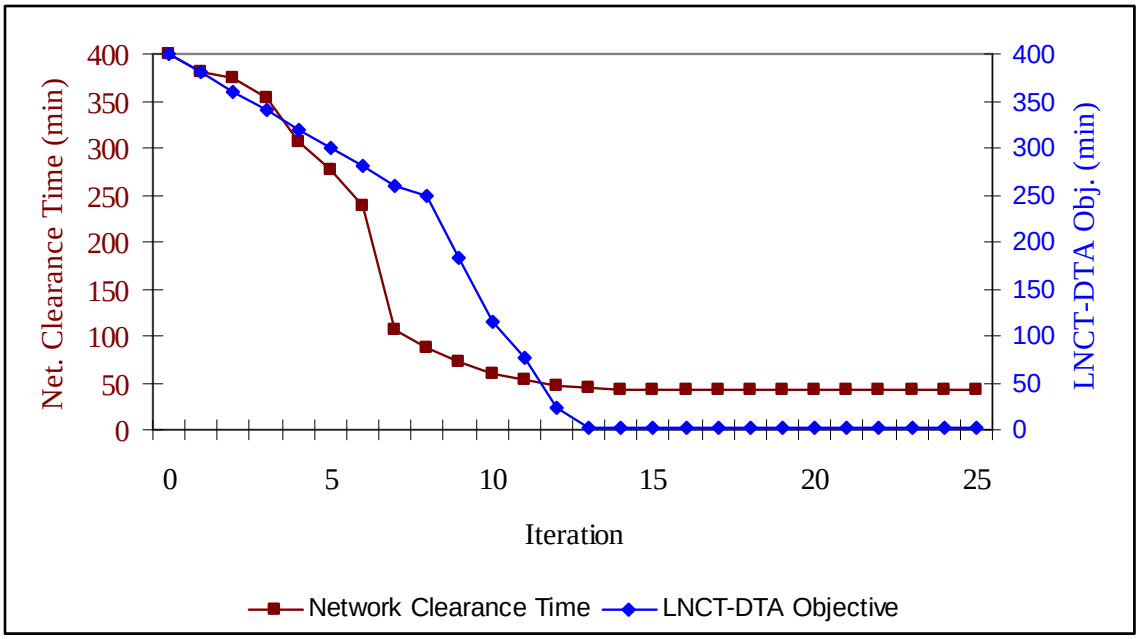

Figure 4.6 Network clearance time and LNCT-DTA objective convergence pattern for LNCT-DTA algorithm for the Nine-node network – 2,000 vehicles

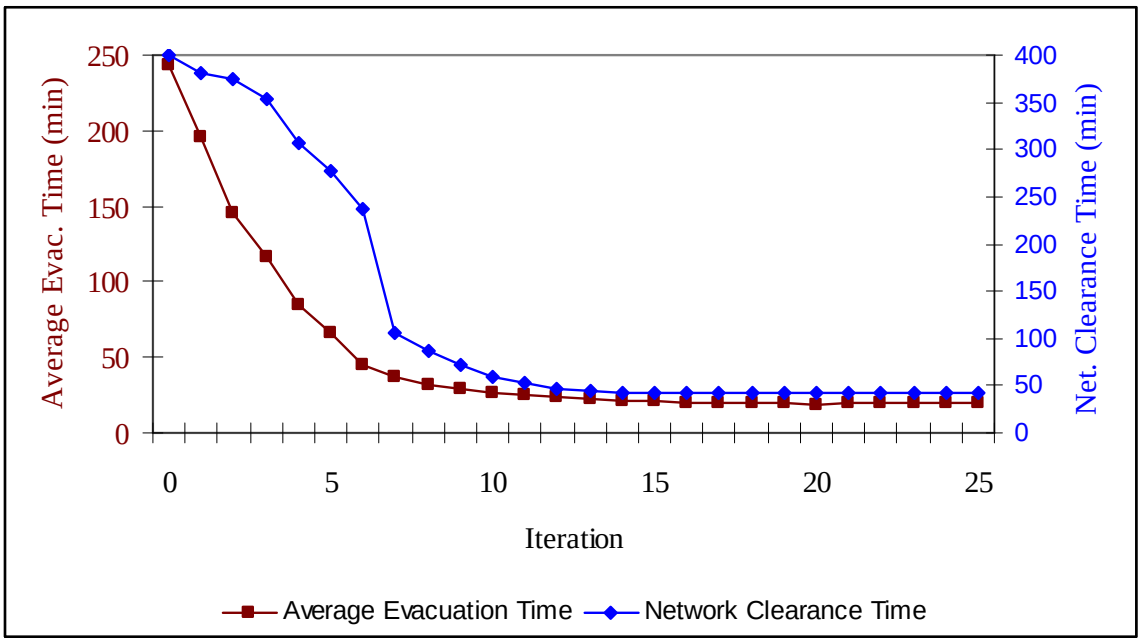

Figure 4.7 Average evacuation time and network clearance time convergence pattern for LNCT-DTA algorithm for the Nine-node network – 5,000 vehicles

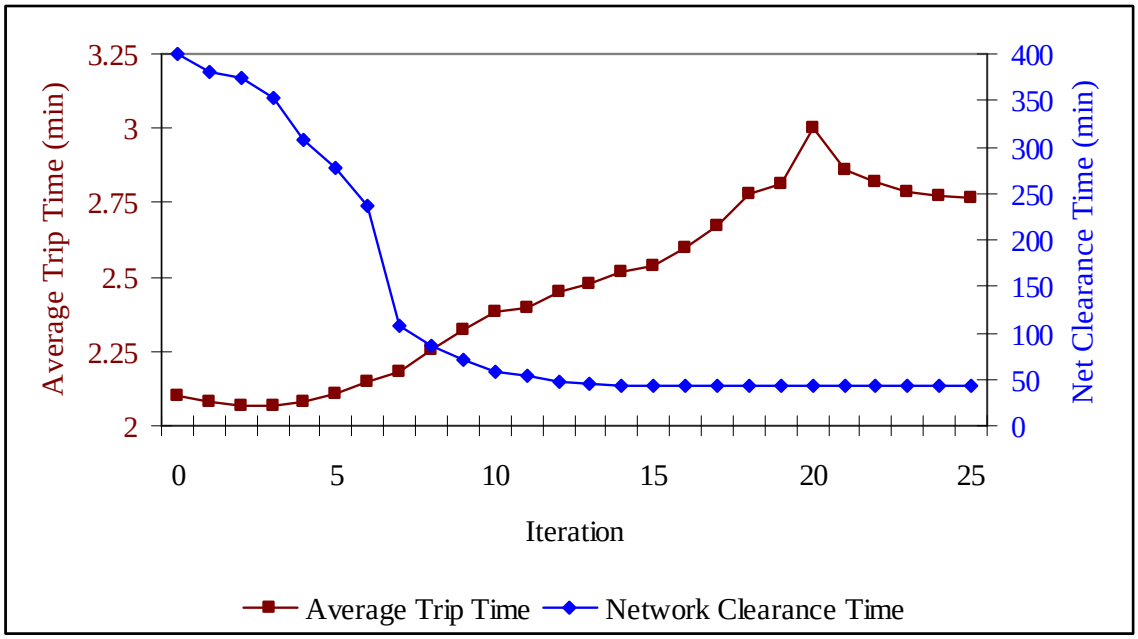

Figure 4.8 Average trip time and network clearance time convergence pattern for LNCT-DTA algorithm for the Nine-Node network – 2,000 vehicles

Table 4.4 Summary of LNCT-DTA optimality results for the Nine-node network – 2,000 vehicles

Measure of Effectiveness	*Initial Conditions*	*Results at Optimality*	*Results after 25 Iterations*
Iteration	0	13	25
Network Clearance Time (min)	64.2	46.32	46.16
Average LNCT-DTA Objective (min)	N/A	2.47	2.77
Average Evacuation Time (min)	24.9	20.71	19.31
Average Trip Time (min)	24.9	2.49	2.77

The same experiment is repeated for a demand level of 5,000 vehicles and a target network evacuation time of 87.8 min. Figure 4.9 depicts the network clearance time and the (transformed) average LNCT-DTA objective value results of the first 75 iterations of the algorithm. The optimal objective value is 3.26 min and is achieved after 49 iterations. The corresponding network clearance time is 88.95 min, a 1.31% increase over the target evacuation time.

The average evacuation time at optimality is 44.65 min, a 0.11% increase over the optimal

objective value (44.6 min) of the associated MNCT-DTA problem. The average trip time is 3.28 min, which is within 1% of the (transformed) average LNCT-DTA objective and essentially means that all vehicles managed to exit the network within the target evacuation time. Moreover, the average trip time represents a 29% improvement over the MNCT-DTA problem (4.63 min). Figure 4.10 shows that the behavior of the network clearance time is, as expected, very similar to that of the average evacuation time. Figure 4.11 shows that the average trip time does drop with a steady the network clearance time. Note that the results do not change much after 75 iterations as reported in Table 4.5.

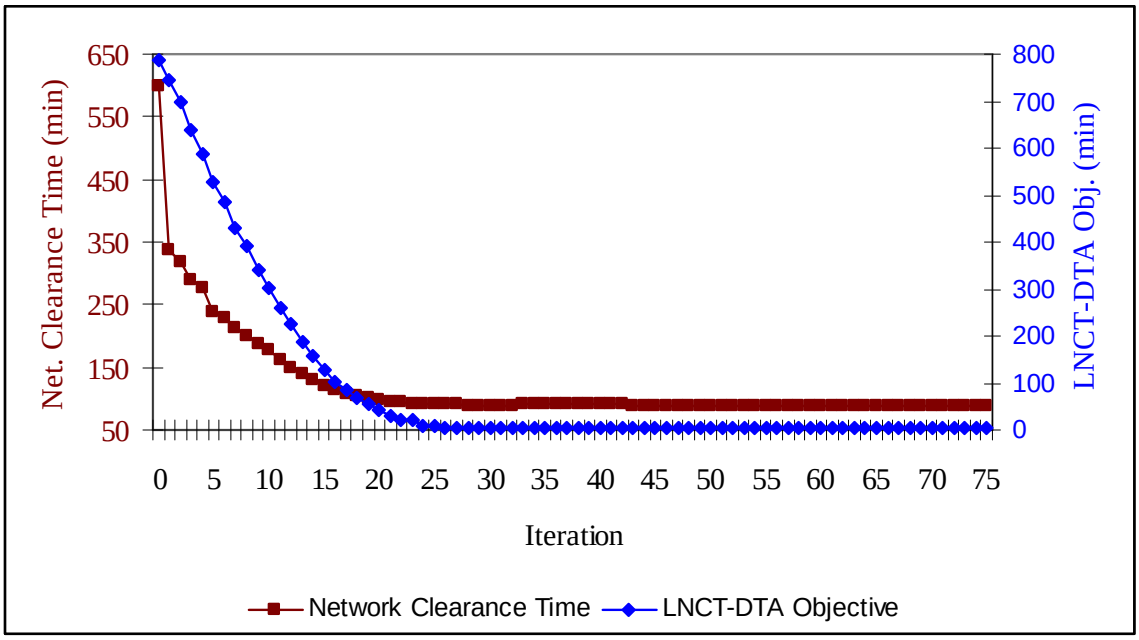

Figure 4.9 Network clearance time and LNCT-DTA objective convergence pattern for LNCT-DTA algorithm for Nine-node network – 5,000 vehicles

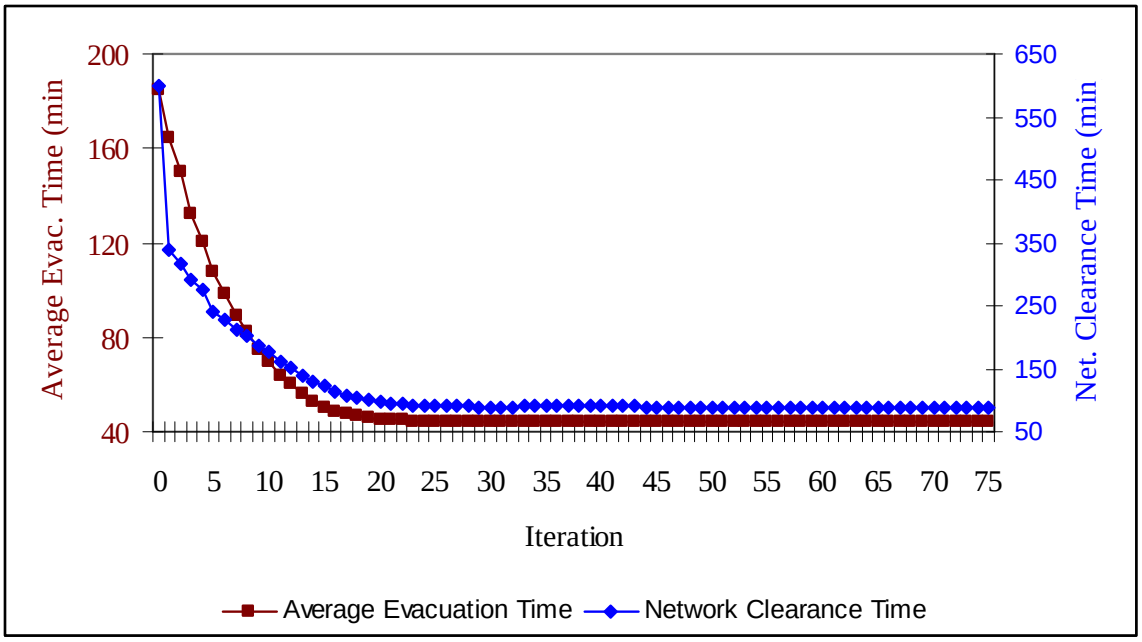

Figure 4.10 Average evacuation time and network clearance time convergence pattern for LNCT-DTA algorithm for Nine-node network – 5,000 vehicles

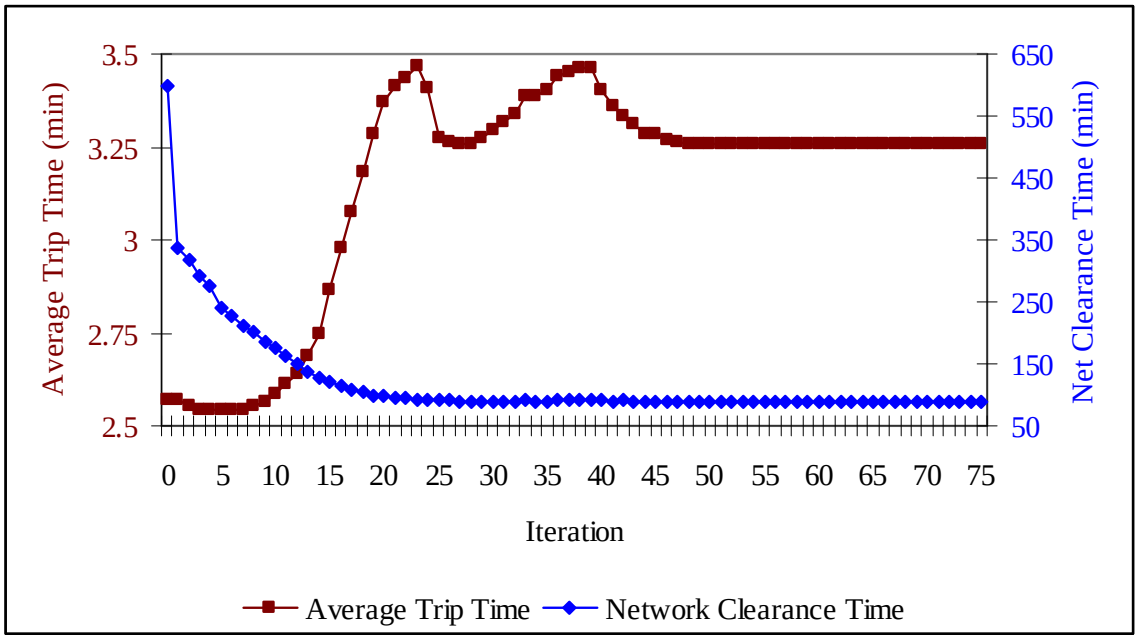

Figure 4.11 Average trip time and network clearance time convergence pattern for LNCT-DTA algorithm for Nine-node network – 5,000 vehicles

Table 4.5 Summary of LNCT-DTA optimality results for the Nine-node network – 5,000 vehicles

Measure of Effectiveness	*Initial Conditions*	*Results at Optimality*	*Results after 75 Iterations*
Iteration	0	49	75
Network Clearance Time (min)	162.6	88.95	88.85
Average LNCT-DTA Objective (min)	N/A	3.25	3.29
Average Evacuation Time (min)	59.5	44.65	44.63
Average Trip Time (min)	59.5	3.28	3.31

The same experiment is repeated for a demand level of 10,000 vehicles and a target network evacuation time of 178.54 min. Figure 4.12 depicts the network clearance time and the (transformed) average LNCT-DTA objective results of the first 75 iterations of the algorithm. The optimal objective value is 10.25 min and is achieved after 66 iterations. The corresponding network clearance time is 175.48 min, a 1.7% decrease over the target evacuation time. The average evacuation time is 90.49 min, a 2.3% increase over the MNCT-DTA problem (88.42 min). The higher average evacuation time coupled with the lower network clearance time suggest that the network clearance time obtained by the associated MNCT-DTA problem could be still be further improved, however, the differences are rather small.

The average trip time is 10.25 min, which is exactly the same as the (transformed) average LNCT-DTA objective since all vehicles managed to exit the network within the target evacuation time. Moreover, the average trip time represents a 27% improvement over the MNCT-DTA problem (6.99 min). Figure 4.13 shows that the behavior of the network clearance time is very similar to that of the average evacuation time. Figure 4.14 shows that the average trip time does indeed drop with a steady the network clearance time. The results do not change much after 75 iterations as reported in Table 4.6.

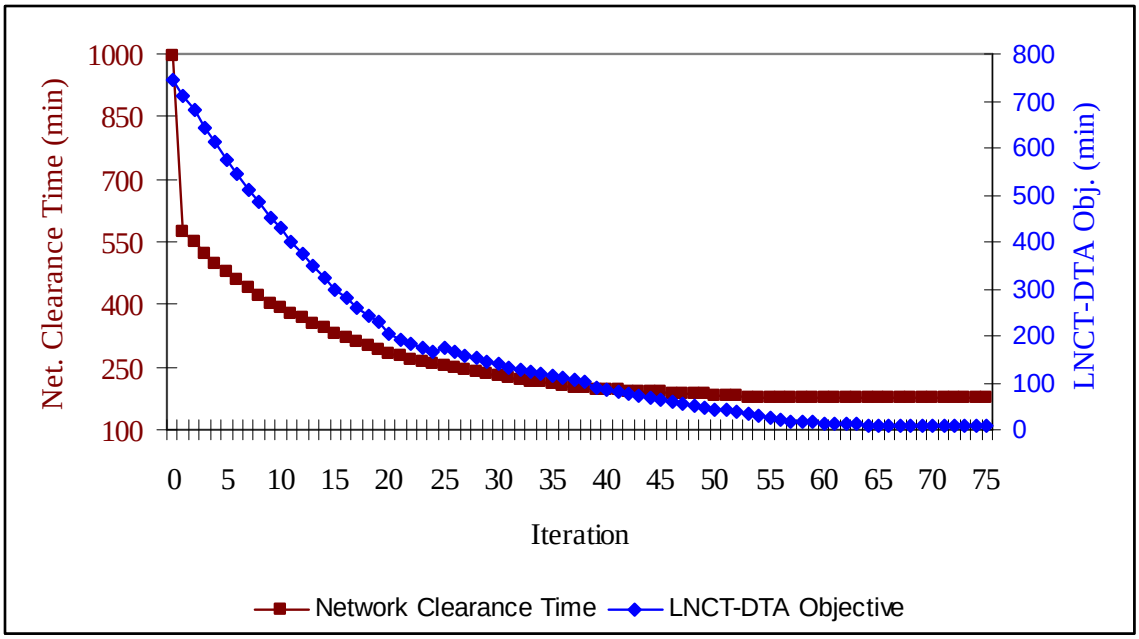

Figure 4.12 Network clearance time and LNCT-DTA objective convergence pattern for LNCT-DTA algorithm for Nine-Node network – 10,000 vehicles

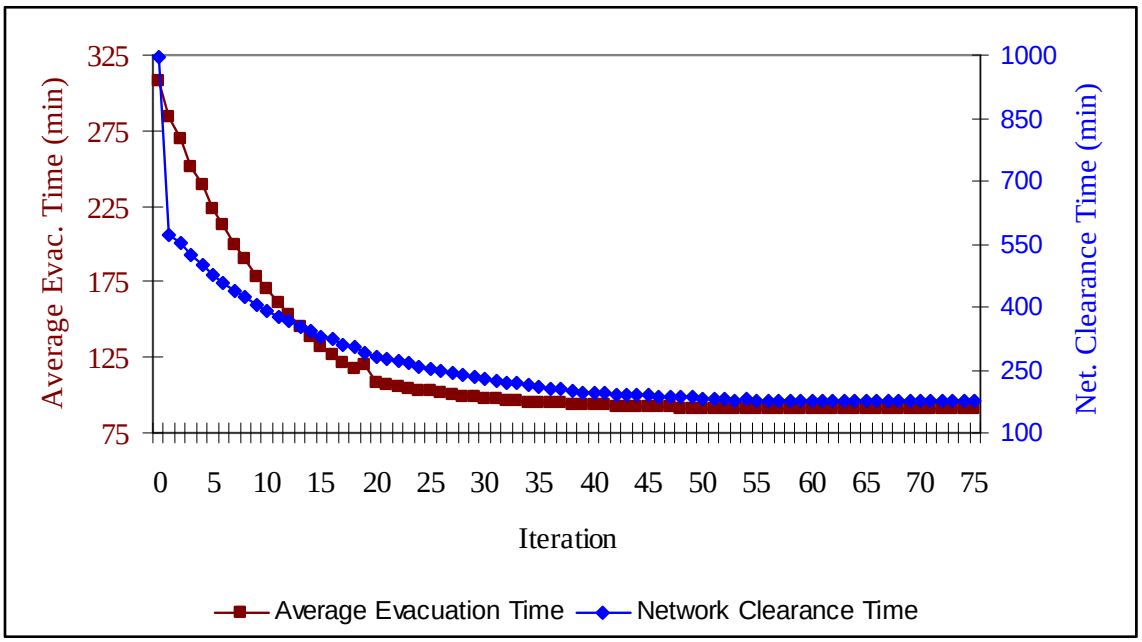

Figure 4.13 Average evacuation time and network clearance time convergence pattern for LNCT-DTA algorithm for Nine-Node network – 10,000 vehicles

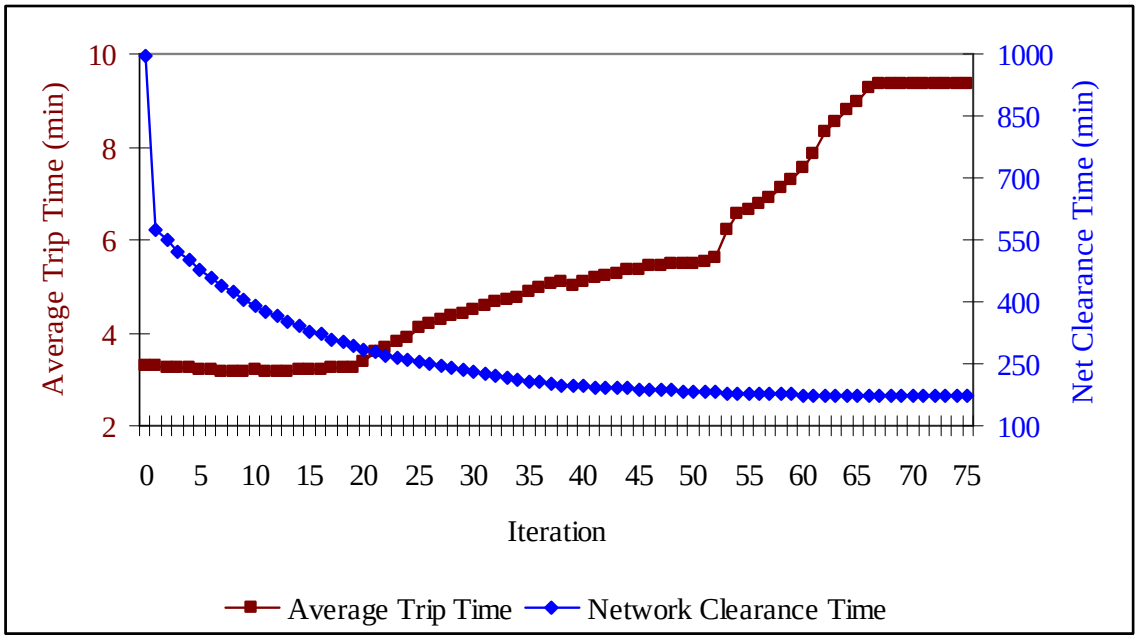

Figure 4.14 Average trip time and network clearance time convergence pattern for LNCT-DTA algorithm for Nine-Node network – 10,000 vehicles

Table 4.6 Summary of LNCT-DTA optimality results for the Nine-node network – 10,000 vehicles

Measure of Effectiveness	*Initial Conditions*	*Results at Optimality*	*Results after 75 Iterations*
Iteration	0	66	75
Network Clearance Time (min)	324.6	175.48	175.77
Average LNCT-DTA Objective (min)	N/A	10.25	11.85
Average Evacuation Time (min)	159.8	90.49	90.67
Average Trip Time (min)	159.8	10.25	11.85

This series of experiments showed that the LNCT-DTA model is capable of minimizing the average trip times for evacuees while still achieving network clearance (and average evacuation) times very close to specified target evacuation times. Since the target evacuation times are obtained from solving the respective MNCT-DTA problem, the LNCT-DTA solutions are in fact equivalent to the ODS-DTA solutions. Table 4.7 cross-compares the LNCT-DTA (or more accurately ODS-DTA) convergence results with MNCT-DTA results.

Table 4.7 Comparison of LNCT-DTA with MNCT-DTA optimal results for the Nine-node network

	LNCT-DTA Optimal Solutions			*MNCT-DTA Optimal Solutions*		
Demand Level (veh)	*Average Evacuation Time (min)*	*Network Clearance Time (min)*	*Average Trip Time (min)*	*Average Evacuation Time (min)*	*Network Clearance Time (min)*	*Average Trip Time (min)*
2,000	20.71	46.32	2.49	19.6	46.1	4.2
5,000	44.65	88.95	3.28	44.60	87.8	4.63
10,000	90.49	175.48	10.25	88.42	178.54	6.99

4.5.2 Experiments on Fort Worth Network

The following set of experiments is aimed at analyzing the performance of the MNCT-DTA, LNCT-DTA, and ODS-DTA algorithms on reasonably sized networks.

4.5.2.1 ***Convergence Pattern Analysis for MNCT-DTA Algorithm***

The first series of experiments aims to examine the convergence pattern of the MNCT-DTA algorithm. The analysis is made for two evacuation demand levels namely, 30,000 vehicles (light-moderate traffic) and 45,000 vehicles (heavy traffic). For each demand level, the analysis is made for three solution points: 1) initial conditions, 2) at minimum average evacuation time (optimal objective value), and 3) after 100 iterations. Zone 2 is designated as the safety destination (see Figure 3.13).

Depicted in Figure 4.15 are the results of the first 100 iterations of the MNCT-DTA algorithm for an evacuation demand of 30,000 vehicles. Initial conditions for such a demand level are a network clearance time of 195.5 min, an average evacuation time of 105.3 min, and an average trip time is 105.3 min as well. The minimum average evacuation time for this scenario is 54.2 min and is achieved after 61 iterations with a corresponding minimum network clearance time of 108.6 min and an average trip time is 39.1 min. Therefore, the MNCT-DTA algorithm managed to improve the network clearance time by 44%, the average evacuation time by 49%, and the average trip time by 63% from initial conditions. After 100

iterations, the average evacuation time is 54.4 min, the network clearance time is 109.7 min, and the average trip time is 39.7 min, all slightly higher than at optimal solution, which also validates the appropriateness of the descent method embedded in the MNCT-DTA solution algorithm. Table 4.8 summarizes the results for the MNCT-DTA algorithm.

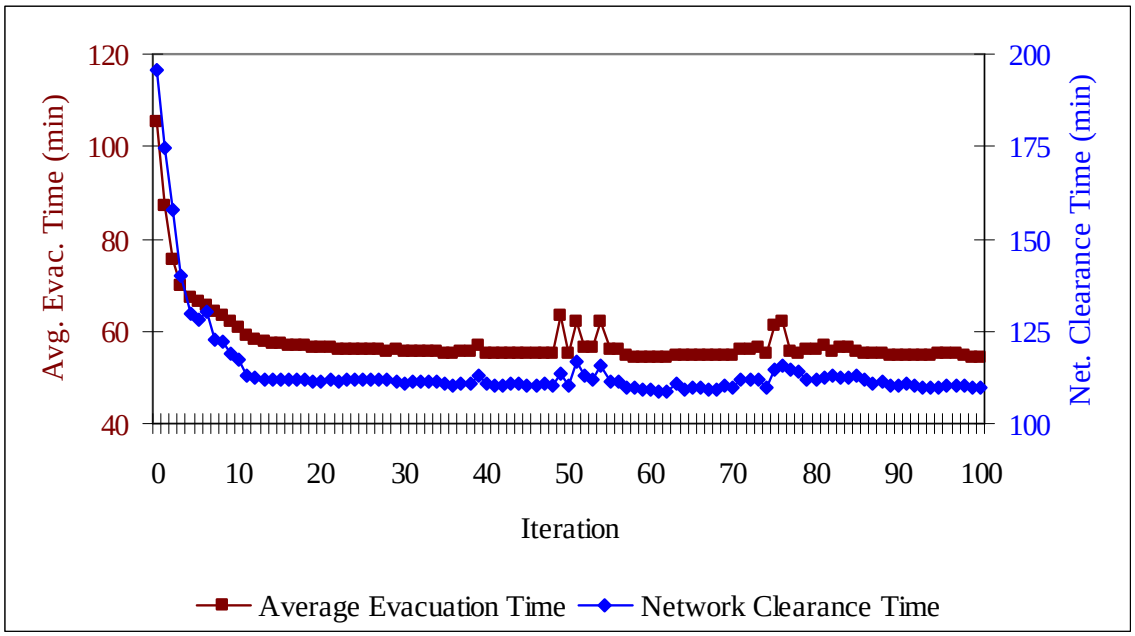

Figure 4.15 Convergence pattern for MNCT-DTA algorithm for Fort Worth network – 30,000 vehicles

Table 4.8 Summary of MNCT-DTA optimality results for Fort Worth network – 30,000 vehicles

Measure of Effectiveness	*Initial Conditions*	*Results at Optimality*	*Results after 100 Iterations*
Iteration	0	61	100
Network Clearance Time (min)	195.5	108.6	109.7
Average Evacuation Time (min)	105.3	54.2	54.4
Average Trip Time (min)	105.3	39.1	39.7

Depicted in Figure 4.16 are the results of the first 100 iterations of the MNCT-DTA algorithm the for an evacuation demand level of 45,000 vehicles. Initial conditions for such a demand level are a network clearance time of 386.3 min, an average evacuation time of 206.9 min and an average trip time is 206.9 min as well. The minimum average evacuation time for

this scenario is 83.4 min and is achieved after 88 iterations with a corresponding minimum network clearance time of 166.8 min and average trip time is 60.1 min. Therefore, the MNCT-DTA algorithm managed to improve the network clearance time by 57%, the average evacuation time by 60%, and the average trip time by 71% from initial conditions. After 100 iterations, the average evacuation time is 83.8 min, the network clearance time is 166.9 min, and the average trip time is 60.8 min, all slightly higher than at optimal solution, which also validates the appropriateness of the descent method embedded in the MNCT-DTA solution algorithm. Table 4.9 summarizes the results for the MNCT-DTA algorithm.

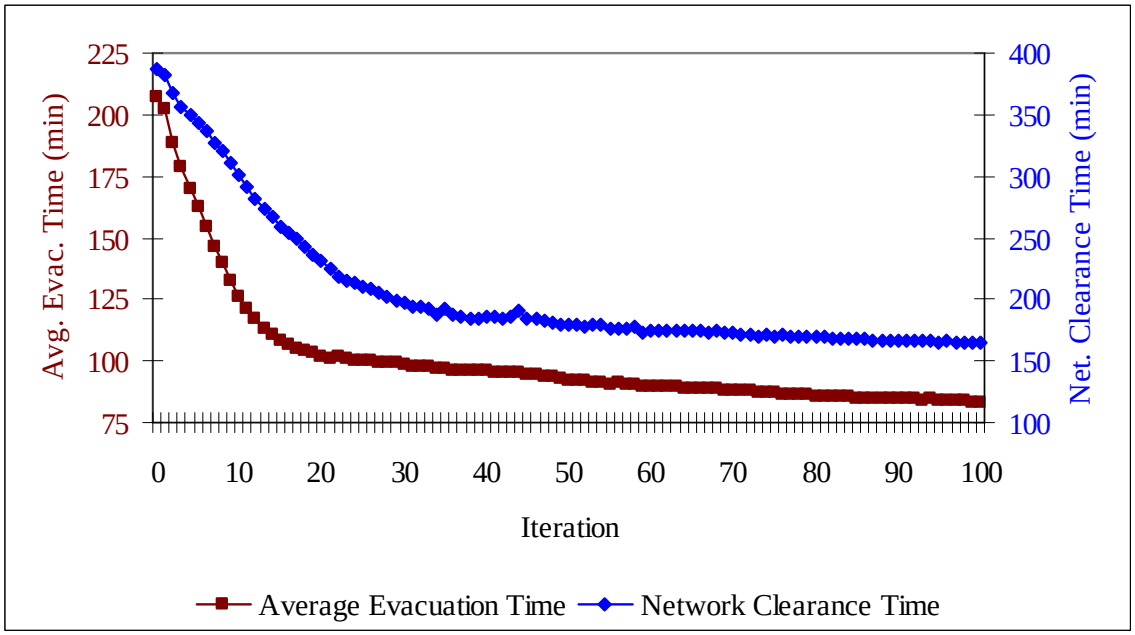

Figure 4.16 Convergence pattern for MNCT-DTA algorithm for Fort Worth network – 45,000 vehicles

Table 4.9 Summary of MNCT-DTA optimality results for Fort Worth network – 45,000 vehicles

Measure of Effectiveness	*Initial Conditions*	*Results at Optimality*	*Results after 100 Iterations*
Iteration	0	88	100
Network Clearance Time (min)	386.3	166.8	166.9
Average Evacuation Time (min)	206.9	83.4	83.8
Average Trip Time (min)	206.9	60.1	60.8

4.5.2.2 *Convergence Pattern Analysis for LNCT-DTA Algorithm*

The first experiment is conducted for an evacuation demand of 30,000 vehicles and a latest evacuation time of 108.6 min. Figure 4.17 depicts the network clearance time and the (transformed) average LNCT-DTA objective results of the first 100 iterations of the algorithm. The optimal objective value is 35.62 min and is achieved after 86 iterations. The corresponding network clearance time is 108.14 min, a 0.4% decrease over the target evacuation time. The average evacuation time at optimality is 53.98 min, a 0.41% decrease over the associated MNCT-DTA problem (54.2 min). The average trip time is 34.83 min, which is slightly less (2.2%) than the (transformed) average LNCT-DTA objective, means that almost all vehicles managed to exit the network within the target evacuation time of 108.6 min. Moreover, the average trip time represents a 10.9% improvement over the associated MNCT-DTA problem (39.1 min). Figure 4.18 shows that the behavior of the network clearance time is, as expected, very similar to that of the average evacuation time. Figure 4.19 shows that the average trip time does indeed drop with a steady the network clearance time. The results do not change much after 100 iterations as reported in Table 4.10.

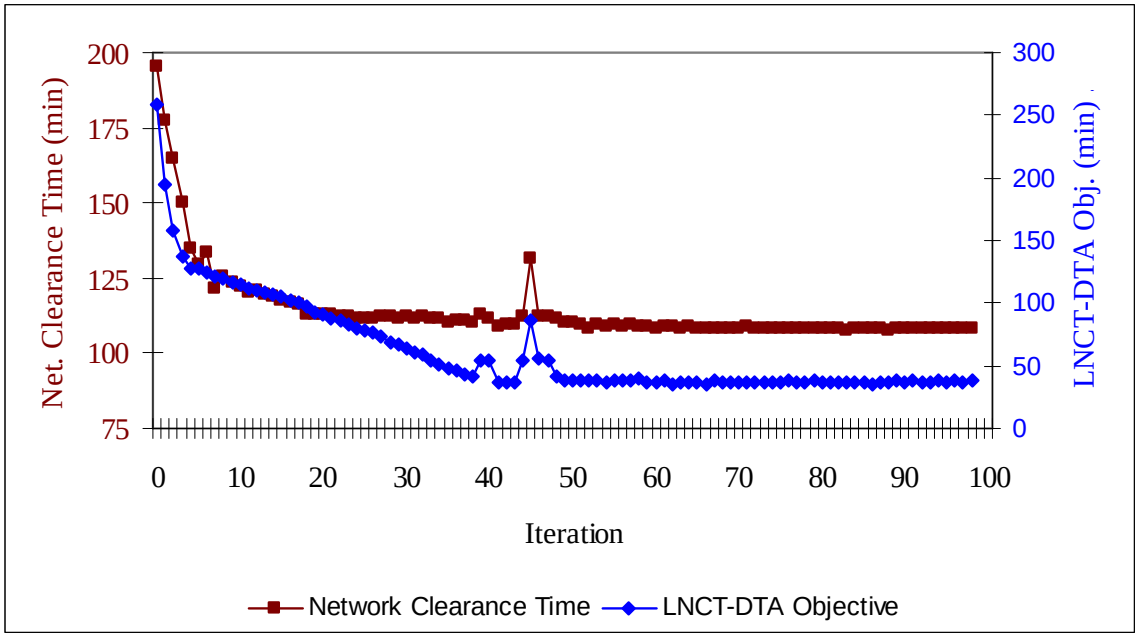

Figure 4.17 Network clearance time and LNCT-DTA objective convergence pattern for LNCT-DTA algorithm on Fort Worth network – 30,000 vehicles

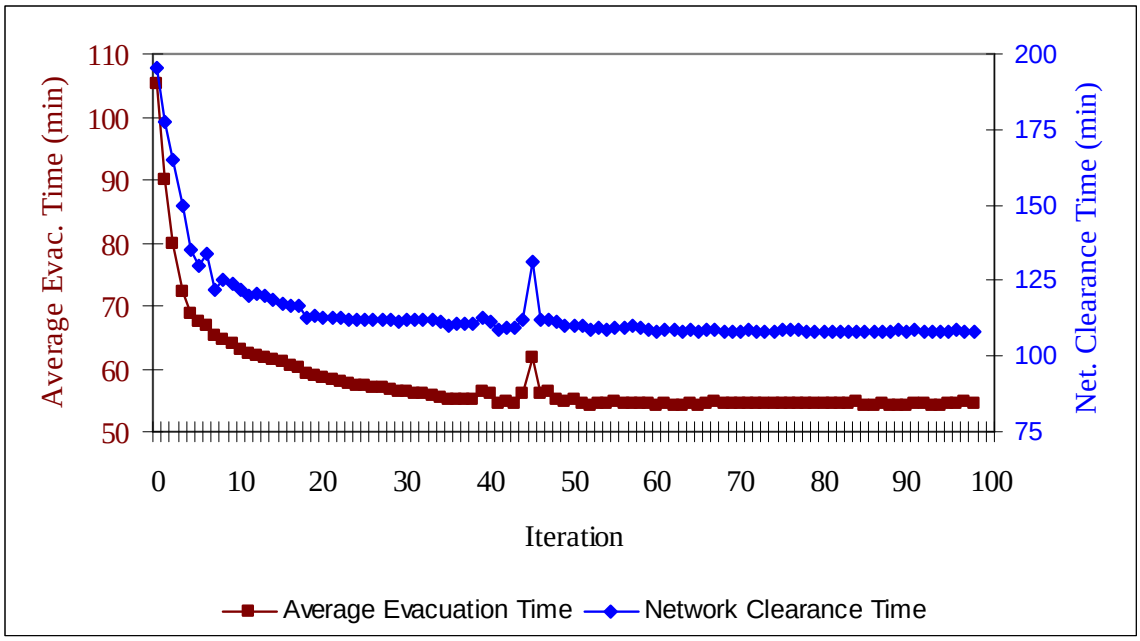

Figure 4.18 Average evacuation time and network clearance time convergence pattern for LNCT-DTA algorithm on Fort Worth network – 30,000 vehicles

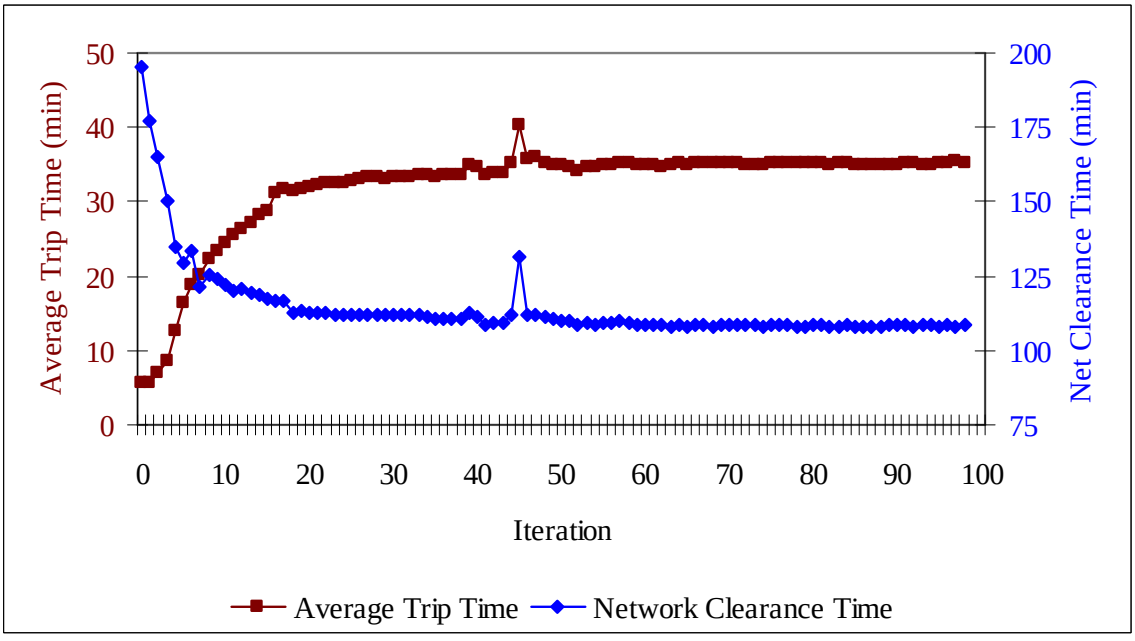

Figure 4.19 Average trip time and network clearance time convergence pattern for LNCT-DTA algorithm on Fort Worth network – 30,000 vehicles

Table 4.10 Summary of LNCT-DTA optimality results for Fort Worth network – 30,000 vehicles

Measure of Effectiveness	*Initial Conditions*	*Results at Optimality*	*Results after 75 Iterations*
Iteration	0	86	100
Network Clearance Time (min)	195.5	108.14	108.36
Average LNCT-DTA Objective (min)	N/A	35.62	36.07
Average Evacuation Time (min)	105.3	53.98	54.37
Average Trip Time (min)	105.3	34.83	35.21

The second experiment is conducted for an evacuation demand of 45,000 vehicles and a latest evacuation time of 166.8 min. Figure 4.20 depicts the network clearance time and transformed (average) LNCT-DTA objective results of the first 100 iterations of the algorithm. The optimal objective value is 45.91 min and is achieved after 92 iterations. The corresponding network clearance time is 168.07 min, a 0.8% decrease over the target evacuation time. The average evacuation time at optimality is 84.82 min, a 1.7% increase over the associated MNCT-DTA problem (83.4 min).

The average trip time is 45.51 min, which is slightly less (0.9%) than the (transformed) average LNCT-DTA objective (45.91 min), means that almost all vehicles managed to exit the network within the target evacuation time of 166.8 min. Moreover, the average trip time represents a 24% improvement over the associated MNCT-DTA problem (60.1 min). Figure 4.21 shows that the behavior of the network clearance time is, as expected, very similar to that of the average evacuation time. Figure 4.22 shows that the average trip time does indeed drop with a steady the network clearance time. The results do not change much after 100 iterations as reported in Table 4.11.

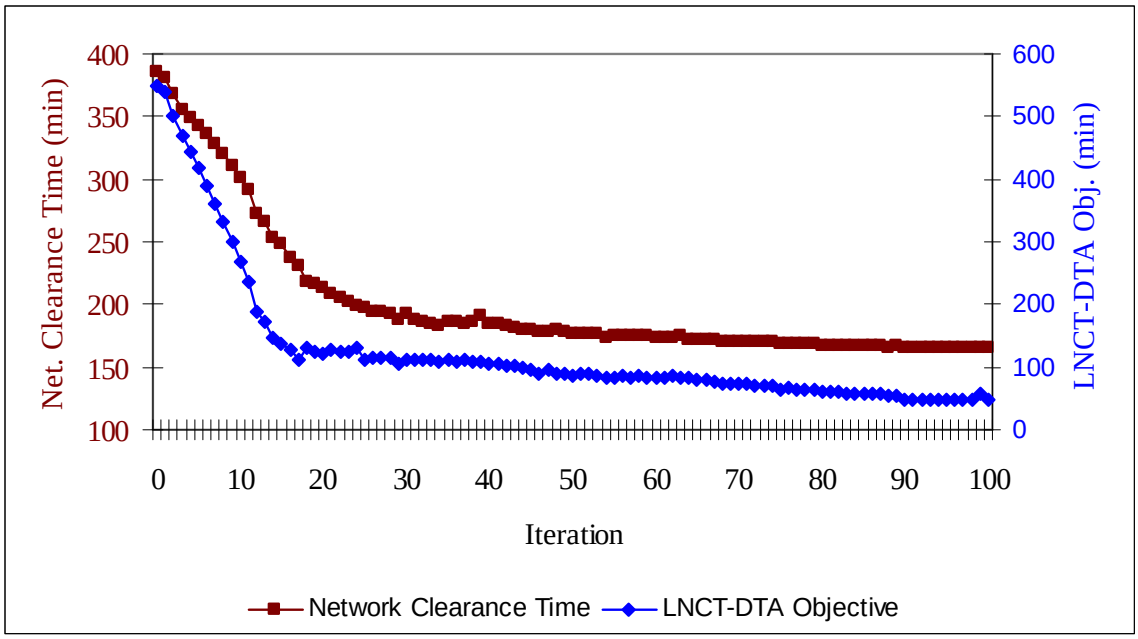

Figure 4.20 Network clearance time and LNCT-DTA objective convergence pattern for LNCT-DTA algorithm on Fort Worth network – 45,000 vehicles

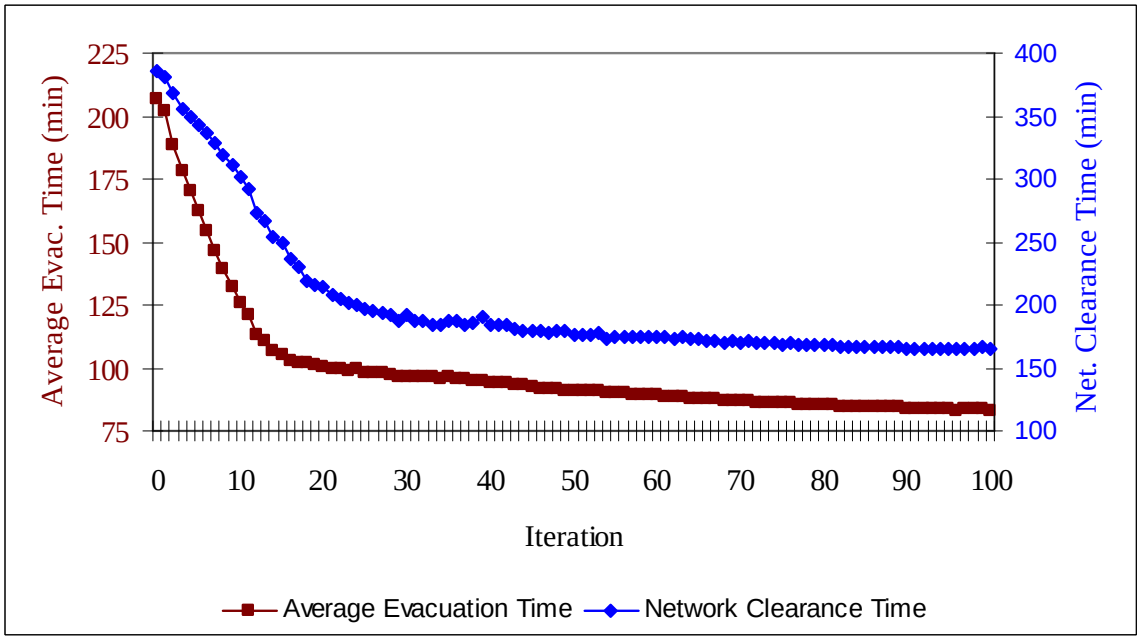

Figure 4.21 Average evacuation time and network clearance time convergence pattern for LNCT-DTA algorithm on Fort Worth network – 45,000 vehicles

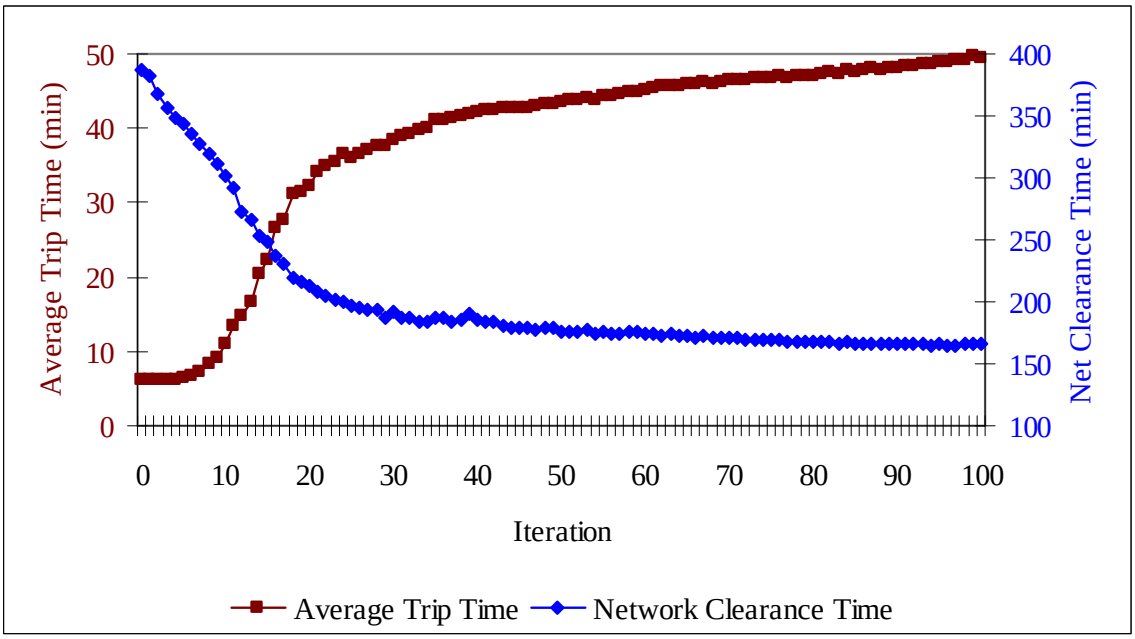

Figure 4.22 Average trip time and network clearance time convergence pattern for LNCT-DTA algorithm on Fort Worth network – 45,000 vehicles

Table 4.11 Summary of LNCT-DTA optimality results for Fort Worth network – 45,000 vehicles

Measure of Effectiveness	*Initial Conditions*	*Results at Optimality*	*Results after 75 Iterations*
Iteration	0	92	100
Network Clearance Time (min)	386.3	168.07	168.66
Average LNCT-DTA Objective (min)	N/A	45.91	46.65
Average Evacuation Time (min)	206.9	84.82	84.51
Average Trip Time (min)	206.9	45.51	45.95

4.5.2.3 ***Convergence Pattern Analysis for ODS-DTA Algorithm***

The ODS-DTA algorithm is a two stage process. The MNCT-DTA problem is solved in the first stage to determine the network clearance time and the LNCT-DTA is solved in the second stage, given the network clearance time from the first stage, to minimize trip times in the network. In this set of experiments however, the second stage, i.e. the LNCT-DTA problem, is solved with the MNCT-DTA solution as the starting solution. That is, the initial solution for the LNCT-DTA problem is not obtained by an AON assignment, but rather from the MNCT-DTA. Such a solution is therefore feasible and is expected to converge faster.

The first experiment pertains to an evacuation demand level of 30,000 vehicles. Initial conditions are a network clearance time of 195.5 min, and average evacuation and trip times of 105.3 min. Figure 4.23, Figure 4.24, Figure 4.25 show the convergence patterns of the network clearance time, average evacuation time, and average trip time, respectively. The first stage of the ODS-DTA algorithm, i.e. the MNCT-DTA algorithm converges after 61 iterations. The minimum network clearance time is reduced by 44% to 108.6 min, the average evacuation time is reduced by 49% to 54.2 min, and the average trip time is reduced by 63% to 39.1 min. The MNCT-DTA solution is then used as the initial solution to the LNCT-DTA algorithm (Stage II) with a target evacuation time of 108.6 min.

The LNCT-DTA algorithm converges after 20 iterations. The network clearance time remains virtually unchanged at 108.71; the average evacuation time is slightly higher at 54.92 or a 1.3% increase; and the average trip time is reduced by 8.7% to 35.71 min. These results compare favorably with the LNCT-DTA results obtained without a feasible starting solution as shown in Table 4.12. The interesting finding is that it only took 20 iterations for the LNCT-DTA algorithm to converge if the MNCT-DTA optimal solution is used as the starting solution as opposed to 86 iterations for the case where an AON assignment is used (not a feasible solution).

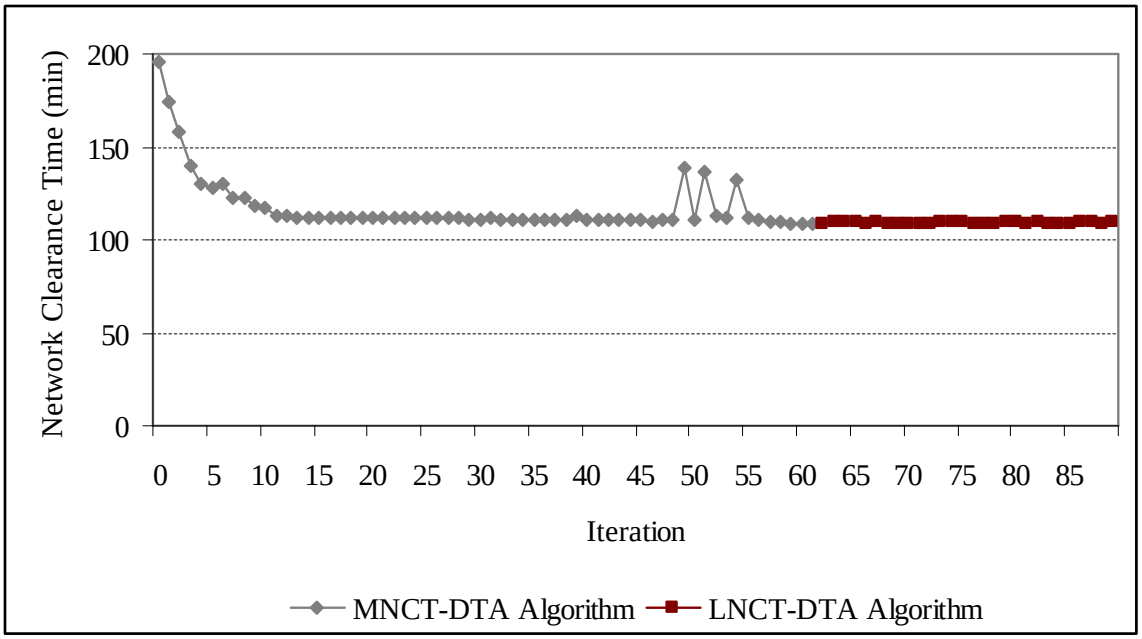

Figure 4.23 Network clearance time convergence pattern for ODS-DTA algorithm for Fort Worth network – 30,000 vehicles

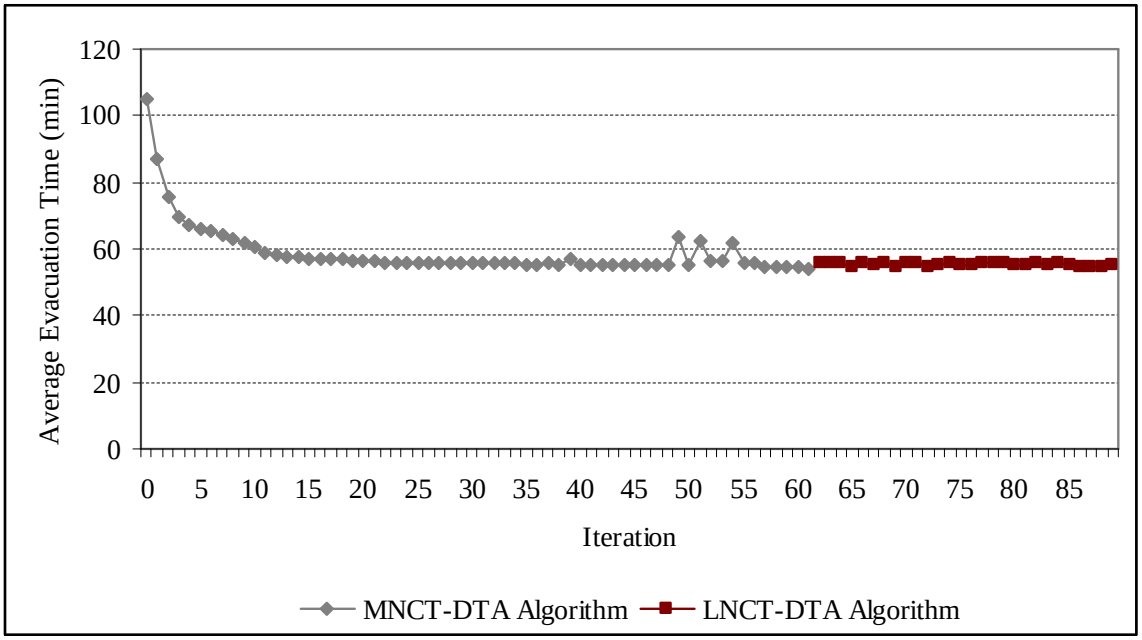

Figure 4.24 Average evacuation time convergence pattern for ODS-DTA algorithm for Fort Worth network – 30,000 vehicles

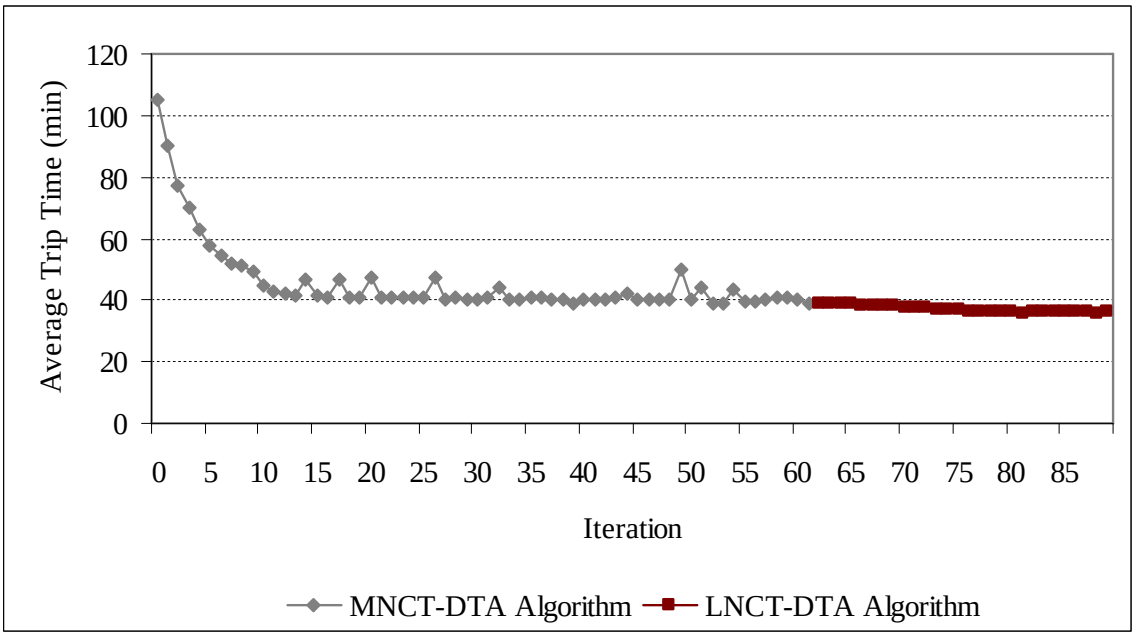

Figure 4.25 Average trip time convergence pattern for ODS-DTA algorithm for Fort Worth network – 30,000 vehicles

Table 4.12 Summary of ODS-DTA optimality results for Fort Worth network – 30,000 vehicles

Measure of Effectiveness	*Initial Conditions*	*Results at End of Stage I (MNCT-DTA)*	*Results at End of Stage II (LNCT-DTA)**	*Results at end of Stand-alone LNCT-DTA***
Iteration	0	61	20 (81 total)	86
Network Clearance Time (min)	195.5	108.6	108.71	108.14
Average LNCT Time (min)	N/A	N/A	36.58	35.62
Average Evacuation Time (min)	105.3	54.2	54.92	53.98
Average Trip Time (min)	105.3	39.1	35.71	34.83

* *Initial solution is obtained from stage I*

** *Initial solution is AON*

The second experiment pertains to an evacuation demand level of 45,000 vehicles. Initial conditions are a network clearance time of 386.3 min, and average evacuation and trip times of 206.9 min. Figure 4.26, Figure 4.27, Figure 4.28 show the convergence patterns of the network clearance time, average evacuation time, and average trip time, respectively. The first stage of the ODS-DTA algorithm, i.e. the MNCT-DTA algorithm converges after 88 iterations. The resulting network clearance time is reduced by 57% to 166.8 min, the average

evacuation time is reduced by 60% to 83.4 min, and the average trip time is reduced by 71% to 60.1 min. The MNCT-DTA solution is then used as the initial solution to the LNCT-DTA algorithm (Stage II) with a target evacuation time of 108.6 min, which converges after 37 iterations. The resulting network clearance time is 1.3% higher than the target evacuation time of 166.8 min, the average evacuation time is slightly higher at 84.4 or a 1.2% increase, and the average trip time is improved by 23% to 46.5 min. These results compare favorably with the LNCT-DTA results obtained without a feasible starting solution as shown in Table 4.13. It only took 37 iterations for the LNCT-DTA algorithm to converge if the MNCT-DTA optimal solution is used as the starting solution as opposed to 92 iterations for the case where no feasible solution is used.

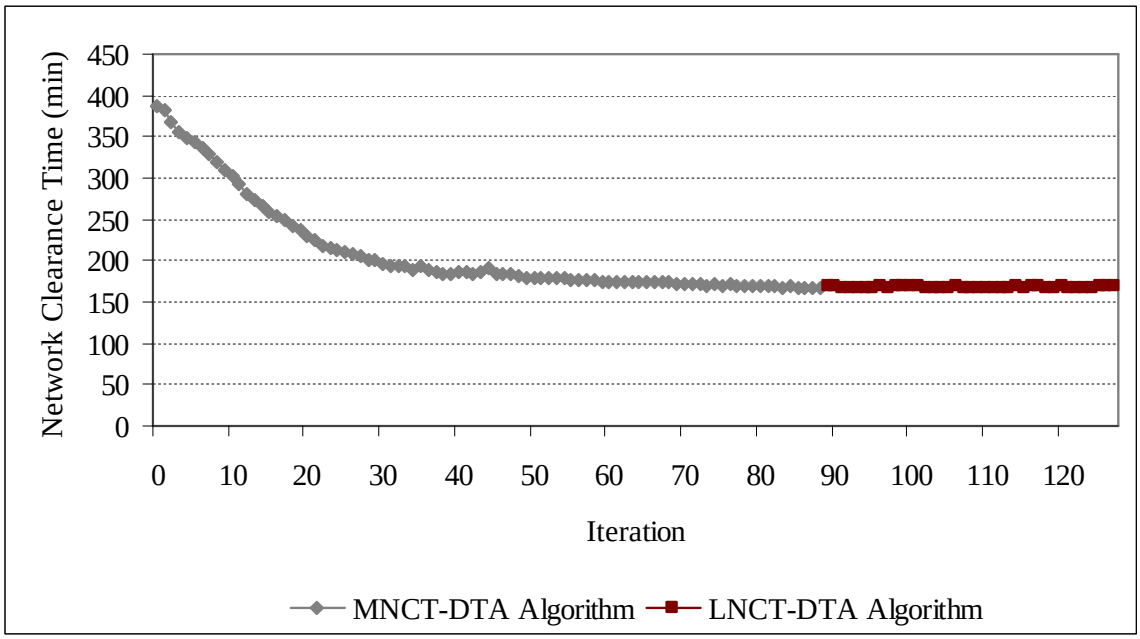

Figure 4.26 Network clearance time convergence pattern for ODS-DTA algorithm for Fort Worth network – 45,000 vehicles

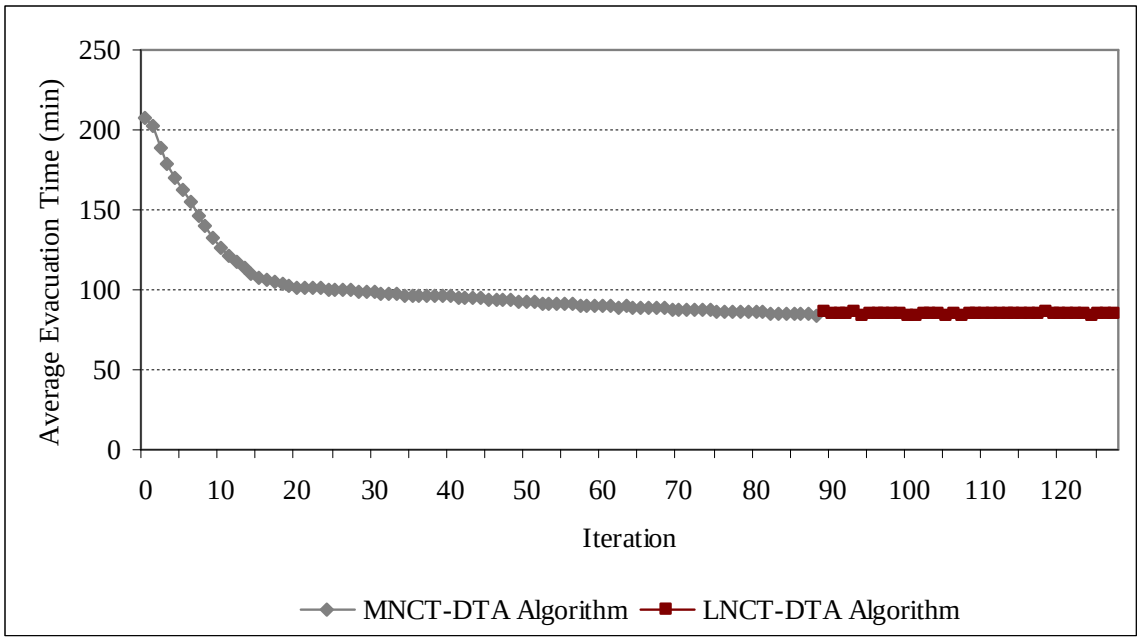

Figure 4.27 Average evacuation time convergence pattern for ODS-DTA algorithm for Fort Worth network – 45,000 vehicles

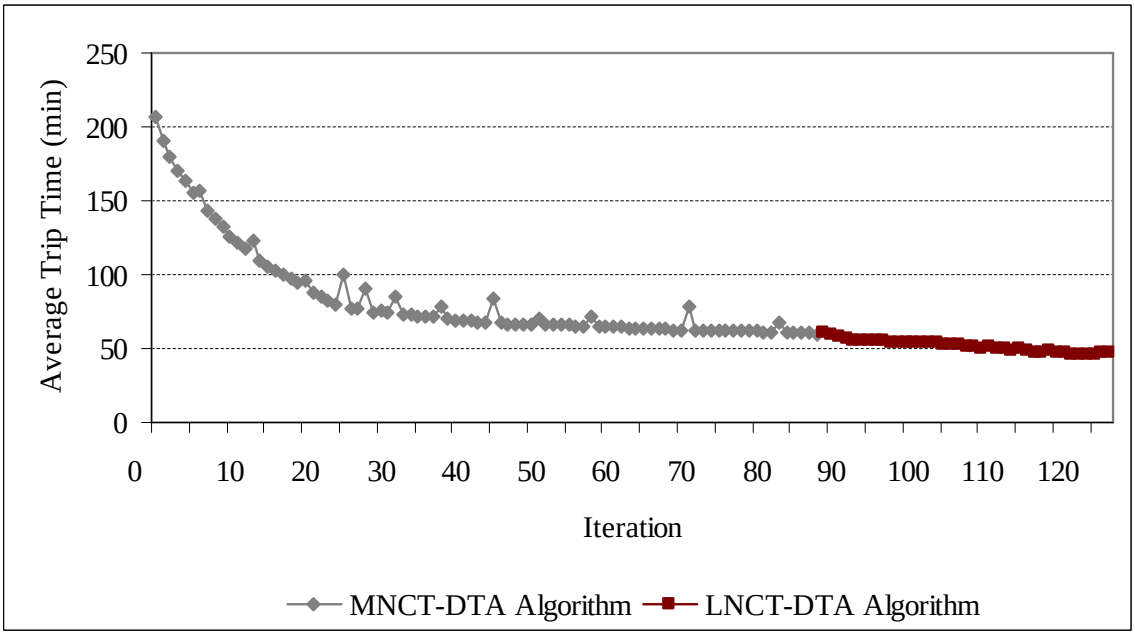

Figure 4.28 Average trip time convergence pattern for ODS-DTA algorithm for Fort Worth network – 45,000 vehicles

Table 4.13 Summary of ODS-DTA optimality results for Fort Worth network – 45,000 vehicles

Measure of Effectiveness	*Initial Conditions*	*Results at End of Stage I (MNCT-DTA)*	*Results at End of Stage II (LNCT-DTA)**	*Results at end of Stand-alone LNCT-DTA***
Iteration	0	88	37 (125 total)	92
Network Clearance Time (min)	386.3	166.8	168.98	168.07
Average LNCT Time (min)	N/A	N/A	47.31	45.91
Average Evacuation Time (min)	206.9	83.4	84.44	84.82
Average Trip Time (min)	206.9	60.1	46.56	45.51

* *Initial solution is obtained from stage I*

** *Initial solution is AON*

4.5.2.4 ***Staging Policy***

The objective of demand scheduling is to evacuate the network in stages rather than simultaneously. Therefore, it is important to compute the staging policy, i.e. how much traffic to evacuate every departure time period. We refer to this distribution as the staging policy. Figure 4.29 depicts the fraction of demand loaded as a function of time for the 30,000 vehicles evacuation demand as imputed from the MNCT-DTA, LNCT-DTA, and ODS-DTA solutions for zone 1.

Figure 4.29 shows the clear differences between the staging policies of the MNCT-DTA and the LNCT-DTA (or ODS-DTA) solutions. In the MNCT-DTA staging policy, and as expected, more demand is concentrated on early departure periods, with total demand spread over 75 min. In contrast, the LNCT-DTA (and ODS-DTA) algorithms shift more demand towards the later departure periods, with a total spread of 90 min.

Another way to look at the inherent differences between the MNCT-DTA and LNCT-DTA (or ODS-DTA) algorithms, is to look at the cumulative demand loading curve. For example, the MNCT-DTA algorithm loads 41% of the demand in the first 5 min, whereas the LNCT-DTA and ODS-DTA algorithms load 31% and 27%, respectively (Figure 4.30).

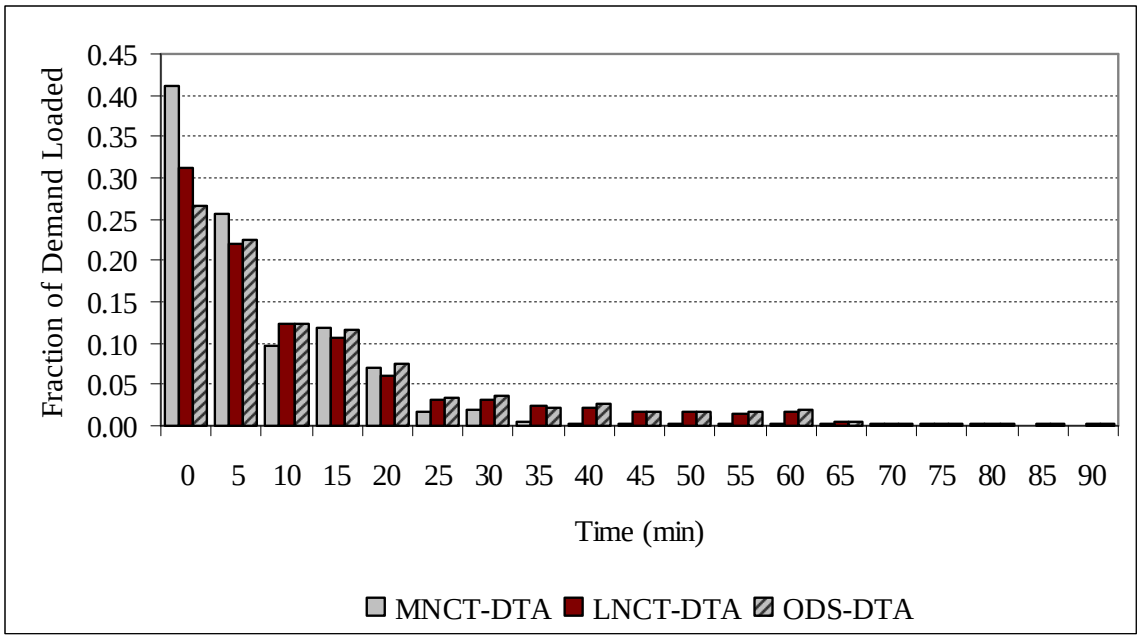

Figure 4.29 Fraction of demand loaded as a function of time for Fort Worth – 30,000 vehicles

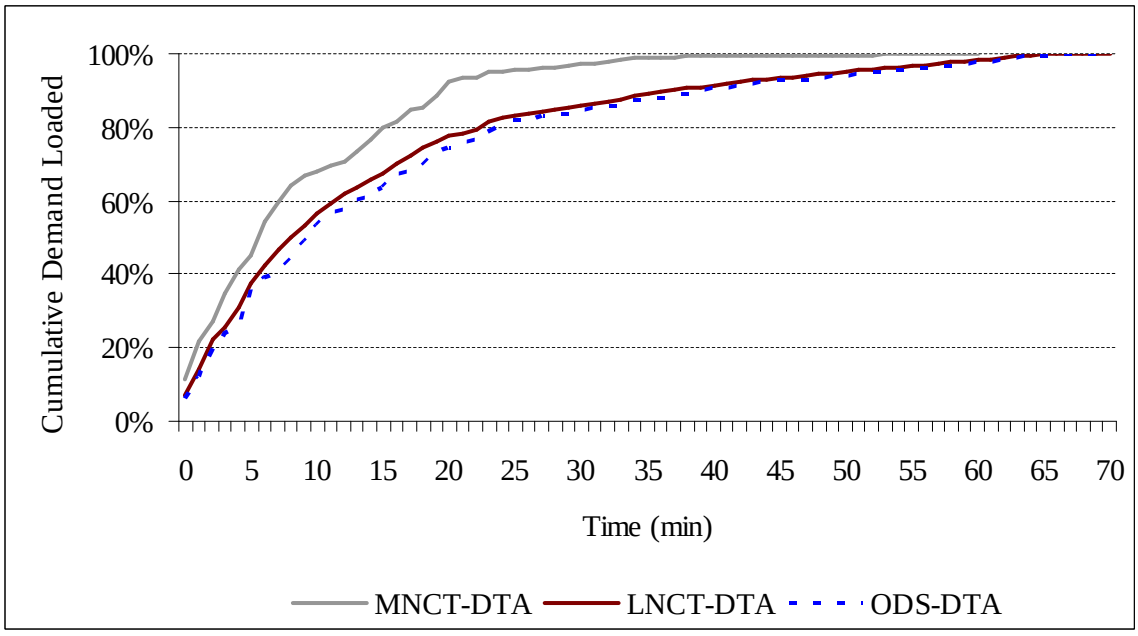

Figure 4.30 Cumulative demand loaded as a function of time for Fort Worth – 30,000 vehicles

Figure 4.31 depicts the fraction of demand loaded as a function of time for the 45,000 vehicles evacuation demand as imputed from the MNCT-DTA, LNCT-DTA, and ODS-DTA solutions for zone 1. The MNCT-DTA staging policy concentrates (or front-loads) the demand on early departure periods, with total demand spread over 100 min. In contrast, the LNCT-DTA and ODS-DTA algorithms shift more demand towards the later departure periods, with a total spread of 130 min. Figure 4.32 shows that the MNCT-DTA algorithm loads 32% of the demand in the first 5 min, whereas the LNCT-DTA and ODS-DTA algorithms load 24% and 20%, respectively. Figure 4.32 also show that there are not much difference between the LNCT-DTA and ODS-DTA solutions.

Note that the network clearance times for all these experiments have been obtained by assuming vehicles follow an SO-type of route choice behavior. While there is no guarantee that vehicles would follow such route a choice behavior, it may be easier to enforce the staging policy instead. Therefore, it would be interesting to know, under pre-trip information provisions, the impact of the staging policies as imputed from the LNCT-DTA or ODS-DTA solutions, on network clearance time versus simultaneous evacuations, however, this is beyond the scope of this dissertation.

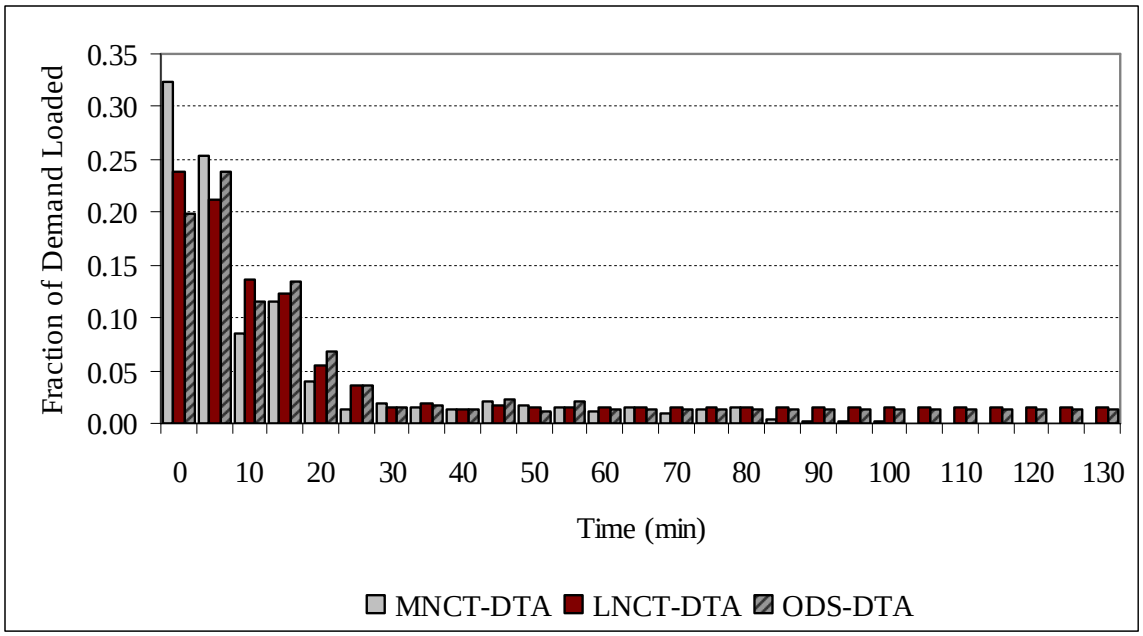

Figure 4.31 Fraction of demand loaded as a function of time for Fort Worth – 45,000 vehicles

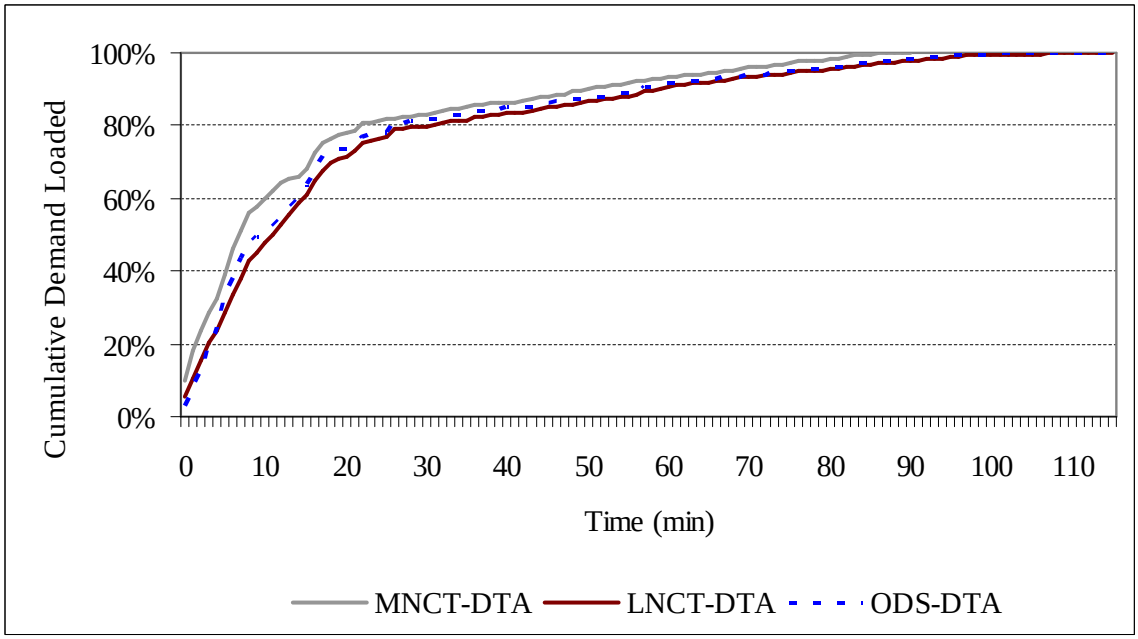

Figure 4.32 Cumulative demand loaded as a function of time for Fort Worth – 45,000 vehicles

5 CONTRAFLOW DESIGN PROBLEMS FOR EVACUATION APPLICATIONS

5.1 CONCEPTS AND NOTATIONS

Let $c_a(t)$ be the travel time for link a at time step t. The relationship between link costs and path costs are defined as:

$$C_{r,s,p}^{\tau} = \sum_t \sum_a c_a(t).\xi_{r,s,p}^{\tau,a}(t) \qquad \forall r,s,p,\tau \tag{5.1}$$

Similarly, let $\tilde{c}_a(t)$ be the marginal travel time for link a at time step t. The relationship between link marginal costs and path marginal costs are defined as:

$$\tilde{C}_{r,s,p}^{\tau} = \sum_t \sum_a \tilde{c}_a(t).\xi_{r,s,p}^{\tau,a}(t) \quad \forall r,s,p,\tau \tag{5.2}$$

Although all links may be reversed, in this study and consistent with current practice, we only consider freeway links and major arterials to be reversible. Consider a directed link $a \in \overline{A}$ with l_a lanes, where $\overline{A}$ is the set of reversible links. In this study, the analysis is based on the concept of coupled links (a, a^{-1}) where a^{-1} is the link running in opposite direction to a [Tuydes (2005)]. Let ω_a be the number of reversible lanes added to or subtracted from link a, i.e. ω_a is algebraic. A positive value for ω_a means that link a will receive an additional ω_a lanes from its coupled link a^{-1} or equivalently link a^{-1} will have $|\omega_a|$ of its lanes reversed, and vice-versa. That is the extra capacity received by link a implies a similar capacity reduction for its coupled link a^{-1}. Mathematically, this can be stated as follows:

$$\omega_a(t) + \omega_{a^{-1}}(t) = 0 \qquad \forall a, a^{-1} \in \overline{A} \tag{5.3}$$

The number of lanes that can be reversed in a given link a is bounded by the existing number of lanes on that link l_a. Moreover, the number of lanes that can be added to a is

bounded by the number of lanes on its coupled link $l_{a^{-1}}$:

$$-l_a \le \omega_a \le l_{a^{-1}} \qquad \forall a, a^{-1} \in \overline{A} \tag{5.4}$$

5.2 THE DISCRETE CONTRAFLOW NETWORK DESIGN PROBLEM

While network design problems are generally UE-based, the contraflow network design problem in this dissertation is SO-based. We refer to the problem as CF-DTA and it is stated as follows: given the time dependent O-D demand desires $d_{r,s}^{\tau}$ and a set of candidate reversible links $\overline{A}$; we want to find the time-dependent path-flow assignments $f_{r,s,p}^{\tau}$ as well as the number of lanes reversed ω_a for each reversible link $a \in \overline{A}$ to minimize the total system travel time subject to feasibility and DTA constraints.

Given: $d_{r,s}^{\tau}, \overline{A}$

Find: $f_{r,\bar{s},p}^{\tau}, \omega_a$

To:
$$\text{Min } Z(\boldsymbol{f}) = \sum_{\tau}\sum_{r}\sum_{s}\sum_{p} C_{r,s,p}^{\tau} f_{r,s,p}^{\tau} \tag{5.5}$$

Subject to:
$$\sum_{p} f_{r,s,p}^{\tau} = d_{r,s}^{\tau} \qquad \forall r, s, \tau \tag{5.5a}$$

$$\omega_a + \omega_{a^{-1}} = 0 \qquad \forall a, a^{-1} \in \overline{A} \tag{5.5b}$$

$$\omega_a - l_{a^{-1}} \le 0 \qquad \forall a, a^{-1} \in \overline{A} \tag{5.5c}$$

$$-l_a - \omega_a \le 0 \qquad \forall a \in \overline{A} \tag{5.5d}$$

$$f_{r,s,p}^{\tau} \ge 0 \qquad \forall r, s, p, \tau \tag{5.5e}$$

DTA constraints (5.5f)

5.3 FIRST-ORDER OPTIMALITY CONDITIONS

The optimality conditions of the model are studied to investigate the underlying assignment principle, which in turn will shape the solution algorithm for the problem. Let $\boldsymbol{L}(\boldsymbol{f},\boldsymbol{\omega},\tilde{\boldsymbol{\pi}},\boldsymbol{\mu},\boldsymbol{\zeta},\boldsymbol{\psi})$ be the Lagrangian of the program (5.5), where $\tilde{\boldsymbol{\pi}}$, $\boldsymbol{\mu}$, $\boldsymbol{\zeta}$, and $\boldsymbol{\psi}$ denote the vector of Lagrangian variables associated with the constraints (5.5a), (5.5b), (5.5c), and (5.5d), respectively.

$$\begin{aligned}\text{Min}\,\boldsymbol{L}(\boldsymbol{f},\boldsymbol{\omega},\tilde{\boldsymbol{\pi}},\boldsymbol{\mu},\boldsymbol{\zeta},\boldsymbol{\psi}) = \sum_{\tau}\sum_{r}\sum_{s}\sum_{p} C^{\tau}_{r,s,p}\cdot f^{\tau}_{r,s,p} - \sum_{\tau}\sum_{r}\sum_{s}\tilde{\pi}^{\tau}_{r,s}\left(d^{\tau}_{r,s} - \sum_{p} f^{\tau}_{r,s,p}\right) \\ + \sum_{a}\mu_a\left(\omega_a + \omega_{a^{-1}}\right) + \sum_{a}\zeta_a\left(\omega_a - l_{a^{-1}}\right) + \sum_{a}\psi_a\left(-l_a - \omega_a\right)\end{aligned} \tag{5.6}$$

The necessary conditions for a minimum of this program are given by the first-order conditions:

$$\frac{\partial \boldsymbol{L}(\boldsymbol{f},\boldsymbol{\omega},\tilde{\boldsymbol{\pi}},\boldsymbol{\mu},\boldsymbol{\zeta},\boldsymbol{\psi})}{\partial \boldsymbol{f}} \geq 0 \tag{5.6a}$$

$$\boldsymbol{f}\frac{\partial \boldsymbol{L}(\boldsymbol{f},\boldsymbol{\omega},\tilde{\boldsymbol{\pi}},\boldsymbol{\mu},\boldsymbol{\zeta},\boldsymbol{\psi})}{\partial \boldsymbol{f}} = 0 \tag{5.6b}$$

$$\frac{\partial \boldsymbol{L}(\boldsymbol{f},\boldsymbol{\omega},\tilde{\boldsymbol{\pi}},\boldsymbol{\mu},\boldsymbol{\zeta},\boldsymbol{\psi})}{\partial \tilde{\boldsymbol{\pi}}} = 0 \tag{5.6c}$$

$$\frac{\partial \boldsymbol{L}(\boldsymbol{f},\boldsymbol{\omega},\tilde{\boldsymbol{\pi}},\boldsymbol{\mu},\boldsymbol{\zeta},\boldsymbol{\psi})}{\partial \boldsymbol{\omega}} \geq 0 \tag{5.6d}$$

$$\boldsymbol{\omega}\frac{\partial \boldsymbol{L}(\boldsymbol{f},\boldsymbol{\omega},\tilde{\boldsymbol{\pi}},\boldsymbol{\mu},\boldsymbol{\zeta},\boldsymbol{\psi})}{\partial \boldsymbol{\omega}} = 0 \tag{5.6e}$$

$$\frac{\partial \boldsymbol{L}(\boldsymbol{f},\boldsymbol{\omega},\tilde{\boldsymbol{\pi}},\boldsymbol{\mu},\boldsymbol{\zeta},\boldsymbol{\psi})}{\partial \boldsymbol{\mu}} = 0 \tag{5.6f}$$

$$\frac{\partial \boldsymbol{L}(\boldsymbol{f},\boldsymbol{\omega},\tilde{\boldsymbol{\pi}},\boldsymbol{\mu},\boldsymbol{\zeta},\boldsymbol{\psi})}{\partial \boldsymbol{\zeta}} \geq 0 \tag{5.6g}$$

$$\boldsymbol{\zeta}\frac{\partial \boldsymbol{L}(\boldsymbol{f},\boldsymbol{\omega},\tilde{\boldsymbol{\pi}},\boldsymbol{\mu},\boldsymbol{\zeta},\boldsymbol{\psi})}{\partial \boldsymbol{\zeta}} = 0 \tag{5.6h}$$

$$\frac{\partial \mathbf{L}\left(\mathbf{f},\boldsymbol{\omega},\tilde{\boldsymbol{\pi}},\boldsymbol{\mu},\boldsymbol{\zeta},\boldsymbol{\psi}\right)}{\partial \boldsymbol{\psi}} \geq 0 \tag{5.6i}$$

$$\boldsymbol{\psi}\frac{\partial \mathbf{L}\left(\mathbf{f},\boldsymbol{\omega},\tilde{\boldsymbol{\pi}},\boldsymbol{\mu},\boldsymbol{\zeta},\boldsymbol{\psi}\right)}{\partial \boldsymbol{\psi}} = 0 \tag{5.6j}$$

$$f_{r,s,p}^{\tau} \geq 0 \quad \forall r,s,p,\tau \tag{5.6k}$$

DTA constraints (5.6l)

Optimality conditions (5.6a), (5.6b), and (5.6c) are the usual SO-DTA optimality conditions. Evaluating the partial derivative $\partial \mathbf{L}\left(\mathbf{f},\boldsymbol{\omega},\tilde{\boldsymbol{\pi}},\boldsymbol{\mu},\boldsymbol{\zeta},\boldsymbol{\psi}\right)/\partial \boldsymbol{\mu}$ with respect to a random link $\dot{a}$ we get:

$$\begin{aligned}\frac{\partial \mathbf{L}\left(\mathbf{f},\boldsymbol{\omega},\tilde{\boldsymbol{\pi}},\boldsymbol{\mu},\boldsymbol{\zeta},\boldsymbol{\psi}\right)}{\partial \mu_{\dot{a}}} &= \frac{\partial \sum_{\tau}\sum_{r}\sum_{s}\sum_{p} C_{r,s,p}^{\tau}\cdot f_{r,s,p}^{\tau}}{\partial \mu_{\dot{a}}} + \frac{\partial \sum_{\tau}\sum_{r}\sum_{s} \tilde{\pi}_{r,s}^{\tau}\left(d_{r,s}^{\tau} - \sum_{p} f_{r,s,p}^{\tau}\right)}{\partial \mu_{\dot{a}}} \\ &+ \frac{\sum_{a}\mu_a\left(\omega_a + \omega_{a^{-1}}\right)}{\partial \mu_{\dot{a}}} + \frac{\sum_{a}\zeta_a\left(\omega_a - l_{a^{-1}}\right)}{\partial \mu_{\dot{a}}} + \frac{\sum_{a}\psi_a\left(-l_a - \omega_a\right)}{\partial \mu_{\dot{a}}} \\ &= \omega_{\dot{a}} + \omega_{\dot{a}^{-1}}\end{aligned} \tag{5.7}$$

Similarly, for $\partial \mathbf{L}\left(\mathbf{f},\boldsymbol{\omega},\tilde{\boldsymbol{\pi}},\boldsymbol{\mu},\boldsymbol{\zeta},\boldsymbol{\psi}\right)/\partial \boldsymbol{\zeta}$, we get:

$$\begin{aligned}\frac{\partial \mathbf{L}\left(\mathbf{f},\boldsymbol{\omega},\tilde{\boldsymbol{\pi}},\boldsymbol{\mu},\boldsymbol{\zeta},\boldsymbol{\psi}\right)}{\partial \zeta_{\dot{a}}} &= \frac{\partial \sum_{\tau}\sum_{r}\sum_{s}\sum_{p} C_{r,s,p}^{\tau}\cdot f_{r,s,p}^{\tau}}{\partial \zeta_{\dot{a}}} + \frac{\partial \sum_{\tau}\sum_{r}\sum_{s} \tilde{\pi}_{r,s}^{\tau}\left(d_{r,s}^{\tau} - \sum_{p} f_{r,s,p}^{\tau}\right)}{\partial \zeta_{\dot{a}}} \\ &+ \frac{\sum_{a}\mu_a\left(\omega_a + \omega_{a^{-1}}\right)}{\partial \zeta_{\dot{a}}} + \frac{\sum_{a}\zeta_a\left(\omega_a - l_{a^{-1}}\right)}{\partial \zeta_{\dot{a}}} + \frac{\sum_{a}\psi_a\left(-l_a - \omega_a\right)}{\partial \zeta_{\dot{a}}} \\ &= \omega_{\dot{a}} - l_{\dot{a}^{-1}}\end{aligned} \tag{5.8}$$

and for $\partial \mathbf{L}\left(\mathbf{f},\boldsymbol{\omega},\tilde{\boldsymbol{\pi}},\boldsymbol{\mu},\boldsymbol{\zeta},\boldsymbol{\psi}\right)/\partial \boldsymbol{\psi}$ we get:

$$\frac{\partial \boldsymbol{L}\,(\boldsymbol{f},\boldsymbol{\omega},\tilde{\boldsymbol{\pi}},\boldsymbol{\mu},\boldsymbol{\zeta},\boldsymbol{\psi})}{\partial \psi_{\dot{a}}} = \frac{\partial \sum_{\tau}\sum_{r}\sum_{s}\sum_{p} C^{\tau}_{r,s,k}\cdot f^{\tau}_{r,s,p}}{\partial \psi_{\dot{a}}} + \frac{\partial \sum_{\tau}\sum_{r}\sum_{s} \tilde{\pi}^{\tau}_{r,s}\left(d^{\tau}_{r,s} - \sum_{p} f^{\tau}_{r,s,p}\right)}{\partial \psi_{\dot{a}}} + \frac{\sum_{a}\mu_a\left(\omega_a + \omega_{a^{-1}}\right)}{\partial \psi_{\dot{a}}} + \frac{\sum_{a}\zeta_a\left(\omega_a - l_{a^{-1}}\right)}{\partial \psi_{\dot{a}}} + \frac{\sum_{a}\psi_{\dot{a}}\left(-l_a - \omega_a\right)}{\partial \psi_{\dot{a}}} = -l_{\dot{a}} - \omega_{\dot{a}} \tag{5.9}$$

Therefore, conditions (5.6f), (5.6g), and (5.6i) will result in obtaining the same set of constraints in program (5.5). Evaluating the partial derivative $\partial \boldsymbol{L}\,(\boldsymbol{f},\boldsymbol{\omega},\tilde{\boldsymbol{\pi}},\boldsymbol{\mu},\boldsymbol{\zeta},\boldsymbol{\psi})/\partial\boldsymbol{\omega}$ with respect to a random reversible link $\dot{a}$ we get:

$$\frac{\partial \boldsymbol{L}\,(\boldsymbol{f},\boldsymbol{\omega},\tilde{\boldsymbol{\pi}},\boldsymbol{\mu},\boldsymbol{\zeta},\boldsymbol{\psi})}{\partial \omega_{\dot{a}}} = \frac{\partial \sum_{\tau}\sum_{r}\sum_{s}\sum_{p} C^{\tau}_{r,s,p}\cdot f^{\tau}_{r,s,p}}{\partial \omega_{\dot{a}}} + \frac{\partial \sum_{\tau}\sum_{r}\sum_{s} \tilde{\pi}^{\tau}_{r,s}\left(d^{\tau}_{r,s} - \sum_{p} f^{\tau}_{r,s,p}\right)}{\partial \omega_{\dot{a}}} + \frac{\sum_{a}\mu_a\left(\omega_a + \omega_{a^{-1}}\right)}{\partial \omega_{\dot{a}}} + \frac{\sum_{a}\zeta_a\left(\omega_a - l_{a^{-1}}\right)}{\partial \omega_{\dot{a}}} + \frac{\sum_{a}\psi_a\left(-l_a - \omega_a\right)}{\partial \omega_{\dot{a}}} \tag{5.10}$$

The classical assumption of no link interactions will not hold in this formulation for coupled links since we have $\omega_{\dot{a}} + \omega_{\dot{a}^{-1}} = 0$, which means that

$$\partial \omega_{\dot{a}} = -\partial \omega_{\dot{a}^{-1}} \tag{5.11}$$

Therefore a change in the capacity of link $\dot{a}$ is expected to influence changes in link flows for both $\dot{a}$ and $\dot{a}^{-1}$. Let us evaluate the first term on the RHS of (5.10):

$$\frac{\partial \sum_{\tau}\sum_{r}\sum_{s}\sum_{p} C^{\tau}_{r,s,p} \cdot f^{\tau}_{r,s,p}}{\partial \omega_{\dot{a}}} = \sum_{\tau}\sum_{r}\sum_{s}\sum_{p}\left(f^{\tau}_{r,s,p}\frac{\partial C^{\tau}_{r,s,p}}{\partial \omega_{\dot{a}}} + C^{\tau}_{r,s,p}\frac{\partial f^{\tau}_{r,s,p}}{\partial \omega_{\dot{a}}} \right) \tag{5.12}$$

Consider the first term on the RHS of (5.12):

$$\begin{aligned}\sum_{\tau}\sum_{r}\sum_{s}\sum_{p} f^{\tau}_{r,s,p}\frac{\partial C^{\tau}_{r,s,p}}{\partial \omega_{\dot{a}}} &= \sum_{\tau}\sum_{r}\sum_{s}\sum_{p} f^{\tau}_{r,s,p}\frac{\partial\left(\sum_{t}\sum_{a} c_a(t)\xi^{\tau,a}_{r,s,p}(t)\right)}{\partial \omega_{\dot{a}}} \\ &= \frac{\sum_{t}\sum_{a}\partial c_a(t)\underbrace{\left[\sum_{\tau}\sum_{r}\sum_{s}\sum_{p}\left(f^{\tau}_{r,s,p}\xi^{\tau,a}_{r,s,p}(t)\right)\right]}_{x_a(t)}}{\partial \omega_{\dot{a}}} \\ &= \sum_{t}\sum_{a} x_a(t)\frac{\partial c_a(t)}{\partial \omega_{\dot{a}}}\end{aligned} \tag{5.13}$$

Now consider the second term on the RHS of (5.12):

$$\begin{aligned}\sum_{\tau}\sum_{r}\sum_{s}\sum_{p} C^{\tau}_{r,s,p}\frac{\partial f^{\tau}_{r,s,p}}{\partial \omega_{\dot{a}}} &= \sum_{\tau}\sum_{r}\sum_{s}\sum_{p} f^{\tau}_{r,s,p}\frac{\partial\left(\sum_{t}\sum_{a} c_a(t)\xi^{\tau,a}_{r,s,p}(t)\right)}{\partial \omega_{\dot{a}}} \\ &= \frac{\sum_{t}\sum_{a} c_a(t)\underbrace{\left[\sum_{\tau}\sum_{r}\sum_{s}\sum_{p}\partial\left(f^{\tau}_{r,s,p}\xi^{\tau,a}_{r,s,p}(t)\right)\right]}_{\partial x_a(t)}}{\partial \omega_{\dot{a}}} \\ &= \sum_{t}\sum_{a} c_a(t)\frac{\partial x_a(t)}{\partial \omega_{\dot{a}}}\end{aligned} \tag{5.14}$$

Equation (5.12) may now be re-written as:

$$\frac{\partial \sum_{\tau}\sum_{r}\sum_{s}\sum_{p} C^{\tau}_{r,s,p} f^{\tau}_{r,s,p}}{\partial \omega_{\dot{a}}} = \sum_{t}\sum_{a} x_a(t)\frac{\partial c_a(t)}{\partial \omega_{\dot{a}}} + \sum_{t}\sum_{a} c_a(t)\frac{\partial x_a(t)}{\partial \omega_{\dot{a}}} \tag{5.15}$$

Note that equation (5.15) could have been easily reached by replacing the objective function in (5.5) by the following link-based objective function:

$$\text{Min } Z = \sum_t \sum_a c_a(t) x_a(t) \tag{5.16}$$

Consider the second term in the RHS of equation (5.10):

$$\begin{aligned} &\frac{\partial \sum_\tau \sum_r \sum_s \tilde{\pi}_{r,s}^\tau \left(d_{r,s}^\tau - \sum_p f_{r,s,p}^\tau \right)}{\partial \omega_{\dot{a}}} \\ &= \frac{\sum_\tau \sum_s \sum_r \left[\sum_t \sum_a \tilde{\pi}_a(t) \xi_{r,s,p}^{\tau,a}(t) \left(d_{r,s}^\tau - \partial \sum_p f_{r,s,p}^\tau \right) \right]}{\partial \omega_{\dot{a}}} \\ &= -\sum_t \sum_a \tilde{\pi}_a(t) \frac{\partial x_a(t)}{\partial \omega_{\dot{a}}} \end{aligned} \tag{5.17}$$

Assuming there are no link interactions, i.e.

$$\frac{\partial c_a(t)}{\partial \omega_{\dot{a}}} = \begin{cases} \neq 0 & \text{if } a = \dot{a}, \dot{a}^{-1}; \forall a \in \overline{A} \\ 0 & \text{otherwise} \end{cases} \tag{5.18}$$

and

$$\frac{\partial x_a(t)}{\partial \omega_{\dot{a}}} = \begin{cases} \neq 0 & \text{if } a = \dot{a}, \dot{a}^{-1}; \forall a \in \overline{A} \\ 0 & \text{otherwise} \end{cases} \tag{5.19}$$

further reduces (5.13) to

$$\sum_\tau \sum_r \sum_s \sum_p f_{r,s,p}^\tau \frac{\partial C_{r,s,p}^\tau}{\partial \omega_{\dot{a}}} = \sum_t \left(x_{\dot{a}}(t) \frac{\partial c_{\dot{a}}(t)}{\partial \omega_{\dot{a}}} + x_{\dot{a}^{-1}}(t) \frac{\partial c_{\dot{a}^{-1}}(t)}{\partial \omega_{\dot{a}}} \right) \tag{5.20}$$

and (5.14) to

$$\sum_{\tau}\sum_{r}\sum_{s}\sum_{p} C^{\tau}_{r,s,p}\frac{\partial f^{\tau}_{r,s,p}}{\partial \omega_{\dot{a}}} = \sum_{t}\left(c_{\dot{a}}(t)\frac{\partial x_{\dot{a}}(t)}{\partial \omega_{\dot{a}}} + c_{\dot{a}^{-1}}(t)\frac{\partial x_{\dot{a}^{-1}}(t)}{\partial \omega_{\dot{a}}} \right) \tag{5.21}$$

and (5.17) to

$$\frac{\partial \sum_{\tau}\sum_{r}\sum_{s} \tilde{\pi}^{\tau}_{r,s}\left(d^{\tau}_{r,s} - \sum_{p} f^{\tau}_{r,s,p} \right)}{\partial \omega_{\dot{a}}} = -\sum_{t}\left(\tilde{\pi}_{\dot{a}}(t)\frac{\partial x_{\dot{a}}(t)}{\partial \omega_{\dot{a}}} + \tilde{\pi}_{\dot{a}}(t)\frac{\partial x_{a'^{-1}}(t)}{\partial \omega_{\dot{a}}} \right) \tag{5.22}$$

Now consider the remaining terms in the RHS of (5.10). Keeping in mind that $\partial \omega_{\dot{a}} = -\partial \omega_{\dot{a}^{-1}}$, we have:

$$\frac{\sum_{a} \mu_{a}(\omega_{a} + \omega_{a^{-1}})}{\partial \omega_{\dot{a}}} = \mu_{\dot{a}} - \mu_{\dot{a}} - \mu_{\dot{a}^{-1}} + \mu_{\dot{a}^{-1}} = 0 \tag{5.23}$$

and

$$\frac{\sum_{a} \zeta_{a}(\omega_{a} - l_{a^{-1}})}{\partial \omega_{\dot{a}}} = \zeta_{\dot{a}} - \zeta_{\dot{a}^{-1}} \tag{5.24}$$

and

$$\frac{\sum_{a} \psi_{a}(-l_{a} - \omega_{a})}{\partial \omega_{\dot{a}}} = -\psi_{\dot{a}} + \psi_{\dot{a}^{-1}} \tag{5.25}$$

The partial derivative $\partial \boldsymbol{L}(\boldsymbol{f}, \boldsymbol{\omega}, \tilde{\boldsymbol{\pi}}, \boldsymbol{\mu}, \boldsymbol{\zeta}, \boldsymbol{\psi}) / \partial \boldsymbol{\omega}$ can now be expressed in a link-based format as follows:

$$\frac{\partial \boldsymbol{L}\ (\boldsymbol{f},\boldsymbol{\omega},\widetilde{\boldsymbol{\pi}},\boldsymbol{\mu},\boldsymbol{\zeta},\boldsymbol{\psi})}{\partial \omega_{\dot{a}}} = \sum_t \begin{bmatrix} \left(x_{\dot{a}}(t)\frac{\partial c_{\dot{a}}(t)}{\partial \omega_{\dot{a}}} - x_{\dot{a}^{-1}}(t)\frac{\partial c_{\dot{a}^{-1}}(t)}{\partial \omega_{\dot{a}}} \right) \\ + \left(c_{\dot{a}}(t)\frac{\partial x_{\dot{a}}(t)}{\partial \omega_{\dot{a}}} - c_{\dot{a}^{-1}}(t)\frac{\partial x_{\dot{a}^{-1}}(t)}{\partial \omega_{\dot{a}}} \right) \\ - \left(\widetilde{\pi}_{\dot{a}}(t)\frac{\partial x_{\dot{a}}(t)}{\partial \omega_{\dot{a}}} - \widetilde{\pi}_{\dot{a}}(t)\frac{\partial x_{a'^{-1}}(t)}{\partial \omega_{\dot{a}}} \right) \end{bmatrix} + \begin{bmatrix} \left(\zeta_{\dot{a}} - \zeta_{\dot{a}^{-1}}\right) \\ + \left(\psi_{\dot{a}^{-1}} - \psi_{\dot{a}}\right) \end{bmatrix} \tag{5.26}$$

The first-order optimality conditions for program (5.6) are summarized below:

$$\left(\widetilde{C}^{\tau}_{r,s,p} - \widetilde{\pi}_{r,s} \right) \geq 0 \qquad \forall r, s, p, \tau \tag{5.27a}$$

$$f^{\tau}_{r,s,p}\left(\widetilde{C}^{\tau}_{r,s,p} - \widetilde{\pi}_{r,s} \right) = 0 \qquad \forall r, s, p, \tau \tag{5.27b}$$

$$\sum_p f^{\tau}_{r,s,p} = d^{\tau}_{r,s} \qquad \forall r, s, \tau \tag{5.27c}$$

$$\left\{ \sum_t \begin{bmatrix} \left(x_a(t)\frac{\partial c_a(t)}{\partial \omega_a} - x_{a^{-1}}(t)\frac{\partial c_{a^{-1}}(t)}{\partial \omega_a} \right) \\ + \left(c_a(t)\frac{\partial x_a(t)}{\partial \omega_a} - c_{\dot{a}^{-1}}(t)\frac{\partial x_{a^{-1}}(t)}{\partial \omega_a} \right) \\ - \left(\widetilde{\pi}_a(t)\frac{\partial x_a(t)}{\partial \omega_a} - \widetilde{\pi}_a(t)\frac{\partial x_{a^{-1}}(t)}{\partial \omega_a} \right) \end{bmatrix} + \begin{bmatrix} \left(\zeta_a - \zeta_{a^{-1}}\right) \\ + \left(\psi_{a^{-1}} - \psi_a\right) \end{bmatrix} \right\} \geq 0 \qquad \forall t, a \in \overline{A} \tag{5.27d}$$

$$\begin{pmatrix} \omega_a + \\ \omega_{a^{-1}} \end{pmatrix} \left\{ \sum_t \begin{bmatrix} \left(x_a(t)\frac{\partial c_a(t)}{\partial \omega_a} - x_{a^{-1}}(t)\frac{\partial c_{a^{-1}}(t)}{\partial \omega_a} \right) \\ + \left(c_a(t)\frac{\partial x_a(t)}{\partial \omega_a} - c_{\dot{a}^{-1}}(t)\frac{\partial x_{a^{-1}}(t)}{\partial \omega_a} \right) \\ - \left(\widetilde{\pi}_a(t)\frac{\partial x_a(t)}{\partial \omega_a} - \widetilde{\pi}_a(t)\frac{\partial x_{a^{-1}}(t)}{\partial \omega_a} \right) \end{bmatrix} + \begin{bmatrix} \left(\zeta_a - \zeta_{a^{-1}}\right) \\ + \left(\psi_{a^{-1}} - \psi_a\right) \end{bmatrix} \right\} = 0 \qquad \forall t, a \in \overline{A} \tag{5.27e}$$

$$\omega_a + \omega_{a^{-1}} = 0 \qquad \forall a, a^{-1} \in \overline{A} \tag{5.27f}$$

$$\omega_a - l_{a^{-1}} \leq 0 \qquad \forall a, a^{-1} \in \overline{A} \tag{5.27g}$$

$$\left(\zeta_a + \zeta_{a^{-1}}\right)\left(\omega_a - l_{a^{-1}}\right) = 0 \qquad \forall a, a^{-1} \in \overline{A} \tag{5.27h}$$

$$-l_a - \omega_a \le 0 \qquad \forall a \in \overline{A} \tag{5.27i}$$

$$\left(\psi_a + \psi_{a^{-1}}\right)\left(l_a + \omega_a\right) = 0 \qquad \forall a, a^{-1} \in \overline{A} \tag{5.27j}$$

$$f_{r,s,p}^{\tau} \ge 0 \qquad \forall r, s, p, \tau \tag{5.27k}$$

DTA Constraints (5.27l)

Note that optimality condition (5.27e) is automatically satisfied since $\left(\omega_a + \omega_{a^{-1}}\right) = 0$ by definition. An assignment principle can be derived from the above optimality conditions for the case when total reversibility is not attained, i.e. optimality conditions (5.27g) and (5.27i) are non-binding:

$$\omega_{\dot{a}} - l_{\dot{a}^{-1}} < 0 \qquad \forall \dot{a}, \dot{a}^{-1} \in \overline{A} \tag{5.28}$$

and

$$-l_{\dot{a}} - \omega_{\dot{a}} < 0 \qquad \forall \dot{a} \in \overline{A} \tag{5.29}$$

which means we must have $\zeta_{\dot{a}} = 0$, $\zeta_{\dot{a}^{-1}} = 0$, $\psi_{\dot{a}} = 0$, and $\psi_{\dot{a}^{-1}} = 0$. Moreover, we have,

$$\frac{\partial c_a(t)}{\partial \omega_{\dot{a}}} = \begin{cases} \neq 0 & \text{if } a = \dot{a}, \dot{a}^{-1}; \forall a \in \overline{A} \\ 0 & \text{otherwise} \end{cases} \tag{5.30}$$

and

$$\frac{\partial x_a(t)}{\partial \omega_{\dot{a}}} = \begin{cases} \neq 0 & \text{if } a = \dot{a}, \dot{a}^{-1}; \forall a \in \overline{A} \\ 0 & \text{otherwise} \end{cases} \tag{5.31}$$

therefore

$$\sum_t \sum_a x_a(t) \frac{\partial c_a(t)}{\partial \omega_{\dot{a}}} = \sum_t \left(x_{\dot{a}}(t) \frac{\partial c_{\dot{a}}(t)}{\partial \omega_{\dot{a}}} - x_{\dot{a}^{-1}}(t) \frac{\partial c_{\dot{a}^{-1}}(t)}{\partial \omega_{\dot{a}}} \right) \tag{5.32}$$

and

$$\sum_t \sum_a c_a(t) \frac{\partial x_a(t)}{\partial \omega_{\dot{a}}} = \sum_t \left(c_{\dot{a}}(t) \frac{\partial x_{\dot{a}}(t)}{\partial \omega_{\dot{a}}} - c_{\dot{a}^{-1}}(t) \frac{\partial x_{\dot{a}^{-1}}(t)}{\partial \omega_{\dot{a}}} \right) \tag{5.33}$$

and

$$\sum_t \sum_a \tilde{\pi}_a(t) \frac{\partial x_a(t)}{\partial \omega_{\dot{a}}} = \sum_t \left(\tilde{\pi}_{\dot{a}}(t) \frac{\partial x_{\dot{a}}(t)}{\partial \omega_{\dot{a}}} - \tilde{\pi}_{\dot{a}^{-1}}(t) \frac{\partial x_{\dot{a}^{-1}}(t)}{\partial \omega_{\dot{a}}} \right) \tag{5.34}$$

thus, optimality condition (5.27d) is further simplified to

$$\left[\begin{array}{l} \sum_t \left(x_{\dot{a}}(t) \frac{\partial c_{\dot{a}}(t)}{\partial \omega_{\dot{a}}} \right) - \sum_t \left(x_{\dot{a}^{-1}}(t) \frac{\partial c_{\dot{a}^{-1}}(t)}{\partial \omega_{\dot{a}^{-1}}} \right) \\ + \sum_t \left(\left(c_{\dot{a}}(t) - \tilde{\pi}_{\dot{a}}(t) \right) \frac{\partial x_{\dot{a}}(t)}{\partial \omega_{\dot{a}}} \right) - \sum_t \left(\left(c_{\dot{a}^{-1}}(t) - \tilde{\pi}_{\dot{a}^{-1}}(t) \right) \frac{\partial x_{\dot{a}^{-1}}(t)}{\partial \omega_{\dot{a}^{-1}}} \right) \end{array} \right] \geq 0 \qquad \forall \dot{a}, \dot{a}^{-1} \in \bar{A} \tag{5.35}$$

We know that condition (5.35) will always be binding at any SO assignment regardless of the lane reversibility variable $\boldsymbol{\omega}$ since replacing $\tilde{\pi}_{\dot{a}}(t)$ by $\left[c_{\dot{a}}(t) + x_{\dot{a}}(t) \frac{\partial c_{\dot{a}}(t)}{\partial x_{\dot{a}}(t)} \right]$ and $\tilde{\pi}_{\dot{a}^{-1}}(t)$ by $\left[c_{\dot{a}^{-1}}(t) + x_{\dot{a}^{-1}}(t) \frac{\partial c_{\dot{a}^{-1}}(t)}{\partial x_{\dot{a}^{-1}}(t)} \right]$ renders (5.35) to be zero. Therefore, there needs to be another (sufficient) condition to simultaneously satisfy optimality condition (5.35). Consider the following equality condition:

$$\sum_t \left(x_{\dot{a}}(t) \frac{\partial c_{\dot{a}}(t)}{\partial \omega_{\dot{a}}} \right) = \sum_t \left(x_{\dot{a}^{-1}}(t) \frac{\partial c_{\dot{a}^{-1}}(t)}{\partial \omega_{\dot{a}^{-1}}} \right) \tag{5.36}$$

Condition (5.36) renders condition (5.35) to be binding and hence it is the sufficient condition we are looking for. It also makes perfect sense as it relates the lane reversibility variables for coupled links and states that optimality occurs when the total increase in system cost due to an additional vehicle is the same for couple links. In simpler terms, optimality

occurs when an additional vehicle will have the same contribution to the system cost whether it is traverses reversible link a or its couple a^{-1}. Simple numerical examples, as we will show shortly, have been found to support condition (5.36).

Therefore, for the case where total reversibility is not attained, the first-order optimality conditions for program (5.6) will be:

$$\left(\tilde{C}^{\tau}_{r,s,p} - \tilde{\pi}_{r,s}\right) \geq 0 \qquad \forall r, s, p, \tau \tag{5.37a}$$

$$f^{\tau}_{r,s,p}\left(\tilde{C}^{\tau}_{r,s,p} - \tilde{\pi}_{r,s}\right) = 0 \qquad \forall r, s, p, \tau \tag{5.37b}$$

$$\sum_{p} f^{\tau}_{r,s,p} = d^{\tau}_{r,s} \qquad \forall r, s, \tau \tag{5.37c}$$

$$\sum_{t}\left(x_a(t)\frac{\partial c_a(t)}{\partial \omega_a}\right) = \sum_{t}\left(x_{a^{-1}}(t)\frac{\partial c_{a^{-1}}(t)}{\partial \omega_{a^{-1}}}\right) \qquad \forall t, a, a^{-1} \in \bar{A} \tag{5.37d}$$

$$\omega_a + \omega_{a^{-1}} = 0 \qquad \forall a, a^{-1} \in \bar{A} \tag{5.37e}$$

$$\omega_a - l_{a^{-1}} < 0 \qquad \forall a, a^{-1} \in \bar{A} \tag{5.37f}$$

$$-l_a - \omega_a < 0 \qquad \forall a \in \bar{A} \tag{5.37g}$$

$$f^{\tau}_{r,s,p} \geq 0 \qquad \forall r, s, p, \tau \tag{5.37h}$$

DTA Constraints (5.37i)

5.4 SIMPLE NUMERICAL EXAMPLES

Two sets of simple examples are conducted in this section to verify the optimality conditions for the CF-DTA problem derived in this chapter. Both sets are conducted over two networks and solved using the nonlinear solver in Microsoft Excel. The first network consists of two links and involves only determination of the lane reversibility variables vector i.e. no flow

assignment is necessary. The second network is a 4-link network involves both flow assignment and lane reversibility. The BPR link delay function is used in the first set of examples, whereas the Greenshields link delay function is used in the second set of examples.

5.4.1 Examples Using BPR Functions

Consider the following BPR volume-delay function:

$$c_a = c_a^{\min}\left(1+\frac{x_a}{y_a}\right)^{\alpha_a} \tag{5.38}$$

where c_a is the link travel time on link a, $c_a^{\min}$ is the minimum travel time on link a corresponding to free-flow conditions, x_a is the volume on link a, y_a is the physical capacity of link a, and α_a is the shape parameter associated with link a. The link capacity may be computed as follows:

$$y_a = (l_a + \omega_a)\cdot L_a.\kappa_a^{\text{jam}} \tag{5.39}$$

where l_a is the original number of lanes for link a, L_a is the length of link a, and κ_a^{jam} is the jam density on link a. Differentiating link cost with respect to flow, we get

$$\frac{\partial c_a}{\partial x_a} = \alpha_a.c_a^{\min}\frac{1}{(l_a+\omega_a)\cdot L_a.\kappa_a^{jam}}\left(1+\frac{x_a}{(l_a+\omega_a)\cdot L_a.\kappa_a^{\text{jam}}}\right)^{\alpha_a-1} \tag{5.40}$$

Differentiating the link cost with respect to lane reversibility variable, we get

$$\frac{\partial c_a}{\partial \omega_a} = -\alpha_a.c_a^{\min}\frac{x_a}{L_a.\kappa_a^{jam}}\frac{1}{(l_a+\omega_a)^2}.\left(1+\frac{x_a}{(l_a+\omega_a)\cdot L_a.\kappa_a^{\text{jam}}}\right)^{\alpha_a-1} \tag{5.41}$$

Example 1

This example is designed to investigate the optimality conditions of coupled links with identical link delay functions. Consider the 2-link network shown in Figure 5.1.

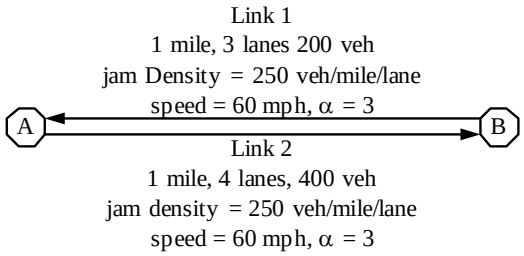

Figure 5.1 Two-link network for example 1

Assume that link travel times are given by the BPR function in (5.38). Assuming no reversibility, ($\omega_1 = \omega_2 = 0$), results in travel times of 2.03 and 2.74 min for links 1 and 2, respectively for an average system travel time of 2.51 min. Allowing for lane reversibility, we get $\omega_1 = -0.67$ and $\omega_2 = 0.67$ lanes. The average system travel time at optimality is 2.42 min, a reduction of 3.6% from initial conditions. The final parameter values show that $x_1 \partial c_1 / \partial \omega_1 = x_2 \partial c_2 / \partial \omega_2 = -158.98$ veh-min/lane, which satisfy optimality condition (5.36). Moreover, the travel times and marginal travel times are equal for links 1 and 2, which is attributed to having the same link cost specification ($\alpha, c^{\min}, \kappa^{\text{jam}}$). Table 5.1 summarizes the parameter values for this example.

Table 5.1 Example 1 optimal parameter values

Parameter	*Link 1*	*Link 2*
x (vehicles)	200	400
ω (lanes)	– 0.67	0.67
l (lanes)	2.33	4.67
c (min)	2.42	2.42
$\frac{\partial c}{\partial \omega}$ (min/lane)	– 0.79	– 0.40
$\frac{\partial c}{\partial x}$ (min/vehicle)	0.0093	0.0046
$x\frac{\partial c}{\partial \omega}$ (veh-min/lane)	– 158.98	– 158.98
$c + x\frac{\partial c}{\partial x}$ (min)	4.28	4.28
Initial objective function value (no lane reversals)		2.51 min
Final objective function value (with reversals)		2.42 min

Example 2

The second experiment is designed to investigate the effect of different link cost functions on optimality condition(5.36). The jam densities, speeds, and the shape parameters are different for links 1 and 2 (Figure 5.2).

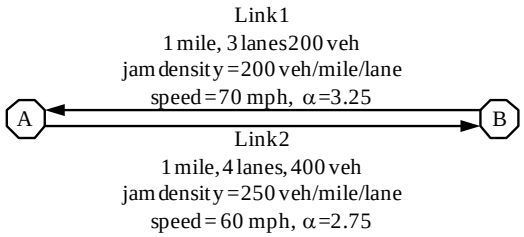

Figure 5.2. 2-link network for example 2

Assuming no reversibility ($\omega_1 = \omega_2 = 0$) results in travel times of 2.18 and 2.52 min for links 1 and 2, respectively for an average system travel time of 2.41 min. Allowing for lane reversibility, we get the link reversibility variables to be $\omega_1 = -0.34$ and $\omega_2 = 0.34$ lanes. The average system travel time at optimality is 2.38 min, a reduction of 1.2% from initial

conditions. The final parameter values show that $x_1 \partial c_1 / \partial \omega_1 = x_2 \partial c_2 / \partial \omega_2 = -161.69$ veh-min/lane, which satisfy optimality condition (5.36). However, unlike case 1, the travel times and marginal travel times are not equal for links 1 and 2 due to the use of different link cost function specifications. Table 5.2 summarizes the parameter values at optimality.

Table 5.2 Example 2 optimal parameter values

Parameter	*Link 1*	*Link 2*
x (vehicles)	200	400
ω (lanes)	– 0.34	0.34
l (lanes)	2.66	4.34
c (min)	2.42	2.37
$\frac{\partial c}{\partial \omega}$ (min/lane)	– 0.81	– 0.40
$\frac{\partial c}{\partial x}$ (min/vehicle)	0.0107	0.0044
$x\frac{\partial c}{\partial \omega}$ (veh-min/lane)	– 161.69	– 161.69
$c + x\frac{\partial c}{\partial x}$ (min)	4.57	4.12
Initial objective function value (no lane reversals)		2.41 min
Final objective function value (with reversals)		2.38 min

Example 3

In this example the number of links is increased to four with links 2 and 3 being reversible (Figure 5.3). The link cost functions are identical for links 2 and 3 and different for links 1 and 4 (Table 5.3). 500 vehicles are going from A to B and 1000 vehicles from B to A.

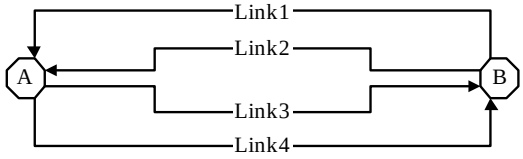

Figure 5.3. 4-link network for example 3

Table 5.3 Link cost function attributes for example 3

Link	*Lanes*	*Length (miles)*	*Jam Density (veh/mile/lane)*	*Free-Flow Speed (mph)*	*Shape Parameter (α)*
1	2	2	250	70	3.25
2	4	1	250	60	3
3	4	1	250	60	3
4	2	1.5	250	65	2.75

Assuming no reversibility, i.e. $\omega_2 = \omega_3 = 0$, the optimal flow assignment for this problem is $x_1 = 378$ veh, $x_2 = 622$ veh, $x_3 = 315$ veh, and $x_4 = 185$ veh with an average system travel time of 3.78 min. Allowing for lane reversibility, we get $\omega_2 = 2.276$ lanes and $\omega_3 = -2.276$ lanes. The optimal flow assignment corresponding to this lane reversibility scheme is $x_1 = 265$ veh, $x_2 = 735$ veh, $x_3 = 202$ veh, and $x_4 = 298$ veh with an average system travel time of 3.32 min, a 12% reduction from initial conditions.

Moreover, parameter values at optimality show that $x_2 \partial c_2 / \partial \omega_2 = x_3 \partial c_3 / \partial \omega_3 = -354.52$ veh-min/lane, which satisfy optimality condition (5.36). The travel times and marginal travel times are equal for links 1 and 2, and link 3 and 4 which verify SO optimality conditions. Furthermore, the travel times and marginal travel times are equal for links 2 and 3 due to the specification of identical link cost functions (in fact all links have equal marginal travel times in this particular example). Table 5.4 summarizes the optimal parameter values for this example.

Table 5.4 Example 3 optimal parameter values

Parameter	*Link 1*	*Link 2*	*Link 3*	*Link 4*
x (vehicles)	265	735	202	298
ω (lanes)	N/A	2.276	– 2.276	N/A
l (lanes)	2	6.276	1.724	2
c (min)	3.68	3.17	3.17	3.48
$\frac{\partial c}{\partial \omega}$ (min/lane)	– 1.26	– 0.48	– 1.76	– 1.36
$\frac{\partial c}{\partial x}$ (min/vehicle)	0.0095	0.0041	0.0150	0.0091
$x\frac{\partial c}{\partial \omega}$ (veh-min/lane)	– 332.99	– 354.52	– 354.52	– 405.3
$c + x\frac{\partial c}{\partial x}$ (min)	6.19	6.19	6.19	6.19
Initial objective function value (no lane reversals)				3.78 min
Final objective function value (with reversals)				3.32 min

Example 4

In this experiment, the link attributes for the 4-link network in Figure 5.3 are designed in such a way that no two links have identical cost attributes (Table 5.5).

Table 5.5 Link attributes for example 4

Link	*Lanes*	*Length (miles)*	*Jam Density (veh/mile/lane)*	*Free-Flow Speed (mph)*	*Shape Parameter (α)*
1	2	2	250	70	3.25
2	4	1	225	60	2.5
3	4	1	275	55	3
4	2	1.5	200	65	2.75

Assuming no reversibility, i.e. $\omega_2 = \omega_3 = 0$, the optimal flow assignment for this problem is $x_1 = 341$ veh, $x_2 = 659$ veh, $x_3 = 340$ veh, and $x_4 = 160$ veh with an average system travel time of 3.58 min. Allowing for lane reversibility, we get $\omega_2 = 1.84$ lanes and $\omega_3 = -1.84$ lanes. The optimal flow assignment corresponding to this lane reversibility scheme is

$x_1 = 252$ veh, $x_2 = 748$ veh, $x_3 = 261$ veh, and $x_4 = 239$ veh with an average system travel time of 3.26 min, a 9% reduction from initial conditions. Moreover, parameter values at optimality show that $x_2 \partial c_2 / \partial \omega_2 = x_3 \partial c_3 / \partial \omega_3 = -358.82$ veh-min/lane, which satisfy optimality condition (5.36). Moreover, the marginal travel times are equal for links 1 and 2, and links 3 and 4, which also verifies SO optimality conditions. Table 5.6 summarizes the parameter values at optimality for this example.

Table 5.6 Example 4 optimal parameter values

Parameter	*Link 1*	*Link 2*	*Link 3*	*Link 4*
x (vehicles)	252	748	261	239
ω (lanes)	N/A	1.84	– 1.84	N/A
l (lanes)	2	5.84	2.16	2
c (min)	3.56	3.09	3.25	3.48
$\frac{\partial c}{\partial \omega}$ (min/lane)	– 1.16	– 0.48	– 1.38	– 1.37
$\frac{\partial c}{\partial x}$ (min/vehicle)	0.0092	0.0037	0.0114	0.0114
$x\frac{\partial c}{\partial \omega}$ (veh-min/lane)	– 292.41	– 358.82	– 358.82	– 326.77
$c + x\frac{\partial c}{\partial x}$ (min)	5.88	5.89	6.22	6.22
Initial objective function value (no lane reversals)				3.58 min
Final objective function value (with reversals)				3.26 min

5.4.2 Examples Using Greenshields Traffic Flow Relationship

In this set of experiments, we will repeat the examples 1 through 4 using the Greenshields traffic model, which relates speed to density as follows:

$$\vartheta_a = \vartheta_a^{\text{free}} \left(1 - \frac{\kappa_a}{\kappa_a^{\text{jam}}} \right)^{\alpha_a} \qquad \forall \kappa_a \le \kappa_a^{\text{jam}} \tag{5.42}$$

This model is different from the "modified" Greenshields model embedded in DYNASMART however; the analysis is just as valid. The link density κ_a can be expressed in terms of flow as follows:

$$\kappa_a = \frac{x_a}{(l_a + \omega_a) \cdot L_a} \tag{5.43}$$

Expressing the speed as the quotient of link length by link travel time, we have:

$$\frac{L_a}{c_a} = \vartheta_a^{\text{free}} \left(1 - \frac{x_a}{(l_a + \omega_a) \cdot L_a . \kappa_a^{\text{jam}}} \right)^{\alpha_a}, \quad \forall \kappa_a \le \kappa_a^{\text{jam}} \tag{5.44}$$

Rearranging the terms we get the following link delay function:

$$c_a = \frac{L_a}{\vartheta_a^{\text{free}} \left(1 - \frac{x_a}{(l_a + \omega_a) \cdot L_a . \kappa_a^{\text{jam}}} \right)^{\alpha_a}}, \quad \forall \kappa_a \le \kappa_a^{\text{jam}} \tag{5.45}$$

Adjusting the model to incorporate lane reversibility variables, we get:

$$c_a = \frac{L_a}{\vartheta_a^{\text{free}} \left(1 - \frac{x_a}{(l_a + \omega_a) \cdot L_a . \kappa_a^{\text{jam}}} \right)^{\alpha_a}}, \quad \forall \kappa_a \le \kappa_a^{\text{jam}} \tag{5.46}$$

Differentiating the link cost with respect to link volume, we get

$$\frac{\partial c_a}{\partial x_a} = \alpha_a \frac{L_a}{\vartheta_a^{\text{free}}} \frac{1}{(l_a + \omega_a) \cdot L_a . \kappa_a^{\text{jam}}} \left(1 - \frac{x_a}{(l_a + \omega_a) \cdot L_a . \kappa_a^{\text{jam}}} \right)^{-\alpha_a - 1}, \quad \forall \kappa_a \le \kappa_a^{\text{jam}} \tag{5.47}$$

Similarly differentiating link cost with respect to link lanes we get:

$$\frac{\partial c_a}{\partial l_a} = -\alpha_a \frac{L_a}{\vartheta_a^{\text{free}}} \frac{x_a}{L_a . \kappa_a^{\text{jam}}} \frac{1}{(l_a + \omega_a)^2} \left(1 - \frac{x_a}{(l_a + \omega_a) \cdot L_a . \kappa_a^{\text{jam}}} \right)^{-\alpha_a - 1}, \quad \forall \kappa_a \le \kappa_a^{\text{jam}} \tag{5.48}$$

Example 5

Consider the 2-link network shown in Figure 5.1. Assume that link travel times are now given by the Greenshields link delay function given in (5.46). Assuming no reversibility, ($\omega_1 = \omega_2 = 0$) results in travel times of 2.53 and 4.63 min for links 1 and 2, respectively for an average system travel time of 3.93 min. Allowing for reversibility, we get $\omega_1 = -0.67$ and $\omega_2 = 0.67$ lanes. The average system travel time at optimality is 3.52 min, a reduction of 10% from initial conditions. The final parameter values show that $x_1 \partial c_1 / \partial \omega_1 = x_2 \partial c_2 / \partial \omega_2 = -472.77$ veh-min/lane, which satisfy optimality condition (5.36). Moreover, the travel and marginal travel times are equal for links 1 and 2, due to the identical cost functions. Table 5.7 summarizes the parameter values for this example.

Table 5.7 Example 5 optimal parameter values

Parameter	*Link 1*	*Link 2*
x (vehicles)	200	400
ω (reversible lanes)	– 0.67	0.67
l (lanes)	2.33	4.67
c (min)	3.52	3.52
$\frac{\partial c}{\partial \omega}$ (min/lane)	– 2.36	– 1.18
$\frac{\partial c}{\partial x}$ (min/vehicle)	0.0276	0.0138
$x\frac{\partial c}{\partial \omega}$ (veh-min/lane)	– 472.77	– 472.77
$c + x\frac{\partial c}{\partial x}$ (min)	9.04	9.04
Initial objective function value (no lane reversals)		3.93 min
Final objective function value (with reversals)		3.52 min

Example 6

In this example, example 2 is now repeated with link costs being given by the Greenshields link delay function. Assuming no reversibility ($\omega_1 = \omega_2 = 0$) results in travel times of 3.2 and

4.07 min for links 1 and 2, respectively for an average system travel time of 3.78 min. Allowing for reversibility, we get $\omega_1 = -0.3$ and $\omega_2 = 0.3$ lanes. The average system travel time at optimality is 3.68 min, a reduction of 2.65% from initial conditions. The final parameter values show that $x_1 \partial c_1 / \partial \omega_1 = x_2 \partial c_2 / \partial \omega_2 = -545.39$ veh-min/lane, which satisfy optimality condition (5.36). However, unlike case 1, the travel times and marginal travel times are not equal for links 1 and 2 due to the specification of different link cost functions. Table 5.8 summarizes the optimal parameter values of this example.

Table 5.8 Example 6 optimal parameter values

Parameter	*Link 1*	*Link 2*
x (vehicles)	200	400
ω (lanes)	– 0.3	0.3
l (lanes)	2.7	4.3
c (min)	3.85	3.59
$\frac{\partial c}{\partial \omega}$ (min/lane)	– 2.73	– 1.36
$\frac{\partial c}{\partial x}$ (min/vehicle)	0.0368	0.0147
$x\frac{\partial c}{\partial \omega}$ (veh-min/lane)	– 545.39	– 545.39
$c + x\frac{\partial c}{\partial x}$ (min)	11.22	9.46
Initial objective function value (no lane reversals)		3.78 min
Final objective function value (with reversals)		3.68 min

Example 7

In this example, example 3 is repeated with link costs being given by the Greenshields link delay function. Assuming no reversibility,($\omega_2 = \omega_3 = 0$) results in $x_1 = 458$ veh, $x_2 = 542$ veh, $x_3 = 298$ veh, and $x_4 = 202$ veh with an average system travel time of 8.61 min. Allowing for reversibility, we get $\omega_2 = 2.203$ lanes and $\omega_3 = -2.203$ lanes. The optimal

flow assignment corresponding to this lane reversibility scheme is $x_1 = 337$ veh, $x_2 = 663$ veh, $x_3 = 192$ veh, and $x_4 = 308$ veh with an average system travel time of 5.72 min, a 34% reduction from initial conditions. Moreover, parameter values at optimality show that $x_2 \partial c_2 / \partial \omega_2 = x_3 \partial c_3 / \partial \omega_3 = -1276.88$ veh-min/lane, which satisfy optimality condition (5.36). The travel times and marginal travel times are equal for links 1 and 2, and link 3 and 4 which verify SO optimality conditions. Furthermore, the travel times and marginal travel times are equal for links 2 and 3 due to the specification of identical link cost functions (in fact all links have equal marginal travel times in this particular example). Table 5.9 summarizes the optimal parameter values for this example.

Table 5.9 Parameter values at optimality for example 7

Parameter	*Link 1*	*Link 2*	*Link 3*	*Link 4*
x (vehicles)	337	663	192	308
ω (lanes)	N/A	2.203	– 2.203	N/A
l (lanes)	2	6.203	1.797	2
c (min)	6.51	5.33	5.33	5.92
$\frac{\partial c}{\partial \omega}$ (min/lane)	– 5.39	– 1.93	– 6.65	– 5.68
$\frac{\partial c}{\partial x}$ (min/vehicle)	0.0319	0.018	0.0622	0.0369
$x\frac{\partial c}{\partial \omega}$ (veh-min/lane)	– 1812.56	– 1276.88	– 1276.88	– 1748.22
$c + x\frac{\partial c}{\partial x}$ (min)	17.28	17.28	17.28	17.28
Initial objective function value (no lane reversals)				8.61 min
Final objective function value (with reversals)				5.72 min

Example 8

In this example, example 4 is repeated with link costs being given by the Greenshields volume delay function. Assuming no reversibility, ($\omega_2 = \omega_3 = 0$), results in $x_1 = 459$ veh,

$x_2 = 541$ veh, $x_3 = 330$ veh, and $x_4 = 170$ veh with an average system travel time of 8.54 min. Allowing for reversibility we get $\omega_2 = 1.872$ lanes and $\omega_3 = -1.872$ lanes. The optimal flow assignment corresponding to this lane reversibility scheme is $x_1 = 348$ veh, $x_2 = 652$ veh, $x_3 = 248$ veh, and $x_4 = 252$ veh with an average system travel time of 5.96 min, a 30% reduction from initial conditions.

Moreover, parameter values at optimality show that $x_2 \partial c_2 / \partial \omega_2 = x_3 \partial c_3 / \partial \omega_3 = -1481.23$ veh-min/lane, which satisfy optimality condition (5.36). Moreover, the travel times and marginal travel times are equal for links 1 and 2, and link 3 and 4 which verify SO optimality conditions. Table 5.10 summarizes the parameter values for this example.

Table 5.10 Parameter values at optimality for example 8

Parameter	*Link 1*	*Link 2*	*Link 3*	*Link 4*
x (veh)	348	652	248	252
ω (lanes)	N/A	1.872	– 1.872	N/A
l (lanes)	2	5.872	2.128	2
c (min)	6.88	5.47	5.72	6.16
$\frac{\partial c}{\partial \omega}$ (min/lane)	– 5.97	– 2.27	– 5.96	– 6.12
$\frac{\partial c}{\partial x}$ (min/veh)	0.0343	0.0205	0.0510	0.0487
$x\frac{\partial c}{\partial \omega}$ (veh-min/lane)	– 2077.03	– 1481.23	– 1481.23	– 1539.68
$c + x\frac{\partial c}{\partial x}$ (min)	18.82	18.82	18.41	18.41
Initial objective function value (no lane reversals)				8.54 min
Final objective function value (with reversals)				5.96 min

5.5 CF-DTA SOLUTION ALGORITHM

Numerical examples 1, 3, 5, and 7 highlighted a special condition, when link cost functions are identical, that renders the link travel time marginals for coupled links to be identical at optimality. Such a condition is rather intuitive and suggests reversing lanes from links with lower marginal costs to links with higher marginal costs until equilibrium in marginal costs is reached. This implies the following simple solution heuristic for a given flow pattern $\boldsymbol{f}$:

Step 1: Given flow pattern $\boldsymbol{f}$, set of reversible links $\overline{A}$. Set iteration counter $\ell = 0$, and the lane reversibility vector $\boldsymbol{\omega}^{(0)} = 0$.

Step 2: Perform dynamic network loading of $\boldsymbol{f}$ using the current number of lanes vector $\boldsymbol{l}^{(\ell)}$. Compute the link total travel time marginals $\tilde{c}_a^{(\ell)}$ for each reversible link $a \in \overline{A}$.

Step 3: If $\left|\tilde{c}_a^{(\ell)} - \tilde{c}_{a^{-1}}^{(\ell)}\right| \le \varepsilon, \forall a \in \overline{A}$ (present convergence threshold), or $\omega_a^{(\ell)} = 1 - l_a^{(\ell)}, \forall a \in \overline{A}$ (total reversibility) stop, or $\ell = \ell_{\max}$ (maximum number of iterations), lane reversible vector $\boldsymbol{\omega}^{(\ell)}$ is optimal, otherwise continue to Step 4.

Step 4: For each coupled links $a, a^{-1} \in \overline{A}$, if $\tilde{c}_a^{(\ell)} > \tilde{c}_{a^{-1}}^{(\ell)}$, reverse a lane from link a^{-1}, i.e. $\omega_{a^{-1}}^{(\ell)} = \omega_{a^{-1}}^{(\ell)} - 1$ and $\omega_a^{(\ell)} = \omega_a^{(\ell)} + 1$. Update lane vector $\boldsymbol{l}^{(\ell+1)} = \boldsymbol{l}^{(\ell)} - \boldsymbol{\omega}^{(\ell)}$ and go to step 2. Set $\ell = \ell + 1$.

5.6 OPTIMAL DEMAND SCHEDULING WITH CONTRAFLOW PROBLEM

In this section, the demand and supply strategies are combined into one model to form the ODS-CF-DTA model.

5.6.1 Problem Statement and Formulation

Consider an urban setting represented by the directed graph $G(N, A)$ with multiple origins $r \in R$, requires evacuation due to an extreme event. Assume that a set of shelter destinations

$s \in \bar{S}$ for that type of event has been identified. Assume that the set of reversible links $\bar{A}$ has been identified. Assume that the total demand to be evacuated at each origin d_r is known and must be evacuated before a target time $\bar{W}$. Additionally, assume that the network is empty at the time of evacuation.

The ODS-CF-DTA problem is therefore to determine the time-dependent path-flow pattern $\boldsymbol{f}$ and the lane-reversibility vector ω that minimize network clearance time W while keeping the total system trip time at a minimum. As in previous models, the destination choice is incorporated by connecting all the destinations s to a super-sink $\bar{s}$ via zero-cost infinite capacity links. This transforms the problem from a multi-destination to a single-destination DTA problem. The problem is inherently bi-objective but is formulated as a single-level minimization program as follows:

Given: $d_r, \bar{s}, \bar{A}$

Find: $f^{\tau}_{r,\bar{s},p}, \omega_a$

To:
$$\text{Min } Z(\boldsymbol{f}) = \sum_{\tau}\sum_{r}\sum_{p} C^{\tau}_{r,\bar{s},p} f^{\tau}_{r,\bar{s},p} \tag{5.49}$$

Subject to:
$$\sum_{\tau}\sum_{p} f^{\tau}_{r,\bar{s},p} = d_r \qquad \forall r \tag{5.49a}$$

$$f^{\tau}_{r,\bar{s},p}\left(\tilde{\chi}^{\tau}_{r,\bar{s},p} - \hat{\pi}_{r,\bar{s}}\right) = 0 \qquad \forall r, p, \tau \tag{5.49b}$$

$$\tilde{\chi}^{\tau}_{r,\bar{s},p} - \hat{\pi}_{r,\bar{s}} \geq 0 \qquad \forall r, p, \tau \tag{5.49c}$$

$$y_a = \left(l_a + \omega_a\right) \cdot L_a . \kappa_a^{\text{jam}} \qquad \forall a \in A^{-1} \tag{5.49d}$$

$$\omega_a + \omega_{a^{-1}} = 0 \qquad \forall a, a^{-1} \in \bar{A} \tag{5.49e}$$

$$\omega_a - l_{a^{-1}} + 1 \leq 0 \qquad \forall a, a^{-1} \in \bar{A} \tag{5.49f}$$

$$1 - l_a - \omega_a \leq 0 \qquad \forall a \in \bar{A} \tag{5.49g}$$

$$f_{r,\bar{s},p}^{\tau} \geq 0 \qquad \forall r, p, \tau \tag{5.49h}$$

DTA Constraints (5.49i)

The objective function is to minimize the average trip times in the network. Constraints (5.49b) and (5.49c) represent the MNCT-DTA optimality conditions, which in combination with constraints (5.49a), (5.49h) and (5.49i) form the ODS-DTA problem. Constraints (5.49e)-(5.49g) are specific to the CF-DTA model. The optimality conditions for this problem will be the aggregation of the ODS-DTA and CF-DTA optimality conditions.

5.6.2 Optimal Demand Scheduling with Contraflow Problem Solution Heuristic

The solution procedure for the ODS-CF-DTA problem is also a two-stage procedure. In Stage I, the MNCT-DTA and CF-DTA problems are combined to solve for the optimal joint flow pattern and lane distribution configuration that results in minimizing the network clearance time. The resulting problem is referred to as MNCT-CF-DTA and is solved in an iterative bi-level framework where an MNCT-DTA problem is solved in the lower level, given current optimal lane configuration to find the optimal flow pattern that minimizes network clearance time and a CF-DTA problem is solved in the upper level, given current optimal flow pattern, to find the optimal lane configuration that minimizes trip times in the network. The process iterates until convergence. In the second stage, an LNCT-DTA problem is solved, given the optimal lane configuration $\boldsymbol{\omega}^*$, minimum network clearance time $\boldsymbol{f}^*$, and using the MNCT-CF-DTA solution as the starting solution.

5.6.3 The MNCT-CF-DTA Solution Algorithm

The solution algorithm for the MNCT-CF-DTA is described in detail below:

Step 1: Initialization

- Set outer-loop iteration counter $k = 1$ and inner-loop iteration counter $\ell = 1$.

- Set lane reversibility vector $\boldsymbol{\omega}^{(\ell=1)} = 0$.
- Let the lane configuration vector $\boldsymbol{l}^{(\ell=1)} = \boldsymbol{l}^{(k)}$
- Connect safety destinations s to super sink $\bar{s}$ with zero-time infinite capacity links.
- Solve for the time-dependent MNCT-DTA marginal cost shortest path tree $\hat{P}_{r,\bar{s}}^{\tau\ (k)}$ for all $(r, \bar{s}, \tau)$ combinations assuming free-flow link travel times.
- For each origin r, search across all shortest paths trees $\hat{P}_{r,\bar{s}}^{\tau\ (k)}, \forall \tau$ and select the departure time and path combination (τ^*, p^*) that results in lowest possible MNCT-DTA marginal cost. Let $\hat{p}_{r,\bar{s}}^{\ (k)}$ be that path, i.e.,:

$$\hat{p}_{r,\bar{s}}^{(k)} = \left(p^*, \tau^*\right) \mid \tilde{\chi}_{r,\bar{s},p^*}^{\tau^*\ (k)} = \min_{\tau,p}\left(\tilde{\chi}_{r,\bar{s},p}^{\tau\ (k)}\right)$$

- Perform an AON of the demand d_r onto $\hat{p}_{r,\bar{s}}^{(k)}$ for every r to obtain path assignments $f_{r,\bar{s},p}^{\tau\ (k)}$.

Inner-Loop: CF-DTA Algorithm

Step 2: Dynamic Network Loading Problem

- Use DYNASMART to simulate path assignments $f_{r,\bar{s},p}^{\tau\ (k)}$ using the current lane configuration vector $\boldsymbol{l}^{(\ell)}$.
- Compute the link total travel time marginals $\tilde{c}_a^{(\ell)}$ for each reversible link $a \in \bar{A}$.

Step 3: Convergence Checking

- If $\left|\tilde{c}_a^{(\ell)} - \tilde{c}_{a^{-1}}^{(\ell)}\right| \le \varepsilon, \forall a \in \bar{A}$ (convergence threshold), or $\omega_a^{(\ell)} = 1 - l_a^{(\ell)}, \forall a \in \bar{A}$ (total reversibility) or $\ell = \ell_{\max}$ (maximum number of inner-loop iterations), stop. Lane reversibility vector $\boldsymbol{\omega}^{(\ell)}$ is optimal. Set $\boldsymbol{l}^{(k+1)} = \boldsymbol{l}^{(\ell)}$, and go to step 5. Otherwise continue to Step 4.

Step 4: Update Number of Lanes

- For each coupled links $a, a^{-1} \in \bar{A}$, if $\tilde{c}_a^{(\ell)} > \tilde{c}_{a^{-1}}^{(\ell)}$, reverse a lane from link a^{-1}, i.e. $\omega_{a^{-1}}^{(\ell)} = \omega_{a^{-1}}^{(\ell)} - 1$ and $\omega_a^{(\ell)} = \omega_a^{(\ell)} + 1$.

- Update lane configuration vector $\boldsymbol{l}^{(\ell+1)} = \boldsymbol{l}^{(\ell)} - \boldsymbol{\omega}^{(\ell)}$.
- Increment inner-loop counter $\ell = \ell + 1$ and go to Step 2.

Outer-Loop: MNCT

Step 5: Dynamic Network Loading Problem

- Use DYNASMART to simulate path assignments $f_{r,\bar{s},p}^{\tau}{}^{(k)}$.
- Estimate time-dependent link travel times $c(\boldsymbol{f}^{(k)})$ and time-dependent link marginal travel times $\tilde{c}(\boldsymbol{f}^{(k)})$ from simulation results.

Step 6: Update Objective Function

- Compute $\tilde{G}_{\text{MNCT}}{}^{(k)}$ according to (4.14).
- Compute average evacuation time (proxy for MNCT-DTA objective) as

$$AET^{(k)} = \frac{\sum_{\tau}\sum_{r}\sum_{p} \chi_{r,\bar{s},p}^{\tau}{}^{(k)} f_{r,\bar{s},p}^{\tau}{}^{(k)}}{\sum_{\tau}\sum_{r}\sum_{p} f_{r,\bar{s},p}^{\tau}{}^{(k)}} \tag{5.50}$$

Step 7: Check Convergence

- Count the number of times the condition $\left| f_{r,\bar{s},p}^{\tau}{}^{(k+1)} - f_{r,\bar{s},p}^{\tau}{}^{(k)} \right| > \varepsilon$ is satisfied for all (r,τ,p) combinations and denote that number by $V(\varepsilon)$.
- If $V(\varepsilon) \le \bar{V}(\varepsilon)$ or $k \le \bar{k}$ then stop, otherwise set $k = k+1$ and go to step 5.

Step 8: Time-Dependent MNCT-DTA Marginal Cost Shortest Path Problem

- Solve for the time-dependent least MNCT-marginal time path tree $\hat{P}_{r,\bar{s}}^{\tau}{}^{(k)}$ for all $(r,\bar{s},\tau)$ combinations using link travel times $c(\boldsymbol{f}^{(k)})$ and link marginal travel times $\tilde{c}(\boldsymbol{f}^{(k)})$.
- Add $\hat{p}_{r,\bar{s}}^{\tau}{}^{(k)}$ for all departure times τ to the active-path set $\bar{P}_{r,\bar{s}}{}^{(k)}$ for each r.

Step 9: Update of Path Assignments

- Find the optimal un-adjusted shifts $\delta_{r,s,p}^{\tau}{}^{(k)}$ for all paths in active set $\bar{P}_{r,\bar{s}}{}^{(k)}$ according to equations (4.15) and (4.16).

- Find the optimal adjusted shifts $\tilde{\delta}^{\tau}_{r,s,p}{}^{(k)}$ for all paths in $\overline{P}_{r,\bar{s}}{}^{(k)}$ according to equations (4.18) and (4.19).
- Update the assignments $f^{\tau}_{r,\bar{s},p}{}^{(k+1)}$ for the next iteration $(k+1)$ using for each (r,τ,p) using (4.20).

5.7 EXPERIMENTAL RESULTS

The following set of experiments is aimed at analyzing the performances of the MNCT-CF-DTA and ODS-CF-DTA algorithms. In these experiments, we assume that each reversible link a will keep at least one lane in the direction of link a. The reason for this is two fold. First, from a logistics point of view, it allows for emergency vehicles and first responders to have complete accessibility, and secondly, from a modeling point of view, it guarantees full network connectivity and consequently better performance of the solution algorithms. We then have:

$$1-l_a \le \omega_a \le l_{a^{-1}} - 1 \qquad \forall a, a^{-1} \in \overline{A} \tag{5.51}$$

5.7.1 Convergence Pattern for the MNCT-CF-DTA Algorithm

The first series of experiments aims to examine the convergence pattern of the MNCT-DTA algorithm. Two evacuation demand levels are considered, namely, 30,000 vehicles (light-moderate traffic) and 45,000 vehicles (heavy traffic). For each demand level, the analysis is made for three solution points: 1) at initial conditions, 2) at minimum average evacuation time (optimal objective value), and 3) after 100 iterations. Zone 2 is designated as the safety destination with all the freeway links being candidates for lane reversal (Figure 5.4).

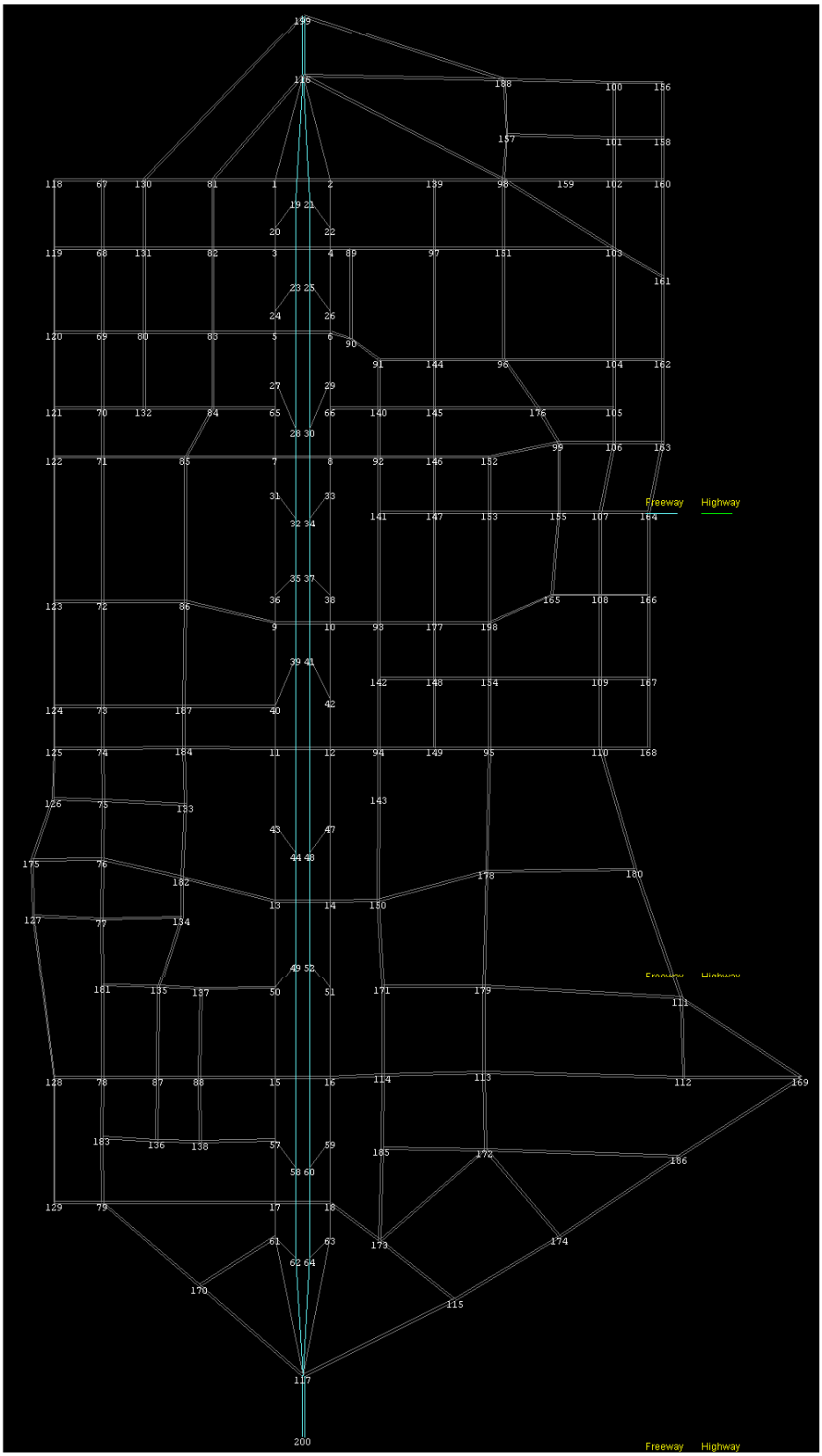

Figure 5.4 Reversible highway lanes in Fort Worth network

Depicted in Figure 5.5 are the results of the first 100 iterations of the MNCT-CF-DTA algorithm for an evacuation demand of 30,000 vehicles. Initial conditions for such a demand level are a network clearance time of 195.5 min, an average evacuation time of 105.3 min, and an average trip time is 105.3 min as well. The minimum average evacuation time is 43.64 min and is reached after 80 (outer-loop) iterations with a corresponding minimum network clearance time of 83.78 min and the average trip time of 30.62 min. Therefore, the MNCT-CF-DTA algorithm managed to improve the network clearance time by 57%, the average evacuation time by 59%, and the average trip time by 71% from initial conditions. Moreover, the contraflow capability within the MNCT-CF-DTA improved the minimum average evacuation time obtained by the MNCT-DTA algorithm (54.2 min) by a further 20% and the network clearance time (108.6 min) by a further 25%.

After 100 iterations, the average evacuation time is 46.91 min, a 7% increase over optimal conditions. The network clearance time is 84.27 min, a 0.6% decrease over optimal conditions. The average trip time is 29.22 min, a 5% decrease over optimal conditions. All these values are slightly different from the values from at optimal solution, which validates the appropriateness of the descent method embedded in the MNCT-CF-DTA solution algorithm. Table 5.11 summarizes the results for the MNCT-CF-DTA algorithm.

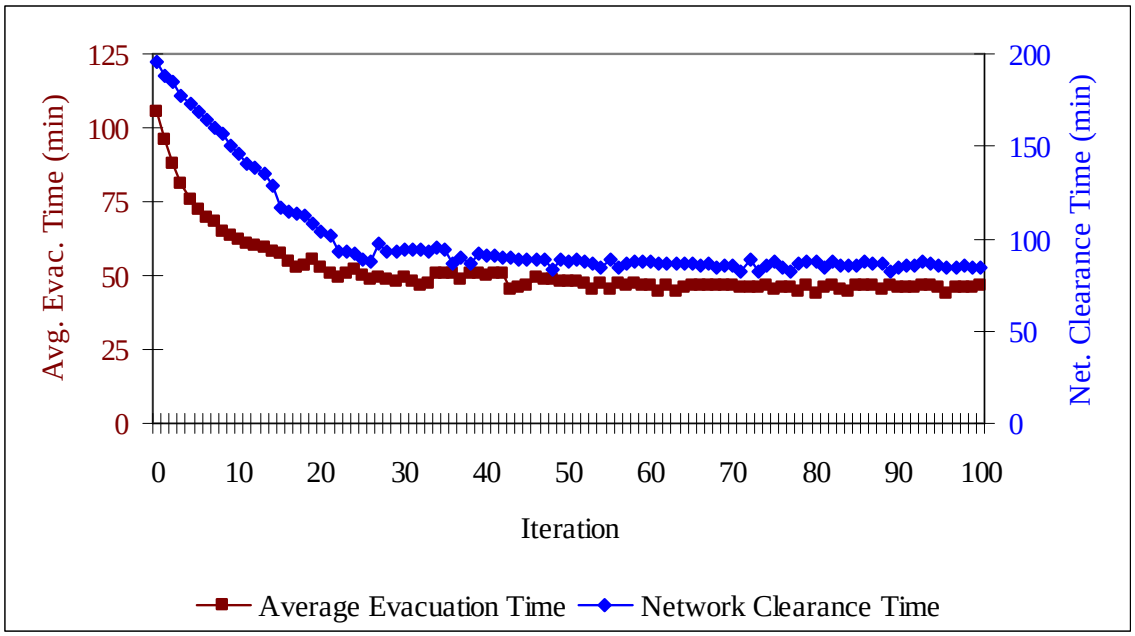

Figure 5.5 Convergence pattern for the MNCT-CF-DTA algorithm
for Fort-Worth network – 30,000 vehicles

Table 5.11 Summary of MNCT-CF-DTA optimality results for Fort Worth network – 30,000 vehicles

Measure of Effectiveness	*Initial Conditions*	*Results at Optimality*	*Results after 100 Iterations*
Iteration	0	80	100
Network Clearance Time (min)	195.5	83.78	84.27
Average Evacuation Time (min)	105.3	43.64	46.91
Average Trip Time (min)	105.3	30.62	29.22

Depicted in Figure 5.6 are the results of the first 100 iterations of the MNCT-CF-DTA algorithm for an evacuation demand of 45,000 vehicles. Initial conditions for such a demand level are a network clearance time of 386.3 min, an average evacuation time of 206.9 min, and an average trip time is 206.9 min as well. The minimum average evacuation time is 61.16 min and is reached after 83 (outer-loop) iterations with a corresponding minimum network clearance time is 122.87 min and an average trip time in the network is 43.67 min. Therefore, compared with initial conditions, the MNCT-CF-DTA algorithm managed to improve the network clearance time by 70% and network clearance time by 68%. Moreover, the contraflow capability within the MNCT-CF-DTA improved the minimum average evacuation

time obtained by the MNCT-DTA algorithm (83.4 min) by a further 27% and the network clearance time (166.8 min) by a further 26%.

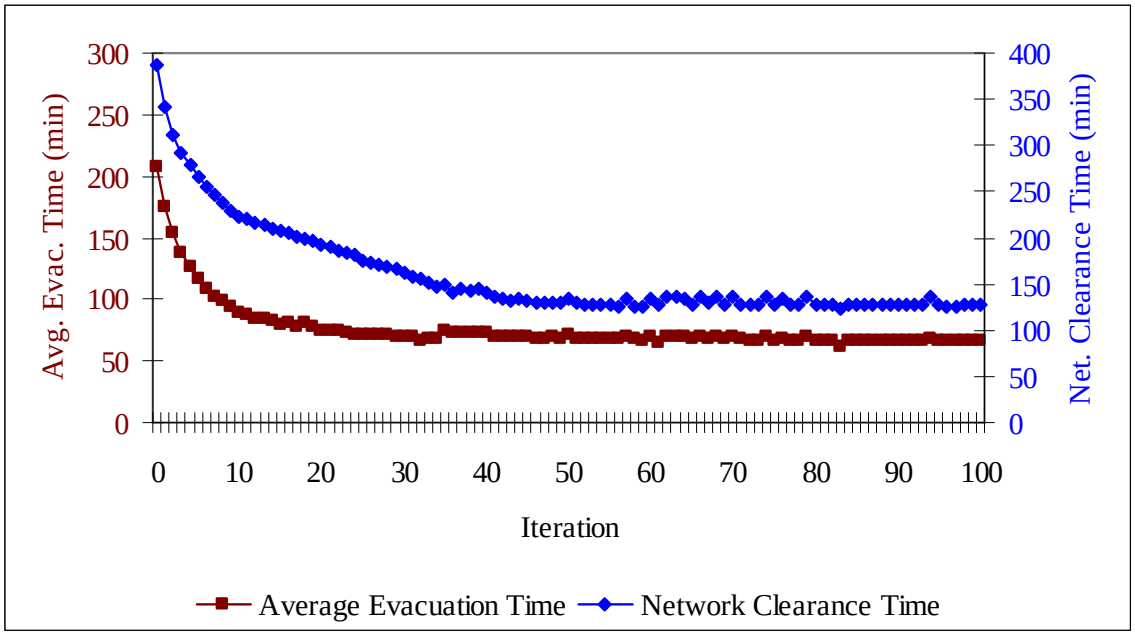

Figure 5.6 Convergence pattern for the MNCT-CF-DTA algorithm
for Fort-Worth network – 45,000 vehicles

After 100 iterations, the network clearance time is 126.54 min, a 2.9% increase over optimal MNCT-CF-DTA conditions. The average evacuation time is 62.73 min, a 2.5% increase over optimal MNCT-CF-DTA conditions. The average trip time is 43.10 min, a 1% decrease over optimal MNCT-CF-DTA conditions. All these values are slightly different from optimal values which validates the appropriateness of the descent method embedded in the MNCT-CF-DTA solution algorithm. Table 5.12 summarizes the results for the MNCT-CF-DTA algorithm.

Table 5.12 Summary of MNCT-CF-DTA optimality results for Fort Worth network– 45,000 vehicles

Measure of Effectiveness	*Initial Conditions*	*Results at Optimality*	*Results after 100 Iterations*
Iteration	0	83	100
Network Clearance Time (min)	386.3	122.87	126.54
Average Evacuation Time (min)	206.9	61.16	62.73
Average Trip Time (min)	206.9	43.67	43.10

5.7.2 Lane Reversibility Simulation Results

Figure 5.7, Figure 5.8, Figure 5.9 and Figure 5.10 show the optimal lanes redistribution of the reversible highway links in Forth Worth network, starting with the freeway links farthest from safety destination. These plots reveal that, no flip-flopping of lane-reversals in the network occurred, which validates the lane-distribution heuristic (CF-DTA) embedded in the MNCT-CF-DTA algorithm. Moreover, the closer the links are to the safety destination, the faster the lane reversibility occurred. For example, for coupled links 117-200 and 200-117, a lane is reversed from 200-117 to 117-200 every iteration of the CF-DTA until full reversibility (Figure 5.10), whereas for links 119-116 and 116-119, which are the farthest from safety, the first reversal is only made after 13 iterations of the algorithm, and in fact, did not even reach require reversibility Figure 5.7. The lane distribution for the sections in-between revealed a smooth transition between these extremes, though all did require full-reversibility at optimality.

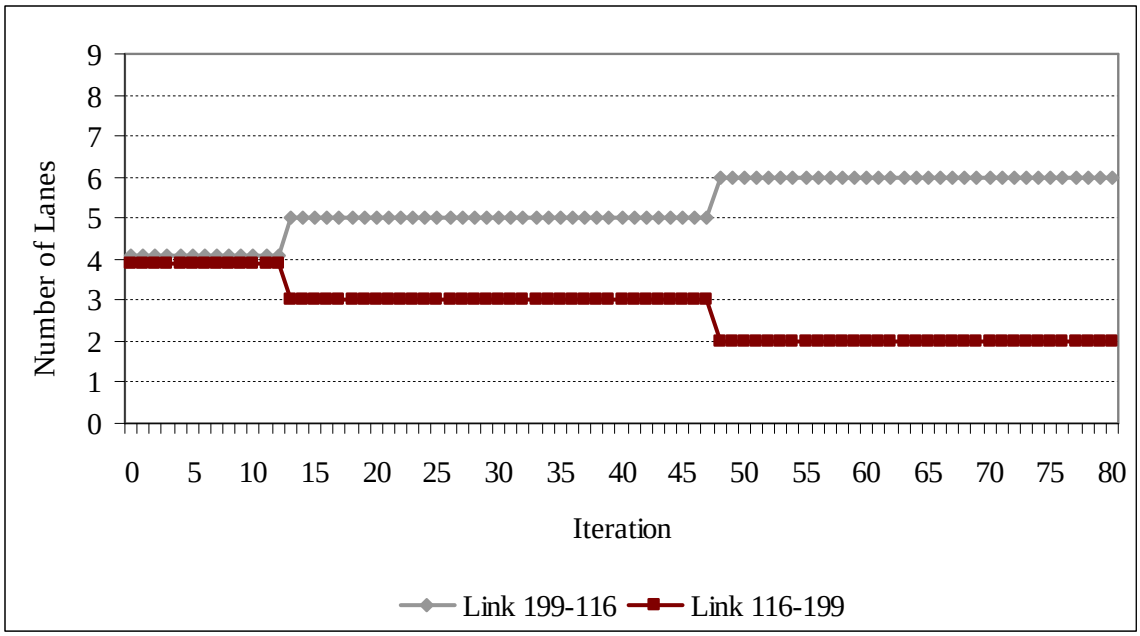

Figure 5.7 Lanes re-distribution for coupled links 119-116 and 116-119

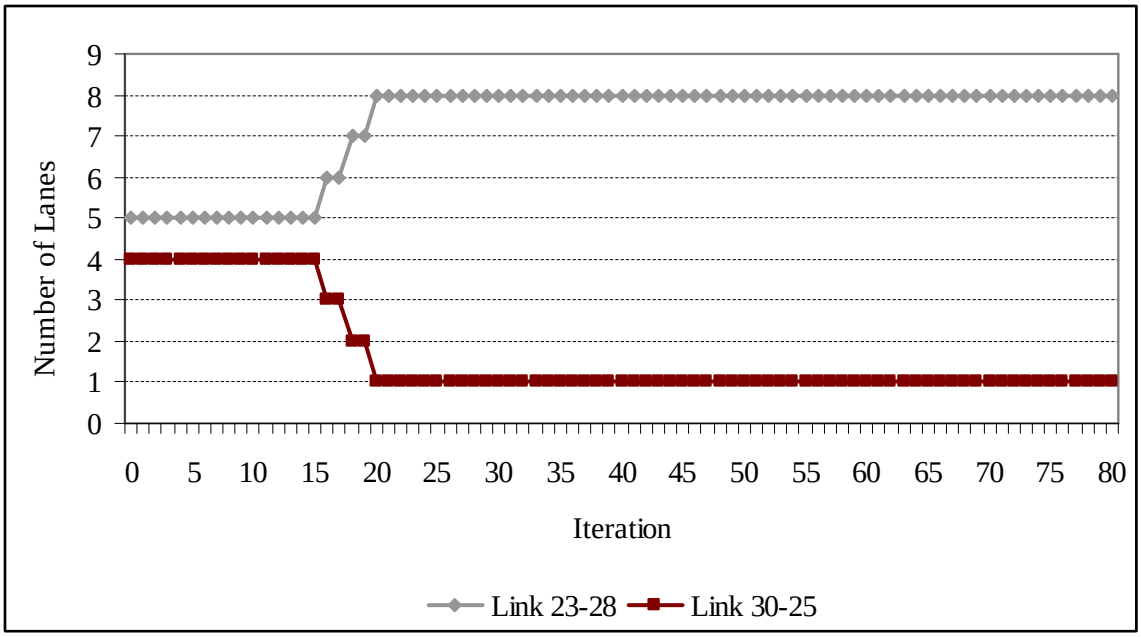

Figure 5.8 Lanes re-distribution for coupled links 23-28 and 30-25

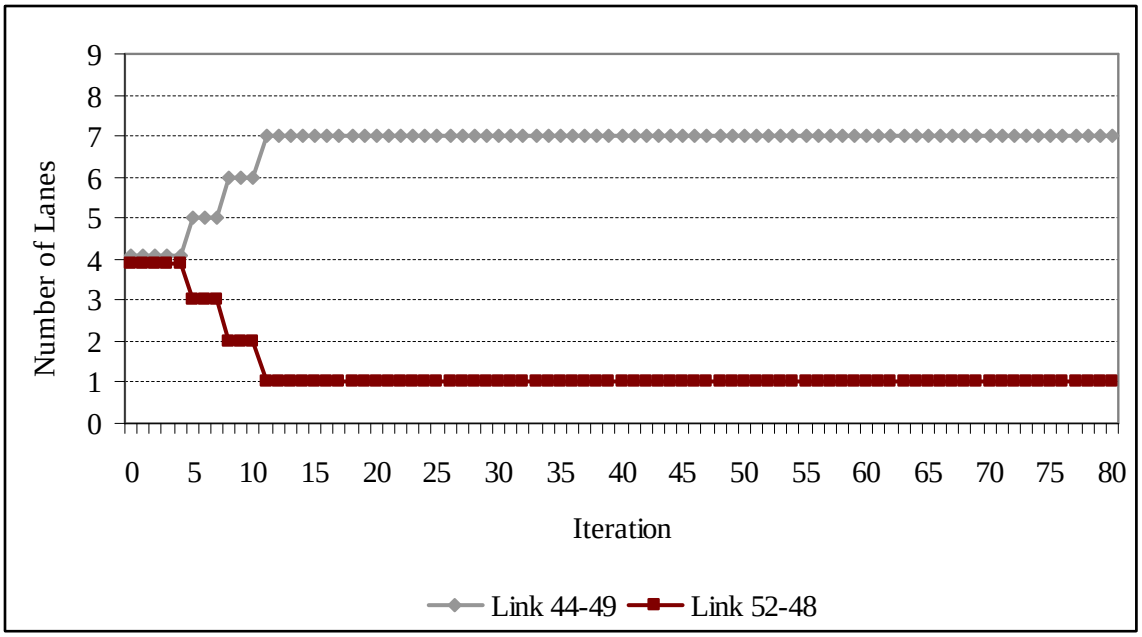

Figure 5.9 Lanes re-distribution for coupled links 44-49 and 52-48

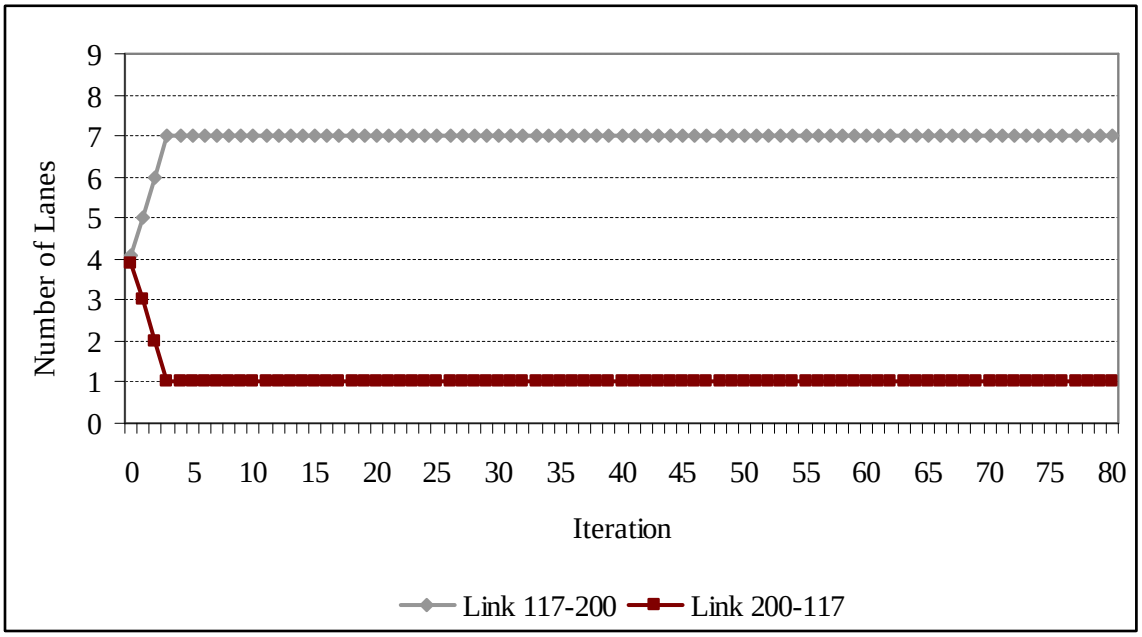

Figure 5.10 Lanes re-distribution for coupled links 117-200 and 200-117

5.7.3 Convergence Pattern Analysis for the ODS-CF-DTA Algorithm

The ODS-CF-DTA algorithm is a two stage process. The MNCT-CF-DTA problem is solved in the first stage to determine the network clearance time and the optimal lane configuration. The LNCT-DTA is then solved in the second stage, given the network clearance time and optimal lane configuration from the first stage, to minimize trip times in the network. In this set of experiments however, the second stage, i.e. the LNCT-DTA problem is solved with the MNCT-CF-DTA solution, i.e. path assignments, as the starting solution. That is, the initial solution for the LNCT-DTA problem is not obtained by an AON assignment but rather from the outcome of solving the MNCT-CF-DTA. Such a solution is therefore feasible and is expected to converge faster.

The first experiment pertains to an evacuation demand level of 30,000 vehicles. Initial conditions are a network clearance time of 195.5 min, and average evacuation and trip times of 105.3 min. Figure 5.11, Figure 5.12, and Figure 5.13 show the convergence patterns of the network clearance time, average evacuation time, and average trip time, respectively.

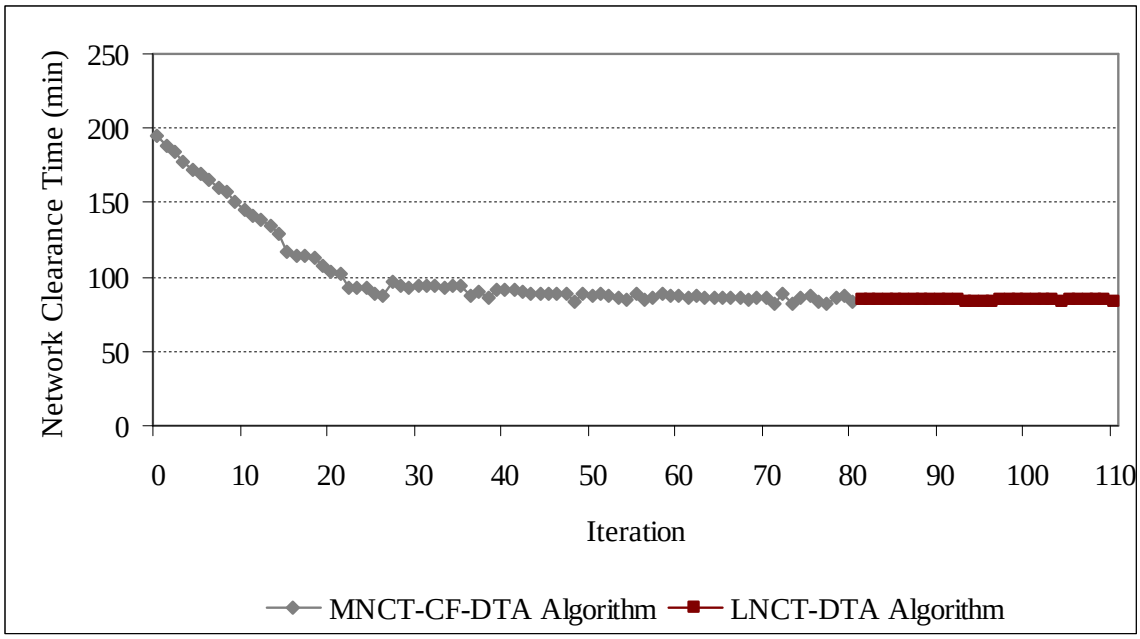

Figure 5.11 Network clearance time convergence pattern for ODS-CF-DTA algorithm for Fort Worth network – 30,000 vehicles

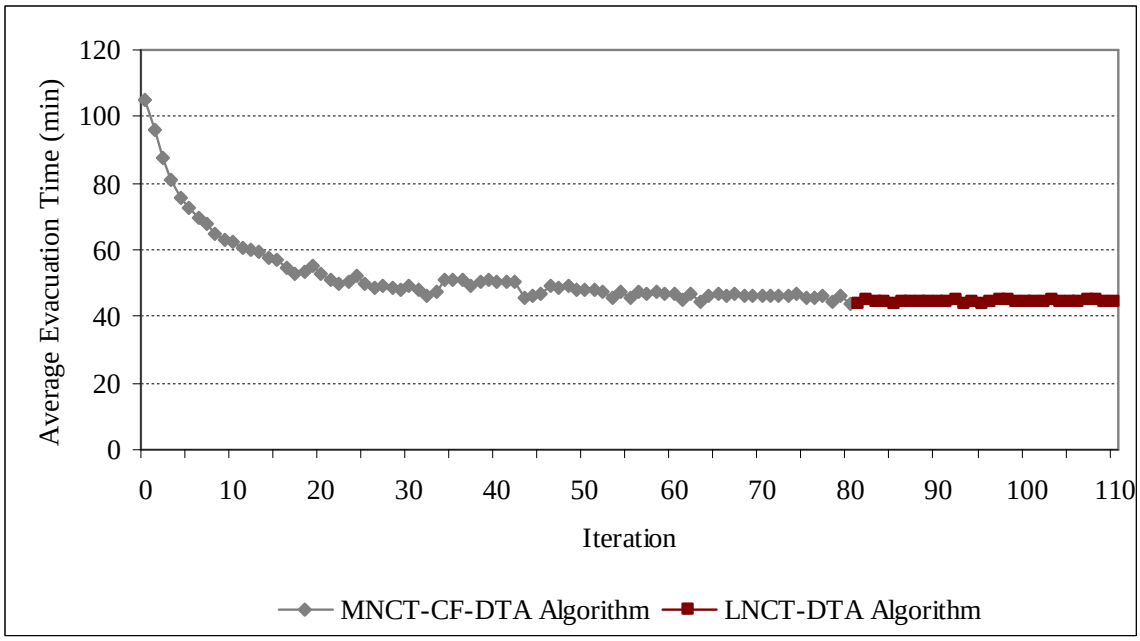

Figure 5.12 Average evacuation time convergence pattern for ODS-CF-DTA algorithm for Fort Worth network – 30,000 vehicles

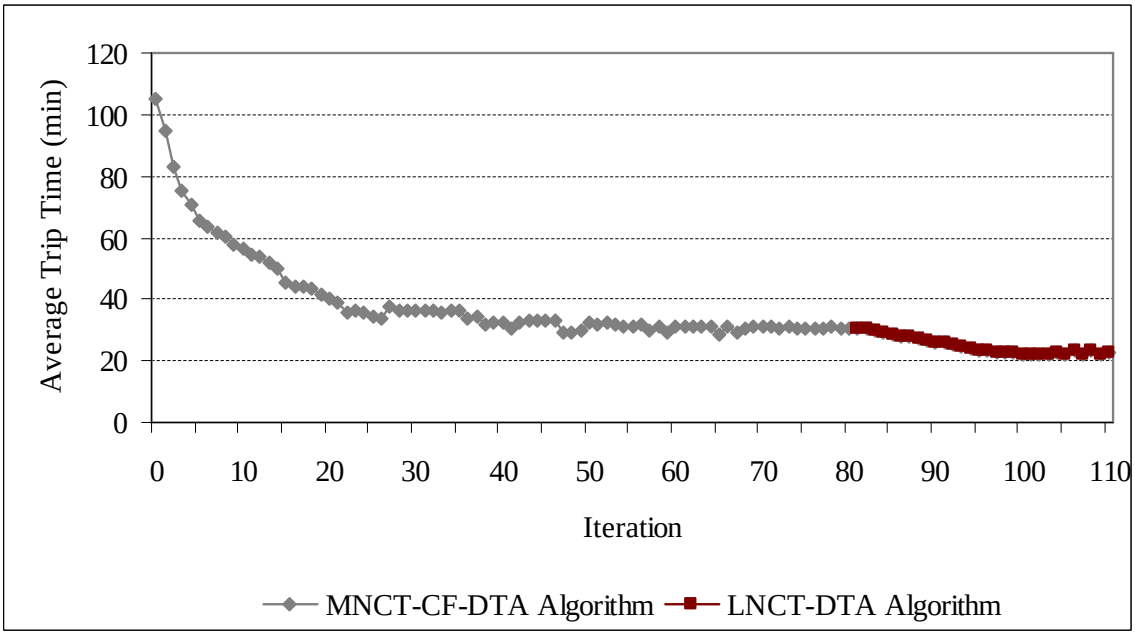

Figure 5.13 Average trip time convergence pattern for ODS-DTA algorithm for Fort Worth network – 30,000 vehicles

The first stage of the ODS-CF-DTA algorithm, i.e. the MNCT-CF-DTA algorithm converges after 80 (outer-loop) iterations. The resulting network clearance time is reduced by 57.14% to 83.78 min, the average evacuation time is reduced by 58.56% to 43.64 min, and the average trip time is reduced by 70.92% to 30.62 min. The MNCT-CF-DTA solution is then used as the initial solution to the LNCT-DTA algorithm (Stage II) with a target evacuation time of 83.78 min. The LNCT-DTA algorithm converges after 26 iterations. The network clearance time is slightly higher (0.92%) at 84.55 min; the average evacuation time is slightly higher at 44.55 min or a 2.09% increase; and the average trip time is reduced by 25.47% to 22.82 min. These results compare favorably with the LNCT-DTA results obtained without a feasible starting solution as shown in (5.13). Note that it only took 26 iterations for the LNCT-DTA algorithm to converge if the MNCT-CF-DTA optimal solution is used as the starting solution as opposed to 86 iterations for the case where no feasible solution is used.

Table 5.13 Summary of ODS-DTA optimality results for Fort Worth network – 30,000 vehicles

Measure of Effectiveness	*Initial Conditions*	*Results at End of Stage I (MNCT-CF-DTA)*	*Results at End of Stage II (LNCT-DTA)**	*Results at end of Stand-alone LNCT-DTA***
Iteration	0	80	26 (106 Total)	86
Network Clearance Time (min)	195.5	83.78	84.55	86.48
Average LNCT Time (min)	N/A	N/A	23.31	22.61
Average Evacuation Time (min)	105.3	43.64	44.55	44.03
Average Trip Time (min)	105.3	30.62	22.82	22.01

* *Initial solution is obtained from stage I*

** *Initial solution is AON*

The second experiment pertains to an evacuation demand level of 45,000 vehicles. Initial conditions are a network clearance time of 386.3 min, and average evacuation and trip times of 206.9 min. Figure 5.14, Figure 5.15 and Figure 5.16 show the convergence patterns of the network clearance time, average evacuation time, and average trip time, respectively. The first stage of the ODS-CF-DTA algorithm, i.e. the MNCT-CF-DTA algorithm converges

after 80 (outer-loop) iterations. The resulting network clearance time is reduced by 68.14% to 122.87 min, the average evacuation time is reduced by 70.23% to 61.16 min, and the average trip time is reduced by 78.89% to 43.67 min. The MNCT-CF-DTA solution is then used as the initial solution to the LNCT-DTA algorithm (Stage II) with a target evacuation time of 122.87 min and final lane reversibility values.

The LNCT-DTA algorithm converges after 24 iterations. The network clearance time is slightly higher (0.75%) at 123.78 min; the average evacuation time is slightly higher at 62.3 min or a 1.86% increase; and the average trip time is reduced by 28.90% to 31.05 min. These results compare favorably with the LNCT-DTA results obtained without a feasible starting solution as shown in Table 5.14. Note that it only took 24 iterations for the LNCT-DTA algorithm to converge if the MNCT-CF-DTA optimal solution is used as the starting solution as opposed to 86 iterations for the case where no feasible solution is used.

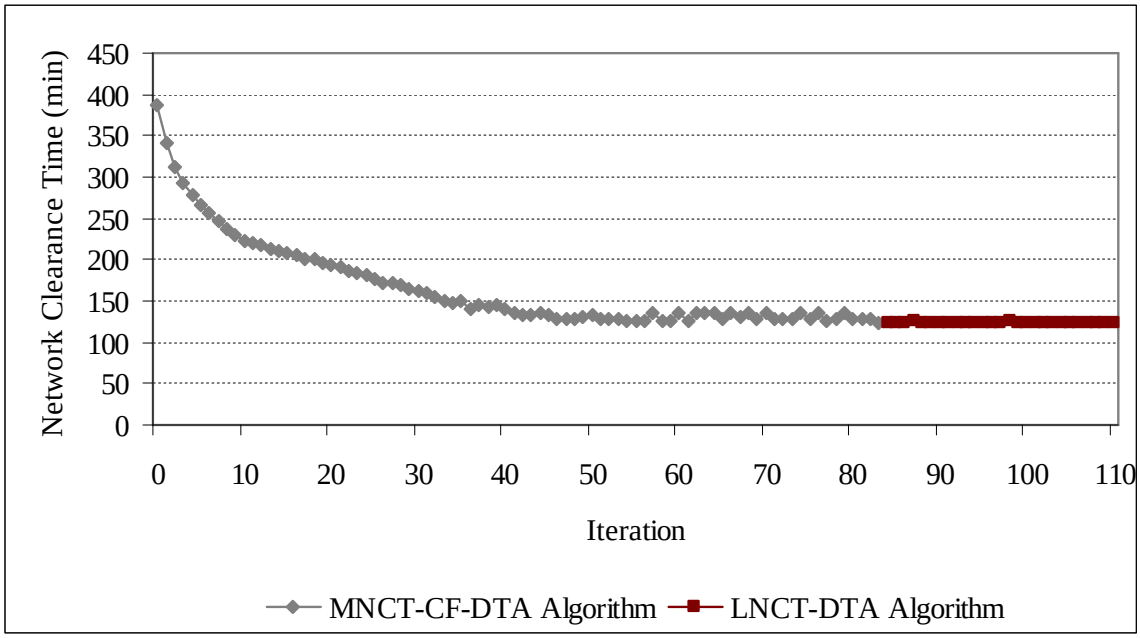

Figure 5.14 Network clearance time convergence pattern for ODS-CF-DTA algorithm for Fort Worth network – 45,000 vehicles

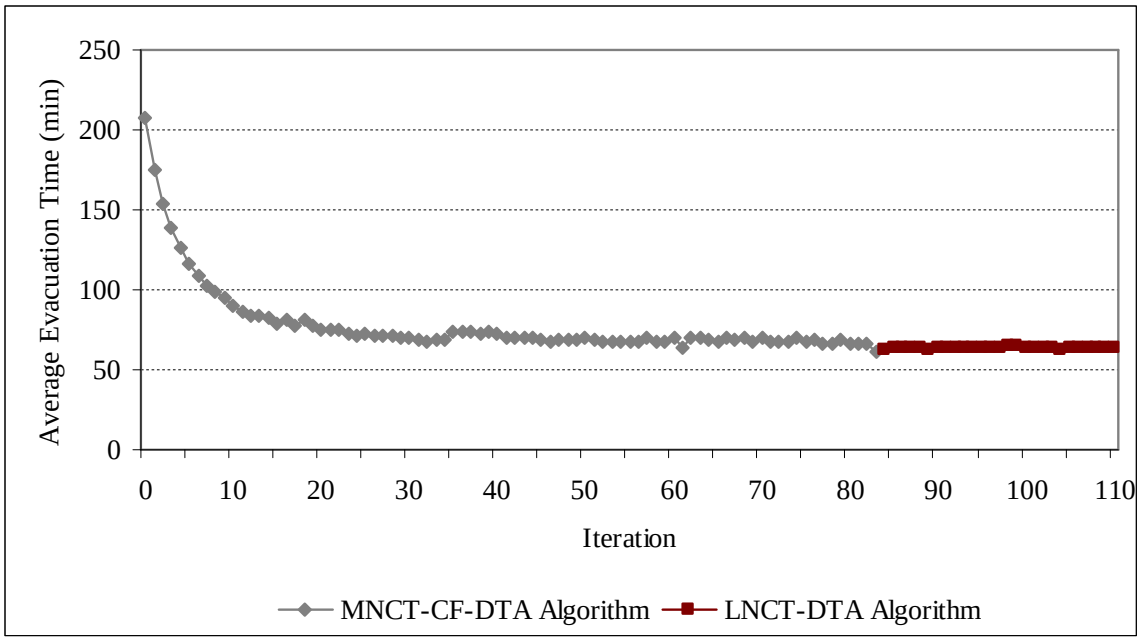

Figure 5.15 Average evacuation time convergence pattern for ODS-CF-DTA algorithm for Fort Worth network – 45,000 vehicles

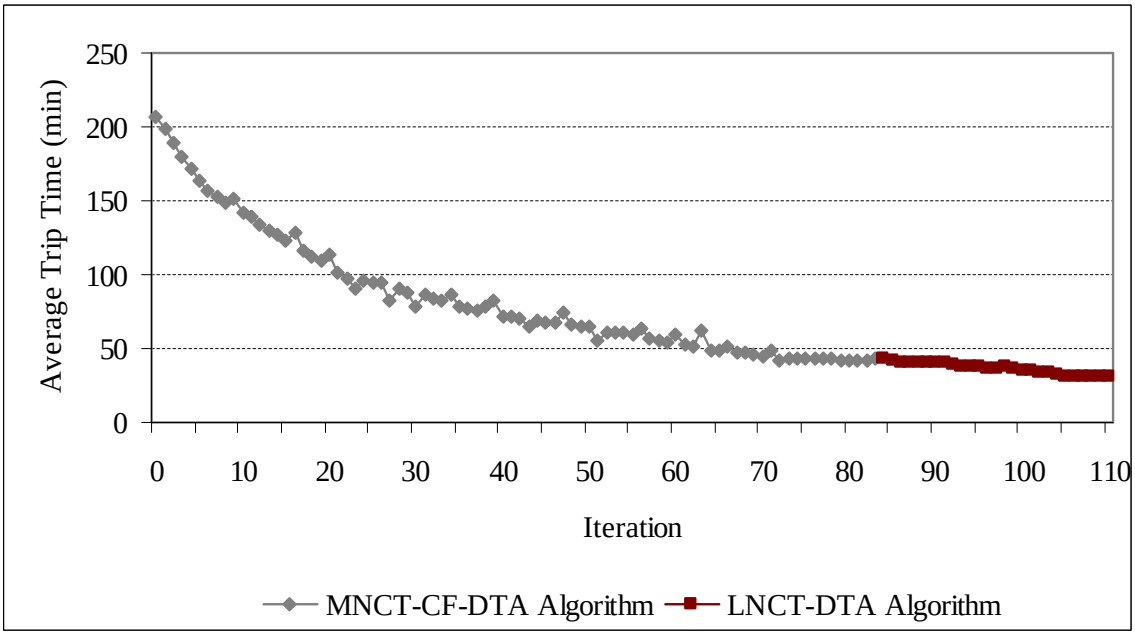

Figure 5.16 Average trip time convergence pattern for ODS-DTA algorithm for Fort Worth network – 45,000 vehicles

Table 5.14 Summary of ODS-DTA optimality results for Fort Worth network – 45,000 vehicles

Measure of Effectiveness	*Initial Conditions*	*Results at End of Stage I (MNCT-CF-DTA)*	*Results at End of Stage II (LNCT-DTA)**	*Results at end of Stand-alone LNCT-DTA***
Iteration	0	83	24 (107 Total)	92
Network Clearance Time (min)	386.3	122.87	123.78	124.12
Average LNCT Time (min)	N/A	N/A	32.11	32.16
Average Evacuation Time (min)	206.9	61.16	62.3	62.22
Average Trip Time (min)	206.9	43.67	31.05	31.01

* *Initial solution is obtained from stage I*
** *Initial solution is AON*

6 SUMMARY OF CONTRIBUTIONS AND FINDINGS

The main focus of this study is to develop Dynamic Traffic Assignment (DTA) models for evacuation that incorporate demand and supply strategies to improve the mobility to safety. Two strategies are considered in this dissertation namely, 1) demand scheduling whereby the evacuation demand is spread over a larger period to alleviate congestion and minimize network clearance time; and 2) contraflow design, whereby lanes are reversed (or capacity is re-distributed) to create a temporary increase in outbound capacity. The development of these models have resulted in research contributions in the fields of operational transportation planning and evacuation management. A summary of the contributions and findings are presented in the following sections.

6.1 RESEARCH CONTRIBUTIONS

This research has several contributions in the fields of operational transportation planning and evacuation management. The first is the estimation of the minimum network clearance time by formulating the Minimum Network Clearance Time (MNCT) DTA problem as a mathematical model. While such a problem is not new, it has not been estimated optimally because previous studies have fixed the departure times (existing evacuation models have always associated evacuees with departure times obtained from demand mobilization curves). This effectively reduces the problem to the classical System Optimal (SO) DTA problem. On the other hand, by treating the departure times, destination, and route choices as decision variables, a better lower bound is obtained. This is achieved by intelligently scheduling the evacuation trips to minimize the network clearance time.

The second contribution of this dissertation is the combination of the MNCT-DTA and the Latest Network Clearance Time (LNCT) DTA models in a bi-objective framework to minimize the network clearance time while keeping the trip times in the network at a minimum. None of the evacuation models reviewed in this dissertation, to the best

knowledge of the author, has this capability.

The third contribution is the determination of the optimal capacity distribution principle for the contraflow network design problem. Previous studies on this topic employed sensitivity or trial-and-error type of analysis in order to find the optimal lane reversibility policy. In this dissertation, the problem is formulated as a minimization problem and a solution algorithm is proposed and tested based on its derived optimality conditions.

The fourth and the main contribution of this dissertation is the integration of demand scheduling and contraflow strategies to minimize network clearance time at a minimum cost to the users (evacuees) in a single framework. Again, to the best knowledge of the author, all the evacuation studies have focused on either demand or supply strategies, but not both.

Finally, and as a by-product of this research, a contribution is made in the field of simulation-based DTA. Since all the evacuation problems formulated in this dissertation are variations of the classical SO-DTA problem, an efficient yet theoretically sound simulation-based solution methodology that outperforms averaging heuristics such as the Method of Successive Averages (MSA) has been developed. In this regards, the work of Lu (2007) on developing a theoretically-sound simulation-based User Equilibrium (UE) DTA model and its solution heuristic is extended to the SO-DTA case along with the necessary modifications.

6.2 RESEARCH SUMMARY AND FINDINGS

6.2.1 Efficient Solution for the Simulation-based SO-DTA Model

All the evacuation problems to be addressed in this dissertation are variations of the classical SO-DTA problem. While SO-DTA models have been formulated analytically in the past, their solution properties have been obtained at the cost realistic traffic flow behavior. On the other hand, the solution quality of simulation-based DTA models has long been questioned despite their ability to handle larger networks and realistically capture traffic dynamics.

At the core of the mistrust in simulation-based DTA models are averaging heuristics such as MSA. While very easy to implement, the lack of derivative information results in improper determination of descent directions, which forces such methods to oscillate and sometimes even diverge. For example, MSA shifts traffic from inferior paths to current optimal (auxiliary) paths using predetermined step sizes with complete disregard to the degree of inferiority. That is slightly inferior paths are penalized as much as the most inferior path and this results in an improper descent direction.

Therefore, it is of great importance to have a hybrid model that combines the theoretical elegance of analytical models with the traffic realism of their simulation counterparts. Candidate traffic simulators must be able to push traffic through the network according to acceptable traffic flow theory – modified Greenshields model in this study – all while packing substantial modeling prowess that includes intersection control, formation and dissipation of queues, information supply strategies, incidents, link closures, link priorities, multiple user classes, and others.

The traffic simulator's main role is therefore to evaluate the path-assignments through simulation and capturing the network state, i.e. link travel times and turn penalties, in the process. The link travel times and turn penalties are then fed into the analytical model to determine the assignments for next iteration. The process then iterates until convergence or a stable solution is found.

6.2.1.1 ***Theoretically Sound Simulation-based SO-DTA Model***

The work done by Lu (2007) on developing a theoretically sound simulation-based UE-DTA problem is extended to the SO-DTA case with appropriate modifications and enhancements made to its solution algorithm. The SO-DTA problem is therefore reformulated via a gap function, as a nonlinear minimization program. An efficient column generation-based optimization framework is then used to integrate a descent method that minimizes the gap

function with DTA constraints being satisfied via a dynamic traffic simulation model. Computational results on both small and large real road networks demonstrate that the proposed SO-DTA algorithm is efficient and effective in obtaining close-to-optimal solutions.

The SO-DTA model is essentially a hybrid model that integrates a traffic simulation model with an analytical model. The major advantage of having a traffic simulation model is to bypass the need to use rudimentary link exit functions or link performance functions to model traffic flow. The SO-DTA model is first formulated as a classical minimization program with the exception that DTA constraints are satisfied through simulation. The optimality conditions are then derived to gain insights in designing its solution algorithm. Given the optimality conditions, the underlying Variational Inequality (VI) formulation of the SO-DTA problem is identified and used to establish solution existence and uniqueness. Nonetheless, the presence of simulation will most probably preclude from having unique solutions. The VI is later reformulated as an equivalent nonlinear minimization program via an appropriate gap function.

A solution framework that integrates both a simulation model and an analytical model is devised to solve the SO-DTA model. The simulation model is responsible for evaluating the time-dependent path-assignments solutions found by the analytical model as well as estimating the link travel times and penalties. A descent method is used to solve the analytical model. The negative of the projected gradient is used to determine the search direction along which the objective function is expected to improve (decrease). A second-order route-swap algorithm is then developed to find the optimal step sizes for the gradient-based search direction on the active (non-zero flow) paths set.

6.2.1.2 ***Analytical Link Travel Time Marginals***

The SO optimality conditions require that path marginal travel times be equilibrated for the

same (r,s,τ) combination. However, the travel time marginals require differentiating the objective function twice with respect to flow (or the link cost once with respect to flow) and this has been cumbersome in the past due to the use of simulation techniques an the lack of a well-behaved link cost function. Hence, the common approach has been to estimate the link cost derivatives, $\partial c(x)/\partial x$, using numerical techniques with all its instability and shortcomings [Peeta (1994)].

To alleviate the instability, this study uses a differentiable link cost function to estimate the link marginal travel times. This is done by expressing link speed term in the Greenshields model as the quotient of the link length by travel time. Then the terms are rearranged to express the link travel time as a function of the link attributes to obtain a continuous differential link-performance function. Moreover, estimating the link marginal travel times analytically requires less computation time and memory than numerical methods, making the proposed descent method more attractive than non-derivative methods.

Tests on a Nine-node network showed that analytical marginals clearly resulted in a stable system trip time whereas numerical marginals resulted in more fluctuations when implemented within an MSA-based solution heuristic. A similar effect is noticed when analyzing the extended convergence pattern for the relative gap.

6.2.1.3 ***Column Generation and Vehicle-based Implementation***

All the models proposed in this study are path-based, which necessitates the explicit storage of the grand path set and assignment results. Although it is straightforward to record all the paths and their assignments in multi-dimensional arrays, memory requirements will grow dramatically with network size, the number of Origin-Destination (O-D) pairs, number of iterations, and planning horizon. To circumvent the intensive memory requirements especially for large-scale network applications of these models, a vehicle-based implementation technique is used throughout this dissertation.

The vehicle-based method, which is only available for traffic simulators that track individual vehicles in the network, extracts the active (non-zero flow) path set and the corresponding flows from vehicle trajectories. Hence, there is no need to enumerate all paths in the network, since non-used paths will never be stored. This is particularly advantageous for large-scale DTA applications, as the total number of feasible path/alternatives generated by the iterative solution algorithm, after a certain number of iterations, could be significantly greater than the total number of vehicles, which is fixed a priori. The benefits are compounded when the column generation technique is used to generate efficient new solutions. Therefore, at most, the model needs to store an additional path per ODT.

Previous experiments [Sbayti et al. (2007), Lu (2007)] show that this vehicle-based implementation technique requires much less computer memory than the typical multi-dimensional grand path set implementation method and is comparable in accuracy to non-vehicle-based implementation techniques.

6.2.1.4 ***Optimal Route-swap Heuristic***

The most important aspect of any simulation-based solution algorithms centers around updating current assignments $\boldsymbol{f}^{(k)}$ for the next iteration to obtain $\boldsymbol{f}^{(k+1)}$. While most simulation-based models shift flow from non-optimal routes to optimal routes, they typically apply a fixed swap rate to the search direction to determine the flow shifts. Still, the determination of the swap rate is problematic. A small swap rate and convergence will take forever to reach, and a large swap-rate and oscillations will occur [Szeto and Lo (2005)]. The general approach has been to parametrically solve for the optimal swap-rate, however, often than not, the resulting optimal swap-rate is network specific, flow-specific, and by all means non-transferable to other networks.

Looking at the units, the swap-rate is actually a factor that converts differences in travel time to vehicles. However, for the units of the swap-rate to be consistent, it must have units of

vehicles/time, which corresponds to the inverse of the second derivative of the objective function with respect to flow. Jayakrishnan et al. (1994) used a similar method based on the inverse Hessian. This study, on the other hand, derives this conversion factor by solving a system of equalities to obtain the optimal swap-rate to equilibrate the set of active paths in the network. The calculated optimal swap-rates are then adjusted for feasibility and applied in the path-assignment update step of the algorithm. The swap-rate computed by this method differs slightly from the diagonal elements of the Hessian matrix used by Jayakrishnan et al. (1994). We refer to this heuristic as the Optimal Route Swap (ORS) heuristic.

Experiments on the Nine-node network demonstrate that ORS guarantees descent at almost each iteration due to the exploitation of local information and derivative information whereas the MSA fluctuates considerably before stabilizing. Experiments on Fort Worth network also shows that the ORS heuristic easily outperforms MSA under two levels of time-varying O-D demand. The ORS heuristic shows consistent convergence properties irrespective of demand levels. This essentially means that the ORS heuristic guarantees, on average, improving the objective function with each additional iteration. The same cannot be said about the MSA. Nonetheless, MSA has been shown to perform satisfactorily under light to medium congestion levels, after which fluctuations take over.

6.2.2 Evacuation Demand Models

Two demand models are developed, namely the MNCT-DTA and the LNCT-DTA model. The former is used to minimize the network clearance time. The latter is used to minimize the system-wide average trip time while ensuring that demand exits the network before a specified target evacuation time. These two models are then combined into one model which we refer to in this dissertation as the Optimal Demand Scheduling (ODS) DTA model, whose objective is to minimize network clearance time at a minimum cost to the network.

6.2.2.1 ***The Minimum Network Clearance Time Problem***

The MNCT-DTA model is formulated as a minimization program by replacing the network clearance time objective by an equivalent yet much simpler objective, the average evacuation time in this case. Figure 6.1 illustrates the difference between trip times and evacuation times.

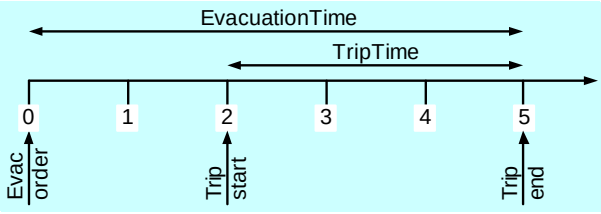

Figure 6.1 Trip time versus evacuation time

The model is then successfully transformed into a structure analogous to an SO-DTA by minimizing an appropriate path-cost function $\chi^{\tau}_{r,s,p}$:

$$\chi^{\tau}_{r,s,p} = \left(\tau + C^{\tau}_{r,s,p} \right) \qquad \forall r, s, p, \tau \tag{6.1}$$

The optimality conditions for the MNCT-DTA model are derived and they show a marked resemblance to the SO-DTA model. Whereas the SO-DTA model aims at equilibrating the path marginal travel times among non-zero path flows for each (r,s,τ), the MNCT-DTA model aims at equilibrating another path cost, $\tilde{\chi}^{\tau}_{r,s,p}$ in this case, among non-zero path-departure time combinations for each (r,s), where

$$\tilde{\chi}^{\tau}_{r,\bar{s},p} = \tau + \tilde{C}^{\tau}_{r,\bar{s},p} \tag{6.2}$$

is the marginal cost incurred by the MNCT-DTA system due to an additional vehicle departing from r to $\bar{s}$ along path p at departure time τ. The optimality conditions for the MNCT-DTA problem can be formally expressed as follows:

$$f^{\tau}_{r,\bar{s},p}\left(\tilde{\chi}^{\tau}_{r,\bar{s},p} - \hat{\pi}_{r,\bar{s}} \right) = 0 \qquad \forall r, p, \tau \tag{6.3a}$$

$$\tilde{\chi}^{\tau}_{r,\bar{s},p} - \hat{\pi}_{r,\bar{s}} \geq 0 \qquad \forall r, p, \tau \tag{6.3b}$$

Optimality condition (6.3a) represents a gap function for the MNCT-DTA problem. Minimizing such a gap function (6.4) is therefore equivalent to solving the original MNCT-DTA problem. Moreover the solution algorithm devised for the SO-DTA problem can be used to solve the MNCT-DTA problem as well.

$$\text{Min } G_{\text{MNCT}}(\boldsymbol{f}) = \sum_{\tau}\sum_{r}\sum_{p} f^{\tau}_{r,\bar{s},p}\left(\tilde{\chi}^{\tau}_{r,\bar{s},p} - \hat{\pi}_{r,\bar{s}}\right) \tag{6.4}$$

Simulation experiments on the Nine-node network show that the MNCT-DTA problem reduced the network clearance time by 28% to 45% and the average trip times by 83% to 93% over initial conditions (simultaneous evacuation). Similarly, simulation experiments on the Fort Worth network show that the MNCT-DTA problem reduced the network clearance time by 44% to 57% and the average trip times by 83% to 96% from initial conditions.

6.2.2.2 ***The Latest Network Clearance Time Problem***

The second demand model developed in this dissertation is LNCT-DTA model, which is formulated by adding arrival time constraints to the classical SO-DTA problem:

$$C^{\tau}_{r,\bar{s},p} \leq \overline{W} \qquad \forall r, p, \tau \tag{6.5}$$

The model is then successfully transformed into a structure analogous to an SO-DTA by minimizing an appropriate path-cost function $\gamma^{\tau}_{r,s,p}$:

$$\gamma^{\tau}_{r,s,p} = \begin{Bmatrix} C^{\tau}_{r,s,p} & (p,\tau) \notin \Re_{r,s};\ \forall r, s, p, \tau \\ C^{\tau}_{r,s,p} + M & (p,\tau) \in \Re_{r,s};\ \forall r, s, p, \tau;\ M >> 0 \end{Bmatrix} \tag{6.6}$$

where M is a large positive number and $\Re_{r,s}$ is the set of restricted path-departure times combinations for pair $r-s$ (vehicles belonging to $\Re_{r,s}$ will exit the network later than the

target evacuation time $\overline{W}$):

$$\Re_{r,s} = \left\{ (p,\tau) \,|\, \left(\tau + C^{\tau}_{r,s,p} \right) \geq \overline{W}; \forall r,s,p,\tau \right\}$$

The optimality conditions for the LNCT-DTA model show a marked resemblance to the SO-DTA model. Whereas the SO-DTA model aims at equilibrating the path marginal travel times among non-zero path flows for each (r,s,τ), the MNCT-DTA model aims at equilibrating another path marginal cost, $\tilde{\gamma}^{\tau}_{r,\bar{s},p}$ in this case, among non-zero path-departure time combinations for each (r,s), where

$$\tilde{\gamma}^{\tau}_{r,\bar{s},p} = \begin{cases} M + \tilde{C}^{\dot{\tau}}_{\dot{r},\bar{s},\dot{p}}; & (p,\tau) \in \Re_{r,\bar{s}}; \forall r,p,\tau;\ M >> 0 \\ \tilde{C}^{\dot{\tau}}_{\dot{r},\bar{s},\dot{p}}; & (p,\tau) \notin \Re_{r,\bar{s}};\ \forall r,p,\tau \end{cases} \tag{6.7}$$

is the marginal cost incurred by the LNCT-DTA system due to an additional vehicle departing from r to $\bar{s}$ along path p at departure time τ. The optimality conditions for the LNCT-DTA problem are formally expressed as follows:

$$f^{\tau}_{r,\bar{s},p} \left(\tilde{\gamma}^{\tau}_{r,\bar{s},p} - \breve{\pi}_{r,\bar{s}} \right) = 0 \qquad \forall r,p,\tau \tag{6.8a}$$

$$\tilde{\gamma}^{\tau}_{r,\bar{s},p} - \breve{\pi}_{r,\bar{s}} \geq 0 \qquad \forall r,p,\tau \tag{6.8b}$$

Optimality condition (6.8a) represents a gap function for the LNCT-DTA problem. Minimizing such a gap function (6.9) is therefore equivalent to solving the original LNCT-DTA problem. Moreover the solution algorithm devised for the SO-DTA problem can also be used to solve the LNCT-DTA problem as well.

$$\text{Min } G_{\text{LNCT}}(\boldsymbol{f}) = \sum_{\tau} \sum_{r} \sum_{p} f^{\tau}_{r,\bar{s},p} \left[\tilde{\gamma}^{\tau}_{r,\bar{s},p} - \breve{\pi}_{r,\bar{s}} \right] \tag{6.9}$$

Simulation experiments on the Nine-node network show that the LNCT-DTA problem, with

target evacuation times set as the minimum network clearance times (as computed from the corresponding MNCT-DTA problems) reduced the average trip times obtained by the MNCT-DTA problem by an additional 27% to 41%. Similarly, simulation experiments on the Fort Worth network show that the LNCT-DTA problem reduced the average trip times obtained by the MNCT-DTA problem by an additional 11% to 24%.

6.2.2.3 *Optimal Demand Scheduling Problem*

Ideally, the best solution to an evacuation problem would be to clear the network in the least amount of time, with the evacuees collectively accruing the least amount of travel times. This is achieved by combining both the MNCT-DTA and LNCT-DTA problems in a bi-objective framework whose solution is obtained in two sequential stages. An MNCT-DTA problem is solved first to determine the minimum network clearance time W^*, and an LNCT-DTA problem is solved in the second stage to minimize system trip time, with a target evacuation time equal to W^*. The second stage can be solved in two approaches. The first approach is to solve it as a typical LNCT-DTA problem, i.e. without a feasible initial solution. The second approach, which will be the one adopted for the ODS-DTA problem, is to solve the LNCT-DTA problem using the MNCT-DTA solution (from stage I) as the initial solution. The initial solution is therefore feasible and will result in a much faster convergence rate.

Simulation results on the Fort Worth show that the ODS-DTA problem is capable of reducing the average trip times in the network obtained by the MNCT-DTA problem by an additional 10% to 25%. Moreover, using the MNCT-DTA solution as the initial solution in stage II, resulted in 30% to 70% less iterations for convergence over the typical LNCT-DTA problem.

6.2.3 Optimal Demand Scheduling with Contraflow Problem

The contraflow network design (CF-DTA) problem is formulated as simulation-based DTA model with an SO objective. Additional constraints are added to account for lane

reversibility. The first order optimality conditions failed to reveal any useful insights to the solution of this problem. However, an reversibility principle is obtained under conditions of no-total reversibility among coupled links.

$$\sum_t \left(x_a(t) \frac{\partial c_a(t)}{\partial \omega_a} \right) = \sum_t \left(x_{a^{-1}}(t) \frac{\partial c_{a^{-1}}(t)}{\partial \omega_{a^{-1}}} \right) \tag{6.10}$$

Condition (6.10) states that, in the case where total reversibility is not attained, optimality occurs when an additional vehicle will have the same contribution to the system cost whether it is traverses reversible link a or its couple a^{-1}. Simple numerical examples show that such a condition holds true. Moreover, numerical examples have found that, under the provision of identical link cost functions for coupled links, the total link travel time marginals must be equal at optimality.

$$\sum_t \left(c_a(t) + x_a(t) \frac{\partial c_a(t)}{\partial x_a} \right) = \sum_t \left(c_{a^{-1}}(t) + x_{a^{-1}}(t) \frac{\partial c_{a^{-1}}(t)}{\partial x_{a^{-1}}} \right) \tag{6.11}$$

Condition (6.11) is extremely important in SO-based DTA models since the travel time marginals (or more appropriately $\partial c_a(t) / \partial x_a$) are readily available, whereas the $\partial c_a(t) / \partial \omega_a$ is problematic to compute or estimate.

The CF-DTA problem is then combined with the ORS-DTA problem to integrate the supply and demand strategies considered in this study. The resulting problem is referred to as the ODS-CF-DTA problem and its solution is a two-stage procedure. In Stage I, the MNCT-DTA and CF-DTA problems are combined to solve for the optimal joint flow pattern and lane configuration that results in minimizing the network clearance time. The resulting problem is referred to as MNCT-CF-DTA and is solved in an iterative bi-level framework whereby an MNCT-DTA problem is solved in the lower level, given current optimal lane configuration to find the optimal flow pattern that minimizes network clearance time and a CF-DTA problem is solved in the upper level, given current optimal flow pattern, to find the optimal lane

configuration that minimizes trip times in the network. The process iterates until convergence. In the second stage, an LNCT-DTA problem is solved, given the optimal lane configuration ω^*, minimum network clearance time f^*, and using the MNCT-CF-DTA solution as the starting solution. Simulation results on the Fort Worth network show that allowing for contraflow further reduced the network clearance time and average trip times obtained from solving an ODS-DTA problem by an additional 20% to 27%.

REFERENCES

Abkowitz, M., and Meyer, E. Technological Advancements in Hazardous Materials Evacuation Planning. *Transportation Research Record,* 1522, pp. 116-121, 1996.

Alam, S. B. and Goulias, K. G. Dynamic Emergency Evacuation Management System Using Geographic Information System and Spatiotemporal Models of Behavior. *Transportation Research Record,* 1660, pp. 92-99, 1999.

Alsnih, R. and Stopher, P. R. A Review of the Procedures Associated with Devising Emergency Evacuation Plans. *Transportation Research Record,* 1865, pp. 89-97, 2004.

Barrett B., Ran, B., and Pillai, R. Developing a Dynamic Traffic Management Modeling Framework for Hurricane Evacuation. *Transportation Research Board*, 79th Annual Meeting, Washington, D.C., No. 00-1595, 2000.

Baxter, D. H. Utilization of Florida's Existing and Future Intelligent Transportation Systems for Enhancing Statewide Transportation System Management During and After Hurricane Evacuations. *ITS America*, 11th Meeting, Miami Beach, Florida, 2001.

Ben-Akiva, M., Bierlaire, M., Bottom, J, Koutsopoulos, H. N., and Mishalani, R. Development of a Route Guidance Generation System for Real-Time Application. *IFAC/IFIP/IFORS Symposium on Transportation Systems*, 8th Meeting, Chania, Greece, 1997.

Ben-Akiva, M., Bierlaire, M., Burton, D., Koutsopoulos, H. and Mishalani, R. Simulated-Based Tools for Dynamic Traffic Assignment: DynaMIT and Applications. *ITS America*, 10th Annual Meeting, Boston, May 1-4, 2000.

Ben-Akiva, M., Koutsopoulos, H. N., and Mishalani, R. DynaMIT: A Simulation-Based System for Traffic Prediction". Paper presented at the *DACCORD Short Term Forecasting Workshop*, Delft, The Netherlands, 1998.

Bertsekas, D. P. *Nonlinear Programming*. Athena Scientific, Belmont, MA, USA, 1995.

Bertsekas, D. P. and Gafni, E. M. *Projected Newton Methods and Optimization of Multi-Commodity Flows. IEEE Transactions on Automatic Control*, 28 (12), pp. 1000-1006, 1983.

Bottom, J. A. *Consistent Anticipatory Route Guidance*. PhD Thesis, Massachusetts Institute of Technology, 2000.

Boyce, D., Lee, D-H., and Ran, B. Analytical Models of the Dynamic Traffic Assignment Problem. *Networks and Spatial Economics*, 1 (3-4), pp. 377-390, 2001.

Bureau of Public Roads (BPR). *Traffic Assignment Manual*. U.S. Dept. of Commerce, Urban Planning Division, Washington D.C., 1964.

Campos, VBG., da Silva, PAL., and Netto, POB. Evacuation Transportation Planning: A Method to Identify Optimal Independent Routes. *International Conference on Urban Transport and the Environment for the 21st Century*, 5th Meeting, Rhodes, Greece, 1999.

Carey, M. Optimal Time-Varying Flows on Congested Networks. *Operations Research*, 35 (1), pp. 58-69, 1987.

Carey, M. and McCartney, M. Behavior of a Whole-Link Travel Time Model Used In Dynamic Traffic Assignment. *Transportation Research Part B*, 36, pp. 85-93, 2002.

Carey, M. and Subrahmanian, E. An Approach To Modelling Time-varying Flows on Congested Networks. *Transportation Research B*, 34, pp. 157-183, 2000.

Chamlet, L. G., Francis, R. L., and Saunders, P. B. Network Models for Building Evacuation. *Management Science*, 28 (1), pp. 86-105, 1982.

Chang, G-L., Mahmassani, H. S. and Herman, R. A Macroparticle Traffic Simulation Model to Investigate Peak-Period Commuter Decision Dynamics. *Transportation Research Record* 1005, pp. 107-120, 1985.

Chen, G. H. and Hung, Y. C. On the Quickest Path Problem. *Information Processing Letters*, 46, pp. 125-128, 1993.

Chen, H-K. and Hsueh, C-F. A Model and an Algorithm for the Dynamic User-Optimal Route Choice Problem. *Transportation Research Part B*, 32 (3), pp. 219-234, 1998.

Chen, X., and B. Zhan. Agent-Based Modeling and Simulation of Urban Evacuation Relative Effectiveness of Simultaneous and Staged Evacuation Strategies. *Transportation Research Board*, 83rd Annual Meeting, 2004.

Chen, Y. L. and Chin, Y. H. The Quickest Path Problem. *Computers and Operations Research*, 17, PP. 153-161, 1990.

Chiu, Y-C., P. Korada, and Mirchandani, P. B. Dynamic Traffic Management for Evacuation. *Transportation Research Board*, 84th Annual Meeting, 2005.

Chiu, Y-C., Zheng, H., Villalobos, J. and Gautam, B. Modeling No-Notice Mass Evacuation Using a Dynamic Traffic Flow Optimization Model, *IIE Transactions* 39, pp. 83-94, 2007.

Chiu, Y-C. Traffic Scheduling Simulation and Assignment for Area-Wide Evacuation. *IEEE Intelligent Transportation Systems Conference*, Washington D.C., 2004.

Choi, W., Francis, R.L., Hamacher, H.W., Tufekci, S., Network Models of Building Evacuation Problems with Flow-Dependent Exit Capacities. *Operational Research*, pp. 1047-1059, 1984.

Choi, W., Hamacher, H. W., and Tufekci, S. Modeling of Building Evacuation Problems by Network Flows with Side Constraints. *European Journal of Operational Research*, 35, pp. 98-110, 1988.

Church, R. L. and Cova, T. J. Mapping Evacuation Risk on Transportation Networks Using a Spatial Optimization Model. *Transportation Research Part C*, 8, pp. 321-336, 2000.

Church, R. L. and Sexton, R. *Modeling Small Area Evacuation: Can Existing Transportation Infrastructure Impede Public Safety*. Final Report, California Department of Transportation, Testbed Center for Interoperability, 2002.

Corps of Engineers (COE) and Southwest Florida Region Planning Council (SWFRPC). *Lee County Florida Flood Emergency Evacuation Plan*. 1979.

Cova, T. J and Church, R. L. Modeling Community Evacuation Vulnerability Using GIS. *International Journal of Geographical Information Science*, 11 (8), pp. 763-784, 1997.

Cova, T. J. and Johnson, J. P. Microsimulation of Neighborhood Evacuations in the Urban-Wildland Interface. *Environment and Planning A*, 34, pp. 2211-2229, 2002.

Cova, T. J. and Johnson, J. P. A Network Flow Model for Lane-based Evacuation Routing. *Transportation Research Part A*, 37, pp. 579-604, 2003.

Cybis, H. B. B. A Dynamic User Equilibrium Assignment Model - A Rigorous Formulation. In: Gartner, N. H., Improta, G. (Eds.), *Urban Traffic Networks: Dynamic Flow Modeling and Control*, Springer, Berlin, pp. 233-250, 1995.

Dafermos, S. Traffic Equilibrium and Variational Inequalities. *Transportation Science*, 14 (1), pp. 42-54, 1980.

Daganzo, C. F. The Cell Transmission Model: A Dynamic Representation of Highway Traffic Consistent With The Hydrodynamic Theory. *Transportation Research B*, 28 (4), pp. 269-287, 1994.

Daganzo,C. F. The Cell Transmission Model, Part II: Network Traffic. *Transportation Research Part B*, 29 (2), pp. 79-93, 1995.

Dash, N. and Morrow, B. H. Return Delays and Evacuation Order Compliance: The Case of Hurricane Georges and the Florida Keys. *Environmental Hazards*, 2, pp. 119-128, 2001.

Dial., R. Algorithm 360: Shortest Path Forest with Topological Ordering. *Communications of the ACM*, 12, pp. 632-633, 1969.

Dong, Z., and Xue, D. Intelligent Scheduling of Contraflow Control Operation Using Hierarchical Pattern Recognition and Constrained Optimization. *IEEE*, pp. 135-140, 1997.

Dunn, C. E. Optimal Routes in GIS and Emergency Planning Applications. *Area*, 24 (3), pp. 259-267.

Fahy, R. F. An Evacuation Model for High Rise Buildings. *International Symposium on Fire Safety Science*, 3rd Meeting, Elsevier, London, pp. 815-823, 1991.

Franzese, O. and Han, L. D. A Methodology for the Assessment of Traffic Management Strategies for Large-Scale Emergency Evacuations. *ITS America*, 11th Meeting, Miami Beach, Florida, 2001.

Friesz, T. L., Luque, J., Tobin, R. L., Wie, B. W. Dynamic Network Traffic Assignment Considered as a Continuous Time Optimal Control Problem. *Operation Research*, 37 (6), pp. 893-901, 1989.

Fu, H., and Wilmot, C. G. A Sequential Logit Dynamic Travel Demand Model for Hurricane Evacuation. *Transportation Research Record*, 1882, pp. 19-26, 2004.

Hamza-Lup, G. L., Hua, K. A., and Peng, R. Applying E-Transportation to Traffic Evacuation Management Under Human-Caused Threats. *IEEE*, pp. 666-673, 2005.

Ghali, M. O. and Smith, M. J. Road Pricing: A New Model for Assessing the Many Options.

Traffic Engineering and Control, 33 (3), pp. 156-157, 1992.

Givens, G. G. Disaster Duty – Prepare to Evacuate, Prime for Alert. *Traffic Digest and Review*, 11, (6), pp. 4-7, 1963.

Graat, E., Midden, C., and Bockholts, P. Complex Evacuation: Effects of Motivation Level and Slope of Stairs on Emergency Egress Time in a Sports Stadium. *Safety Science*, 31, pp. 127-141, 1999.

Mahmassani., H. S., and G. L. Chang. On Boundedly-Rational User Equilibrium in Transportation Systems. *Transportation Science*, 21, pp. 88-89, 1987.

Hamacher, H. W., and Tjandra S. A. Mathematical Modeling of Evacuation Problems: A State of The Art. In *Pedestrian and Evacuation Dynamics* (Schreckinberg, M. and Sharma, S. D. eds.), Springer, 227-266, 2002.

Han A. F. TEVACS: Decision Support System for Evacuation Planning in Taiwan. *Journal of Transportation Engineering*, 116 (6), pp. 821-830, 1990.

Han L. D. and Yuan F. Evacuation Modeling and Operations Using Dynamic Traffic Assignment and Most Desirable Destination Approaches. *Transportation Research Board*, 84th Annual Meeting, Washington, D.C., No. 05-2401, 2005.

Hawas, Y. and Mahmassani, H. S. Comparative Analysis of the Robustness of Centralized and Distributed Route Control Systems in Incident Situations. *Transportation Research Record* 1537, pp. 83-90, 1997.

HMM Associates. Evacuation Time Estimates for Area Near Pilgrim Station. Report prepared for Boston Edison Company, Boston, 1980.

Ho, J. K. A Successive Linear Optimization Approach to the Dynamic Traffic Assignment Problem. *Transportation Science*, 14 (4), pp. 295-305, 1980.

Hobeika A. G., Kim S., and Beckwith R. E. A Decision Support System for Developing Evacuation Plans around Nuclear Power. *Interfaces*, 24 (5), pp. 22-35, 1994.

Hobeika, A. G., Kim., C. Comparison of Traffic Assignments in Evacuation Modeling. *IEEE Transactions on Engineering Management*, 45 (2), pp. 192-198, 1998.

Hobeika, A. G., Radwan, A. E., and Jamei, B. Transportation Actions to Reduce Evacuation Times under Hurricane/Flood Conditions: A Case Study of Virginia Beach city. Transportation Research Board, 74th Annual Meeting, Washington, D.C. 1985

Hobeika, A.G. TEDSS: A Software for Evacuating People around Nuclear Power Stations. 7th International Conference on Applications of Advanced Technologies in Transportation, ASCE, Reston, Va., pp. 688–695, 2002.

Hobeika, A.G. and Jamei, B. MASSVAC: A Model for Calculating Evacuation Times under Natural Disasters. Conference on *Computer Simulation in Emergency Planning*, La Jolla, California, 15 (1), 1985.

Huang, H. -J. and Lam, W. H. K. Modeling and Solving the Dynamic User Equilibrium Route and Departure Time Choice Problem in Network with Queues. *Transportation Research Part B*, 36 (3), pp. 253-273, 2002.

Houston, W. An Evacuation Model. US Nuclear Regulatory Commission, Working Paper, Washington DC, 1975.

Irwin, M. D., and Hurlbert, J. S. A Behavioral Analysis of Hurricane Preparedness and Evacuation in Southwestern Louisiana. Louisiana Population Data Center, Louisiana State Univ., Baton Rouge, La., 1995.

Jang, W., Ran, B., and Choi, K. A Discrete Time Dynamic Flow Model and a Formulation and Solution Method for Dynamic Route Choice. *Transportation Research Part B*, 39 (7), pp. 593-620, 2005.

Janson, B. N. Convergent Algorithm for Dynamic Traffic Assignment. *Transportation Research Record* 25, pp. 69-80, 1991a.

Janson, B. N. Dynamic Traffic Assignment for Urban Road Networks. *Transportation Research Part B*, 25, pp. 143-161, 1991b.

Jarvis, J. R. and D. H. Ratliff. Some Equivalent Objectives for Dynamic Network Flow Problems. *Management Science*, 28, pp. 106-109, 1982.

Jayakrishnan, R., Mahmassani, H. S., and Hu, T.-Y. An Evaluation Tool for Advanced Traffic Information and Management Systems in Urban Networks. *Transportation Research Part C*, 2 (3), pp. 129-147, 1994.

Jayakrishnan, R., Tsai, W. K., Prashker, J. N., and Rajadhyaksha, S. A Faster Path-Based Algorithm for Traffic Assignment. *Transportation Research Record* 1443, pp. 75-83, 1994.

Jayakrishnan, R., Tsai, W. K. and Chen, A. A Dynamic Traffic Assignment Model with Traffic-Flow Relationships. *Transportation Research C*, 3 (1), pp. 51-72, 1995.

Kagaris, D., Pantziou, G. E., Tragoudas, S. and Zaroliagis, C. D. Transmissions in a Network with Capacities and Delays. *Networks*, 33 (3), pp. 167-174, 1999.

Kisko, T. M., Francis, R. L. EVACNET+: A Computer Program to Determine Optimal Evacuation Plans *Fire Safety Journal*, 9, pp. 211-220, 1985.

KLD Associates. Formulations of the DYNEV and I-DYNEV Traffic Simulation Models Used in ESF. Report prepared for Federal Emergency Management Agency, Washington, D.C, 1984.

Kwon E. and Pitt S. Evaluation of Emergency Evacuation Strategies for Downtown Event Traffic Using a Dynamic Network Model. *Transportation Research Board*, 84th Annual Meeting, Washington, D.C., No. 05-2164, 2005.

Larsson, T. and Patriksson, M. Simplicial Decomposition with Disaggregated Representation for the Traffic Assignment Problem. *Transportation Science*, 26, pp. 4-17, 1992.

Leonard D., Grower P., and Taylor N. CONTRAM: Structure of the Model. Technical Report 178, TRRL, 1989.

Lepofsky, M., Abkowitz M. and Cheng P. Transportation Hazard Analysis in Integrated GIS Environment. *Journal of Transportation Engineering*, 119 (2), pp. 239-254, 1993.

Lewis, D.C. Transport Planning for Hurricane Evacuations. *ITE Journal*, 55 (8), pp. 31-35, 1985.

Lewis, D.C. September's Great Escape: New Information System Helps Manage Hurricane Evacuations. *Roads and Bridges*, 39 (9), pp. 40–42, 2001.

Li Q. and Wang Y. GIS-Based Emergency Evacuation Computer Simulation System. Integrating Mobility Safety and Security. *ITS America 2004*, 14th Annual Meeting and Exposition, 2004.

Lieberman, E., Andrews, B., Davilla, M., and Yedlin, M. Macroscopic Simulation for Urban Traffic Management: The TRAFLO Model. FHWA-RD-80, Federal Highway Administration, 1983.

Lieberman, E. B. and Andrews, B. J. TRAFLO – A New Tool to Evaluate Transportation Management Strategies. *Transportation Research Record*, 772, pp. 9-15, 1980.

Lighthill, M. H. and Whitham, G. B. On Kinematic Waves-II. A Theory of Traffic Flow on Long Crowded Roads. *Proceedings* of the Royal Society (London), A229, 1178, pp. 317-345, 1955.

Liu Y., Lai X., and Chang G. A Two-Level Integrated Optimization Model for Planning of Emergency Evacuation: A Case Study of Ocean City under Hurricane Evacuation. *Transportation Research Board*, 84th Annual Meeting, Washington, D.C., No. 05-1786, 2005b.

Liu, H., Wenteng X., Jeff Ma, Ban, X., and Mirchandani, P. Dynamic Equilibrium Assignment with Microscopic Traffic Simulation. *Proceedings* of the 8th IEEE Conference on Intelligent Transportation Systems. Vienna, Austria, September 13-16, 2005c.

Liu, Y., Zou, N., and Chang, G-L. An Integrated Emergency Evacuation System for Real-Time Operations: A Case Study of Ocean City, Maryland under Hurricane Attacks, 2005a.

Lo, H. K. and Szeto, W. Y. A Cell-Based Variational Inequality Formulation of the Dynamic User Optimal Assignment Problem. *Transportation Research Part B*, 36 (5), pp. 421-443, 2002.

Lovas, G .G. Models of Wayfinding in Emergency Evacuations. *European Journal of Operation Research*, 105, pp. 371-389, 1998.

Li, Y, Ziliaskopoulos, A.K., and S. T. Waller. Linear Programming Formulations for System Optimum Dynamic Traffic Assignment with Arrival Time-based and Departure time-based Demands. *Transportation Research Record*, 1667, pp. 52-59, 1999

Lu, C-C. Multi-Criterion Dynamic Traffic Assignment Models and Algorithms for Road Pricing Applications with Heterogeneous Users. *Ph. D dissertation*, The University of Maryland, College Park, 2007.

Mahmassani H. S., et. al. Effect of Real-Time Information on Network Performance under Alternative Dynamic Assignment Rules, PTRC 21st Annual Meeting, 1993b.

Mahmassani, H. S. Dynamic Traffic Simulation and Assignment: Models, Algorithms and Application to ATIS/ATMS Evaluation and Operation. In *Operations Research and Decision Aid Methodologies in Traffic and Transportation Management*, Labbe, M., Laporte, G., Tanczos, K., and Toint, P. (eds.), 1998.

Mahmassani, H. S. and Jayakrishnan, R. System Performance and User Response under Real-Time Information in a Congested Traffic Corridor. *Transportation Research Part A*, 25 (5), pp. 293-307, 1991.

Mahmassani, H. S., Hu, T., Peeta, S. and Ziliaskopoulos, A. Development and Testing of Dynamic Traffic Assignment and Simulation Procedure for ATIS/ATMS Applications, *Technical Report* DTFH6-90-R-00074-FG, Center for Transportation Research, The University of Texas at Austin, 1992.

Mahmassani, H. S., Peeta, S., Hu, T. Y., and Ziliaskopoulos, A. Dynamic traffic assignment with multiple user classes for real-time ATIS/ATMS applications. *Proceedings* of the Advanced Traffic Management Conference, Federal Highway Administration, U.S. Department of Transportation, Washington, D.C., 91–114, 1993.

Mahmassani, H. S. and Peeta, S. System Optimal Dynamic Assignment for Electronic Route Guidance in a Congested Traffic Network, *Proceedings* of the Second International Capri Seminar on Urban Traffic Networks, Capri, Italy, 1992.

Mahmassani, H. S. Dynamic Network Traffic Assignment and Simulation Methodology for Advanced Systems Management Applications. *Networks and Spatial Economics*, 1, pp. 267-292, 2001.

Mahmassani, H. S. A Distributed Simulation Architecture for Intelligent Transportation Systems Evaluation and Operation. *Proceedings* of the Second LAAS International Conference on Computer Simulation, Beirut, Lebanon, September 1997.

Merchant D. K. and Nemhauser G. L. Optimality Conditions for a Dynamic Traffic Assignment Model. *Transportation Science*, 12, pp. 200-207, 1978b.

Merchant D. K. and Nemhauser G. L. A Model and an Algorithm for the Dynamic Traffic Assignment Problems. *Transportation Science*, 12, 183-199, 1978a.

Moeller, M., Urbanik, T., and Desrosiers. CLEAR (Calculates Logical Evacuation and Response) A Generic Transportation Network Model for the Calculation of Evacuation Time Estimates, NUREG/CR 2504 (PNL3770), U.S. Nuclear Regulatory Commission, Washington D.C., 1982.

Morrow, R. B. Implementing ITS for Hurricane Evacuations in Florida. *ITE Journal*, April, pp. 46-50, 2002.

Nagurney, A. Network Economics: A Variational Inequality Approach. Kluwer Academic Publishers, Boston, MA, USA, 1998.

Oak Ridge National Laboratory (ORNL). Oak Ridge Evacuation Modeling System (OREMS) User's Guide, Oak Ridge, Tn., 1995.

Oak Ridge National Laboratory (ORNL). Oak Ridge Evacuation Modeling System (OREMS) User's Guide, Oak Ridge, Tn., 1999.

Patriksson, M. The Traffic Assignment Problem: Models and Methods. VSP, Utrecht, The Netherlands, 1994.

Peeta, S. and Ziliaskopoulos, A. K. Foundations of Dynamic Traffic Assignment: the Past, the Present and the Future. *Networks and Spatial Economics*, 1 (3/4), pp. 233-265, 2001.

Peeta, S. and Mahmassani, H. S. Multiple User Class Real-Time Traffic Assignment for On-Line Operations: A Rolling Horizon Solution Framework. *Transportation Research C*, 3, pp. 83-98, 1995b.

Peeta, S. and Mahmassani, H. S. System Optimal and User Equilibrium Time-Dependent Traffic Assignment in Congested Networks. *Annals of Operations Research*, 60, pp. 81-113, 1995a.

Peeta, S. System Optimal Dynamic Traffic Assignment in Congested Networks with Advanced Information Systems. *Ph. D Dissertation*, The University of Texas at Austin, 1994.

Petruccelli U. Urban Evacuation in Seismic Emergency Conditions. *ITE Journal*, 73 (8), pp. 34-38, 2003.

Pidd M., F. N. de Siva and Eglese R. W. A Simulation Model for Emergency Evacuation. *European Journal of Operational Research*, 90, pp. 413-419, 1996.

Post, Buckley, Schuh & Jernigan, Inc. (PBS&J). Southeast United States Hurricane Evacuation Traffic Study: Evacuation Travel Demand Forecasting System. *Technical Memorandum* 2. Final Report, Tallahassee, Fl, 2000a.

Post, Buckley, Schuh & Jernigan, Inc. (PBS&J). Southwest Louisiana Hurricane Evacuation Study: Transportation Model Support Document. Tallahassee, Fla, 2000b.

Post, Buckley, Schuh & Jernigan, Inc. (PBS&J). Southeast Louisiana Hurricane Evacuation Study: Transportation Model Support Document." Tallahassee, Fl, 2001.

Post, Buckley, Schuh & Jernigan, Inc. (PBS&J). Southeast United States Hurricane Evacuation Study, Evacuation Traffic Information System (ETIS). Prepared for US Army Corps of Engineers, Mobile District and US Department of Transportation, 2001.

Post, Buckley, Schuh and Jernigan (PBS&J). Evacuation Travel Demand Forecasting System. *Technical Memorandum* 2, Southeast United States Hurricane Evacuation Study, 2000c.

PRC Voorhees. Evacuation Planning Package. *Transportation Research Board*, 61st Annual Meeting, Washington, D.C., 1982.

Radwan A. E., Hobeika A. G., and Sivasailam D. A Computer Simulation Model for Rural Network Evacuation under Natural Disasters. *ITE journal*, pp. 25-30, 1985.

Ran B. and Boyce D. E. Modeling Dynamic Transportation Networks – An Intelligent Transportation System Oriented Approach. Springer-Verlag, Heidelberg, 1996.

Ran, B., Boyce, D. E., and LeBlanc, L. J. A New Class of Instantaneous Dynamic Traffic Assignment Models. *Operations Research*, 4 (1), pp. 192-202, 1993.

Ran, B., Hall, R. W., and Boyce, D. E. A Link-Based Variational Inequality Model for Dynamic Departure Time/Route Choice. *Transportation Research* 30, pp. 31-46, 1996.

Rathi A. K. and Solanki R. S. Simulation of Traffic Flow during Emergency Evacuations: A Microcomputer Based Modeling System. *Proceedings* of the Winter Simulation Conference, 1993.

Regional Development Service (RDS). Executive Summary of a Socioeconomic Hurricane Impact Analysis and a Hurricane Evacuation Impact Assessment Tool (Methodology) for Coastal North Carolina: A Case Study of Hurricane Bonnie. Department of Sociology and Department of Economics, East Carolina University, Greenville, N.C, 1999.

Richards, P. I. Shock Waves on the Highway. *Operation Research*, 4 (1), pp. 42-51, 1956.

Sattayhatewa P. and Ran B. Developing A Dynamic Traffic Management Model For Nuclear Power Plant Evacuation. *Transportation Research Board*, 79th Annual Meeting., 2000.

Sbayti, H., and Mahmassani, H. S. Optimal Scheduling of Evacuation Operations. *Transportation Research Record*, 1964, pp 238-246, 2006.

Sbayti, H., Lu, C.-C., and Mahmassani, H. S. Efficient Implementations of the Method of Successive Averages in Simulation-Based DTA Models for Large-Scale Network Applications. *Transportation Research Record*, 2029, pp 22-30, 2007.

Sheffi, Y. *Urban Transportation Networks: Equilibrium Analysis with Mathematical Programming Methods*. Prentice-Hall, New Jersey, USA, 1985.

Sheffi, Y., H. Mahmassani, W. B. Powell. Evacuation Studies for Nuclear Power Plant Sites: A New Challenge for Transportation Engineers. *ITE Journal*, 51 (6), pp. 25-28, 1982a.

Sheffi, Y., Mahmassani, H., and Powell, W. A Transportation Network Evacuation Model, *Transportation Research Part A*, 16 (3), pp. 209-218, 1982b.

Simon, H. A Behavioral Model of Rational Choice. *Quarterly Journal of Economics*, 69 (1), pp. 99-118, 1955.

Sisiopiku V. P., Jones S., Sullivan A., Sullivan A. J., Patharkar S,. and Tang X. Regional Traffic Simulation for Emergency Preparedness. Technical Report 03226, Transportation Center for Alabama, 2004.

Smith, M. J. A New Dynamic Traffic Model and the Existence and Calculation of Dynamic User Equilibria on Congested Capacity-Constrained Road Networks. *Transportation Research B*, 25, pp. 49-53, 1993.

Smith, M. J. and Wisten, M. B. A Continuous Day-To-Day Traffic Assignment Model and the Existence of a Continuous Dynamic User Equilibrium. *Annals of Operations Research*, 60, pp. 59-79, 1995.

Southworth, F. Regional Evacuation Modeling: A State-of-the-Art Review. ORNL/TM-11740, Oak Ridge National Laboratory, Oak Ridge, Tn., 1990.

Stern E. and Sinuany-Stern Z. A Behavioral-Based Simulation Model for Urban Evacuation. *Regional Science Association*, 66, p. p87-103, 1989.

Szeto, W. Y. and Lo, H. K. Non-Equilibrium Dynamic Traffic Assignment. *Proceedings* of the *16th International Symposium on Transportation and Traffic Theory*, Mahmassani, H. S. (Ed.) Elsevier, USA, pp. 427-445, 2005.

Theodoulou, G., and B. Wolshon. Modeling and Analyses of Freeway Contraflow to Improve Future Evacuations. *Transportation Research Board*, 83rd Annual Meeting, 2004.

Tong, C. O. and Wong, S. C. A Predictive Dynamic Traffic Assignment Model in Congested Capacity-Constrained Road Networks. *Transportation Research Part B*, 34 (8), pp. 625-644, 2000.

Townsend, J. HURREVAC support site http://www. hurrevac.com, 2003.

Tufekci, Suleyman and Kisko. Regional Evacuation Modeling System (REMS): A Decision Support System for Emergency Area Evacuations. *Computers Industrial Engineering*, 21 (1-4) pp. 89-93, 1991.

Tuydes, H. Network Traffic Management under Disaster Conditions. Ph.D. Dissertation Thesis. Northwestern University, December 2005b.

Tuydes, H. and A. Ziliaskopoulos. Network Re-Design to Optimize Evacuation Contraflow. Transportation Research Board, 83rd Annual Meeting, 2004.

Tuydes, H. and A. Ziliaskopoulos. Tabu-Based Heuristic for Optimization of Network Evacuation Contraflow. Transportation Research Board, 84th Annual Meeting, 2005a.

Urbanik, T. Texas Hurricane Evacuation Study. Texas Transportation Institute, College Station, TX., 1978.

Urbanik, T. and Desrosler, A. E. An Analysis of Evacuation Time Estimates around 52 Nuclear Power Plant Sites: An Evacuation. Report NUREG/CR 7856, Volume 1, U.S. NRC, Rockville, Md., 1981.

Urbina E. and Wolshon B. National Review of Hurricane Evacuation Plans and Policies: A Comparison and Contrast of State Practices. *Transportation Research Part A*, 37 (3), pp. 257-275, 2003.

van Aerde, M. and Yagar, S. Dynamic Integrated Freeway/Traffic Signal Networks: A Routing-based Modelling Approach. *Transportation Research A*, 22 (6), pp. 445-453, 1988.

Lin, W. H. and Ahanotu, D. Validating the Basic Cell Transmission Model On A Single Freeway Link. PATH Technical Report 95-3, University of California at Berkeley, 1995.

Wardrop, J. G. Some Theoretical Aspects of Road Traffic Research. Proceedings *of Institute of Civil Engineers*, II (1), pp. 325-378, 1952.

Wie, B.-W., Tobin, R. L., Friesz, T. L., and Bernstein, D. A Discrete Time, Nested Cost Operator Approach to the Dynamic Network User Equilibrium Problem. *Transportation Science*, 28, pp. 79-92, 1995.

Wilmot C. G., and Meduri N. A Methodology to Establish Hurricane Evacuation Zones. *Transportation Research Board*, 84th Annual Meeting, Washington, D.C., No. 05-1363, 2005.

Wilmot, C. G., and Mei, B. Comparison of Alternative Trip Generation Models for Hurricane Evacuation. *Transportation Research Board*, 82nd Annual Meeting, Washington, D.C., 2003.

Wolshon B., Urbina, E., Wilmot, C., and Levitan, M. Review of Policies and Practices for Hurricane Evacuation. I: Transportation Planning, Preparedness, and Response. *Natural Hazards Review*, August pp. 129 – 142, 2005b.

Wolshon, B. One Way Out: Contraflow Freeway Operation Hurricane Evacuation. *Natural Hazards Review*, 2 (3), pp. 105-112, 2001.

Wolshon, B., Urbina, E., Levitan, M., and Wilmot, C. Review of Policies and Practices for Hurricane Evacuation. II: Traffic Operations, Management, and Control. *Natural Hazards Review*, 6 (3), pp. 143-161, 2005a.

Xue, D., and Dong, Z. An Intelligent Contraflow Control Method for Real-Time Optimal Traffic Scheduling Using Artificial Neural Network, Fuzzy Pattern Recognition, and Optimization. *IEEE Transactions on Control Systems Technology*, 8 (1), pp. 183-191, 2000.

Yamada, T. A Network Approach To A City Emergency Evacuation Planning. *International Journal of Systems Science*, 27 (10), pp. 931-936, 1996.

Yang and Koutsopoulos, H. N. A Microscopic Traffic Simulator for Evaluation of Dynamic Traffic Management Systems. *Transportation Research Part C*, 4 (3), pp. 113-129, 1996.

Yuan, F., Han, L., Chin, S-M, and Howang, H. A Proposed Framework for Simultaneous Optimization of Evacuation Traffic Destination and Route Assignment. Transportation Research Board, 85th Annual Meeting, Washington D.C., 2006.

Zaragoza, D. P., Burris M. W., and Mierzejewski, E. A. Hurricane Evacuation Traffic Analysis and Operational Measures. Report No: WPI 0510807, Final Report, Florida Department of Transportation, 1998.

Ziliaskopoulos, A. K., and Mahmassani, H. S. Time Dependent Shortest-Path Algorithm for Real-Time Intelligent Vehicle Highway System Applications. *Transportation Research Record*, 1408, pp. 94-100, 1993.

Ziliaskopoulos, A. K., and Lee, S. A Cell Transmission Based Assignment-Simulation Model for Integrated Freeway/Surface Street Systems. Transportation Research Board, 75th Annual Meeting, Washington, D.C., 1996.

Ziliaskopoulos, A. K., and Mahmassani, H. S. On Finding Least Time Paths Considering Delays for Intersection Movements. *Transportation Research Part B*, 30 (5), pp. 359-367, 1996.

Ziliaskopoulos, A. K., and Waller, S. T. An Internet Based Geographic Information System that Integrates Data, Models and Users for Transportation Applications. *Transportation Research Part C*, 8, pp. 427-444, 2000.

Ziliaskopoulos, A. K., Waller, S. T., Li, Y., and Byram, M. Large-Scale Dynamic Traffic Assignment: Implementation Issues and Computational Analysis. *Journal of Transportation Engineering*, 130 (5), pp. 585-593, 2004.

Ziliaskopoulos, A. K and Chang E. An Inner Approximation Algorithm for the Time Varying Network User Equilibrium Problem. (Paper submitted to *Transportation Science*) 2005.

Ziliaskopoulos, A.K. A Linear Programming Model for the Single Destination System Optimum Dynamic Traffic Assignment Problem. *Transportation Science*, 34 (1), pp. 37-49, 2000.